

AD-A008 526

INTRASYSTEM ELECTROMAGNETIC COMPATIBILITY ANALYSIS PROGRAM. VOLUME I. USER'S MANUAL ENGINEERING SECTION

J. L. Bogdanor, et al

McDonnell Aircraft Company

Prepared for:

Rome Air Development Center

December 1974

DISTRIBUTED BY:

NTIS

**National Technical Information Service
U. S. DEPARTMENT OF COMMERCE**

UNCLASSIFIED

SECURITY CLASSIFICATION OF THIS PAGE (When Data Entered)

REPORT DOCUMENTATION PAGE		READ INSTRUCTIONS BEFORE COMPLETING FORM
1 REPORT NUMBER RADC-TR-74-342, Volume I (of four)	2 GCVT ACCESSION NO.	3 RECIPIENT'S CATALOG NUMBER AD-A0008 526
4 TITLE (and Subtitle) INTRASYSTEM ELECTROMAGNETIC COMPATIBILITY ANALYSIS PROGRAM Volume I - User's Manual Engineering Section		5 TYPE OF REPORT & PERIOD COVERED Final Report 19 May 72 - 19 Nov 73
		6 PERFORMING ORG REPORT NUMBER None
7 AUTHOR(s) J.L. Bogdanor R.A. Pearlman M.D. Siegel		8 CONTRACT OR GRANT NUMBER(s) F30602-72-C-0277
9 PERFORMING ORGANIZATION NAME AND ADDRESS McDonnell Aircraft Company McDonnell Douglas Corporation Box 516, St. Louis, MO 63166		10 PROGRAM ELEMENT, PROJECT, TASK AREA & WORK UNIT NUMBERS PE 62702F JO 45400127
11 CONTROLLING OFFICE NAME AND ADDRESS Rome Air Development Center (RBCT) Griffiss Air Force Base, New York 13441		12 REPORT DATE December 1974
		13 NUMBER OF PAGES 320
14 MONITORING AGENCY NAME & ADDRESS (if different from Controlling Office) Same		15 SECURITY CLASS (of this report) Unclassified
		15a DECLASSIFICATION DOWNGRADING SCHEDULE N/A
16 DISTRIBUTION STATEMENT (of this Report) Approved for public release. Distribution unlimited.		
17 DISTRIBUTION STATEMENT (of the abstract entered in Block 20, if different from Report) Same		
18 SUPPLEMENTARY NOTES None		
<div style="text-align: center;"> Reproduced by NATIONAL TECHNICAL INFORMATION SERVICE US Department of Commerce Springfield, VA 22151 </div>		
19 KEY WORDS (Continue on reverse side if necessary and identify by block number) Electromagnetic Compatibility Electromagnetic Interference Radio Frequency Interference Computer Programs		
20 ABSTRACT (Continue on reverse side if necessary and identify by block number) This user's manual describes the operation and usage of the Intrasystem Electromagnetic Compatibility Analysis Program (IEMCAP). IEMCAP is a USA Standard FORTRAN program for computer-aided implementation of electromagnetic compatibility (EMC) at all stages of an Air Force system's life cycle, applicable to aircraft, space/missile, and ground-based systems. Extensive knowledge of computers is not required to use the program and all inputs are in easy to		

DD FORM 1 JAN 73 1473

EDITION OF 1 NOV 65 IS OBSOLETE

PRICES SUBJECT TO CHANGE
UNCLASSIFIED

SECURITY CLASSIFICATION OF THIS PAGE (When Data Entered)

UNCLASSIFIED

SECURITY CLASSIFICATION OF THIS PAGE(When Data Entered)

20. ABSTRACT (continued)

use, free-field format.

This volume, the Engineering Section, contains descriptions of the program, its organization, analytic basis, operating principles, and logic flow. The system model employed in IEMCAP for the various analysis tasks is presented. The systems approach is derived from basic communications equations in analytic form and then quantized to sampled spectra for digital computers.

This volume also contains a discussion of the program operation. The overall flow through the program is discussed and the major routines and sub-programs are identified. Each of these is then discussed in detail including flow charts and narratives describing their operation.

A complete operation of all mathematical models used in IEMCAP is included. The emitter and receptor spectrum model equations are described including their derivations. The transfer models, which compute emitter to receptor coupling, are similarly described.

UNCLASSIFIED

SECURITY CLASSIFICATION OF THIS PAGE(When Data Entered)

PREFACE

This documents work conducted by McDonnell Aircraft Company, St. Louis, Missouri, on the Intrasystem Electromagnetic Compatibility (EMC) Analysis Program, sponsored by Rome Air Development Center, Griffiss Air Force Base, New York, under Contract F30602-72-C-0277, Job Order 45400127 from 19 May 1972 to 19 November 1973. Mr. James C. Brodock (RBCT) was the RADC Project Engineer.

This volume is the Engineering Section of the User's Manual, containing descriptions of the program, its organization, analytic basis, operating principles, and logic flow. Volume II, the Usage Section of the User's Manual, contains instructions for preparing the input data, running the program and interpreting the resulting output. Volume III contains detailed descriptions of all subroutines, variables and constants used in the program. Volume IV contains complete FORTRAN source listings and detailed flow charts.

Contributions to this contract effort from Mrs. C.E. Clark, Mr. R.E. Plummer, Dr. C.D. Skouby, and Mr. G.L. Weinstock are gratefully acknowledged.

Information on these documents and on how to obtain a magnetic tape listing of the program may be obtained from Mr. Brodock, RADC/RBCT, Griffiss AFB, NY 13441.

This report has been reviewed by the RADC Information Office (OI) and is releasable to the National Technical Information Service (NTIS). At NTIS it will be available to the general public, including foreign nations.

This technical report has been reviewed and approved for publication.

APPROVED:



JAMES C. BRODOCK
Project Engineer

APPROVED:



JOSEPH J. NARESKY
Chief, Reliability and Compatibility Division

FOR THE COMMANDER:



CARLO P. CROCETTI
Chief, Plans Office

TABLE OF CONTENTS - Volume I

<u>Section</u>	<u>Title</u>	<u>Page</u>
1	INTRODUCTION & SUMMARY	15
1.1	Organization of Manual	15
1.2	Background	15
1.3	Purpose	16
1.4	Approach	16
1.5	Analysis Techniques	17
1.5.1	Data Organization	17
1.5.2	Basic Analysis Approach	17
1.5.3	Representation of Port Spectra	20
1.5.4	Maximum System Size	22
1.5.5	IEMCAP Logic Flow	22
1.6	Units Used in IEMCAP	25
1.7	Interface with EMC Engineer	25
2	SYSTEMS APPROACH	28
2.1	Definitions	28
2.1.1	Sample Frequency	28
2.1.2	Sample Frequency Interval	28
2.1.3	Spectrum Sample Point	28
2.1.4	Port	29
2.1.5	Source or Emitter	29
2.1.6	Receptor	29
2.1.7	Adjustment Limit	29
2.1.8	Initial Spectrum Displacement Factor	29
2.1.9	Required Spectrum	29
2.1.10	Non-Required Spectrum	30
2.1.11	Emitter Bandwidth and Receptor Bandwidth	30
2.1.12	Standard Instrument Bandwidth	30
2.1.13	Default	32
2.1.14	Harmonics	32
2.1.15	EMC Specifications	32
2.1.16	Backsearch	32
2.1.17	Broadband Spectrum	32
2.1.18	Narrowband Spectrum	33
2.1.19	Integrated EMI Margin	33
2.2	System Model	34
2.2.1	System Mathematical Basis	35
2.2.1.1	Point EMI Margin Calculations	37
2.2.1.2	Integrated Margin Calculations	41
2.2.2	Background for Computer Implementation of System Equations	45
2.2.2.1	Spectrum Quantization	45
2.2.2.2	Origin of Emission and Susceptibility Spectra	49
2.2.3	Programmed System Equations and Their Program Application	51
2.2.3.1	Emitter Adjustment	51
2.2.3.2	Receptor Adjustment	55

TABLE OF CONTENTS - Volume I (Continued)

<u>Section</u>	<u>Title</u>	<u>Page</u>
	2.2.3.3 Integrated EMI Margin Calculation	56
	2.2.3.4 Use of Integrated EMI Margin	59
3	PROGRAM OPERATION	61
3.1	IDIPR Routines	61
3.1.1	Input Decode Routine	61
3.1.2	Initial Processing Routine	64
3.1.3	Spectrum Model Routines	64
3.1.4	Wire Map Routine	65
3.2	TART Routines	65
3.2.1	Specification Generation Routine	68
3.2.2	Comparative EMI Analysis Routine	68
3.2.3	Coupling Model Routine	69
3.3	Data Files	69
3.3.1	Permanent Files	69
3.3.2	Working Files	70
3.3.3	Scratch Files	71
3.4	Restart Capability	71
4	INPUT DECODE AND INITIAL PROCESSING ROUTINE	73
4.1	Input Decode Routine (IPDCOD)	73
4.2	Initial Processing Routine (IPR)	75
4.3	Spectrum Model Routine (SPCMDL)	77
5	TASK ANALYSIS ROUTINE	85
5.1	Specification Generation Routine (SGR)	85
5.1.1	SGR Description	85
5.1.2	SGR Operation	86
5.1.2.1	Coupling Path Routine (COUPLE)	89
5.1.2.2	Emitter Margin Calculation and Spectrum Adjustment Routine (EMCASA)	94
5.1.2.3	Total Signal Calculation and Receptor Spectrum Adjustment	105
5.1.2.4	Integrated EMI Margin Computation	109
5.2	Comparative EMI Analysis Routine (CEAR)	109
5.2.1	CEAR Description	109
5.2.2	CEAR Operation	110
5.2.2.1	Baseline EMI Survey Analysis	110
5.2.2.2	Trade-off Analysis with Transfer Changes	110
5.2.2.3	Trade-off Analysis with Spectrum Changes Only	115
5.2.2.4	Specification Waiver Analysis	115

TABLE OF CONTENTS - Volume I (Continued)

<u>Section</u>	<u>Title</u>	<u>Page</u>
5.3	Transfer Model Routines	117
5.3.1	Antenna Coupled Transfer Function Evaluation Routine (ACTFER)	117
5.3.1.1	Antenna-to-Antenna	117
5.3.1.2	Antenna-to-Wire	117
5.3.2	Wire-to-Wire Transfer Function Routine (WTWIFR)	125
5.3.3	Case-to-Case Transfer Function Routine (CTCTFR)	139
5.3.4	Filter Routine (FILTER)	140
5.3.5	Environmental Field Routine (ENVIRN)	140
6	MODELS	144
6.1	Emitter Models	144
6.1.1	Power Spectrum of Binary Frequency-Shift Keying	144
6.1.2	Spectrum Model for Amplitude Modulation with Stochastic Process	149
6.1.3	Spectrum Model for Angle Modulation with Stochastic Process	150
6.1.4	Spectral Characteristics of Single Sideband Amplitude, Phase and Frequency Modulation with a Stochastic Process	152
6.1.5	A Simplified Model for Calculation of the Bounds on the Emission Spectra of Chirp Radars	156
6.1.6	PCM/AM - NRZ Model	160
6.1.7	Pulse Position Modulation	164
6.1.8	PCM/AM - Biphase	170
6.1.9	Spectral Analysis of PAM-FM Signal	174
6.1.10	Pulse Duration Modulation	184
6.1.11	Control and Signal Waveform Analysis	189
6.2	Receptor Modeling	202
6.3	Transfer Models	203
6.3.1	Filter Models	203
6.3.2	Simplified Theoretical Ground Wave Model	211
6.3.3	Antenna Model	215
6.3.4	Intravehicular Propagation Model	217
6.3.5	Field-to-Wire Compatibility Analysis	223
6.3.6	Wire-to-Wire Coupling	230
6.3.7	Case-to-Case Coupling	245
6.4	Programmed Formulas	246
6.4.1	Spectrum Models	246
6.4.1.1	RF Modulations	246
6.4.1.2	Signal/Control Modulations	270
6.4.1.3	Non-Required Emission and Susceptibility	283

TABLE OF CONTENTS - Volume I (Continued)

<u>Section</u>	<u>Title</u>	<u>Page</u>
6.4.2	Transfer Model Equations	289
6.4.2.1	Filter Models	289
6.4.2.2	Field Propagation Model	292
	6.4.2.2.1 Aircraft/Spacecraft Propagation Model	292
	6.4.2.2.2 Ground Propagation Model	297
6.4.2.3	Field-to-Wire (via Aperture)	299
6.4.2.4	Wire-to-Wire Coupling Model	301
6.4.2.5	Case-to-Case Coupling Model	309
	List of References	310
	Appendix A - Signals, Noise and Interference in a Linear Device	312

LIST OF FIGURES - Volume I

<u>Figure No.</u>	<u>Title</u>	<u>Page</u>
1	Port Termination Impedance Configuration	19
2	IEMCAP Functional Flow	23
3	IEMCAP Typical Task Flow	27
4	Standard Instrument Bandwidth	31
5	System Approach Identifies Arrays of Emitter and Receptor Ports with Coupling Paths	34
6	Broadband Integrated Margin Approach	42
7	Narrowband Integrated Margin Approach	44
8	Quantization of Spectra and Log-Linear Interpolation	47
9	Quantization of Received Power	49
10	Spectrum Sampling Accuracy Depends on Number of Assigned Frequencies	50
11	Emitter Adjustment to a Safety Margin Below Receptor Susceptibility	53
12	IDIPR Section of IEMCAP, Top Level Functional Flow	62
13	TART Section of IEMCAP, Top Level Functional Flow	66
14	Functional Flow of Input Decode Routine	74
15	Functional Flow, Initial Processing Routine	76
16	Spectrum Model Routine	79
17	Required Emitter Spectrum Models	83
18	Required Susceptibility Spectrum Models	84
19	Specification Generation Routine Functional Flow Diagram	87
20	COUPLE Subroutine	90
21	Emitter Margin Calculation and Spectrum Adjustment Routine Functional Flow	95

LIST OF FIGURES - Volume I (Continued)

<u>Figure No.</u>	<u>Title</u>	<u>Page</u>
22	Initial Emitter Spectrum Diagram	102
23	Adjustment of Emitter Point for Compatibility at E_2	103
24	Parallel Adjustment of Emitter Line Segment $E_2 - E_3$ for Compatibility at R_4	103
25	Rotation of Emitter Line Segment $E_2' - E_3'$	104
26	Receptor Signal and Spectrum Adjustment Routine Functional Flow Diagram	106
27	Comparative EMI Analysis Routine Functional Flow Diagram	111
28	Antenna-Coupled Transfer Function Evaluation Routine (ACTFER)	118
29	Field to Wire (FTW) Subroutine	124
30	Wire to Wire Transfer Routine (WTWTFR)	126
31	Case to Case Transfer Routine (CTCTFR)	139
32	Environmental Field Routine	141
33	Spectrum Envelope of Chirp Radar	157
34	Chirp Radar Algorithm	158
35	Autocorrelation Function of Total PPM Waveforms	167
36	Two Biphase States	170
37	Two Independent PDM Waveforms	185
38	Autocorrelation Function of Total PDM Waveform	186
39	Single Voltage Pulse	189
40	Pulse Train	191
41	Rectangular Pulse Train	194
42	Trapezoidal Pulse Train	195

LIST OF FIGURES - Volume I (Continued)

<u>Figure No.</u>	<u>Title</u>	<u>Page</u>
43	Triangular Pulse Train	196
44	Sawtooth Pulse Train	197
45	High-Frequency Exponential Pulse Train	198
46	Damped Sinusoid	200
47	Single Tuned Filter	204
48	Transformer Coupled Filter	206
49	Example of Third Order Butterworth Filter	208
50	Two-Ray Optics Representation (Ground Wave Model)	211
51	Gain Over Free Space vs. Distance	212
52	Maximum Plane Earth Distance vs. Frequency	214
53	Maximum Allowable Antenna Height vs. Frequency	214
54	Antenna Pattern Beam Angles	217
55	Model Used to Approximate Aircraft	218
56	Distance Between Two Antennas When One is Located Off Fuselage and a Portion of Path is Around Fuselage	220
57	Distance Between Two Antennas When Both are Off the Fuselage and Path is Around Fuselage	220
58	Typical Propagation Path With Wing Shading	221
59	Diffraction Coordinate System When Propagation Path is Around Wing Edge	223
60	Transmission Line Illuminated by Electromagnetic Field	224
61	Parallel Wires Over a Ground Plane	232
62	Circuit Representative of Capacitive Coupling Between Parallel Wires Over a Ground Plane	232
63	Shielded Emitter Wire Segment	234

LIST OF FIGURES - Volume I (Continued)

<u>Figure No.</u>	<u>Title</u>	<u>Page</u>
64	Circuit Representative of Inductive Coupling Between Parallel Wires Over a Ground Plane	237
65	Inductive Model for Unbalanced, Twisted Emitter Wire Pair	241
66	Inductive Model for Unbalanced, Twisted Receptor Wire Pair	242
67	Port Termination Impedance Configuration	244
68	CW	246
69	PDM/AM	247
70	PCM/AM - NRZ	248
71	PCM/AM - BIPHASE	249
72	PPM/AM	250
73	MORSE	252
74	FSK	254
75	PAM/FM	255
76	RADAR RECT	256
77	RADAR TRAP	257
78	RADAR COSINE-SQUARE	258
79	RADAR GAUSSIAN	259
80	CHIRP	261
81	AM-DSB	262
82	AM-DSB/SC	263
83	SSB-LOWER	264
84	SSB-UPPER	265
85	FM	266

LIST OF FIGURES - Volume I (Continued)

<u>Figure No.</u>	<u>Title</u>	<u>Page</u>
86	VOICE	267
87	CLIPPED VOICE	268
88	NON-VOICE	269
89	PDM	270
90	PCM - NRZ	271
91	PCM/AM - BIPHASE	272
92	PPM	273
93	MORSE	275
94	PAM	276
95	ESPIKE	277
96	RECTANGULAR	278
97	TRAPEZOIDAL	279
98	TRIANGULAR	280
99	SAWTOOTH	281
100	DAMPED SINUSOID	282
101	Model Used to Approximate Aircraft	293
102	Distance Between Two Antennas When One is Off Fuselage and a Portion of Path is Around Fuselage	295
103	Distance Between Two Antennas When Both Are Off Fuselage and the Path is Around Fuselage	295
104	Diffraction Coordinate System When Propagation Path is Around Wing Edge	297
105	Circuit Representative of Capacitive Coupling Between Parallel Wires Over a Ground Plane	302
106	Circuit Representative of Inductive Coupling Between Parallel Wires Over a Ground Plane	305

LIST OF FIGURES - Volume I (Continued)

<u>Figure No.</u>	<u>Title</u>	<u>Page</u>
107	Inductive Model for Unbalanced, Twisted Emitter Wire Pair	307
108	Inductive Model for Unbalanced, Twisted Receptor Wire Pair	308

LIST OF TABLES - Volume I

<u>Table No.</u>	<u>Title</u>	<u>Page</u>
1	Port Emission and Susceptibility Tests and Frequency Ranges	21
2	Maximum System Size	22
3	IEMCAP Spectrum Units Used Internally	33
4	Bandwidth Factor	40
5	Port Coupling Path Codes	93
6	Flow Symbols Used in Emitter Margin Calculation and Spectrum Adjustment Flow	99
7	Symbols Used in Receptor Spectrum Adjustment Flow	108
8	Flow Symbols in ACTFER Subroutine	123
9	Flow Symbols in FTW Subroutine	125
10	Flow Symbols in WTWTFR Subroutine	137
11	Flow Symbols in CTCTFR Subroutine	140
12	Math Flow Symbols in ENVIRN	142

Section 1

INTRODUCTION & SUMMARY

This manual describes the technical basis, operation, and usage of the Intrasytem Electromagnetic Compatibility Analysis Program (IEMCAP) developed for the Air Force by McDonnell Aircraft Company (MCAIR) under Contract Number F30602-72-C-0277. IEMCAP is a computerized analysis program which facilitates the engineering of cost-effective EMC into present and future weapons systems.

1.1 ORGANIZATION OF MANUAL

This manual and the IEMCAP Computer Program Documentation provide complete and thorough information on the program. This manual is divided into two volumes. Volume I, the Engineering Section, presents a complete discussion of the analytic basis, technical background, program organization, and program operation. It also describes the mathematical models used and the basic equations involved. Volume II, the Usage Section, describes procedures and formats for preparing the input data, executing the program, and interpreting the resulting computer output. An example test case is included to illustrate program use.

The IEMCAP Computer Program Documentation contains detailed descriptions of all subroutines, variables, and constants used in the program. It also presents the contents of all data storage files and storage arrays. Detailed flow charts and a complete program listing are included in supplements.

1.2 BACKGROUND

Performance of modern weapons systems is increasingly dependent upon the compatible functioning of electrical and electronic subsystems. The typical system of today includes numerous such subsystems with their associated interconnecting wires and, often, with large numbers of antennas for transmission and reception of required signals. The power and information signals occupy a wide range of the electromagnetic spectrum, resulting in the need for carefully designed control measures to confine them within the spatial, spectral, and temporal limits necessary to avoid disruptive interference. Electromagnetic Compatibility (EMC) assurance is thus increasingly an integral and crucial part of subsystem and system design engineering. Computerized EMC analysis, as provided by IEMCAP, is a needed tool for establishing and maintaining cost-effective interference control throughout the life time of a weapons system.

Methods presently available for specifying, monitoring, and controlling EMC of subsystems and systems involve the imposition of general purpose specifications and testing limits applicable to all equipment and system types. A system comprised of equipment meeting these general interference criteria is not necessarily an interference-free system. On the other hand, if EMC is achieved under these circumstances, many of the interference

safety margins in the end item may be far greater than necessary. This lack of correlation between equipment and total system EMC performance may adversely affect system economy. If the interference criteria are not stringent enough, fix efforts and schedule delays add significant cost penalties. The other extreme of overspecifying has the effect of driving upward equipment and subsystem costs and weights at the outset.

IEMCAP is a link between equipment and subsystem EMC performance and total system EMC characteristics. It provides the means for tailoring EMC requirements to the specific system, whether it be ground based, airborne, or a space/missile system. This is accomplished in IEMCAP by detailed modeling of the system elements and the various mechanisms of electromagnetic transfer among them to perform the following tasks:

- o Provide a data base which can be continually maintained and updated to follow system design changes.
- o Generate EMC specification limits tailored to the specific system.
- o Evaluate the impact of granting waivers to the tailored specifications.
- o Survey a system for incompatibilities.
- o Assess the effect of design changes on system EMC.
- o Provide comparative analysis results on which to base EMC trade-off decisions.

1.3 PURPOSE

The purpose of this contract was to develop a computerized analysis program to provide economical implementation of EMC at all stages of an Air Force system's life cycle, from conceptual studies of new systems to field modification of old systems. This capability is provided for ground, aircraft and space/missile systems. Further, the program should be capable of running on a wide variety of computers and can be run with reasonable efficiency.

1.4 APPROACH

IEMCAP incorporates state-of-the-art communications and EMC analysis math models into a routine which efficiently evaluates the spectra and the transfer modes of electromagnetic energy between generators and receptors within the system. Although a number of separate EMC computer programs and mathematical models had been developed, there remained the need to combine and augment them to obtain a unified, multi-purpose analysis tool.

IEMCAP combines these capabilities into a versatile framework which facilitates modification as the state-of-the-art progresses. This provides a flexibility in updating the program as new or improved mathematical models are developed, and it provides a program which may be easily applied to a

wide variety of EMC analysis and design problems by utilization of only the necessary modules for the specific problem.

The program is designed for use by an EMC systems engineer with a minimum of computer experience. The input data requirements, program control, and output formats are easily learned and engineering oriented. The input data is directly obtainable from system and subsystem operational specifications or measured data. For ease of use, all data input to IEMCAP is in free-field format. The entries may be placed anywhere on the punched cards.

To allow it to be run on a wide range of computers, the program is written in USA standard FORTRAN language. It also runs with approximately 67K (decimal) words of computer core memory.

1.5 ANALYSIS TECHNIQUES

1.5.1 Data Organization

Air Force systems of the types described above contain vast numbers of emitters and receptors of electromagnetic energy. There are a wide variety of types varying from antennas to wires to leakage through box cases. To organize these into a form convenient for collection and utilization by the user and the program, a hierarchy structure is defined. The system (aircraft, spacecraft, or ground) is divided into subsystems which are groups of equipments performing related tasks. For example, an aircraft system might have a navigation subsystem which is composed of several equipments such as a transmitter-receiver unit, a display unit, and a navigation computer. The physical boxes comprising the subsystem are defined as equipments, and electromagnetic energy may enter or leave these equipments via ports. Ports are designated as emitters or receptors (or both). An emitter port generates electromagnetic energy, and a receptor port is susceptible to electromagnetic energy. Ports within an equipment are assumed compatible with each other.

Ports may be intentional or unintentional. An example of an unintentional port is leakage into or out of an equipment case. An example of an intentional port is a connector pin through which AC power, signals, etc. are brought into or out of the equipment. Such ports are connected to wires or antennas.

1.5.2 Basic Analysis Approach

All intentional ports must generate and/or receive certain types of signals to perform their intended function. The signals or responses which are intentionally generated and coupled from port to port are called operationally required and cannot be altered without affecting system operation. In addition to the required signals, there may be additional undesired outputs and/or responses. These are called operationally non-required. For example, an emitter can have non-required outputs in the form of harmonics, and a receptor can have an undesired response in the form of an image response. It should be noted that unrequired

responses may be produced both by unrequired signals and/or by required signals which are unintentionally coupled to the wrong ports.

An incompatibility is said to exist when sufficient signal from an emitter port, or ports, is unintentionally coupled to a receptor port to exceed its susceptibility threshold. Required signals and responses, by definition, cannot be restricted by EMC specification. The non-required signals and responses are spurious and can be controlled; that is, limits can be set for them such that the system is compatible. These limits are called EMC specifications. Ideally, if all ports have no emissions and susceptibilities exceeding these limits, the system is compatible. An important task of IEMCAP is the generation of a set of specification limits tailored to the specific system under analysis.

The emissions and susceptibilities, both required and non-required, are represented in IEMCAP by spectra. For each emitter port, a two-component spectrum represents the power levels produced over the frequency range. The broadband component represents continuous emissions, which vary slowly with respect to frequency; while the narrowband component represents discrete emissions, which vary rapidly with respect to frequency. The broadband components are in units of power spectral density, and the narrowband are in units of power. Thus, each emitter can be considered to have two spectra: broadband and narrowband.

For each receptor, a spectrum represents the susceptibility threshold over the frequency range. The susceptibility level is defined as the minimum received signal which will produce a response at a given frequency.

For each intentional port, a portion of the frequency range is defined as the required range. All signals within this range are required and cannot be adjusted. Outside this range limits may be set for the maximum emission and minimum susceptibility levels. Within the required range, the spectrum is defined by a mathematical model of signal level versus frequency. This can be either from equations of the frequency domain representation of the signal or directly from a user-defined spectrum. Outside the required range, assumed levels are used for the port spectra. During specification generation, if these assumed spectrum levels cause interference, they are adjusted such that there is compatibility. By adjusting the spectra of emitters and receptors for compatibility, the maximum non-required emission and minimum susceptibility levels are obtained which will produce a compatible system. To prevent too stringent specifications from being generated, each spectrum has an adjustment limit.

While any values could be used for the initial non-required spectra, IEMCAP uses the limits of military EMC specifications MIL-STD-461A and MIL-I-6181D. The initial levels may be relaxed or tightened from these if desired. These specifications are used for a variety of reasons. First, they are widely used and most EMC engineers are familiar with them. Those portions of the port spectra not requiring adjustment remain at the usual specification levels. Also, if new equipments are added to a system

containing existing equipment developed and tested to these specifications, the IEMCAP-generated specifications will be at the same general levels and not require radical changes in EMC design. This also facilitates adapting an equipment from one system to another system.

The general approach in performing the various tasks is two-fold. First an emitter-receptor port pair is selected and their type, connection, wire routing, etc. are quickly examined to determine if a coupling path exists. If a path exists the received signal is computed at the receptor and compared to the susceptibility level. In addition to the emitter-receptor port pair analysis, the program also computes the total signal from all emitters coupled into each receptor acting simultaneously. Details of the two analyses are discussed in Section 2.2.

In determining the port spectra and in other phases of the analysis, the port termination impedance must be known. A wide variety of terminations can exist in the system, but for the most part they can be represented by a series resistor and inductor with a shunt capacitor, as illustrated in Figure 1. Various combinations can be specified by setting the appropriate component value to zero. However, at least one component must be non-zero.

Power transfer relationships in IEMCAP are normalized to a one ohm impedance. The actual port impedances that are input to the program are then used to appropriately transform these power relationships.

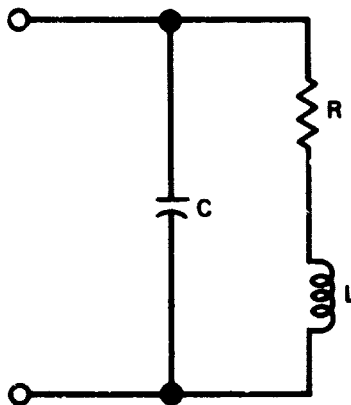


FIGURE 1
PORT TERMINATION IMPEDANCE CONFIGURATION

GP74 0267 105

1.5.3 Representation of Port Spectra

IEMCAP is required to analyze a large number of ports with reasonable run times and reasonable computer core memory requirements. At the same time, it must quickly evaluate the coupling from any type of emitter port into any type of receptor port and use this to perform the variety of tasks discussed in Section 1.1 above and be adaptable to future tasks. For specification generation, the spectra must be easily adjustable at the frequencies where incompatibilities are found as well as allow efficient incorporation of the adjustments for further adjustment. For trade-off and waiver analyses, the spectra and interference of modified ports must be efficiently compared to those from previous runs. Also, the spectra must be stored on files and readily used for future analyses.

In view of the above criteria, IEMCAP uses a sampled spectrum technique in which each spectrum amplitude is sampled at various frequencies across the range of interest. Considering the requirement of MIL-STD-461A of 3 frequencies per octave from 30 Hz to 18 GHz, this requires approximately 90 sample frequencies. This is reasonable resolution for EMC specifications in which limits of emission and susceptibilities are set and can apply over large regions of the spectrum. (If greater resolution is desired, IEMCAP allows the user to specify specific frequencies.) To avoid missing narrow peaks between sample frequencies, IEMCAP samples the spectrum in the interval half-way between the sample frequency and each of its neighboring sample frequencies. For emission spectra, the maximum in the interval is used, and for susceptibility spectra the minimum is used. This effectively quantizes the spectra with respect to the sample frequencies.

To minimize core memory and data file size requirements, a table of sample frequencies is defined for an equipment, and all spectra of ports within that equipment are quantized to them. This eliminates storing a table of sample frequencies for each port which, considering the maximum system size discussed in 1.5.4 below, saves 50,400 words of file storage plus the input/output time required to store and retrieve them. (For 90 frequencies and for 600 ports this requires 54,000 words just to store frequencies. Storing 90 frequencies for 40 equipments requires 3,600 words, saving 50,400 words.)

The equipment frequency tables can be defined using two options. First, the user may specify the upper and lower frequency limits, the maximum number of frequencies (up to 90), and the number of frequencies per octave. The program then generates a table of geometrically spaced frequencies within the specified limits. Optionally, the user may specify the upper and lower frequency limits, the maximum number of frequencies and a number of specific frequencies (up to the maximum number) of interest. The program then generates geometrically spaced frequencies to fill in the number of frequencies not specified. For example, if the maximum number of frequencies to be used is 90 and 10 are user specified, the program generates 80 geometrically spaced frequencies over the specified frequency range and inserts the 10 user frequencies at the appropriate places. (The number of frequencies per octave is ignored if the latter option is used.)

The range of frequencies covered by the analysis is controlled by the user. The program will accept any range from 30 Hz to 18 GHz, but, if desired, the user may concentrate all 90 frequencies over a smaller interval within this range.

Each port is categorized by function into one of six types, each type having its own sub-interval of frequencies within the overall frequency range. These sub-intervals, adapted from MIL-STD-461/462 ranges for the port function, are shown in Table 1. The non-required spectrum model routines will generate zero emission and susceptibility outside these sub-intervals.

Thus, IEMCAP represents the spectra as amplitudes within up to 90 contiguous intervals across the frequency range of interest quantized to the sample frequencies. This representation meets the above criteria and allows for flexibility and program efficiency. It also allows the program to be divided into two sections, each running in approximately 64 to 67K (decimal) of core memory. With this arrangement, the program is readily adaptable to a wide variety of computers; and machine-dependent techniques, such as overlaying, are not required. One section of the program contains the data management and spectrum model routines, and the other contains the analysis and transfer model routines. Each section is executed separately so that both are not in core at one time.

Table 1

PORT EMISSION AND SUSCEPTIBILITY TESTS AND FREQUENCY RANGES

PORT FUNCTION	EMITTER		RECEPTOR	
	MIL-STD-462 Test(s)	Freq Range (Hz)	MIL-STD-462 Test(s)	Freq Range (Hz)
RF	CE06	14K-18G	CS04	14K-18G
Power	CE02/03	30-50M	CS01/02	30-400M
Signal	CE02/04	30-1G	CS02/04	30-10G
Control	CE02/04	30-1G	CS02/04	30-10G
EED	—	—	CS02/04	30-10G
Eqpt Case	RE02	14K-10G	RS03/04	14K-10G

1.5.4 Maximum System Size

A typical aircraft, spacecraft, or ground system can contain thousands of ports. If every emitter port had to be analyzed in conjunction with every receptor port, the run time, core memory size, and file storage would be extremely large. Therefore, the maximum system size shown in Table 2 was established. For each equipment, the 15 ports include the case leakage, and, therefore, 14 intentional ports are allowed.

Table 2

MAXIMUM SYSTEM SIZE

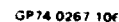
EQUIPMENTS	40
PORTS PER EQUIPMENT	15
TOTAL PORTS (40 x 15)	600
APERTURES	10
ANTENNAS	50
FILTERS	20
WIRE BUNDLES	10
SEGMENTS PER BUNDLE	10
WIRES PER BUNDLE	50

1.5.5 IEMCAP Logic Flow

As discussed above, IEMCAP is divided into two sections, and the basic flow through them is shown in Figure 2. These sections are executed independently with intermediate data storage on a number of disk or tape files known as working files. Depending on the analysis and the size of the system being analyzed, the program sections can be executed in succession or run separately. For small systems or a small number of updates, the first setup would probably be used. However, for a large system the first section can be run independently until data errors have been eliminated, at which time the second section would be run.

A brief description of the function performed by each program section is given below. These are described in detail in Sections 3, 4, and 5.

The first section of IEMCAP, called the Input Decode and Initial Processing Routine (IDIPR), is divided into three basic routines (Figure 2). The Input Decode Routine (IPDCOD) reads and decodes the free-field input



23

data from punched cards and checks the data for errors. If an error is found, a message is printed along with the card containing the error, and the program continues. If, after all cards have been processed, there were errors, the program normally stops. (The user can override this error stop if desired.)

If there are no input errors, the program proceeds into the Initial Processing Routine (IPR). This routine performs data management, interfaces with the spectrum models, and generates the working files. Data defining the system and all of its components is stored on a magnetic disk or tape called the Intrasystem File (also called the Intrasystem Signature File or ISF). This file is a data base which is maintained by IPR, incorporating changes in the system design. For a given run, the system to be analyzed can be defined from punched cards only, from a previously created ISF, or from an old ISF updated by cards. IPR assembles and merges the data to be analyzed and writes this data on a new ISF for future runs and on the working files for analysis. During this process IPR interfaces with the spectrum math model routines. These utilize the user-specified port spectrum parameters to compute the spectrum amplitudes quantized to the equipment sample table frequencies for each port. From IPR, the program enters the Wire Map Routine which generates cross-reference map arrays for use by the wire coupling math models during analysis. At this point, execution of IDIPR terminates. The computer can either stop or continue into the second section, depending on the job setup.

The second section of IEMCAP, called the Task Analysis Routine (TART), uses the data compiled by IDIPR to perform the desired analysis task. This is one of the four tasks summarized below:

- o Specification Generation - Adjusts the initial non-required emission and susceptibility spectra such that the system is compatible, where possible. The user-specified adjustment limit prevents too stringent adjustments. A summary of interference situations not controlled by EMC specifications is printed. The adjusted spectra are the maximum emission and minimum susceptibility specifications for use in EMC tests.
- o Baseline System EMC Survey - Surveys the system for interference. If the maximum of the EMI margins over the frequency range for a coupled emitter-receptor port pair exceeds the user-specified printout limit, a summary of the interference is printed. Total received signal into each receptor from all emitters is also printed.
- o Trade-off Analysis - Compares the interference for a modified system to that from a previous specification generation or survey run. The effect on interference of antenna changes, filter changes, spectrum parameter changes, wire changes, etc. can be assessed from this.

- o Specification Waiver Analysis - Shifts portions of specific port spectra as specified and compares the resulting interference to that from a previous specification generation or survey run. From this the effect of granting waivers for specific ports can be assessed.

TART is composed of two basic routines (Figure 2). The Specification Generation Routine (SGR) performs the first task above, and the Comparative EMI Analysis Routine (CEAR) performs the remaining three. These interface with the coupling math model routines to compute the transfer ratios between emitter and receptor ports.

1.6 UNITS USED IN IEMCAP

In general, IEMCAP employs rationalized Meter-Kilogram-Second (MKS) units internally for all quantities involved in program computations. Input and output data for the program are typically expressed in the more common engineering units, such as inches, feet, miles, etc. However, the program performs all unit conversions internally, both on input data and on output data.

1.7 INTERFACE WITH EMC ENGINEER

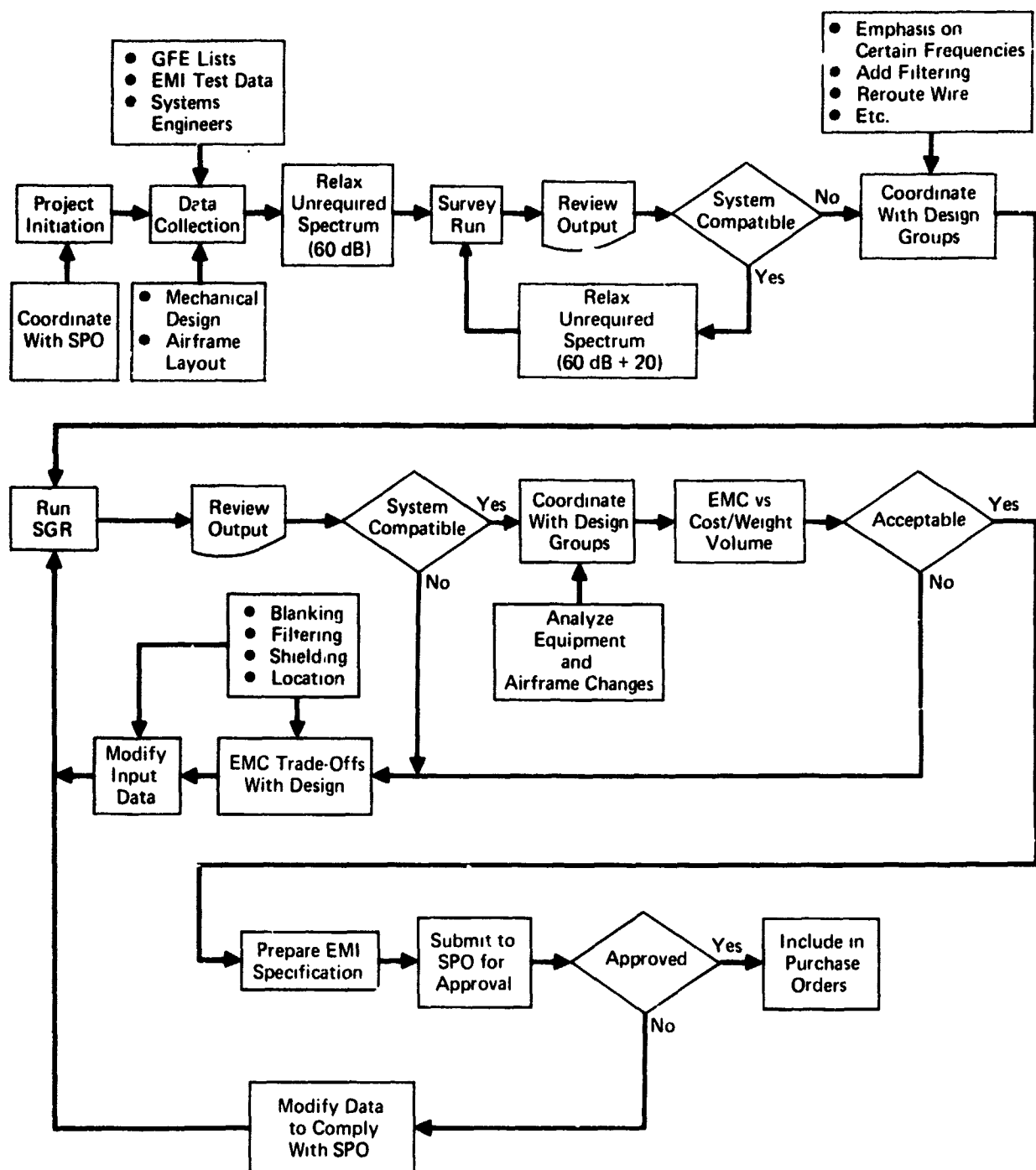
The program mechanization described in the preceding paragraphs has been designed to reserve the important decision-making to the using EMC engineer. He is provided good resolution of the spectral characteristics of his system by the program output and is, therefore, able to employ the best strategies he can devise to correct system deficiencies at minimum cost and with minimum weight penalties. Left to its own devices, a conceivable program could make these decisions arbitrarily and, in the process, impose unrealistic and costly specifications on many equipments in the system when, more than likely, treatment of only a few equipments would cure the problems that had emerged in the analysis.

An example of the inadvisability of programming all decision-making into the program is furnished by a particular test case analysis performed using IEMCAP. In this system, an integrated EMI margin turned out to be +38 dB. This startlingly high level of power above receptor susceptibility could be interpreted by the computer program as a signal and drive all emitter spectra downward by some rule which could, in some instances, result in excessive requirements. The EMC engineer would, on the other hand, recognize that the +38 dB figure had resulted, in large part, from the fact that his input data had specified a tunable transmitter as though its narrowband transmissions were occurring in each of its assignable 1500 channels simultaneously. Thus, he would see that some 32 dB ($10 \log 1500$) of the seeming catastrophic interference would not be present in the real world. He would proceed either to modify his input data, or otherwise, to interpret the integrated EMI margin figure in the appropriate manner so as not to unduly penalize (overspecify) his system elements.

Having the program automatically correct for tunable transmitters, such as the one above, could cause gross errors. The tunable portion of the emitter spectrum can fall in an insensitive range of the receptor spectrum where no interference results, but a possible spurious emission in the sensitive portion could cause interference. "Correcting" the integrated margin for the tunable portion of the emitter which caused negligible interference would falsely reduce the interference from the non-tunable spur. The engineer must use this in his interpretation of the program outputs.

Early in the development of the IEMCAP system approach, it was concluded that the program could not be designed to be a substitute for the strategies of the competent EMC engineer for all system situations and still achieve the cost-saving objectives that prompted its development. The program was accordingly designed to maximize the benefits obtainable from computerized specification generation on new systems and equipments whose spectral characteristics are largely unknown in advance. A typical task flow is shown in Figure 3. As shown, the strategy employed by the engineer for this new system using IEMCAP is to initially relax the non-required spectrum requirements of the baseline MIL-STD-461 by a considerable amount in the program input. Then he performs a computer run to see how the system holds up under these "noisy" conditions. Interference occurring in this initial run will cause automatic adjustments, resulting in a set of interference limits that, hopefully, are an improvement over the stringent MIL-SPEC requirements. Instances of large interference will be evident in the program output and these are then amenable to the application of engineering judgement in their treatment during the next run through the program.

To successfully implement this program the EMC engineer must work closely with, and have the confidence of the project systems engineers. If the EMC engineer just runs IEMCAP and gives the final adjusted specification numbers to the design groups, generally, the specifications will not be optimum for cost. The system design engineer must be involved in the trade-offs made during specification generation. For example, it may be easier to adjust a receptor than an emitter, to increase the transfer loss by moving a wire from one bundle to another, to add a discrimination capability to software, to add blanking, to reassign frequencies, to "live" with the EMI, etc.



GP74 0267 107

FIGURE 3
IEMCAP TYPICAL TASK FLOW
(INITIAL SPECIFICATION GENERATION)

Section 2

SYSTEMS APPROACH

2.1 DEFINITIONS

The ensuing descriptions of the systems model use numerous expressions. The following definitions are provided for clarification. These definitions are presented here as concisely as possible and are discussed in greater detail in other sections of this document.

2.1.1 Sample Frequency

The spectrum of any emitter or receptor is sampled at N frequencies stored in a table at the equipment level. N is user specified and must be large enough for at least one frequency per octave over the user specified frequency range but not greater than 90. These frequencies may be positioned anywhere between 30 Hz and 18 GHz (or any other frequency range within this region as specified by the user). The user should specify those frequencies to model spectrum regions of interest such as a receiver response function. The remainder of the N frequencies that the user does not specify are automatically generated by the program and are geometrically spaced.

Presently, the program has a maximum of 90 frequencies per equipment. Ninety (90) was chosen because it allows three frequencies per octave from 30 Hz to 18 GHz as required by MIL-STD-461/462. It also is a practical limit considering accuracy, computer core requirements and running time.

2.1.2 Sample Frequency Interval

To include all peak emissions and responses, the sampled spectrum is examined in the interval half way between the sample frequency and the next lower and higher sample frequencies. At the lowest frequency, the interval extends below it by half the interval from the first to the second frequency but not below zero. Similarly, at the highest frequency, the interval is extended above it by half the amount to the next lower frequency. For example, assume sample frequencies of 2 MHz, 4 MHz, 8 MHz and 16 MHz. The sample intervals are:

2 MHz	(1 MHz to 3 MHz)
4 MHz	(3 MHz to 6 MHz)
8 MHz	(6 MHz to 12 MHz)
16 MHz	(12 MHz to 20 MHz)

2.1.3 Spectrum Sample Point

Each emission and susceptibility spectrum is stored at the port level as a table of amplitudes at the sample frequencies. The program generates these tables from the user defined parameters in conjunction with the spectrum mathematical models. To ensure that all peaks are included, the maximum amplitude in the sample frequency interval is used for emitters and the minimum is used for receptors. Each such amplitude and its

corresponding frequency defines a spectrum sample point. Once these points are established, the program computes the amplitudes between them by log-linear interpolation. The methods used to establish the sample point amplitude are discussed in Section 2.2.

2.1.4 Port

A port is a point of entry or exit of electromagnetic energy from an equipment or device. Ports are either receptors, emitters or both. Typical ports would be connector pins, coax connectors, and equipment cases. Each port is classified by function as RF, power, signal, control, EED or leakage through the equipment case.

2.1.5 Source or Emitter

Source and emitter are used interchangeably throughout this report in the text and program flowcharts. This refers to a port which generates electromagnetic energy.

2.1.6 Receptor

This is a port that receives electromagnetic energy.

2.1.7 Adjustment Limit (adjlim)

The adjustment limit is a user specified parameter and is the maximum amount to which the non-required spectrum of an emitter or receptor can be adjusted. It is specified at the port level as part of the source and/or receptor spectrum data.

2.1.8 Initial Spectrum Displacement Factor (sdfs and sdfr)

The spectrum displacement factor for sources (sdfs) and receptors (sdfr) is a user-defined number, in dB, that deliberately loosens or tightens the Military Specification EMI limits used as a starting point in generating specifications with IEMCAP. This is specified at the port level.

2.1.9 Required Spectrum

This is the portion of a port spectrum required for operation. A receptor may have a certain required sensitivity within some frequency range, and an emitter may have a required output within a certain range. The required spectrum is not adjusted during specification generation. The user can specify up to ten (10) specific amplitudes and frequencies for the required spectrum of each port. Alternatively, the time domain parameters describing the required signal may be specified, and the spectrum is generated by the appropriate math model.

2.1.10 Non-Required Spectrum

This includes the portion of an emitter or receptor spectrum other than the required portion described above. This non-required spectrum may be adjusted (to a user defined limit) during specification generation by increasing or decreasing the initial amplitudes by the required amount.

2.1.11 Emitter Bandwidth and Receptor Bandwidth

To compute the received signal from a broadband emitter, the bandwidth of the receptor must be used. Within their required frequency ranges, emitters and receptors have known bandwidths which are used in the program. In the non-required ranges, the program uses a set of standard instrument bandwidths (defined below) to characterize the amount of power seen by the receptor from the broadband emitter. Since the bandwidths are unknown, the bandwidths used to establish the military specification levels are used.

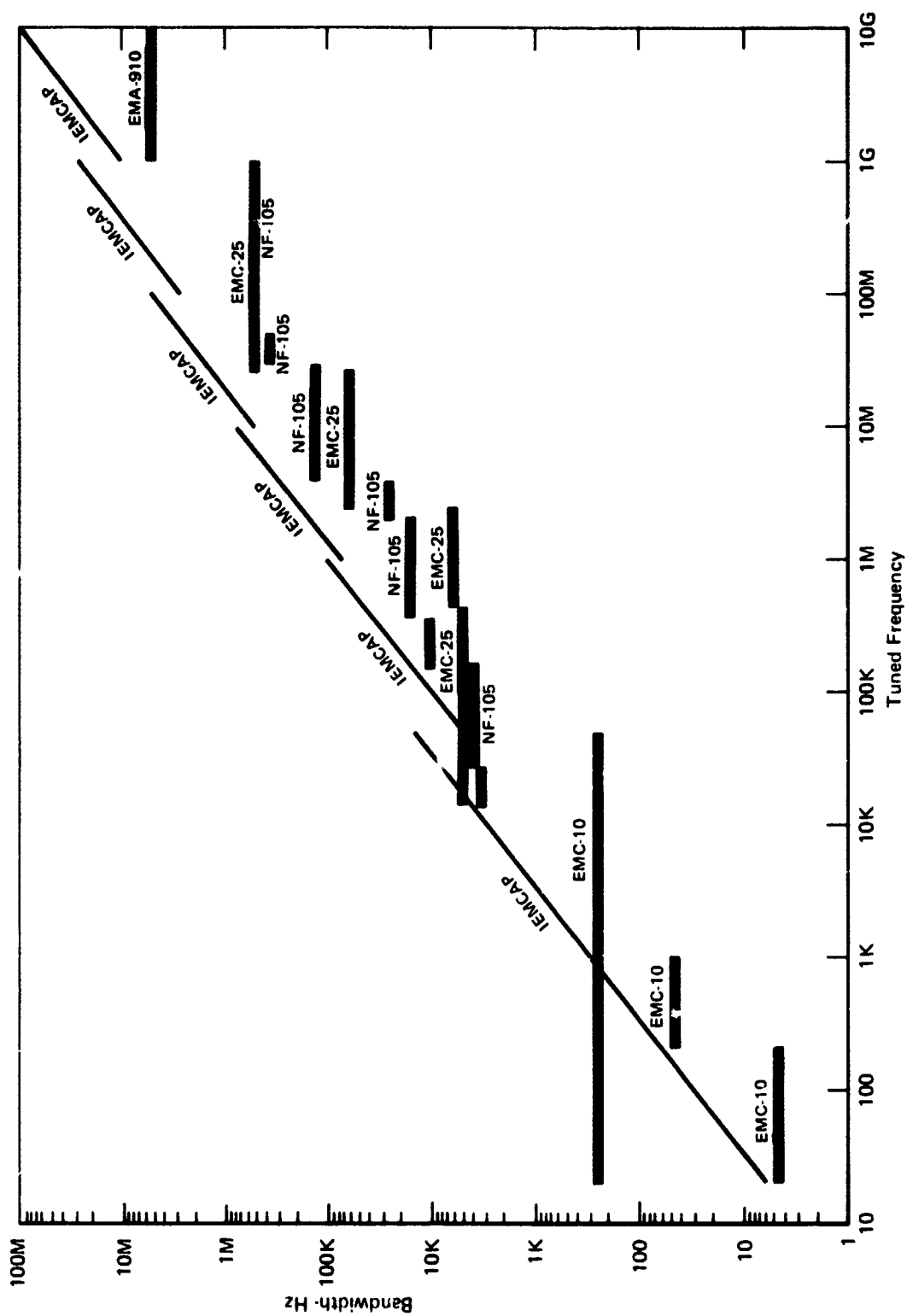
2.1.12 Standard Instrument Bandwidth

This is the maximum bandwidth of the test instrument used to establish and measure the non-required broadband emission spectra. It is defined as follows:

$B_{std} = 30\% f_o$	$30 \text{ Hz} < f_o \leq 50 \text{ KHz}$
$10\% f_o$	$50 \text{ KHz} < f_o \leq 1 \text{ MHz}$
$7\% f_o$	$1 \text{ MHz} < f_o \leq 10 \text{ MHz}$
$5\% f_o$	$10 \text{ MHz} < f_o \leq 100 \text{ MHz}$
$2.5\% f_o$	$100 \text{ MHz} < f_o \leq 1 \text{ GHz}$
$1\% f_o$	$1 \text{ GHz} < f_o \leq 18 \text{ GHz}$

where f_o is the tuned frequency of interest. B_{std} is plotted in Figure 4 along with the bandwidths of many commonly used EMC test receivers. As shown, these instruments all have bandwidths less than B_{std} . When used in conjunction with the non-required broadband spectra, it represents the maximum power detected by the measuring device if the emitter were producing noise at the specification level.

The power received by a given receptor from broadband signals depends on the receptor bandwidth. Within the receptor required frequency range the receptor bandwidth is known and can be used. In the non-required range, the bandwidth is not known since, by definition, it is the non-required region of the spectrum which specification generation determines. Therefore, the standard instrumentation bandwidth, from which the emitter broadband non-required levels are established, is used. That is, where the receptor bandwidth is unknown and the emission is non-required, the standard bandwidth is used to determine the power received.



GP14 0267 108

FIGURE 4 STANDARD INSTRUMENT BANDWIDTH

2.1.13 Default

A default is a value or option automatically assigned to an input parameter if not supplied by the user. An example of a default is the computation of an aircraft fuselage radius from the wing root if the radius is not specified. Also, unless otherwise specified, the equipment frequency table will contain 89 frequencies from 30 Hz to 18 GHz spaced 3 per octave.

2.1.14 Harmonics

Harmonics are spurious emissions from RF ports which are at integral multiples of the fundamental frequencies. The second harmonic is at twice the fundamental, the third is at three times, etc. The amplitudes at the harmonics are specified in dB relative to the fundamental amplitude. These override the MIL-STD-461A or MIL-I-6181D levels normally used in the non-required frequency ranges.

2.1.15 EMC Specifications

These are curves representing the maximum emission and minimum susceptibility non-required levels for emitters and receptors, respectively, such that the system is compatible over the entire frequency range of interest. The specification limits generated by this program use MIL-STD-461 or MIL-I-6181D as a basis. A suggested specification document using program generated limits and a sample test procedure are presented in Appendix A of Volume II of this manual.

2.1.16 Back-Search

This term applies to a procedure used in the Emitter Margin Calculation and Spectrum Adjustment Routine in TART during the emitter spectrum adjustment phase of specification generation. Since emitter and receptor table frequencies will not necessarily coincide, after adjusting a given emitter spectrum amplitude for compatibility, the routine searches back through the receptor frequencies between the present emitter frequency and the previous one. If incompatibilities are found at the intervening receptor frequencies, the emitter amplitudes on either side are further adjusted for compatibility. This process is discussed in detail in Section 5.1.2.2.

2.1.17 Broadband Spectrum

The broadband spectrum is a power spectral density (the power per unit frequency) which is slowly varying with respect to the bandwidth of the measuring device. The power received is equal to the broadband level times the minimum of the emission and receiver bandwidths. The units used internally by IEMCAP for these spectra are given in Table 3.

2.1.18 Narrowband Spectrum

The narrowband spectrum represents discrete power, in that a given quantity of power is concentrated all at a discrete frequency. Physically there is always a finite bandwidth, but when this bandwidth is much smaller than the bandwidth of the receiving device, the power appears to be concentrated at one frequency, and the power received is independent of the bandwidth of the receiver. The internal units are shown in Table 3.

TABLE 3

IEMCAP SPECTRUM UNITS USED INTERNALLY

Spectrum Type	Radiated (Equipment Cases)	Conducted (All Other Ports)
Broadband Emission	dB rel 1 $\mu\text{V}/\text{m}/\text{MHz}$	dB rel 1 $\mu\text{A}/\text{MHz}$
Narrowband Emission	dB rel 1 $\mu\text{V}/\text{m}$	dB rel 1 μA
Susceptibility	dB rel 1 $\mu\text{V}/\text{m}$	dB rel 1 μA

2.1.19 Integrated EMI Margin

The integrated EMI margin is an overall figure of merit representing the ratio of the power received by the receptor to susceptibility over the entire frequency range. The program computes the margin per bandwidth at all spectrum sample frequencies (both emitter and receptor). For broadband emissions, the received signal is the power contained in one receptor bandwidth, as defined in 2.1.11. This level is compared to the power required to produce a response in the receptor at the sample frequency. This ratio per bandwidth is integrated over the range of frequencies to obtain the broadband component of the integrated margin.

For narrowband emissions, the power received is independent of the receptor bandwidth, and the integral becomes a summation. The narrowband signal can be represented by one delta function in the center of the receptor bandwidth. The narrowband spectra are limits in that no single delta function can exceed the specified level. If a measuring instrument is connected to this port and tuned across the band, the program assumes that the instrument reads exactly this specification level everywhere. This is equivalent to having one delta function per instrument bandwidth across the band with amplitudes at the spectrum level. These narrowband levels are assumed to vary linearly from sample point to sample point for the summation. The integrated margin is the sum of the broadband and narrowband components.

2.2 SYSTEM MODEL

The system model for IEMCAP employs the standard EMC approach of identifying all ports in the system having potential for undesired signal coupling. These ports are divided into arrays of emitter ports and of receptor ports having identifiable coupling paths. A simplified diagram of this approach is given in Figure 5 where each element of an array of N_S emitters is considered to have a coupling path to one or more elements of an array of I_R receptors. In this simplified diagram only three coupling paths are shown, illustrating the general idea that more than one emitter can couple to a given receptor and further illustrating that a given emitter can couple to more than one receptor.

All emitters in a system are characterized by emission spectra and all receptors are characterized by susceptibility spectra. All ports and coupling media are assumed to have linear characteristics. Emissions from the various emitter ports are assumed to be statistically independent so that signals from several emitters impinging at a receptor port combine on an RMS or power basis.

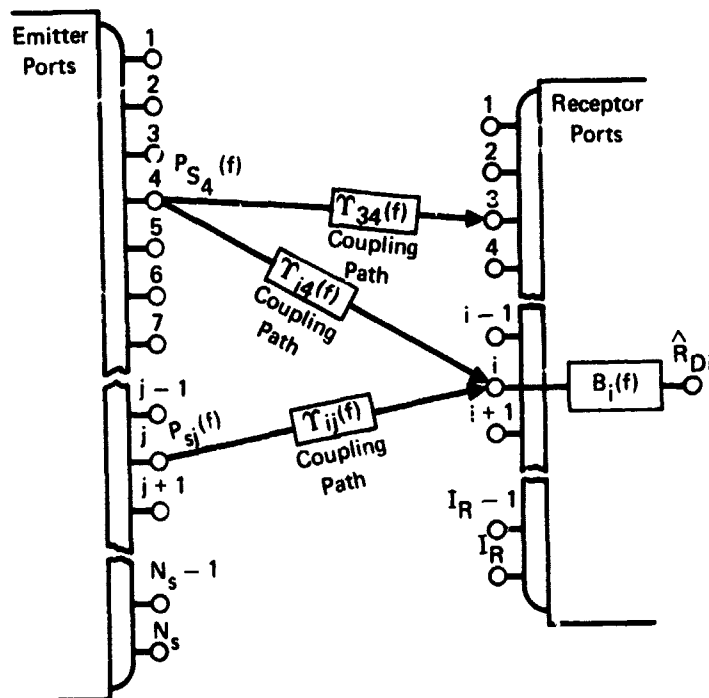


FIGURE 5
SYSTEM APPROACH IDENTIFIES ARRAYS OF EMITTER
AND RECEPTOR PORTS WITH COUPLING PATHS

The function of IEMCAP is to determine, by analysis, whether signals from one or more emitters entering a receptor port cause interference with the required operation of that receptor. Electromagnetic interference (EMI) is assessed in the program by computation of an "EMI Margin" for each receptor port. This EMI Margin is just the ratio of power received at a receptor port to that receptor's susceptibility. Actually, the program computes the margin in decibels; the more positive the number in decibels the greater is the interference while the more negative the number in decibels the greater is the compatibility.

The program performs the interference analyses by exercising various programmed formulas corresponding to mathematical models of emitters, of receptors, of the signal transfer mechanisms between emitters and receptors and of the system. The mathematical models of emitters and receptors in the program correspond to the required portion of their spectra. The program also contains routines to compute the non-required spectra of emitters and receptors. These non-required spectra are initially based on the interference curves of MIL-STD-461 and MIL-I-6181, displaced in level as specified by the user.

The discussion in the paragraphs immediately following is a development of the system mathematical model employed in IEMCAP. This mathematical formulation brings together all of the emitter, receptor and transfer models into a single linear system model. The discussion initially treats spectra and transfer mechanisms as continuous functions to aid understanding of the system concept. Subsequently, quantized versions of these functional relationships, required for their implementation on a digital computer, are developed.

2.2.1 System Mathematical Basis

The basis for all calculations performed by each of the functions of IEMCAP is the linear relationship for power coupled from an emitter, through a transfer medium, and received by a receptor. The general communication theory equation relating power spectral density at the detector of a receptor to power spectral density present at an emitter's output port is expressed as follows:

$$\text{o.p.s.d.} = \eta_{sj}(f) T_{ij}(f) \beta_i(f) \quad (1)$$

where

o.p.s.d. = output power spectral density (in watts/Hz) received by receptor i (at its detector) from emitter j,

$\eta_{sj}(f)$ = output power spectral density (in watts/Hz) at the terminals of source j (including cw power as delta functions),

$T_{ij}(f)$ = power transfer function of the coupling medium between source j and receptor i,

$\beta_1(f)$ = receptor response function relating power at the detector to power at the input terminals.

The broadband and narrowband components of the received power spectral density may be computed separately by considering the broadband and narrowband components of the output power spectral density of the source j . Thus, the power spectral density of source j is expressed as:

$$\eta_{Sj}(f) = \eta_{SNj}(f) + \eta_{SBj}(f) \quad (2)$$

where

$\eta_{SBj}(f)$ = the broadband power spectral density of source j

and

$\eta_{SNj}(f)$ = narrowband power spectral density of source j (composed of delta functions at the frequencies of the cw signals.)

Using Equation (2), Equation (1) can be written as follows:

$$\text{o.p.s.d.} = \eta_{SNj}(f) T_{ij}(f) \beta_1(f) + \eta_{SBj}(f) T_{ij}(f) \beta_1(f) \quad (3)$$

Since the narrowband power spectral density is composed of delta functions, η_{SNj} is accordingly expressed as

$$\eta_{SNj}(f) = \left[\sum_{t=1}^M P_t \delta(f - f_t) \right]_j \quad (4)$$

where

\hat{P}_t = the power, in watts, contained in the narrowband signal at frequency f_t ,

$\delta(x)$ = the Dirac delta function,

and

M = the total number of narrowband signals present in the frequency range being considered.

Using the expression, (4), for narrowband spectral density, Equation (3) is now written:

$$\text{o.p.s.d.} = \left[\sum_{t=1}^M \hat{P}_t \delta(f - f_t) \right]_j T_{ij}(f) \beta_1(f) + \eta_{SBj}(f) T_{ij}(f) \beta_1(f) \quad (5)$$

Received power, in watts, at the receptor's detector is obtained by integrating Equation (5) over a frequency range of interest. This integration is formally written as follows:

$$\begin{aligned} \hat{P}_{Dij} = & \int_{f_a}^{f_b} \left[\sum_{t=1}^M \hat{P}_t \delta(f - f_t) \right]_j T_{ij}(f) \beta_i(f) df \\ & + \int_{f_a}^{f_b} \eta_{SBj}(f) T_{ij}(f) \beta_i(f) df \end{aligned} \quad (6)$$

where

\hat{P}_{Dij} = the power, in watts, at the detector of receptor i due to all emissions from source j,

f_a = the lower frequency in the range of interest,

f_b = the higher frequency in the range of interest.

Evaluation of the integrals in Equation (6) is carried out in IEMCAP through the use of approximations since, as will be clear, the program contains information on spectra at a finite number of discrete frequency points. The program determines compatibility by computing two types of EMI margins: 1) point margins and 2) integrated margins. The approximations used in these two types of margin calculation, while different, are closely related.

2.2.1.1 Point EMI Margin Calculations

The point EMI margins are determined by computing the ratio of power incident at a receptor's input terminal to the susceptibility power level of the receptor. Since emitters normally require separate specifications on broadband and narrowband emissions, the program computes separate broadband and narrowband margins. The narrowband margin calculation is developed first in the following. The first task in this development will be to show the equivalence between the margin calculated at the receptor's detector and the margin calculated at the receptor's input terminal.

Confine attention first of all to the narrowband term in Equation (6) and define a narrowband power spectral density at a point frequency, f_p , incident at the filter input terminals as follows:

$$\bar{P}_{pj} \delta(f - f_p) = \hat{P}_{pj} \delta(f - f_p) T_{ij}(f_p) \quad (7)$$

That is, the power spectral density at the filter input terminals is obtained as the product of the transfer function between emitter and receptor with the narrowband power spectral density at the terminals of the source j at frequency f_p .

Using (6), the p^{th} component of the detector narrowband received power is

$$(\hat{P}_{Dij})_{NBp} = \int_{f_a}^{f_b} \bar{P}_{pj} \delta(f-f_p) \beta_i(f) df \quad (8)$$

Carrying out the indicated integration over frequencies in (8) gives

$$(\hat{P}_{Dij})_{NBp} = \bar{P}_{pj} \beta_i(f_p) \quad (9)$$

Thus, the output power of the filter is equal to the product of the input power of the p^{th} narrowband signal with the power transfer function of the filter evaluated at $f = f_p$. If this output signal power exceeds the detector threshold power or "standard response"* power level of K_i watts, then an interference situation results. An appropriate definition of narrowband point margin is, accordingly:

$$\hat{M}_{NB} = (\hat{P}_{Dij})_{NBp} / K_i \quad (10)$$

This EMI Margin is evaluated by comparing interference signal power at the device detector with the detector standard response. A more convenient measure of EMI margin for the IEMCAP program is to compare the interference signal power at the filter input terminals to the input susceptibility power level for the device defined as follows:

$$\hat{K}_i = \hat{S}_i(f_p) \beta_i(f_p) \quad (11)$$

Equation (11) is a definition of that input power level (susceptibility), $\hat{S}_i(f_p)$ which, when transformed through the filter, just produces a response at the threshold of the detector. Because of the linearity of the filter, the transfer function, $\beta_i(f_p)$, may be eliminated between Equations (9) and (11) with the result

$$\hat{M}_{NB} = \frac{(\hat{P}_{Dij})_{NBp}}{\hat{K}_i} = \frac{\bar{P}_{pj}}{\hat{S}_i(f_p)} \quad (12)$$

That is, a narrowband EMI Margin, defined in Equation (10), in terms of detector signal power and detector standard response, is equivalently given in Equation (12) in terms of input terminal narrowband power and an input terminal susceptibility power level. In IEMCAP all EMI Margins are

* See Appendix A for a discussion of "standard response" and for guidelines for its determination and utilization.

computed in terms of input terminal interference power levels and input terminal susceptibility.

Next consider Equation (6) for the broadband input from the j th source to the i th receptor:

$$(\hat{P}_{Di j})_{BB} = \int_{f_a}^{f_b} \eta_{SBj}(f) T_{ij}(f) \beta_i(f) df \quad (13)$$

Now, define a power spectral density due to source j as seen at the terminals of receptor i :

$$\bar{\eta}_{SBj}(f) = \eta_{SBj}(f) T_{ij}(f) \quad (14)$$

Then, Equation (13) becomes

$$(\hat{P}_{Di j})_{BB} = \int_{f_a}^{f_b} \bar{\eta}_{SBj}(f) \beta_i(f) df \quad (15)$$

Equation (15) is of the form of a linear filter response (output power) to a broadband power spectral density input, $\bar{\eta}_{SBj}(f)$. Subsequent theoretical descriptions of EMI margin calculations will be based on the linear filter response to power at its terminals and will utilize the transformation concept of Equation (15).

Equation (11), given previously as the relationship between the standard response of a receptor to its susceptibility power level for narrowband signals, can be used to eliminate $\beta_i(f)$ in equation (15) by writing the expression as follows:

$$\hat{K}_i = \hat{S}_i(f) \beta_i(f) \quad (16)$$

Then, Equation (15) is written, using Equation (16), as

$$(\hat{P}_{Di j})_{BB} = \int_{f_a}^{f_b} \frac{\bar{\eta}_{SBj}(f) \hat{K}_i}{\hat{S}_i(f)} df \quad (17)$$

Then, the broadband point margin evaluated at the receptor's detector is evidently obtained by dividing both sides of Equation (17) by the constant power level, \hat{K}_i , as follows:

$$\hat{M}_{BB} = \frac{(\hat{P}_{Dij})_{BB}}{\hat{K}_i} = \int_{f_a}^{f_b} \frac{\bar{\eta}_{SBj}(f)}{\hat{S}_i(f)} df \quad (18)$$

The broadband point margin (i.e. margin at a single frequency point f_p) is evaluated by an approximate solution of the integral of Equation (18). The approximation consists of assuming that the input power spectral density, $\bar{\eta}_{SBj}$ and the receptor susceptibility, $\hat{S}_i(f)$, are both constant over an interval of integration centered on the frequency point of interest. In particular, it is assumed that the interval of integration, $f_b - f_a$, is identical to a bandwidth factor, B , whose value is chosen in the program according to the rules set forth in Table 4. In non-required regions the bandwidth factor used is representative of the bandwidth of laboratory instruments. If a required region is involved, the choice of bandwidth factor is logical as is apparent in the table. Using the approximations and assumptions just described the integral of Equation (18) reduces to a simple product as follows:

$$\hat{M}_{Bij} = \bar{\eta}_{SBj}(f_p) B / \hat{S}_i(f_p) = \hat{P}_{TBij}(f_p) / \hat{S}_i(f_p) \quad (19)$$

where

$\hat{P}_{TBij}(f_p) = \bar{\eta}_{SBj}(f) B$ = the piecewise constant power at the i^{th} receptor terminals computed from the product of the input power spectral density of emitter j with the bandwidth factor associated with frequency f_p .

and

$\hat{S}_i(f_p)$ = piecewise constant susceptibility of the i^{th} receptor at frequency f_p .

TABLE 4
BANDWIDTH FACTOR

EMITTER	RECEPTOR	BANDWIDTH
Required	Required	Min (B_{emit} , B_{rec})
Required	Unrequired	Min (B_{emit} , B_{std})
Unrequired	Required	B_{rec}
Unrequired	Unrequired	B_{std}

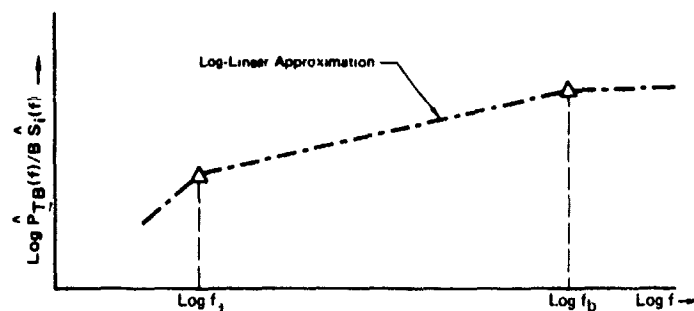
Note that the input power spectral density need not be constant over the bandwidth for Equation (19) to hold; real measuring instruments and receptor devices, characterized by the bandwidth factor, B , will effectively integrate the power spectrum over that bandwidth yielding a power response that is equivalent to the product of the bandwidth with the mean value of the power spectral density. The receptor susceptibility will similarly be measured as a constant level within the measuring instrument bandwidth.

Use of the Point Margins - The point margins calculated in the program for a single emitter coupled to a receptor are used in the Specification Generation Routine (SGR) portion of IEMCAP to gauge the amount of adjustment needed, if any, of the emitter for compatibility with the receptor at each of several points across the frequency range common to the two devices. This is done separately for narrowband and broadband emissions, as mentioned previously, with the objective of generating separate narrowband and broadband emission specifications for the emitter. The details of these emitter adjustments will be elaborated in later sections of the report. Subsequent sections will also bring out in considerable detail the calculation of a third point margin required in the program to determine the adjustments needed for a receptor when considering the total signal present at each receptor point frequency from the entire array of emitters coupling to the receptor. This total signal point margin calculation combines narrowband and broadband signals and results in the generation of a single susceptibility specification for the receptor in SGR. Evident is the fact that the frequency intervals, over which power quantities are considered piecewise constant, need not be contiguous or non-overlapping for the point margin calculations.

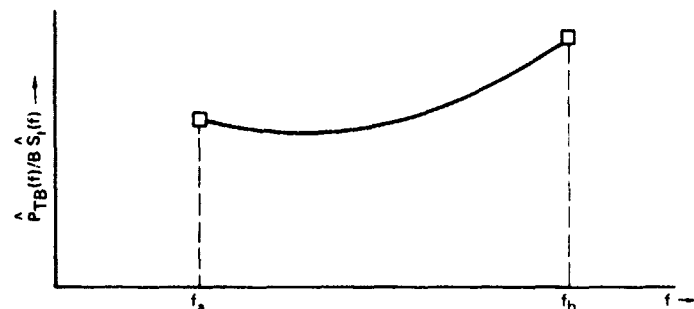
2.2.1.2 Integrated Margin Calculations

Integrated EMI margins applicable across enlarged frequency intervals are now derived by extension of Equations (8) and (18). The concept of "margin density" will be defined and utilized in the derivation of the integrated margin expressions. The integrand of the expression in Equation (18) is recognized to be of the form of a "margin density" although it was not previously identified as such. The idea of margin density is readily understood for broadband signals where the ratio of input power spectral density, in watts per Hertz, to the receptor susceptibility, in watts, has units of a dimensionless power ratio (a "margin") per Hertz.

Broadband Integrated Margin - The approach taken in the program for broadband integrated margin calculations is illustrated by the diagram of Figure 6. Shown in the figure are the logarithmic values of the broadband point margins previously calculated, using Equation (19), at two successive frequency points, modified by subtracting the logarithm of the bandwidth factor, B , applicable at each frequency point. Subtracting the logarithm of bandwidth from the logarithm of the point margin corresponds, of course, to dividing the piecewise constant power ratio of Equation (19) by the bandwidth factor. The result of this operation on the point margins is to convert them to piecewise constant logarithmic "margin densities". The program converts these piecewise constant logarithmic margin densities to piecewise log-linear margin density functions by straight-line connection of the point margin densities



a) Log-Linear Approximation of Broadband Margin Function



b) Broadband Margin Density Function Derived from Log-Linear Margin Function

FIGURE 6

BROADBAND INTEGRATED MARGIN APPROACH

in log-log coordinates. This operation is illustrated in Figure 6(a) by the straight segmented line connecting the point values between the two successive frequency points labeled f_a and f_b in the figure. Worth noting is the fact that the frequency interval, $f_b - f_a$, involved in this discussion differs from the interval involved in Equation (18) and is typically only a small portion of the entire common frequency range of interest for an emitter-receptor pair. Hence, the log-linear approximation to the margin density function must be repeated for each of several contiguous frequency intervals in order to approximate the margin density function over the entire common frequency range from the lowest frequency point, f_{lo} , to the highest frequency point, f_{hi} . Later discussion will show how the resultant piecewise log-linear approximations to the margin density function will tend always to result in a conservative upper bound envelope function compared to the actual input spectral data.

Broadband integrated margin in the interval from frequency f_a to frequency f_b is accomplished in the program by taking the antilog^a of the piecewise log-linear margin function depicted in Figure 6(a), resulting in the exponential curve of Figure 6(b). This resultant margin density function is integrable between the frequencies f_a and f_b as follows:

$$\hat{M}_{IB} \int_{f_a}^{f_b} = \int_{f_a}^{f_b} \frac{\hat{P}_{TB}(f)}{B \hat{S}_1(f)} df \quad (20)$$

where

$$\hat{M}_{TB} \int_{f_a}^{f_b} = \text{the broadband integrated margin between the frequencies } f_a \text{ and } f_b,$$

$$\hat{P}_{TB}(f)/B \hat{S}_i(f) = \text{the broadband margin density function derived from the piecewise log-linear margin density function between frequencies } f_a \text{ and } f_b.$$

Narrowband Integrated Margin - Calculation of narrowband integrated margin again involves use of a margin density function which is derived from the narrowband point margins previously calculated in the program at discrete frequencies. Here the justification for the use of a margin density differs somewhat from the broadband case in that narrowband spectra, by definition, consist of discrete spectral lines whose units are power level, in watts, at discrete frequencies. The levels of discrete spectral lines emanating from an emitter, and the associated receptor susceptibility level used in calculating the point margins, are invariably established or verified in practice by an instrument having a finite bandwidth. Consequently, the narrowband point margins are, in reality, "margin densities" in the sense that they are margins occurring within an instrument (or receptor device) bandwidth. Thus, the narrowband point margins, divided by the associated bandwidth factor, B, are piecewise constant margin densities in the neighborhoods of their frequency points. This is the initial assumption made in the program for the purpose of calculating narrowband integrated margins. The program also assumes that the bandwidth factor is constant over an interval between two successive frequency points involved in a narrowband integrated margin calculation.

Since the frequency points at which narrowband point margins are calculated in the program may be separated by more or less than the widest bandwidth involved, use of the piecewise constant margin densities directly in an integrated margin formulation would generally contain errors of either: a) omission of portions of the spectrum, b) undue amounts of power attributed to those portions of the spectrum where bandwidths overlap, or c) both types of error. The approach used by the program overcomes both types of error by converting the piecewise constant margin densities to piecewise linear margin densities; i.e. the program assumes that the margin density function for narrowband signals is a straight line connecting the values of margin density at two successive frequencies, f_a and f_b . Figure 7 is a graphical picture of this assumption in which the frequencies f_a and f_b are shown rather widely separated compared to a bandwidth known to the program in that frequency region.

The graphical picture of Figure 7 shows that the assumption of a piecewise linear margin density function for narrowband signals is

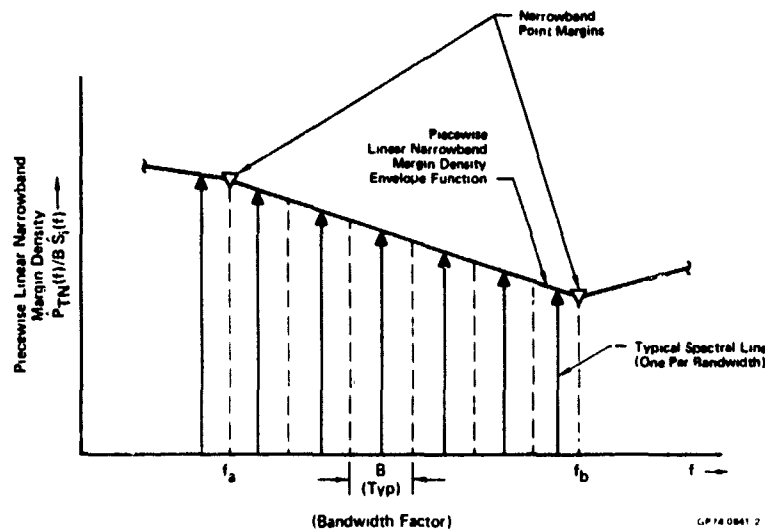


FIGURE 7
NARROWBAND INTEGRATED MARGIN APPROACH

equivalent to the assumption that the spectrum between the end points of a frequency region of interest is filled with one spectral line per bandwidth. In non-required regions of the spectrum this assumption is a compromise (probably worst case) estimate of the distribution of narrowband emissions. The adjusted military specification curves used in non-required regions are intended as bounds which narrowband emissions should not exceed and certainly do not represent extremely dense distributions of spectral lines.

With the assumptions of the preceding paragraphs in mind the narrowband integrated margin is written as follows:

$$\hat{M}_{IN} \Bigg|_{f_a}^{f_b} = \int_{f_a}^{f_b} \frac{\hat{P}_{TN}(f)}{B \hat{S}_i(f)} df \quad (21)$$

where

$$\hat{M}_{IN} \Bigg|_{f_a}^{f_b} = \text{the narrowband integrated margin between the frequencies } f_a \text{ and } f_b,$$

$$\hat{P}_{TN}(f)/B \hat{S}_i(f) = \text{the piecewise linear narrowband margin density function formed by straight line connection of the piecewise constant margin density values at frequencies } f_a \text{ and } f_b,$$

B = the bandwidth, in Hertz, known to the program at the upper frequency limit.

Since the integrand of Equation (21) is always assumed to be a linear function of frequency or a constant value, the solution of the integral is seen to be simply the area of a trapezoid as follows:

$$\hat{M}_{IN} \int_{f_a}^{f_b} = \frac{1}{2} \left[\frac{\hat{P}_{TN}(f_a)}{B \hat{S}_i(f_a)} + \frac{\hat{P}_{TN}(f_b)}{B \hat{S}_i(f_b)} \right] [f_b - f_a] \quad (22)$$

The program separately computes broadband and narrowband integrated margins applicable over the entire common frequency range of an emitter-receptor pair and these are separately printed out following emitter adjustments in SGR. After receptors have been adjusted the program recomputes the broadband and narrowband integrated margins and then combines these into a total signal integrated margin. These several stages of integrated margin calculation are performed and printed out to aid the user in identifying specific contributors to system incompatibility or, conversely, to identify where excessively stringent specifications are being imposed.

Equations (19) and (12) will be seen to correspond respectively to the calculations performed in IEMCAP for the broadband and narrowband EMI margins for a single emitter coupling to a receptor within a frequency sub-range contained within the overall common frequency range. Further, Equations (20) and (22) are the basis for IEMCAP calculations of integrated EMI margin, encompassing both broadband and narrowband coupled signals.

2.2.2 Background for Computer Implementation of System Equations

The preceding discussion forms the general background theory underlying the system EMI calculations performed by IEMCAP. It was shown that the program calculates EMI Margins based on the power present at a receptor's input terminals, from one or more emitters, compared with the receptor's susceptibility power level.

The EMI Margins calculated in the program and the adjustments to achieve compatibility are performed at several discrete sample frequencies that are established to represent the spectra of emitters and receptors. This quantization of spectra in terms of frequency is necessary for numerical computation.

2.2.2.1 Spectrum Quantization

The manner of spectrum quantization in IEMCAP is described now. One is interested in representing each spectrum from some lowest frequency of interest to some highest frequency; e.g., a spectrum of interest might extend from 30 Hz to 18 GHz. To achieve this spectrum representation, the program employs a set of N discrete sample frequencies. The maximum value N may have for any equipment in a system being studied is ninety. To avoid missing

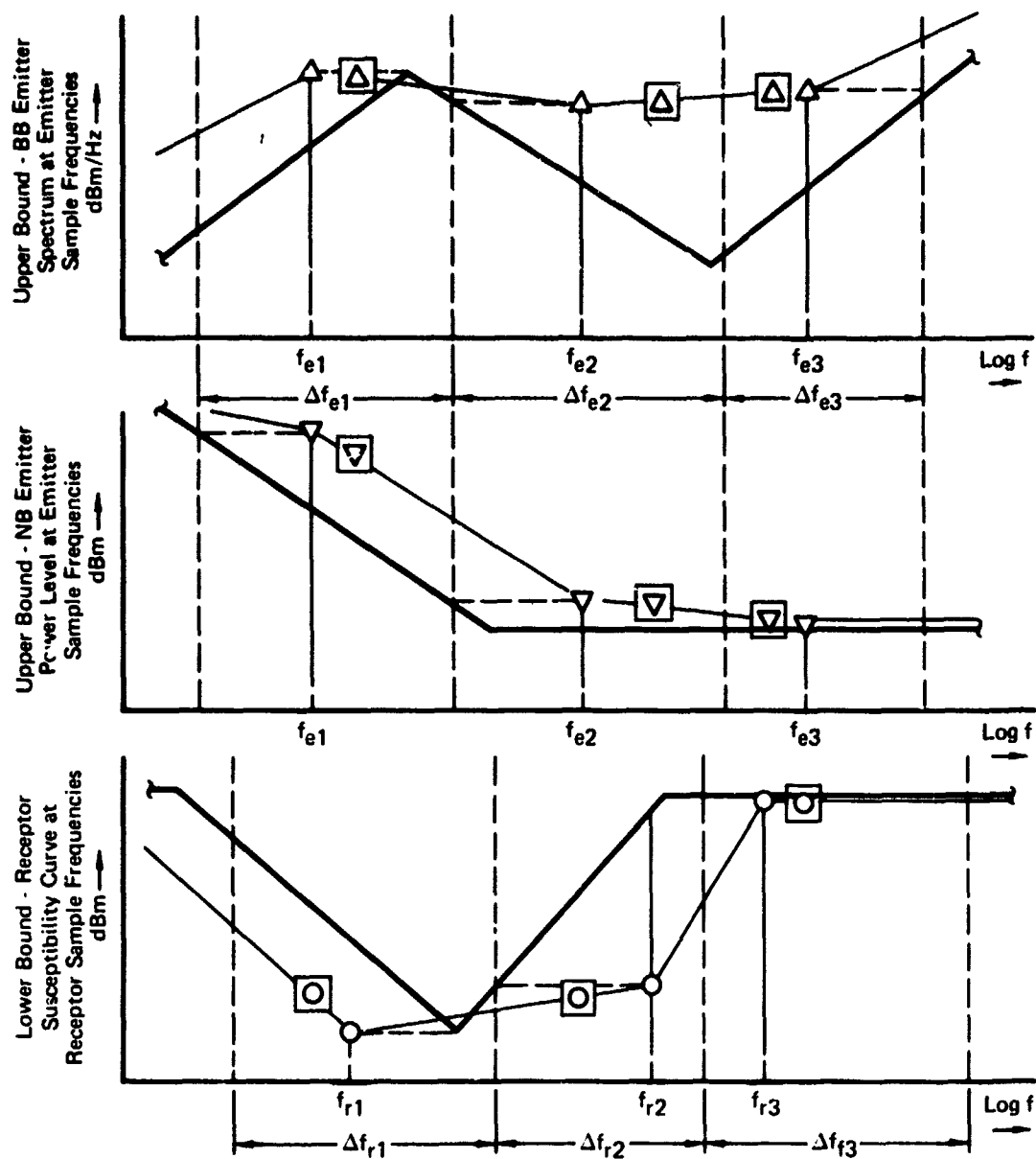
narrow peaks in a spectrum, the program associates with each sample frequency, f_k , a frequency interval, Δf_k , which contains the sample frequency. The set of frequency intervals for an equipment are contiguous and span the entire frequency range. This set of frequency intervals, $\{\Delta f_k\}$, corresponding to the set of sample frequencies, $\{f_k\}$, is determined in the program as follows:

1. for every interior sample frequency f_k (i.e. not first or last sample frequency), the frequency interval Δf_k is bounded by a lower frequency $f_{Lk} = f_k - \frac{f_k - f_{k-1}}{2}$ and an upper frequency $f_{Hk} = f_k + \frac{f_{k+1} - f_k}{2}$
2. Δf_1 (the first sample frequency interval) is bounded by a lower frequency of $f_1 - \frac{f_2 - f_1}{2}$ and by an upper frequency of $f_1 + \frac{f_2 - f_1}{2}$, except that the lower boundary is not allowed to extend to negative frequencies.
3. Δf_N (the last sample frequency interval) is bounded by a lower frequency of $f_N - \frac{f_N - f_{N-1}}{2}$ and by an upper frequency of $f_N + \frac{f_N - f_{N-1}}{2}$.

It will become clear that the intervals, Δf_k , are used to define the process of quantization to the sample frequencies and not for the computation of power received by a receptor.

Illustrations of the use of the frequency intervals to represent spectra of emitters and receptors are now given. Figure 8 shows hypothetical spectrum diagrams for an emitter and a receptor. Three curves are shown: one each for the broadband and narrowband emission spectra and a receptor susceptibility curve. The figure illustrates three typical sample frequencies, f_e , for emitters along with their associated frequency intervals. Also shown are three typical receptor sample frequencies, f_r , (usually different from f_e) and their associated frequency intervals. The Spectrum Model Routine (SPCMDL) performs the spectrum quantization to the sample frequencies resulting in stored files of spectra for later use by SGR in calculations of margins and in adjustment of spectra for compatibility.

The spectrum quantization process involves a worst case representation of broadband emission spectrum, narrowband power level and receptor susceptibility. The program (SPCMDL) searches for the maximum value of emitter spectrum (and narrowband level) in each emitter frequency interval and assigns that maximum value to the sample frequency in the interval. For receptors the program searches for the minimum susceptibility level in the receptor sample frequency interval and assigns that minimum level to the sample frequency in the interval. This maximum (minimum for receptors) value determination is accomplished by computing the levels at the frequency interval boundaries (by log-linear interpolation) and comparing these levels



- Legend
- \triangle = Quantized Broadband Spectrum
 - \triangle (in square) = Broadband Spectrum Interpolated to Receptor Frequencies
 - ∇ = Quantized Narrowband Power Level
 - ∇ (in square) = Narrowband Power Level Interpolated to Receptor Frequencies
 - \circ = Quantized Receptor Susceptibility
 - \circ (in square) = Receptor Susceptibility Interpolated to Emitter Frequencies
- BB = Broadband; NB = Narrowband

GP74 0841 3

FIGURE 8
QUANTIZATION OF SPECTRA AND LOG-LINEAR INTERPOLATION

with those of any known levels within the interval (such as at spectrum breakpoint frequencies). The maximum (minimum for receptor susceptibility) of these known and computed levels in the associated interval is assigned to the sample frequency in that interval. Hence, the upper bound and lower bound labels on the ordinates of the curves in Figure 8.

After the quantization of emitter and receptor spectra, the frequency intervals are no longer used in the program. Instead, margin calculations, adjustments, etc., are performed using the sample frequencies themselves with their quantized spectrum values. In cases where the value for an emitter spectrum or power level is needed at a frequency point intermediate to the emitter sample frequencies, log-linear interpolation of the values between the nearest sample frequencies is used. Similarly, where receptor susceptibility level is needed at frequencies other than receptor sample frequencies, log-linear interpolation is again used. It will later be seen that emission levels at receptor sample frequencies and susceptibility levels at emitter sample frequencies will be needed in the program. Therefore, the log-linear interpolated values of these quantities, as illustrated in Figure 8, will always be computed by the program. One can recognize that, with these data available, the program is able to calculate point margins at every sample frequency (both emitter and receptor) involved in a coupled emitter-receptor pair.

The quantized spectra discussed in the preceding paragraphs enable the program to calculate point narrowband and broadband margins for evaluation of single emitter-receptor compatibility, adjustment of the emitter spectra as needed and generation of emitter narrowband and broadband emission specifications. As mentioned previously, an additional point margin is needed to evaluate compatibility of a receptor to the total emission environment due to all coupled emitters acting simultaneously. Consequently, the program calculates a "total power" quantity in each receptor frequency interval and assigns this power level to the receptor sample frequency. This assumed piecewise constant power level is subsequently compared with the assumed piecewise constant susceptibility level at the sample frequency for calculation of a total power point margin used in compatibility analysis and in the receptor adjustment routine.

The determination of "total power" received by a receptor is accomplished by examining a single coupled emitter at a time, storing the "maximum value" of the power received from that emitter and adding this to the "maximum value" of power received from each of the other coupled emitters. Separate "maximum values" are found for narrowband signals and for broadband signals (product of broadband spectrum with bandwidth) and these are both added to the "maximum values" similarly obtained for all emitters. The "maximum value" used here is found as follows (see Figure 9). The received power is found from a) known levels at emitter frequencies found within the receptor sample frequency interval (the program calculates interval boundary frequencies to determine when other frequencies are interior to the interval) and, b) narrowband and broadband values are computed at the receptor sample frequency (by log-linear interpolation between neighboring emitter frequencies). The largest narrowband signal and the largest broadband signal of all those examined in the interval are selected as the "maximum values". These are added to the "maximum values" determined for all other coupled emitters (after taking the antilog) to obtain the "total received signal" which is assigned to the receptor sample frequency.

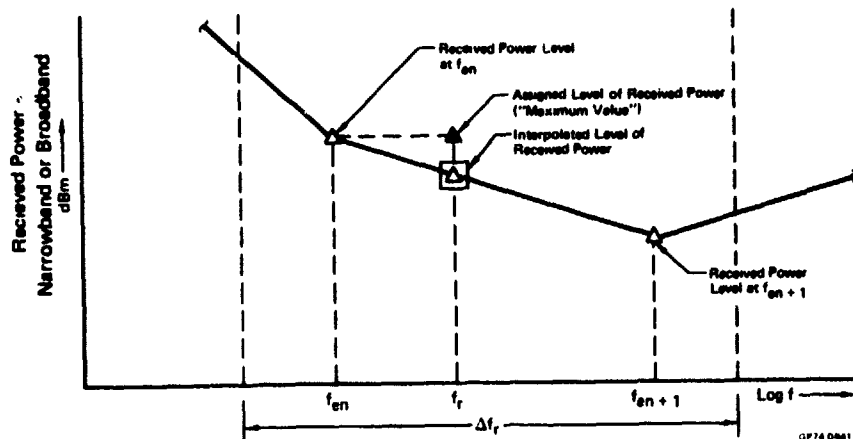


FIGURE 9
QUANTIZATION OF RECEIVED POWER

2.2.2.2 Origin of Emission and Susceptibility Spectra - The program determines emission and susceptibility spectra in one or more of three ways: a) a user-specified required spectrum, b) a user-specified spectrum model with which the program computes required spectra and, c) outside the required frequency range the spectra are initially based on MIL-STD-461A or MIL-I-6181D specification curves as displaced by a user input to the program. Spectrum amplitudes based on these methods are assigned in the program to the sample frequencies for emitters and receptors. If the parameters do not happen to provide data at the specific sample frequencies for emitters or receptors, the program computes values at these sample frequencies by log-linear interpolation between the frequencies at which the data are available in the program. For example, for the non-required portion of some spectra the program would have stored data only at the frequencies corresponding to the end points and break points of the military specification limit curves. Data are obtained at any intermediate sample frequency points by the log-linear interpolation process.

The program is seen to be capable of establishing a signal level at a receptor for any frequency occurring between any pair of sample frequencies; this is accomplished routinely by the log-linear interpolation process. This fact, along with the generally worst-case assignment of spectrum levels to the sample frequencies, could raise the question of accuracy of spectrum representation in the program for those instances when the user may wish to obtain considerable fidelity in the program of either the user-defined spectrum or a spectrum model. The qualified answer to this question is that the accuracy will depend upon the user's judicious selection of sample frequencies in relation to the spectrum of interest.

Figure 10 illustrates how the user-assigned sample frequencies in the vicinity of a particular emission spectrum can result in either a rather gross representation of that spectrum in the program or, otherwise, can result in a quite faithful representation. The figure represents a typical emission spectrum envelope for an emitter, and it is assumed that the user wishes the program to follow this envelope to some accuracy. He accordingly assigns sample frequencies in the region of this spectrum. In general,

these should be at break points in the curve. For example, assignment of only the frequencies f_1 , f_4 and f_7 would yield a rather gross representation of the spectrum as indicated by the dashed curve in the figure since the program interpolates between sample points. Assignment of the frequencies f_1 , f_3 , f_5 and f_7 would result in a much more faithful representation of the spectrum, as illustrated by the interrupted curve. Assignment of additional frequencies, such as f_2 and f_6 would produce even more faithful representation of the spectrum skirts than previously. If even more accuracy in the skirt region were required, then additional frequencies should be assigned in these portions. Note, however, that increased resolution in one part of a spectrum decreases the resolution in the remainder since the total number of sample frequencies cannot exceed 90.

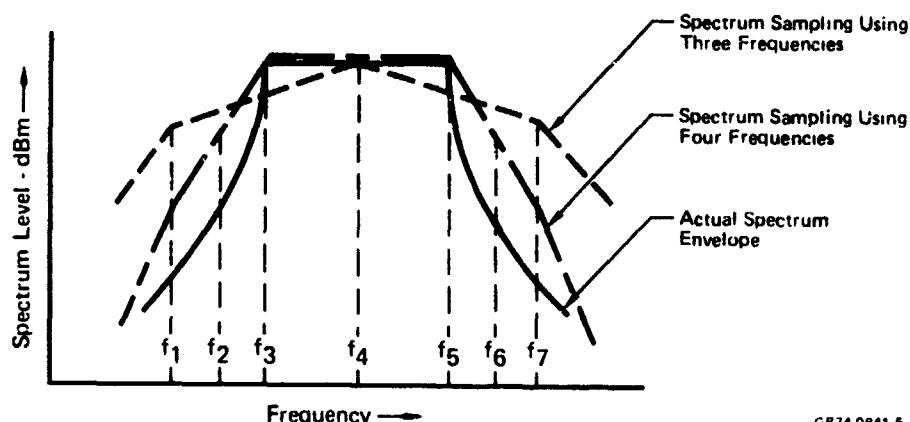


FIGURE 10
SPECTRUM SAMPLING ACCURACY DEPENDS ON NUMBER OF
ASSIGNED FREQUENCIES

In the preceding discussion of spectrum sampling accuracy, the statement that the program can accurately represent a spectrum needs amplification. In the emitter example of the preceding paragraph, it is clear that the discussion pertained to a port of some equipment and that, in the particular case discussed, an emission spectrum model had been specified as the required portion of the spectrum for that port. This spectrum model would have been defined by the user in terms of the modulation type, a carrier frequency and a bandwidth factor. These are the primary parameters that would be specified at the port level. The program would then compute the spectrum using the appropriate mathematical model (Section 6) for the required portion in conjunction with the user-displaced military specification limits for the non-required portion. The program data for this spectrum would consist of the spectrum levels at the equipment sample frequencies. Thus, for the program to provide details of the required spectrum in the manner indicated in the preceding paragraph, the user must assign equipment sample frequencies with suitable relationships to the required spectrum envelope associated with the port of interest. If the required portions of the spectra of several ports in an equipment were of interest, considerable judgement would be necessary to appropriately share the equipment frequencies among these ports while retaining adequate sampling of the remainder of the equipment spectrum.

In the case of user-supplied spectra (say from test data), he will want to include sufficient frequencies (up to a maximum of ten) in his input data for the port to appropriately represent the spectrum of interest. The program will quantize these port spectra to the equipment sample frequencies. The analysis will include frequencies corresponding to the input port frequencies only if the user also assigns them to the equipment sample frequency table. Clearly, the user cannot assign ten independent spectrum values to all fifteen ports of an equipment and expect the program to perform analyses at all of these frequencies because of the ninety frequency limit for the equipment.

It will be appreciated that, for the majority of situations, this general independence of the equipment frequency table from the port input data frequencies is advantageous. This arrangement allows the user to change the equipment frequency table without the necessity of also changing the frequencies of all the ports. However, the flexibility is present to achieve coincidence of port and equipment frequencies if the user wants this.

2.2.3 Programmed System Equations and Their Program Application

With quantized spectra established for emitters and receptors in accordance with the procedures described in the foregoing material, the stage is set for describing the equations used and the operation of the program in determining EMI Margins and in performing spectrum adjustments.

2.2.3.1 Emitter Adjustment - After the initial spectra have been computed, the initial operation in SGR is to compute the power incident at a particular receptor's terminals (say the i th receptor) from an emitter (say the j th emitter) in the emitter array coupled to the receptor. Narrowband and broadband power are computed separately, and the objective is to compare these power levels with the susceptibility levels of the receptor for determination of resultant point EMI Margins. The power computation is performed as follows:

$$\hat{P}_{Tij}(f_k) = \hat{P}_{jN}(f_k)T_{ij}(\Delta f_k) + \hat{P}_{jB}(f_k)T_{ij}(\Delta f_k)B \quad (23)$$

where

$\hat{P}_{Tij}(f_k)$ = power (in watts) transmitted from emitter j to the terminals of receptor i contained within a standard bandwidth, B ,

$\hat{P}_{jN}(f_k)$ = the narrowband emission power level of emitter j , at emitter frequency f_k (assumed piecewise constant),

$\hat{P}_{jB}(f_k)$ = maximum value of $\eta_{SBj}(f)$ in the Δf_k interval, of the emitter (assumed piecewise constant),

$T_{ij}(\Delta f_k)$ = the value of the power transfer function, $T_{ij}(f)$, at the frequency f_k ,

Δf_k = the frequency interval associated with the emitter sample frequency, f_k ,

and

B = a bandwidth factor associated with the power level in the k^{th} frequency interval. Table 4 is a list of rules followed by the program in choosing the bandwidth factor to be used in calculations. B_{std} in this table has been defined in Section 2.1.12.

With these power levels available at each sample frequency, the program compares them with the assumed piecewise constant receptor susceptibility levels. This comparison is accomplished by computation of narrowband and broadband point EMI Margins as follows:

$$\hat{M}_{Nij}(f_k) = \bar{P}_{jN}(f_k) / \hat{S}_i(f_k) \quad (24)$$

and

$$\hat{M}_{Bij}(f_k) = \bar{P}_{jB}(f_k) / \hat{S}_i(f_k) \quad (25)$$

where

$\hat{M}_{Nij}(f_k)$ = the narrowband point EMI Margin at the k^{th} sample frequency due to narrowband power at the receptor's terminal from the j^{th} emitter applicable in a standard bandwidth,

$\hat{M}_{Bij}(f_k)$ = the broadband point EMI Margin at the k^{th} frequency due to broadband power at the receptor's terminal from the j^{th} emitter applicable in a standard bandwidth,

$\hat{S}_i(f_k)$ = the assumed piecewise constant susceptibility of receptor i at the k^{th} frequency,

$\bar{P}_{jN}(f_k) = \hat{P}_{jN}(f_k) T_{ij}(\Delta f_k)$ = the assumed piecewise constant narrowband power at the terminals of receptor i due to emitter j at the k^{th} frequency,

$\bar{P}_{jB}(f_k) = \hat{P}_{jB}(f_k) T_{ij}(\Delta f_k) B$ = the assumed piecewise constant maximum value of broadband power at the terminals of receptor i due to emitter j at the k^{th} frequency.

These point EMI Margins are actually computed in dB and their forms are accordingly

$$M_{Nij}(f_k) = P_{jN}(f_k) - S_i(f_k) \text{ dB} \quad (26)$$

and

$$M_{Bij}(f_k) = P_{jB}(f_k) - S_i(f_k) \text{ dB} \quad (27)$$

If interference conditions (margin greater than the user-defined adjustment safety margin, asm) are found at any frequency, the program adjusts the emitter non-required narrowband and broadband spectra such that the margin equals $-asm$ or to the adjustment limit. Figure 11 illustrates the general approach to emitter spectrum adjustment. In the figure, a considerable portion of the unadjusted quantized emitter spectrum is seen to be above the quantized receptor susceptibility spectrum, indicating electromagnetic interference. The program searches for pairs of receptor frequencies straddling an emitter frequency and, where interference exists in the non-required portion of the emitter spectrum, it adjusts the amplitude at the emitter frequency downward to a level below receptor susceptibility by $-asm$ provided this adjustment can be accomplished within the adjustment limit. It then back-searches through the receptor frequencies between the present and previous emitter frequencies and adjusts the line segment formed by these two points for compatibility at each receptor frequency. In the example shown, all required emitter adjustments were achieved without exceeding the adjustment limit. If interference is found in the required portion of the emitter spectrum, no adjustments are made by the program. If both narrowband and broadband spectra require adjustment at a given frequency, the spectrum adjustment of each component is increased another 3 dB so that the combined narrowband and broadband received signals are compatible. The emitter adjustment procedure is described in detail in Section 5.1.2.2.

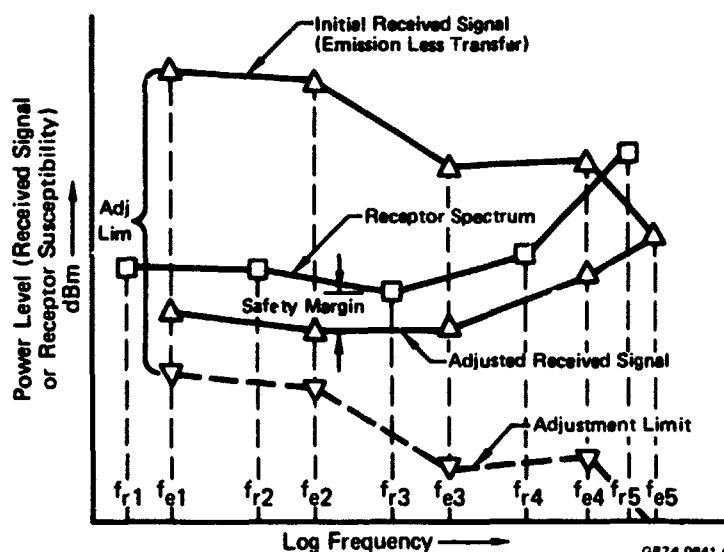


FIGURE 11
EMITTER ADJUSTMENT TO A SAFETY MARGIN
BELOW RECEPTOR SUSCEPTIBILITY

The safety margin and adjustment limits are quantities that the user defines and inputs to the program. Some guidelines for establishing their values are now discussed.

The adjustment limit (adjlim) is the maximum amount, in dB, from the initial amplitude that the program will adjust each non-required spectrum during specification generation. This prevents extremely stringent specifications from being generated. If, after a portion of a spectrum has been adjusted to this limit and the receptor cannot be adjusted for compatibility, an interference condition persists, the program will print out a summary of this interference so that the user can then decide upon special measures to handle the problem.

The user must decide upon a value for adjlim for each port spectrum and specify this value in his input data. No universal rule can be stated regarding the value to assign to this quantity except to say that it should correspond with realistic and economical EMI control measures and should result in EMI limits that are verifiable using standard laboratory instruments and procedures. A reasonable starting value could be guided by the amount of the user specified initial displacement of the military specification limit curves employed in the program for non-required spectra. For example, if the spectra displacement factor (sdfs for emitters and sdf for receptors) was chosen as 40 dB, then it might be reasonable to let the program adjust portions of a spectrum back to the military specification limit level. Thus, in this case the user could also specify an adjustment limit (adjlim) of 40 dB and would anticipate that the resultant adjusted spectrum would be realizable.

The adjustment safety margin (asm) is a factor that the user specifies at the system level. It is the minimum compatible ratio, in dB, of the received power in each segment of a receptor frequency range to the receptor susceptibility in that range. Where emitter or receptor spectra require adjustment, the program will adjust the spectra to this safety margin provided the adjustment limit is not exceeded. Then, the spectra will be piecewise compatible across the entire frequency range except for possible interference in required ranges or wherever the adjustment limit prevents achievement of compatibility (unresolved interference).

A single universally applicable value for the adjustment safety margin (asm) is not advisable; user judgement is required in choosing a value of asm for the particular system being considered. The asm should include, among other factors, the uncertainty in measured data included in the program input for emitters and receptors involved in a given EMI assessment. Possibly the user could be guided in selecting a value for the asm by the safety margins specified in MIL-E-6051D; i.e., a minimum of -6 dB margin for systems in which electroexplosive devices (EED's) are not involved and a minimum of -20 dB for systems that include EED's. With a value of asm in this range specified for the system and with values of spectra displacement factor (sdf) specified for each port, a survey run of the program would then reveal to the user whether the asm and spectra displacement factors were combining to generate reasonable interference limit specifications. The information on which to base a judgement of reasonableness of limits (i.e., limits that are neither too stringent nor too relaxed) is provided by the integrated EMI margin available in the program output for each receptor.

Returning now to the emitter adjustment procedure, the power computations and initial emitter adjustment are repeated for every single emitter coupled to the i^{th} receptor. The entire process is then repeated for every receptor in the receptor array until, finally, all emitters have been adjusted to individual compatibility, if possible, with all receptors at every emitter and receptor sample frequency across the common band of interest. This results in a set of piecewise compatible EMI margins for every single emitter into every single receptor. Both narrowband and broadband margins have been considered, as mentioned previously. It is clear that these margins are all tentative at this point; emitters are, as much as possible, individually compatible with receptors as a result of the foregoing procedure, but the compatibility of the combination of all coupled emitters to a receptor has yet to be examined.

2.2.3.2 Receptor Adjustment - The next step in SGR is to compute maximum total power from all emitters coupling to a receptor within each receptor sample frequency interval and to compare this total power with the receptor's susceptibility level in the manner described in paragraph 2.2.2.1 and illustrated previously in Figure 9. The total signal is a composite, representing the sum of the "maximum values" of signals occurring within a given receptor sample frequency interval from all emitters coupled to it. Thus, total composite signal point margins are computed (narrowband and broadband signals are combined) from adjusted emitters. If these margins indicate interference at any receptor sample frequency, the receptor susceptibility level at that point is adjusted (except for frequencies included in the receptor required spectrum) for compatibility with the total received signal by the safety margin or to the adjustment limit. This process is repeated for every receptor in the receptor array for the system. Section 5.1.2.3 gives further details of the receptor adjustment procedure in SGR.

The equation for computation of total emitter power at the i^{th} receptor's port in the k^{th} receptor frequency interval is written as follows:

$$\hat{P}_{Ti}(f_k) = \sum_{j=1}^{N_s} T_{ij}(\Delta f_k) [\hat{P}_{jN}(f_k)_{\max} + \hat{P}_{jB}(f_k)_{\max} B] \quad (28)$$

where

$\hat{P}_{Ti}(f_k)$ = the total of the maximum values of combined narrowband and broadband power from all emitters coupling to the i^{th} receptor in its k^{th} frequency interval (assumed piecewise constant),

$\hat{P}_{jN}(f_k)_{\max}$ = the "maximum value" of narrowband power from the j^{th} emitter coupling to the i^{th} receptor in its k^{th} frequency interval,

$\hat{P}_{jB}(f_k)_{\max}$ = the "maximum value" of broadband power spectral density from the j^{th} emitter coupling to the i^{th} receptor in its k^{th} frequency interval,

$T_{ij}(\Delta f_k)$ = the value of the power transfer function, $T_{ij}(f)$, at the receptor frequency, f_k ,

B = the bandwidth factor associated with the receptor frequency, f_k ,

N_S = the total of all emitters in the system.

The equation for the total emitter signal EMI margin (using combined narrowband and broadband maximum signals in each sample interval) is

$$\hat{M}_{Ti}(f_k) = \hat{P}_{Ti}(f_k) / \hat{S}_i(f_k) \quad (29)$$

or, in dB

$$M_{Ti}(f_k) = P_{Ti}(f_k) - S_i(f_k) \text{ dB} \quad (30)$$

The result of the emitter and receptor adjustment procedures described thus far is a set of adjusted emitter and receptor spectra that are piecewise compatible across their required frequency ranges except for possible interference situations occurring in the required spectra of the emitters and receptors and where the adjustment limits have prevented adjustments to compatibility. The program thus prints out these sets of total signal EMI margins, some of which may represent the unresolved interference situations just described.

The next step in SGR is to return to the single emitter-to-receptor pair and to re-compute the EMI margins resulting from the adjusted spectra for both the j^{th} emitter and the i^{th} receptor. Separate narrowband and broadband margins are computed at each sample frequency for the single emitter input using the formulas of Equations (26) and (27) where the received power values and receptor susceptibility level now include the adjustments performed by the program. At each frequency these margins are now compatible or, otherwise, represent unresolved interference.

2.2.3.3 Integrated EMI Margin Calculation - If an emitter is adjusted exactly for a zero dB EMI margin relative to a receptor in one or more sample frequency intervals, the integrated signal across the band may still cause interference. As an aid in determining this effect, the program computes, in addition to the margin at each frequency, an EMI margin integrated across the entire frequency range of interest. This integration is accomplished piecewise, from sample frequency to sample frequency. This result is printed on the interference summary output for each emitter-receptor pair. Also, the summation of the integrated margin obtained for the total signal into each receptor is computed. Narrowband and broadband integrated margin components are computed separately and summed.

The approach to calculation of both the broadband and the narrowband integrated margins was developed in considerable detail in Paragraph 2.2.1.2. In that discussion the integration was performed over the frequency range between two successive frequencies at which the point margins were known in the program. From the above discussion of the procedure for emitter adjustment it is clear that these point margins (both broadband and narrowband) were computed at all emitter and receptor sample frequencies involved in an emitter-receptor pair analysis. Consequently, the program makes use of all these data points in the computation of integrated margins. Integration over the entire common frequency range is achieved by summing the integrals obtained from each of the contiguous frequency segments formed by the succession of emitter and receptor sample frequencies taken in combination (a total of up to 180 frequency points across the band). If the general frequency of this set of points formed by the combined emitter and receptor sample frequencies is denoted f_r , then f_r and f_{r+1} are, respectively, the lower and upper limits of integration in the integrals of Equations (20) and (21) given previously.

The actual formulas used in the program in performing the computations of integrated margin are presented in the following for both the broadband and narrowband cases. These formulas employ the index, r , to denote one of the set of combined emitter and receptor frequencies as described above.

The equation for broadband integrated margin encompassing the entire common frequency range is given as follows:

$$\hat{M}_{IBij} = \sum_{r=1}^{N_C} g_{12B} \quad (31)$$

where

N_C = the combined total of all emitter and receptor sample frequencies in the frequency range from f_{10} to f_{hi} ,

$$\begin{aligned} g_{12B} &= \int_{f_r}^{f_{r+1}} g_{rB} \left(\frac{f}{f_r} \right)^a df = \frac{g_{rB}}{(a+1)} \left[\frac{f_{r+1}^{a+1}}{f_r^a} - f_r \right]; \\ &= g_{rB} f_r \log_e \left(\frac{f_{r+1}}{f_r} \right) \text{ for } a = -1; \\ &= 1/2 (g_{(r+1)B} + g_{rB}) (f_{r+1} - f_r) \text{ for } |a| > 25 \end{aligned}$$

and

$$a = \frac{\log_{10} (g_{(r+1)B} / g_{rB})}{\log_{10} (f_{r+1} / f_r)}, \quad g_{rB} = \frac{\hat{P}_{jB}(f_r)}{\hat{BS}_i(f_r)}$$

B = bandwidth factor applicable at each sample frequency.

Note that a straight line integration is used where the slope is steep ($|a| > 25$).

The g_{rB} in the above formulas is seen to be exactly the broadband margin density function derived from the piecewise constant broadband point margins and employed in the integral of Equation (20). The functional dependence on frequency is obtained simply from the equation of a straight line connecting successive point margin densities in log-log coordinates.

The narrowband integrated margin across the entire common frequency range is again a summation of terms of the form of Equation (22) over all N_C sample frequencies as follows:

$$\hat{M}_{INij} = \sum_{r=1}^{N_C} \frac{(g_{rN} + g_{(r+1)N})(f_{r+1} - f_r)}{2} \quad (32)$$

where

$$g_{rN} = \frac{\hat{P}_{jN}(f_r)}{\hat{BS}_i(f_r)},$$

$\hat{P}_{jN}(f_r)$ = narrowband power received by i^{th} receptor from j^{th} emitter

$\hat{S}_i(f_r)$ = susceptibility of i^{th} receptor

B = bandwidth factor applicable to the frequency segment from f_r to f_{r+1}

The integrated margins computed by equations (31) and (32) are combined to give a composite margin and this margin is then computed for each emitter coupling to a receptor. The total integrated margin for that receptor is then computed as the sum of the margins due to all N_s emitters. The composite integrated margin is accordingly given by:

$$\hat{M}_{ITi} = \sum_{j=1}^{N_s} (\hat{M}_{IBij} + \hat{M}_{INij}) \quad (33)$$

2.2.3.4 Use of Integrated EMI Margin - The total integrated EMI margin developed in the preceding section is used in the interactive process involved in interference limit optimization. It is provided to the user as an overall measure of the compatibility of a receptor with its entire emission environment. From the earlier definition of the point margins (from which the integrated margin is derived) it is clear that the integrated

margin is an approximate measure of the total power present at a receptor's detector compared to that receptor's standard response. Hence, the integrated margin is an EMI figure-of-merit, indicating (within the accuracy of the program approximations) how well spectra associated with a receptor have been adjusted to minimize total received power compared to the standard response.

The integrated EMI margin provides the interactive mechanism by which the engineer is enabled to optimize the system EMI specification limits. The engineer will probably exercise the program two or more times in an effort to optimize safety margins and adjustment limits toward values that drive the integrated margin figures for the system receptors toward values that are optimum in the sense that spectra are neither too stringently controlled nor too relaxed. This interactive approach is desirable in the interest of maximizing system economy and conserving system weight as these are influenced by EMI controls.

To illustrate the interactive approach, it will be supposed that the integrated margin for some receptor is a rather large positive number in dB. The engineer will accordingly want to apply corrections to his input data to drive this number, on the next pass through the program, to some moderately negative value in dB. This could be accomplished by applying corrections to all spectra, i.e., increasing the safety margin. However, the greatest economy should result if the corrections are limited to only those particularly offensive interferers or especially susceptible receptors. These are identifiable in the program printout of the interval-by-interval EMI margins. The engineer can thus decide upon selective corrections to be made aimed at curing the actual offenders without penalizing (over-specifying) the remaining portions of spectra. A specific example of such a selective corrective measure would be a decision to shield a wire or, possibly, to relocate a wire.

It is clear from the discussion thus far that a "good" integrated margin is probably one whose value in dB is moderately negative. Neither large negative numbers nor large positive numbers are desirable since these represent, respectively, excessive (therefore uneconomical) interference control and unacceptably high interference. It will be understood that a moderately positive integrated margin may sometimes be unavoidable; a particular situation might involve unresolved interference from required signals or spectra adjusted to their practical limit that will either have to be lived with or else will require other control measures, such as blanking, to remove the interference.

Section 3

PROGRAM OPERATION

A brief discussion of the IEMCAP organization and overall logic flow was presented in Section 1.5.5. In this section, the major routines are identified and discussed to show the overall program operation. In sections 4 and 5, details of these routines and their subprograms are discussed.

As discussed in Section 1.5.5, IEMCAP consists of two sections which are executed separately. The first section (IDIPR) reads, validates, and decodes user input; manages and assembles the data for analysis; generates the initial port spectra; and writes this data on permanent and working data storage files. The second section, TART, uses this data and the transfer models to perform specification generation, baseline survey, trade-off, and waiver analyses.

3.1 IDIPR ROUTINES

The Input Decode and Initial Processing Routine (IDIPR) consists of four basic subprograms. Figure 12 shows the overall logic flow through them and identifies the basic functions and data files used by each. The four subprograms are the Input Decode Routine (IPDCOD), Initial Processing Routine (IPR), Spectrum Model Routines (SPCMDL), and the Wire Map Routine (WMR). The basic operation of these is discussed below.

3.1.1 Input Decode Routine

All user program control and data inputs to IDIPR are on punched cards in a free field format. Basically, the inputs are in the form of statements in which the parameters may be punched into any columns in the cards. The basic format is a keyword, an equals sign, and the parameters separated by commas. Blanks are ignored so that entries may be indented and grouped for clarity. The parameters and subparameters on these cards must be in the prescribed order. Examples of these input statements are

```
EXEC = SGR, NEW
```

and

```
SYSTEM = AIR, 0, 0, 0, -6., -100
```

The first is a control statement which directs the program to execute specification generation from new data. The second is a data entry defining the system as an aircraft and giving basic run parameters applying to the system. This format is discussed in detail in Volume II of this manual.

The IPDCOD reads these cards, decodes them, and tests for a number of possible errors. Syntax errors, such as two commas in a row, an invalid code word, etc. are included in these checks. Also, IPDCOD checks for the proper number of parameters and subparameters for the particular type of

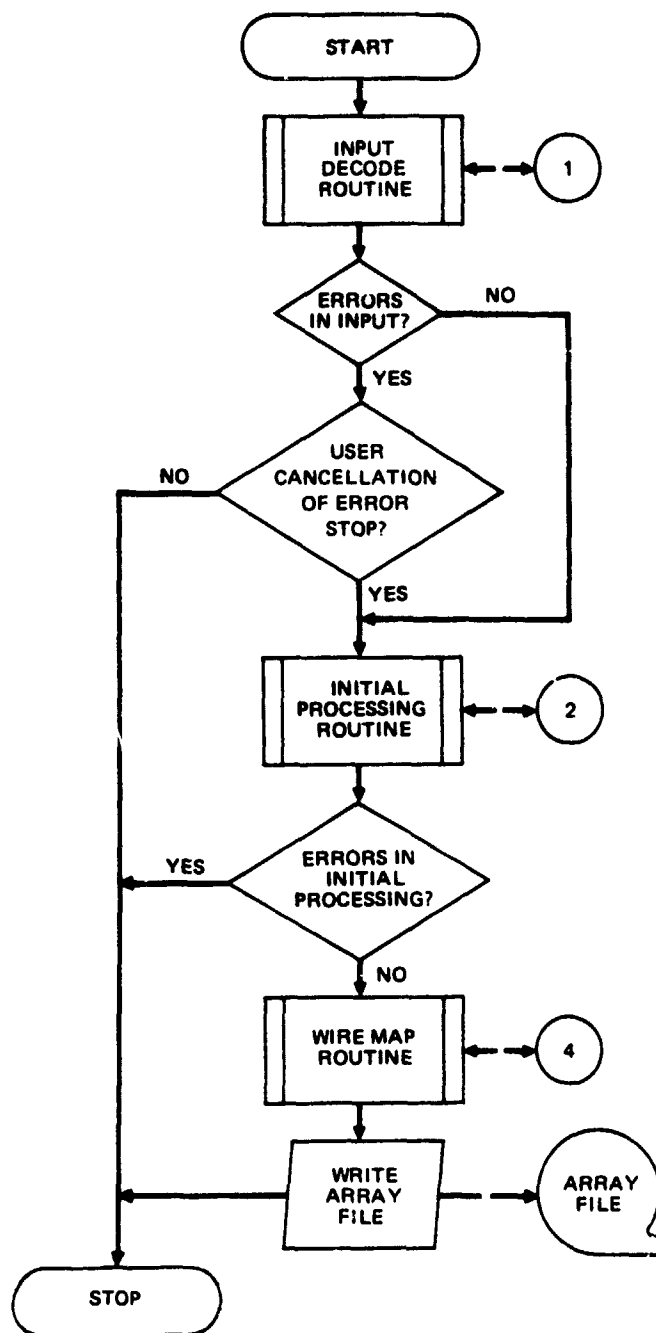


FIGURE 12
IDIPR SECTION OF IEMCAP TOP LEVEL FUNCTIONAL FLOW

GP74 0267 109

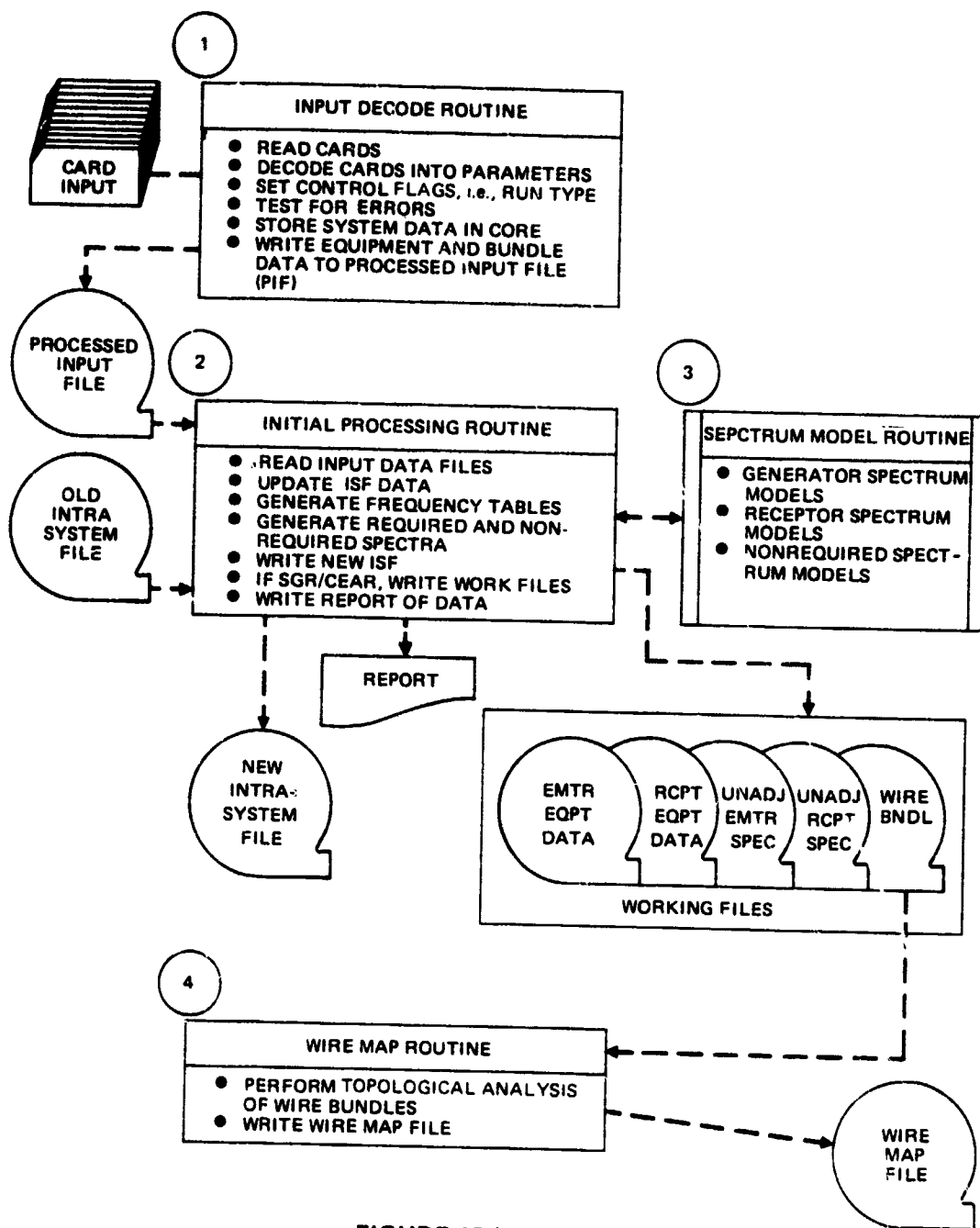


FIGURE 12 (Continued)
IDIPR SECTION OF IEMCAP TOP LEVEL FUNCTIONAL FLOW

JF 74 02, 110

entry and proper order in the hierarchy. If an error is found, the card contents are printed along with a diagnostic message explaining the nature of the error. The card is deleted from the processed data, and processing continues. The error-free data is written on a file called the Processed Input File (PIF) for temporary storage. If there were no errors during input decode, the program continues into the Initial Processing Routines. But if there were errors, the program stops unless overridden by user directive. (This user option to cancel the normal error stop is available for certain runs as discussed in detail in Volume II.)

3.1.2 Initial Processing Routine

For any given run, the system to be analyzed can be defined from card input only, from data stored during a previous run on an Intrasystem File (ISF), or from the old ISF data modified by card input. IPR assembles this data and processes it for analysis. In doing this, it performs three basic functions.

The first function is to merge the data from the old ISF with card input, if required. The data from the old ISF and the PIF, which contains the decoded input card data, are compared. Data from the old ISF may be deleted, replaced by new data from the PIF, or new data may be added.

During this process, the second function, generation of initial spectra, is performed. When a new equipment is encountered, the sample frequency table is generated, as discussed in Section 1.5.3. When a new or modified port is encountered, the Spectrum Model Routine (SPCMDL) is called to generate the spectrum amplitudes at the sample frequencies.

The third function is to write the processed input data and initial spectra onto a new ISF for future runs and onto a number of working files for analysis. All data processed is also summarized in a printed report.

The working files provide intermediate storage between IDIPR and TART. A number of files are used so that the data can be divided for efficient analysis and consecutive files can be used. Use of consecutive files is in accordance with USA Standard FORTRAN and allows adaptation of IEMCAP to computers without random access files.

During IPR processing, additional error checks are made. If an error is encountered, a diagnostic message is printed and the program continues. Basically, errors detected are those in the merge and model input parameters, such as a pulse width exceeding the period between pulses.

3.1.3 Spectrum Model Routines

These routines compute required and non-required spectra for emitters and receptors using mathematical models. (These are discussed in detail in Section 6.) The spectrum routines can be grouped as follows:

- o Required Emitter - These compute required emission spectra from user-supplied parameters. They include various RF modulation types such as AM, FM, SSB, and chirp radar as well as signal waveforms such as rectangular pulses, sawtooth, and damped sinusoid.
- o Required Receptor - These compute required susceptibility spectra from user-supplied parameters. The susceptibility is assumed to have a flat frequency response over the required frequency range if not user supplied spectra. For RF receptors, the user-supplied susceptibility level is used, while for signal or control receptors, a susceptibility of twenty dB below the operating level is assumed.
- o Non-required Emitter - These compute non-required emission spectra based on MIL-STD-461A, MIL-I-6181D, or MIL-STD-704 specification for RF, signal/control, equipment cases, and power lines.
- o Non-required Receptor - These compute non-required susceptibility spectra, based on MIL-STD-461A or MIL-I-6181D specifications for RF, signal/control, equipment cases, and power lines. An electro-explosive device model is also included.

3.1.4 Wire Map Routine

A bundle is defined as a group of wires which, for at least some portion of their length, can run next to each other. To specify the routing, segments are defined in which no branching or change of direction takes place. The end points of the segments are identified and located in the system by giving their coordinates. Complex "trees" of segments can thus be specified. The routing of individual wires through the tree is specified by giving the segment end points through which the wire passes.

The Wire Map Routine (WMR) processes the data in the above form and generates cross-reference map arrays relating wires, segments, end points, and ports. These map arrays are written onto the Wire Map File for use during analysis.

3.2 TART ROUTINES

The Task Analysis Routine (TART) section of IEMCAP performs the designated analysis tasks. The functional flow and major components of TART are shown in Figure 13. First, TART reads the system data and run parameters from the files generated by IDIPR. Then the appropriate task driver routine is entered. If the task specified is SGR, the Specification Generation Routine (SGR) is entered; otherwise the Comparative EMI Analysis Routine (CEAR) is entered. These two routines interface with the working files, coupling path model, and analysis routines to perform the specified task. The coupling path routines determine if a path exists and computes the transfer ratio if it does. The analysis and spectrum adjustment routines use the emitter, receptor, and transfer ratio spectra to compute the received signal and EMI margins for emitter-receptor port pairs as well as the total signal from all coupled emitters into each receptor. These routines also adjust the non-required spectra for SGR runs.

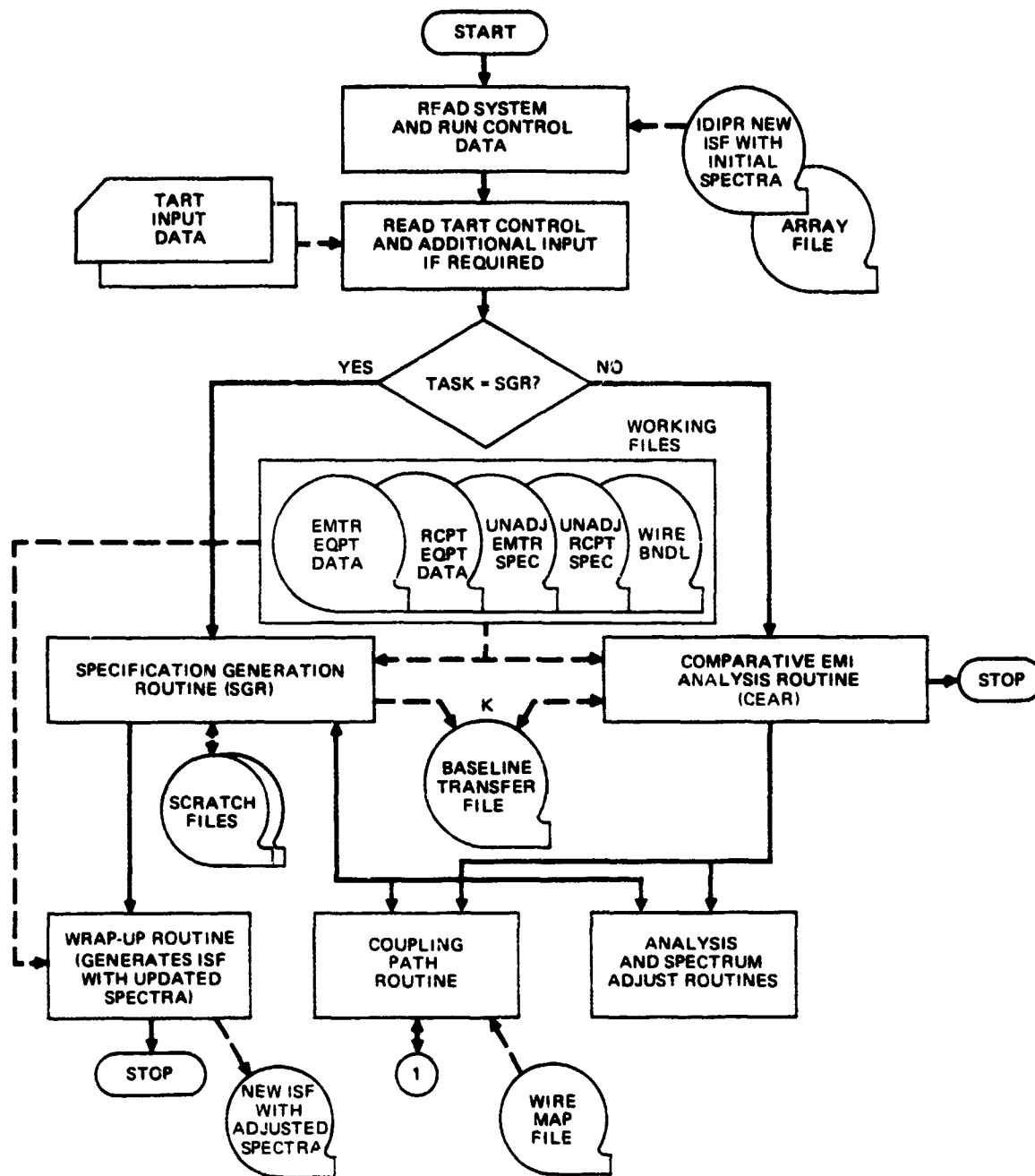
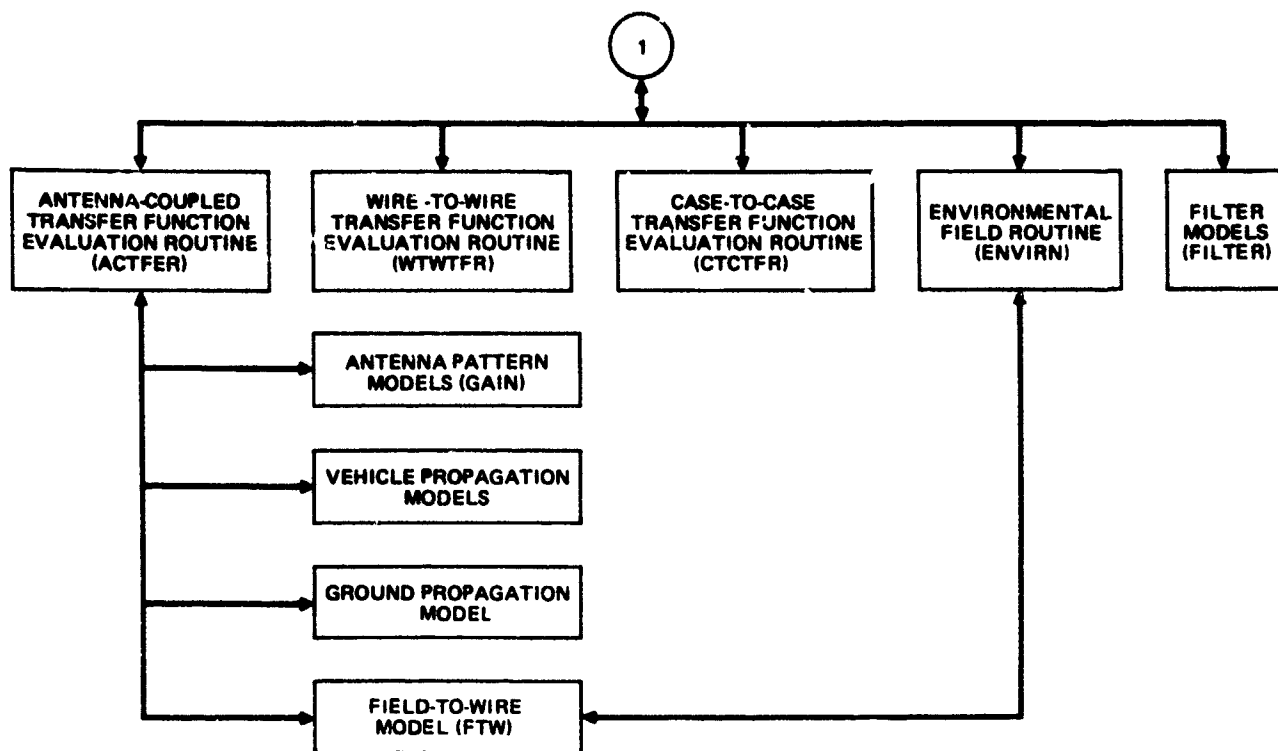


FIGURE 13
TART SECTION OF IEMCAP TOP LEVEL FUNCTIONAL FLOW

GP74 0267 76



GP74-0267-77

FIGURE 13 (Continued)
PART SECTION OF IEMCAP TOP LEVEL FUNCTIONAL FLOW

3.2.1 Specification Generation Routine

This section of the program determines the EMC test limit specifications for the non-operationally required portions of the emitter port output and receptor port susceptibility spectra such that the system is compatible (where compatibility is possible). The user specifies the applicable MIL-STD-461 or MIL-I-6181D limits (plus or minus a displacement, if desired) for each port which are used by IDIPR to generate the initial spectra. These are used as a starting point by SGR, which revises the spectra, where possible, to produce a compatible system. SGR also supplies a list of interference situations which cannot be resolved by EMC specification limit adjustments. These cases require other techniques such as blanking, rearrangement of equipment locations, and the like.

EMC specifications will normally be generated during the conceptual phase of system development or when new subsystems are added to an existing system. The limits generated are furnished to the subsystem builder as a part of the overall subsystem specification. Since these subsystems will be under development, very little will be known about each equipment except for basic inputs and outputs and locations within the system. These specifications will therefore be based on the best available data. At a later date, the specification can be regenerated with more precise data, or the waiver analysis routine can be used to test specific deviations from previously computed specifications.

3.2.2 Comparative EMI Analysis Routine

CEAR performs the baseline survey, trade-off, and waiver analysis tasks, as discussed in Section 1.5.5. During the baseline survey, EMI margins are computed between coupled emitters and receptors as well as from the total received signal and environmental field into each receptor. This data is stored on a permanent file, called the Baseline Transfer File (BTF), for future runs. SGR also generates this file during its run.

For trade-off and waiver analyses, CEAR computes the EMI margins between added ports or changed ports, and compares these to the data stored on the BTF. A summary of each situation showing the baseline and modified system margins and the change is printed. The comparative analysis provides a variety of uses as a design aid to assess the effect of:

- o Added ports
- o Any change in an existing port spectrum, connection, location, antenna gain, wire shielding, etc.
- o Any change in the system such as added obstacles between antennas, aircraft model parameter changes, etc.
- o A shift in a portion of a port spectrum (specification waiver analysis).

3.2.3 Coupling Model Routine

This routine determines if a coupling path exists between two ports. If a path exists, the appropriate math model routines are used to compute the transfer ratio of all frequencies of interest. The models are:

- o Antenna-Coupled Transfer - This includes antenna-to-antenna and antenna-to-wire coupling on an aircraft (winged vehicle), a spacecraft (wingless vehicle), and over ground. Antenna model, and shading (diffraction) models for propagation around wings and fuselage are included.
- o Wire-to-Wire Transfer - These routines compute coupling within a wire bundle. Transfer models between open, shielded, and double shielded wires with both balanced and unbalanced configurations are included.
- o Case-to-Case Transfer - This model computes coupling resulting from electromagnetic leakage from equipment cases.
- o Filter Models - These routines compute losses due to filters between the emitter and receptor ports and the coupling medium. Models for single tuned stage, Butterworth, low-pass, and band reject filters are included.
- o Environmental Field Models - These routines compute the coupling of external and internal environmental electromagnetic fields, if present, to receptor ports.

3.3 DATA STORAGE FILES

There are three types of files used by IEMCAP for data storage: permanent, working, and scratch. Permanent files are generally tape or disk and used to store data and analysis results for use in subsequent runs. Working files are usually disk and provide temporary storage for the data in a form for use by the various analysis routines. They also provide intermediate data storage between IDIPR and TART. Scratch files are used for temporary storage within IDIPR and TART.

3.3.1 Permanent Files

These files are generally saved after a run or are input from a previous run. They are the old and new (updated) Intrasytem Signature Files and the Baseline Transfer File. A description of these follows:

Intrasytem Signature File (ISF) - This is also called the Intrasytem File (the two terms are used interchangeably). It contains all of the input data defining the system and the port spectra. Each time IDIPR is run, a new ISF containing any updates is generated. Hence the ISF is a data base file which can be maintained to incorporate any changes to the system design.

In a given run, there may be up to three ISF's. The old ISF, if present, was created during a previous run and is used as input to the given run. The new ISF is generated by IDIPR during the given run containing updates from card input, if present. If SGR is being run, an additional new ISF is generated during the TART execution. This file is the same as the IDIPR generated new ISF except it contains the adjusted port spectra.

Baseline Transfer File - This file is generated by TART during SGR or survey runs and contains the received signals, transfer ratios, and EMI margins for all coupled port pairs and from the total signal and environmental field into each receptor at all frequencies. It is an input to TART for waiver analysis and trade-off analysis runs.

3.3.2 Working Files

These files may or may not be saved for a given run, depending on whether IDIPR and TART are run independently or are run consecutively as one job. If run separately, for example to check the input data for errors only, the working files must be saved for TART. They can also be saved for restart in the event of errors. These files are as follows:

Unadjusted Emitter Spectrum File (UESF) - This file, as generated by IDIPR during initial processing, contains the initial broadband and narrow-band spectra for all emitter ports. During specification generation runs, SGR adjusts these spectra and writes them on the Adjusted Emitter Spectrum File (AESF). After all emitters have been examined and adjusted in conjunction with a given receptor, the AESF and UESF are swapped, and the process is repeated for the next receptor. For analysis tasks other than SGR, the UESF is used only as input by TART since no spectrum adjustments are made.

Unadjusted Receptor Spectrum File (URSF) - This file is the same as the UESF above except it contains receptor port spectra.

Emitter Equipment Data File (EEDF) - This file, built during initial processing, contains all equipment and port parameters except the port spectra for emitter ports. Because TART selects each receptor and analyzes all emitter ports in conjunction with it, data for emitters and receptors is placed on separate files for efficient processing. If a given port is both an emitter and receptor, the data is on both files.

Receptor Equipment Data File (REDF) - This is the same as the EEDF above except it contains receptor data.

Wire Bundle File (BUNDLE) - This file, built during initial processing contains all wire bundle data for the system. This data is in the form specified in IDIPR input data as described in Section 3.1.4.

Wire Map File - This file, built during initial processing, contains processed wire bundle data in the form of cross-reference map arrays generated by the Wire Map Routine (Section 3.1.4). This data is used as input to the wire-to-wire and field-to-wire transfer model routines in TART.

Array - This file, built during initial processing, contains basic system data, control flags, data change codes, and other data for use by TART.

3.3.3 Scratch Files

These files are used completely within either IDIPR or TART for temporary data storage. They are generally not saved after a run, but some share the same physical file as a permanent or work file which is saved. The PIF may be saved for restart. These files are as follows:

CARDIN - This file is used by IDIPR to store the card images of the input cards during input decode. It is later overwritten and used as the Wire Map File.

Processed Input File (PIF) - This file is built by IDIPR during input decode. For new jobs (no old ISF exists), the format of the PIF is the same as the ISF except there are no emitter and receptor spectra. For modify (updating an old ISF) jobs, the system data is not written on the PIF, but the equipment and wire bundle data are written in the same format as on the ISF.

Adjusted Emitter Spectrum File (AESF) - This file is used by TART during specification generation and contains the adjusted spectra for the emitter ports. The logical unit switches back and forth between AESF and UESF files each time the emitter spectra are re-adjusted as discussed above for the UESF.

Adjusted Receptor Spectrum File (ARSF) - This file is the same as the AESF except that it contains the adjusted receptor spectra.

SGR Scratch File (SGRF) - This is used during specification generation to store adjusted emitter spectra and transfer functions used in the determination of unresolved interference. The logical unit used is the one which was not used to store the final adjusted emitter spectra.

Scratch Transfer File (SCHTR) - This file is used by TART during specification generation and contains the transfer ratio from each coupled emitter into the receptor at each frequency.

3.4 RESTART CAPABILITY

IEMCAP saves analysis results at several stages of execution and provides file updating capability to use those on subsequent runs to avoid re-processing data. During Input Decode, error-free data is written to the Processed Input File. If errors occur during decoding, IDIPR halts after printing all errors and offending cards. The user can use the PIF as he does the old ISF file and update it with corrected data on the following run. An option also allows the user to proceed into Initial Processing even though errors occurred. Spectra will be generated for those ports which the data was found error-free. The results of Initial Processing, which performs file updates

and generates initial spectra for new and modified ports, are saved on the ISF. This file can be updated as many times as are needed until the user is satisfied with the result. If the SGR/CEAR option has been selected and provisions made to save the work files, the user is ready to run TART whenever IDIPR executes without error.

Section 4

INPUT DECODE AND INITIAL PROCESSING ROUTINE

This section describes the detailed operation of the IDIPR routines and subprograms discussed in general in Section 3.1.

4.1 INPUT DECODE ROUTINE (IPDCOD)

As discussed in Section 3.1.1, IPDCOD reads, decodes, and checks for errors all card input to IDIPR and writes the results on the Processed Input File. The inputs are in the form of statements consisting of a keyword, an equals sign, and a number of parameters separated by commas. The general form is

$$\text{KEYWORD} = P_1, P_2, P_3, \dots P_n$$

KEYWORD identifies the type of data. For example, EXEC indicates execution control parameters, and FUSLGE indicates aircraft fuselage parameters. The parameters may be numbers, specific alphanumeric codes, or user-supplied alphanumeric identification names (ID's). For most keyword types the number of parameters is fixed, and the proper number must be given or an error results. In some cases, a parameter is replaced by a set of subparameters enclosed in parenthesis. For example

$$\text{KEYWORD} = P_1, P_2, (\overbrace{sp_1, sp_2, \dots}^{P_3}), \dots P_n$$

Each set of subparameters counts as one in the parameter count. For modify runs, in which an old ISF data is updated by card input, the keyword is followed by an M, D, or A in parenthesis to indicate that the data is to be modified (data on the card is to replace the old ISF data), deleted, or added. (See Section 2.3 of Volume II for a detailed description of the input format.)

The IPDCOD routine flow, in which these cards are decoded and stored, is shown in Figure 14. A card is read, and the individual characters placed into storage arrays. Blanks are suppressed. If the last non-blank character is a comma, indicating continuation, the next card is read and its contents are appended. This continues until a 10 card "supercard" is constructed or until a card is found not terminated in a comma. Each card is temporarily stored on the file CARDIN for later listing.

The portion of the supercard array prior to the equals sign is decoded first. Each character in the array is examined in sequence until an equals sign is located indicating the end of the keyword. If no equals is found, to be valid the keyword must be EODATA. This indicates the end of data and is the only card allowed without an equals sign. An error message is printed if this is not the case. If there was an equals sign and the job is a modify run, the presence of a modify code in parenthesis just before the equals is tested. If not present, the status is assumed to be add.

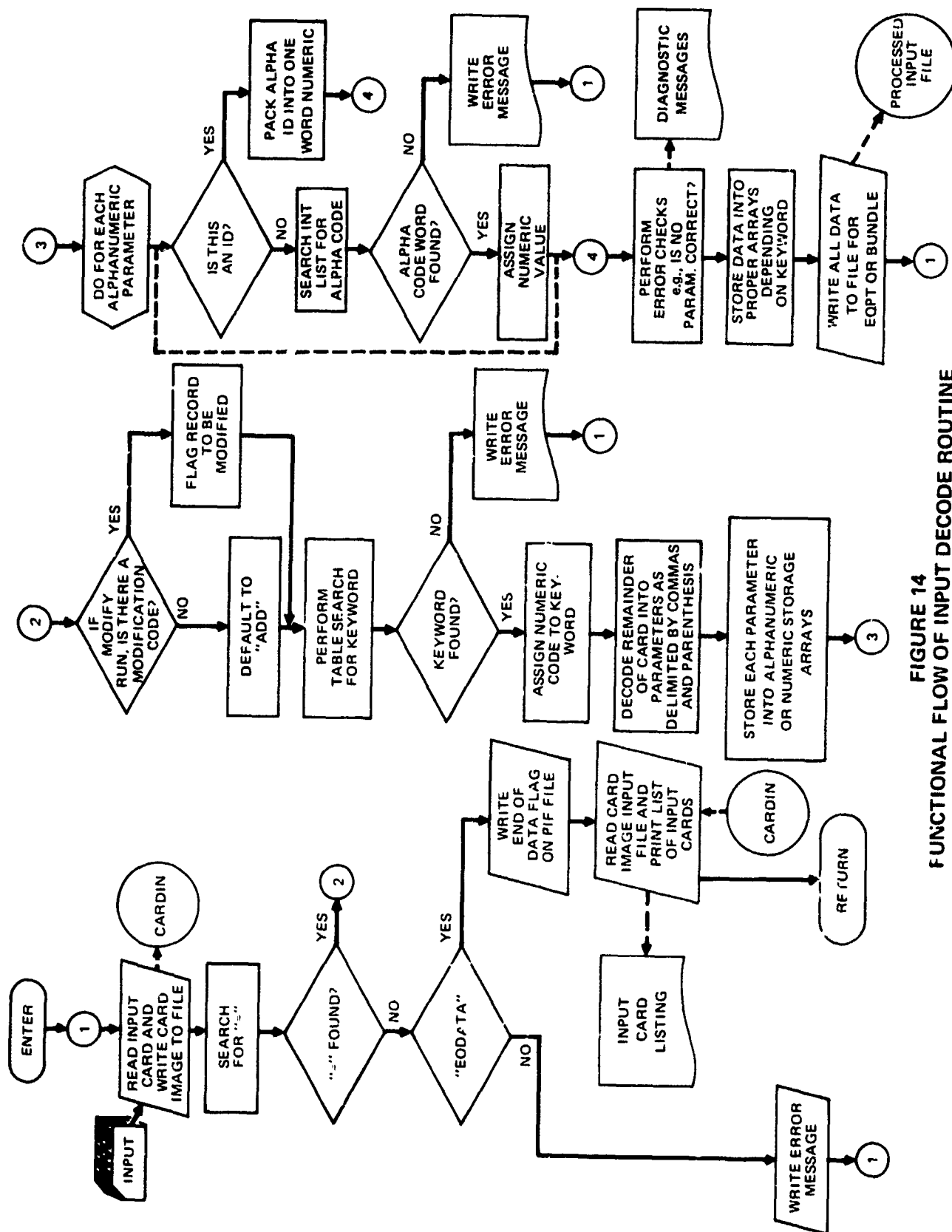


FIGURE 14
FUNCTIONAL FLOW OF INPUT DECODE ROUTINE

Next, the first two characters in the keyword are compared to the internal table of valid keywords. If no match is found, an error is printed. If the keyword is found, a numeric code equivalent is assigned and stored.

The remainder of the supercard following the equals is then scanned. When a delimiter (comma or parenthesis) is encountered, indicating the end of a parameter, the parameter is tested to determine if it is a number or an alphanumeric code or ID. If a number, its value is determined and stored. If alphanumeric, the characters are temporarily stored. After the supercard has been scanned, each of these alphanumeric parameters are tested to determine if it is an ID or a code. If it is an ID, the characters are packed into one word using the IEMCAP internal code. (See Volume II, Section 4.3 for explanation of this code.) If the alphanumeric code is not an ID it must be one of a number of specific codes associated with the keyword. The first two characters are compared to the list of valid codes, and if valid, an equivalent numeric code is assigned and stored. If the code is invalid, an error message is printed. After the alphanumeric parameters have been processed, the number of parameters detected is checked against the number associated with the keyword, and an error message is printed if incorrect.

If there are no errors in the supercard, the parameters are stored in appropriate arrays. If there was an error, the card is deleted, i.e., the data is not stored; and a message to this effect is printed.

System level data (system parameters, flags, common component parameters, etc.), subsystem data, and wire bundle data are stored on the PIF. The subsystem data (equipment, port, and source/receptor hierarchy) is stored by equipment. Likewise, the wire bundle data (bundle, segment, endpoint, and wire hierarchy) is stored on the PIF by bundle. The routine continues processing input cards until the EODATA card is read. A complete listing of all input cards is then printed, and the routine returns control to the main program.

In the program the functions described are performed by a number of subroutines. The basic subroutine is CARDIN. See the IEMCAP Computer Program Documentation for further program details.

4.2 INITIAL PROCESSING ROUTINE (IPR)

As discussed in Section 3.1.2, this routine assembles the data for a given analysis and interfaces with the spectrum model routines to generate the initial spectra. It then generates a new ISF and the working files. The basic subroutine containing IPR in the program is MERGE. A functional flow diagram of IPR is shown in Figure 15.

For any given run, the job status is either new, old, or modify. For a new job, the data is entirely from card input stored on the PIF; for an old job, entirely from an old ISF; and for a modify job, from old ISF data updated by card input stored on the PIF. The first step in the routine, therefore, is to set the appropriate control variables for the proper input files. If the job status is new, the primary input is from the PIF. Otherwise the primary input is from the old ISF. For modify jobs, a secondary input is the PIF.

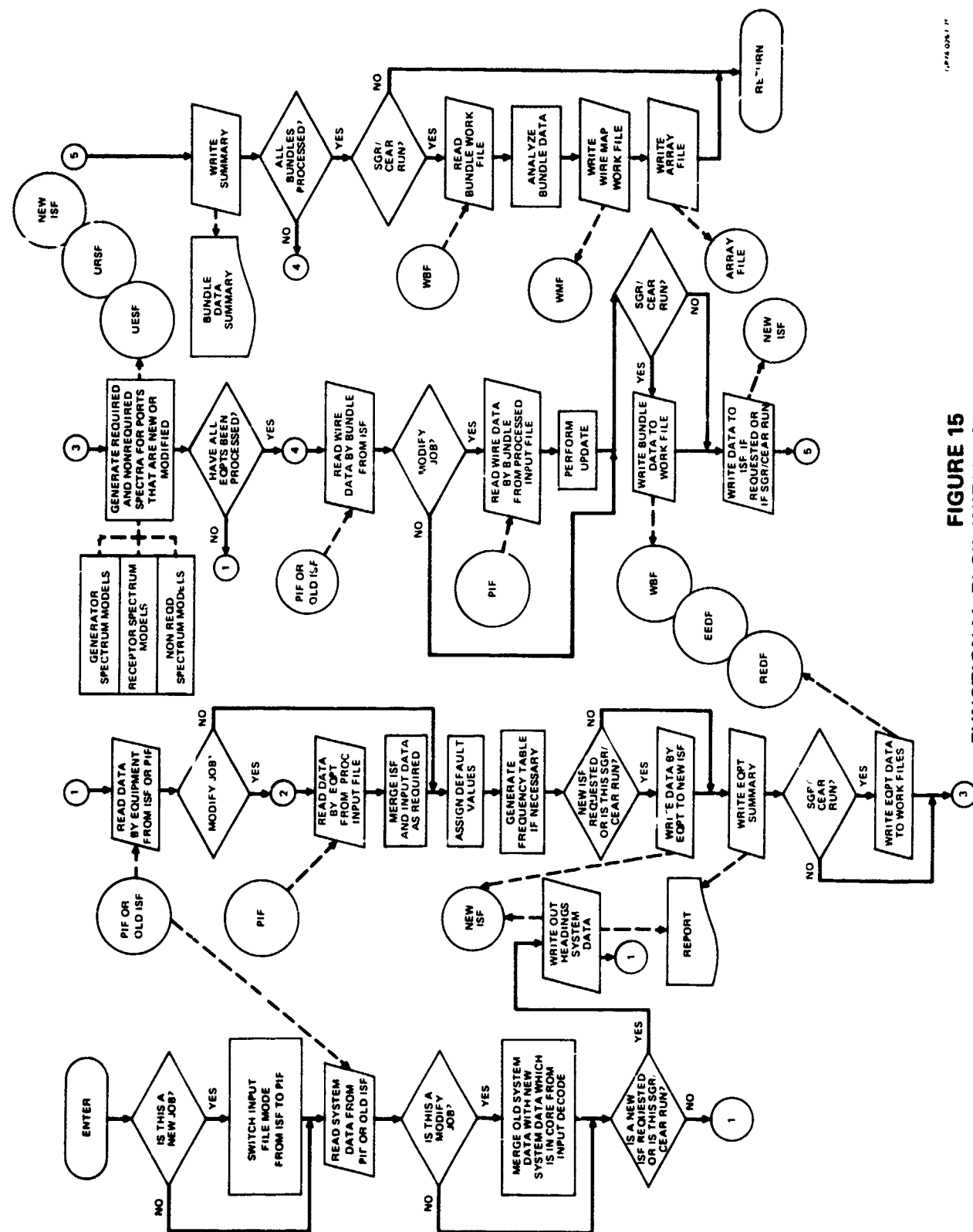


FIGURE 15
FUNCTIONAL FLOW INITIAL SPECTRA PROCESSING

The system level data is processed first. The baseline system data is read from the primary input (PIF or old ISF as defined above). If the job status is modify, the newly defined system data is still in core from IPDCOD. The new data is merged with (i.e., used to update) the old data as read from the old ISF. If not a modify run, the merge operation is skipped. When IDIPR is run alone to check input data, the user can control the generation of the new ISF. Otherwise, it is automatically generated. If it is to be generated the system data is written on the new ISF and printed in the report.

The subsystem data is processed next. All equipment, port, and source/receptor parameters associated with a given equipment are read from the primary input. If the status is modify, the updating data is read from the PIF and used to add, delete, or replace the primary input parameters, as required. After this, any missing or zero parameters for which default values are available are identified, and the default values are assigned. The spectrum sample frequency tables are generated next if non-existent or changed. The equipment processed data is then written on the new ISF, on the emitter and receptor equipment data working files, and printed in the report, as required.

The routine then generates initial spectra for ports which have been added or modified using the spectrum math model routines. This process is discussed in detail in Section 4.3. All spectra are written on the unadjusted emitter and receptor spectrum working files, the new ISF, and printed in the report, as required.

When all equipments have been thus processed, the routine then processes the wire bundle data in a similar manner. The bundle, segment, endpoint, and wire parameters associated with a given bundle are read from the primary input. If necessary, it is merged with data from the PIF, as with the equipment data. The processed data is written on the Wire Bundle File, the new ISF, and printed in the report, as required. The above is repeated until all bundles have been processed.

The Wire Map Routine is then called to generate the cross-reference arrays which are written on the Wire Map File. This routine is discussed in Section 4.4.

Finally, the routine writes the basic run parameters and control flags on the array file. It then returns to the main program.

4.3 SPECTRUM MODEL ROUTINE (SPCMDL)

This routine interfaces the IPR and the various math model routines which compute the port spectra. IPR provides the table of sample frequencies associated with the equipment and the user-defined input parameters for the port spectra. From these, SPCMDL utilizes the appropriate math model routines to generate tables of amplitudes quantized to the sample table frequencies over the range for the particular port type (Table 1). The quantization process is discussed in Section 2.2.2.1.

Figure 16 shows the flow through SPCMDL. Emission spectra are computed first. The routine selects a sample frequency from the table and determines the interval boundary frequencies. (See Section 2.2.2.1). It then determines if the port is an equipment case. If so, there is no termination impedance or required frequency range. The maximum broadband and narrowband emission levels and the minimum susceptibility level in the interval are determined. There is a provision in which the user may provide his own narrowband or broadband spectrum or both for an equipment case. User provided spectra for an equipment case overrides the military specification levels of MIL-STD-461A and MIL-I-6181D. The user spectrum is quantized to the selected sample frequency.

If the port is not an equipment case, it has a termination impedance, and the magnitude of the impedance is evaluated. (See Figure 1 for impedance configuration.) SPCMDL then checks the port type. If it is a powerline or an electroexplosive device (EED), there is no required frequency range. The appropriate model is called to determine the spectrum levels.

If the port is not one of the above types, it is either a radio frequency (RF) or a signal/control port and has a required frequency range. The sample interval is tested to determine if any part of it is within this range. If so and the spectrum is user-defined by frequencies and amplitudes, LOGLIN, which determines the maximum emission and minimum susceptibility level within the sample interval, is called. For an RF port a user frequency is relative to the carrier. In this case, SPCMDL positions the defined RF spectrum about the carrier before quantization. If an RF port carrier is tunable, the carrier is positioned at the frequency closest to the sample frequency as the worst case before the minimum or maximum level in the interval is determined.

If the sample interval is within the required range and the spectrum is not user defined, the Required Emission Spectrum Model driver (SCARFE) or Required Susceptibility Spectrum Model driver (SCARFR) is called, which in turn calls the appropriate math model routine to compute the spectrum level. All of these models produce curves which are monotonically increasing or decreasing or at a peak within the sample interval. If the peak (or minimum for susceptibility) is within the interval, this level is used. If the curve is increasing or decreasing, the model is called at each boundary frequency, and the maximum or minimum of these levels is used. For RF ports, the carrier, if tunable, is positioned as close to the sample frequency as allowed by the tuning range.

If the sample frequency is outside the required range, the MIL-STD-461A or MIL-I-6181D curve evaluation routines are called, and the maximum or minimum level (including the displacement factor) is determined. For RF ports, the sample interval is tested to determine if a carrier harmonic is contained within the interval. If so, the level at the harmonic is used if greater than the military specification level previously computed.

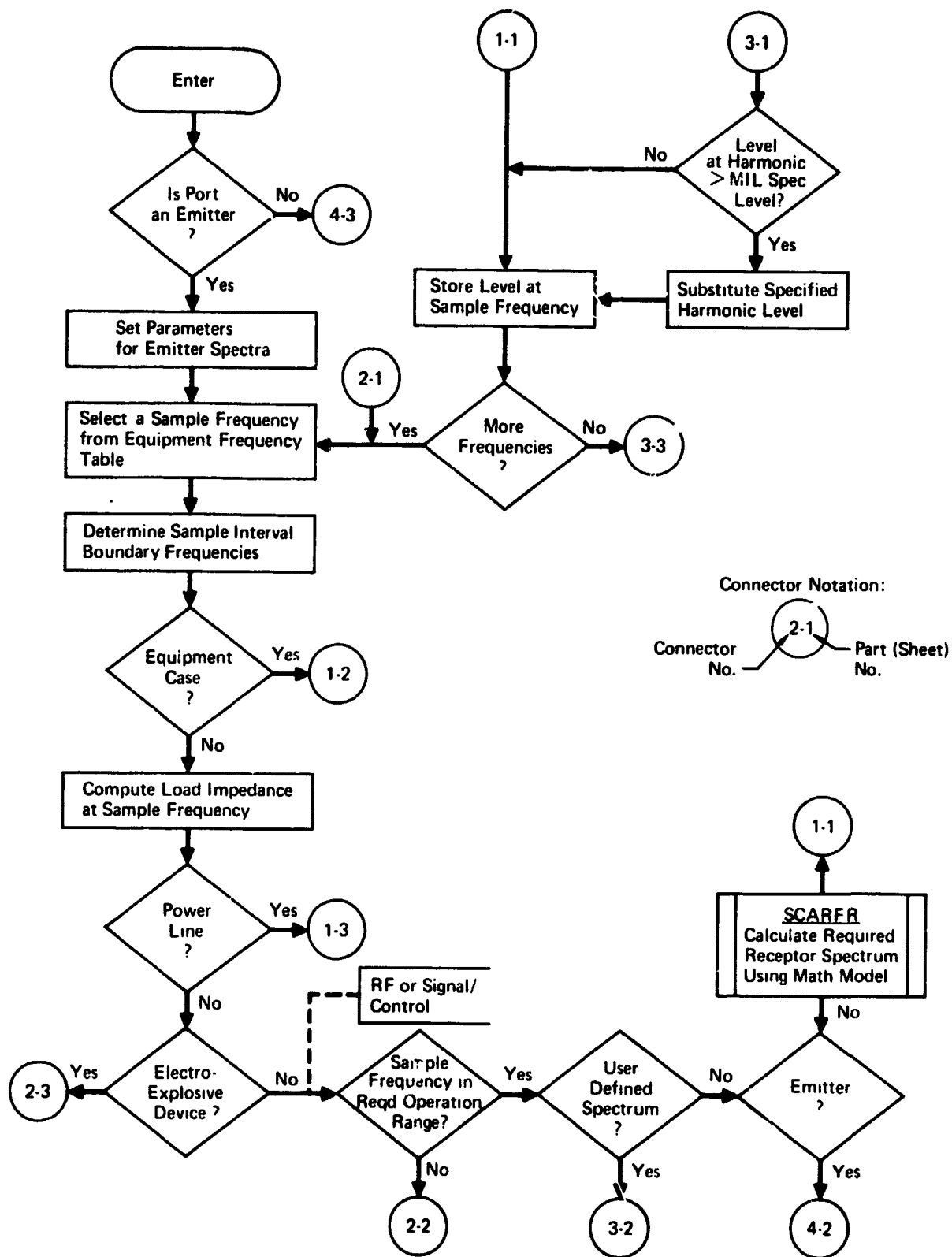


FIGURE 16
SPECTRUM MODEL ROUTINE (SPCMDL)
 (Part 1 of 3)

GP74 0267 71

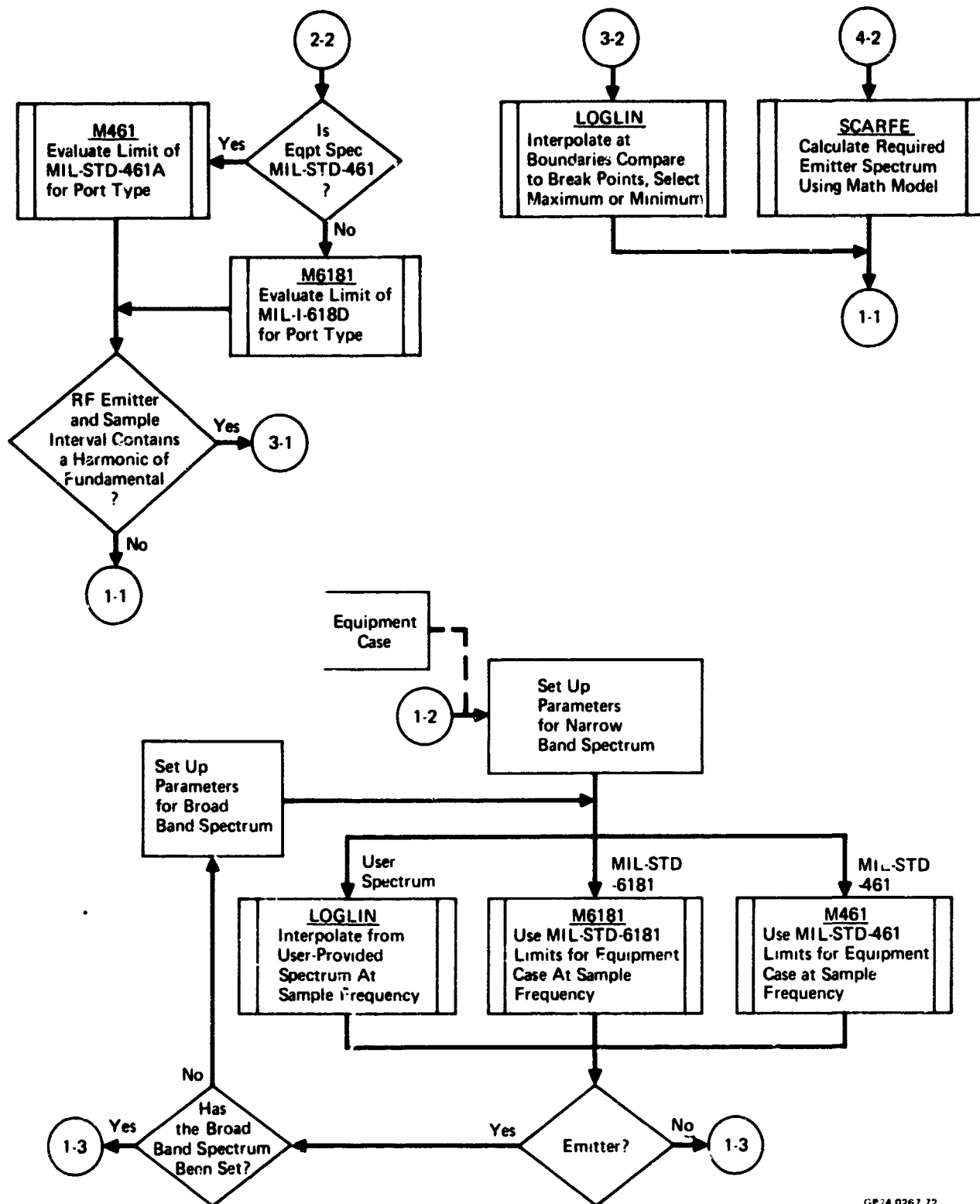
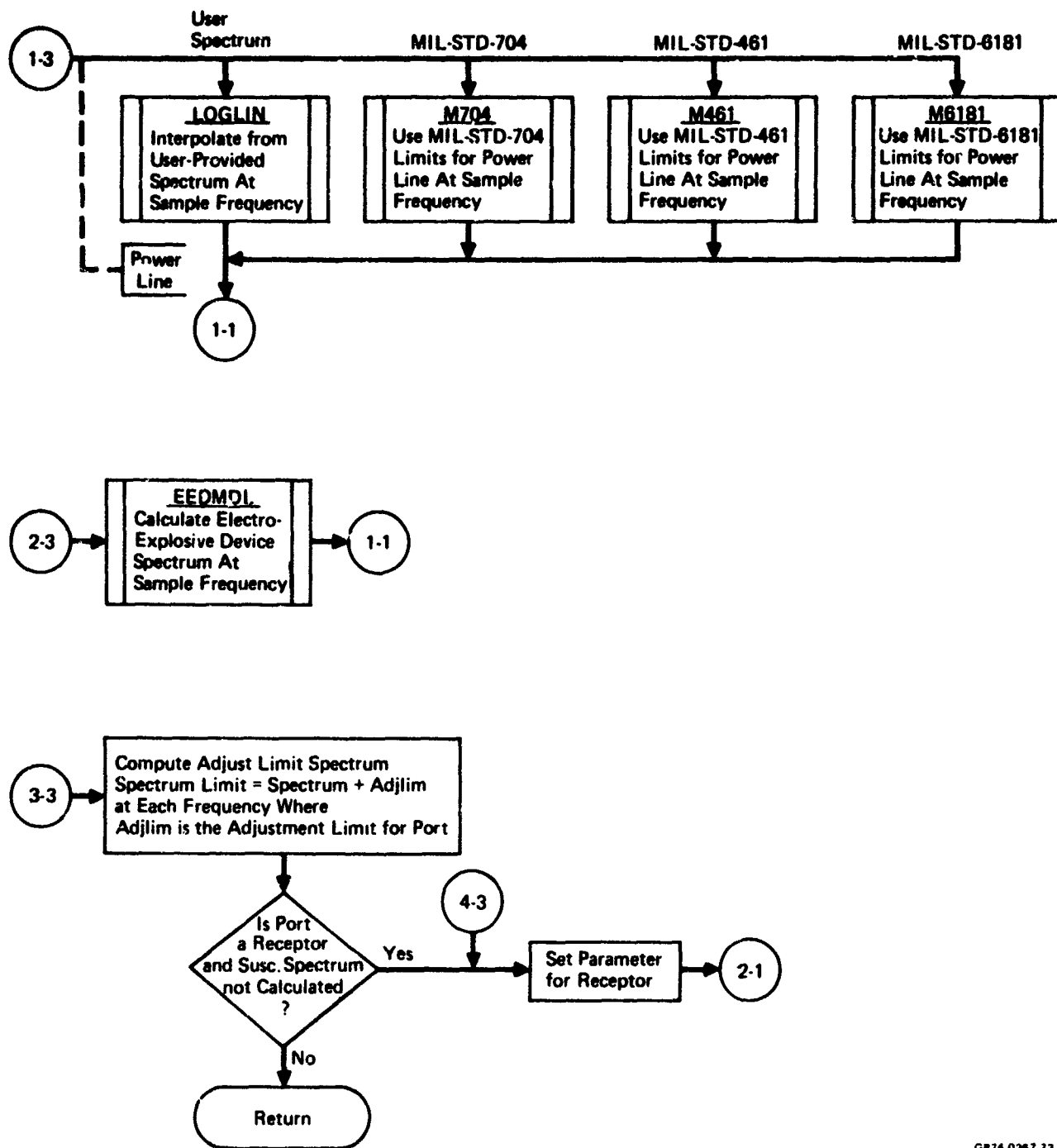


FIGURE 16 (Continued)
SPECTRUM MODEL ROUTINE (SPCMDL)
(Part 2 of 3)

GP 74 0267 72



GP74 0267 73

FIGURE 16 (Continued)
SPECTRUM MODEL ROUTINE (SPCMDL)
(Part 3 of 3)

The sampled spectrum level is stored, and the above process is continued until levels have been determined at all sample frequencies within the frequency range for the port type for emission and/or susceptibility as required. The adjustment limit curve amplitudes are then computed from the spectra. At each sample frequency, the spectrum adjustment limit displacement factor (adjlim) is added to the emission spectrum levels and subtracted from the susceptibility levels. These displaced levels are stored along with the spectrum levels. The routine then returns control to the IPR.

o Unrequired Spectrum Models (M461, M6181, M704)

These subroutines provide the spectrum specifications corresponding to MIL-STD-461A, MIL-I-6181D or MIL-STD-704. When linear interpolation is required, the subroutine LOGLIN is called by these routines, which determines the maximum or minimum level in the sample interval. The initial spectrum displacement factors, sdfs and sdfr, are added to or subtracted from these levels respectively for emitters and receptors.

o Required Emission Spectrum Models (SCARFE)

The routine SCARFE (see Figure 17) calculates the required spectrum levels of a signal/control or RF emitter. For an RF port SCARFE calls one of four subroutines, depending on the modulation/signal (MODSIG) code. For a simple CW signal, it calls the subroutine CW; for pulse modulation, it calls subroutine PULSE; for a radar (pulse modulated RF), it calls subroutine RADAR; and for analog modulation, it calls subroutine ANLOG. The ANLOG routine, in turn, calls VOICE, clipped voice (CVOICE), non-voice (NVOICE), or frequency modulation (FM). For a signal or control port, SCARFE calls the subroutine SIGCON, which also may call VOICE or CVOICE. These models are discussed in detail in Section 6.

o Required Susceptibility Spectrum Models (SCARFR)

The routine SCARFR (see Figure 18) calculates the required susceptibility spectrum levels of a signal/control or RF receptor port. For RF ports, the user-provided sensitivity is used; otherwise the susceptibility is set to 20 dB below the operating voltage or current.

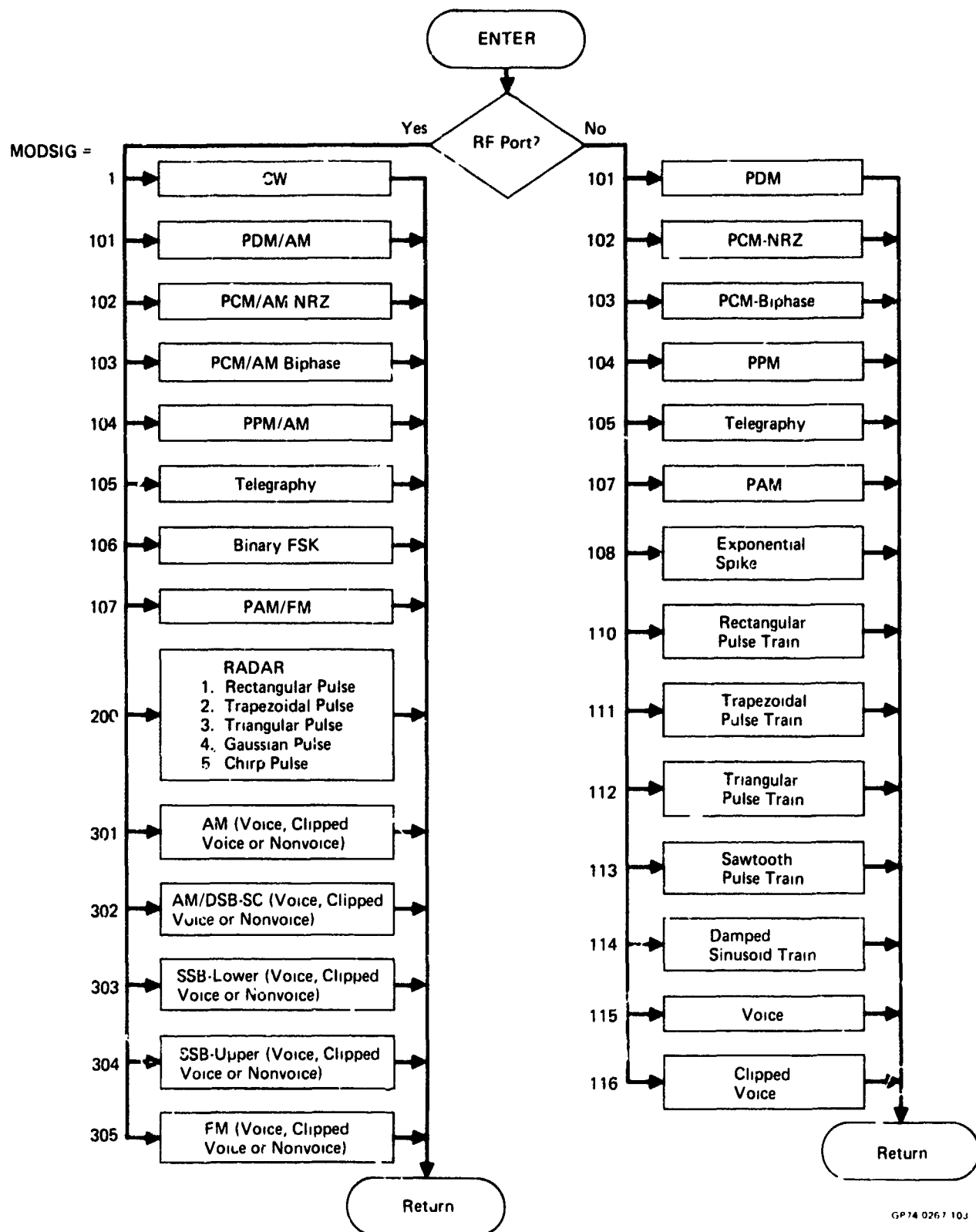
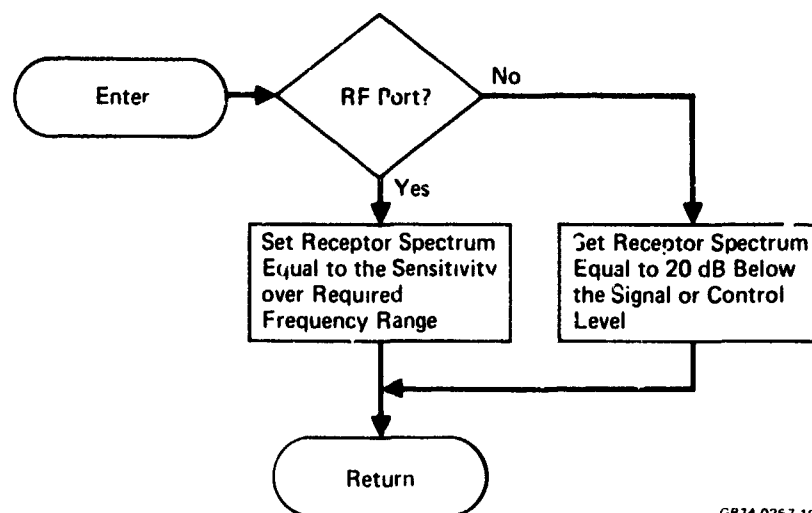


FIGURE 17
REQUIRED EMITTER SPECTRUM MODELS
(SCARFE)



GP74 0267 102

FIGURE 18
REQUIRED SUSCEPTIBILITY SPECTRUM MODELS
(SCARFR)

Section 5

TASK ANALYSIS ROUTINE

This Task Analysis Routine (TART) section of IEMCAP performs the four basic analysis tasks previously discussed. The functional flow and major components of TART are shown in Figure 13. First, TART reads the system data and run parameters from the new ISF and Array files as generated by IDIPR. Then the appropriate task driver routine is entered. If the task specified is SGR, the Specification Generation Routine (SGR) is entered, otherwise the Comparative EMI Analysis Routine (CEAR) is entered. These two routines interface with the work files, coupling path model, and analysis routines to perform the specified task. The coupling path routines determine if a path exists and compute the transfer ratio if it does. The analysis and spectrum adjustment routines use the emitter, receptor, and transfer ratio spectra to compute the received signal and EMI margins for emitter-receptor port pairs as well as the total signal from all coupled emitters into each receptor. These routines also adjust the non-required spectra for SGR runs.

5.1 SPECIFICATION GENERATION ROUTINE (SGR)

5.1.1 Description

SGR attempts to adjust the non-required portions of the port spectra, initially computed in IPR, to produce a compatible system. These spectra are limits. That is, an emitter cannot generate outputs greater than the non-required spectrum levels, and a receptor cannot respond to received signals less than these levels or interference will result. For the analysis, each port is assumed to emit and respond at these levels. For each emitter-receptor port pair in the system with a coupling path between them, the received signal is computed using the assumed maximum emission levels. This signal is compared to the assumed minimum susceptibility levels over the frequency range, and where the susceptibility level is exceeded in the emitter non-required range, the emission levels are reduced such that the margin is equal to the user-defined adjustment safety margin (asm) or to the adjustment limit level whichever is greater.

When each emitter has been adjusted in conjunction with each receptor, the receptor spectra are adjusted. The received signal from each emitter with a coupling path to a given receptor is computed using the adjusted emission spectra and summed. The susceptibility spectrum levels are then compared to this total signal, and where the level is exceeded in the non-required range, the susceptibility is raised such that the margin is asm or to the adjustment limit level whichever is less.

As a result of this process, a set of port spectra are generated such that the system will be compatible if not exceeded. These, then, are EMC specification limits to which the equipment ports can be tested. The test methods are discussed in Volume II, Appendix A.

After the adjustment process, a number of port pairs may exist which are still incompatible. This is called unresolved interference and results from required emissions and responses, non-required spectra adjusted to their limits, and from non-adjustable spectra of previously procured equipments. Consequently, after receptor adjustment, SGR recomputes the interference between adjusted emitters and adjusted receptors. If the maximum of the EMI margin exceeds a user-specified printout limit (empl), the case is printed as unresolved interference along with a summary of the spectrum levels and the EMI margins.

5.1.2 Routine Operation

A flow diagram of SGR is shown in Figure 19. After all files are rewound and pointers are initialized, the routine selects the first receptor port and calls the Receptor File Read (RCPTRD) routine which reads the equipment and spectrum data from the working files. SGR then searches for emitter ports coupled to the selected receptor. The Emitter File Read (EMTRD) routine is called to read the equipment and spectrum data for an emitter port, and the Coupling Path (COUPLE) routine is called. COUPLE tests the port pair type and connection to determine if a path exists, and if it does, it calls the appropriate transfer model routine to compute the transfer ratio at each emitter and receptor frequency common to the two ports. (The operation of COUPLE is discussed in Section 5.1.2.1.)

If a coupling path does exist, the Emitter Margin Calculation and Spectrum Adjustment (EMCASA) routine is called to adjust the emitter broadband and narrowband spectra. (EMCASA is discussed in Section 5.1.2.2.) The transfer ratio arrays are then saved on a scratch file for later use. Also, a summary is printed showing the adjusted spectrum levels, adjusted EMI margins, received signal levels, amount of adjustment, integrated EMI margin, and other pertinent information. (See Volume II, Section 4.2 for description and examples of SGR outputs.)

The emitter spectra, adjusted or not, are then written on the Adjusted Emitter Spectrum File (AESF), and EMTRD is again called to select the next emitter. This process continues until the last emitter has been selected. At that time, the emitter work files are rewound, and the adjusted and unadjusted spectrum file logical unit indices are swapped. The emitter spectra adjusted in conjunction with the currently selected receptor will now be read and adjusted in conjunction with the next receptor. This swapping of adjusted and unadjusted files, therefore, results in cumulative adjustment of the emitter port spectra in conjunction with all receptors.

After the above process has been repeated for all receptor ports, each receptor spectrum is adjusted in conjunction with the total signal. The first receptor port is again selected and the Receptor Signal and Spectrum Adjustment Routine (Section 5.1.2.3) is entered. It uses the finally adjusted emitter spectra and the transfer ratio arrays, previously stored on the scratch transfer file, to compute the total signal at each receptor from all emitters coupled to it and adjusts the susceptibility spectrum accordingly. During this, the matched emitter spectra and transfer ratios are temporarily stored on another scratch file.

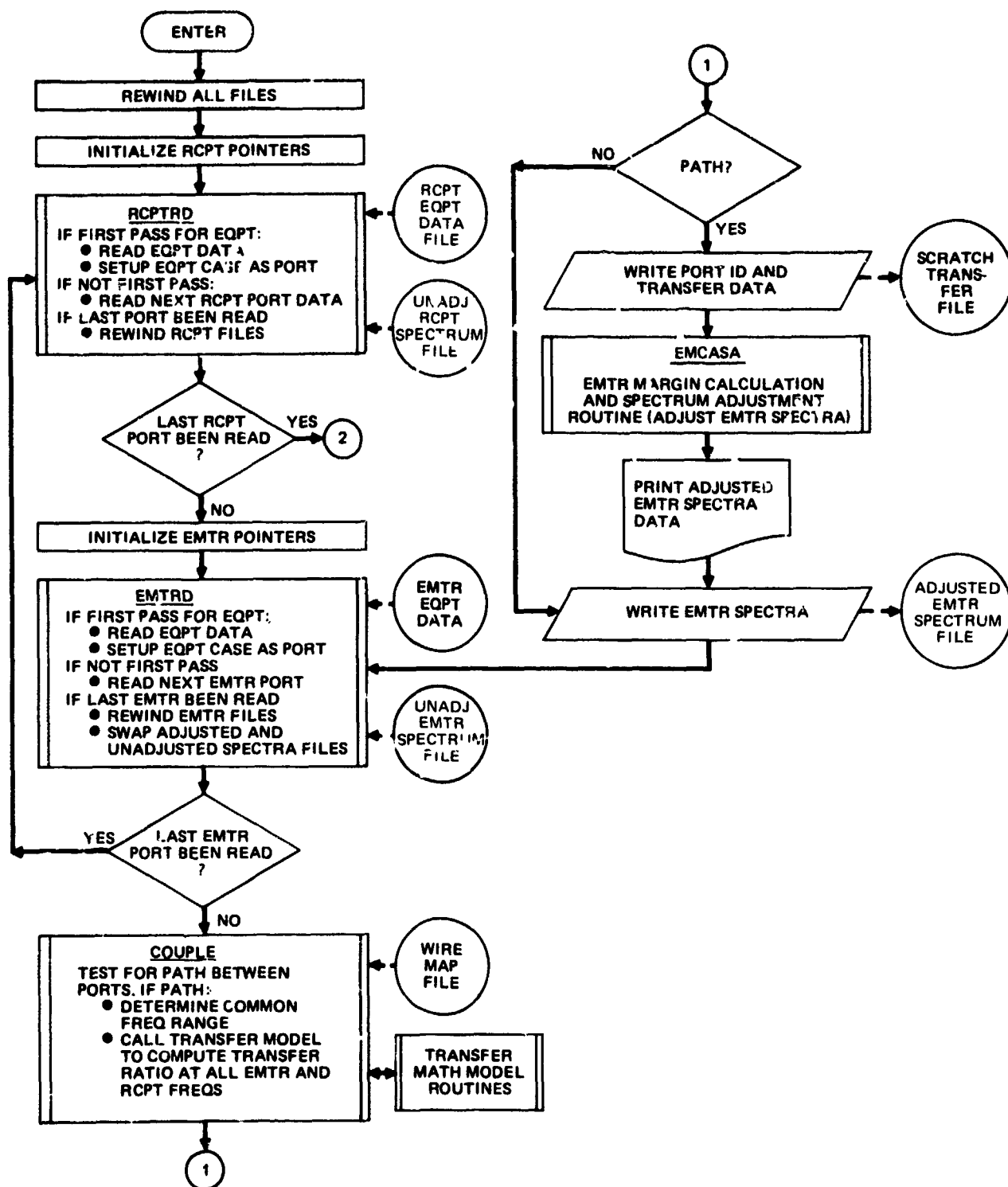
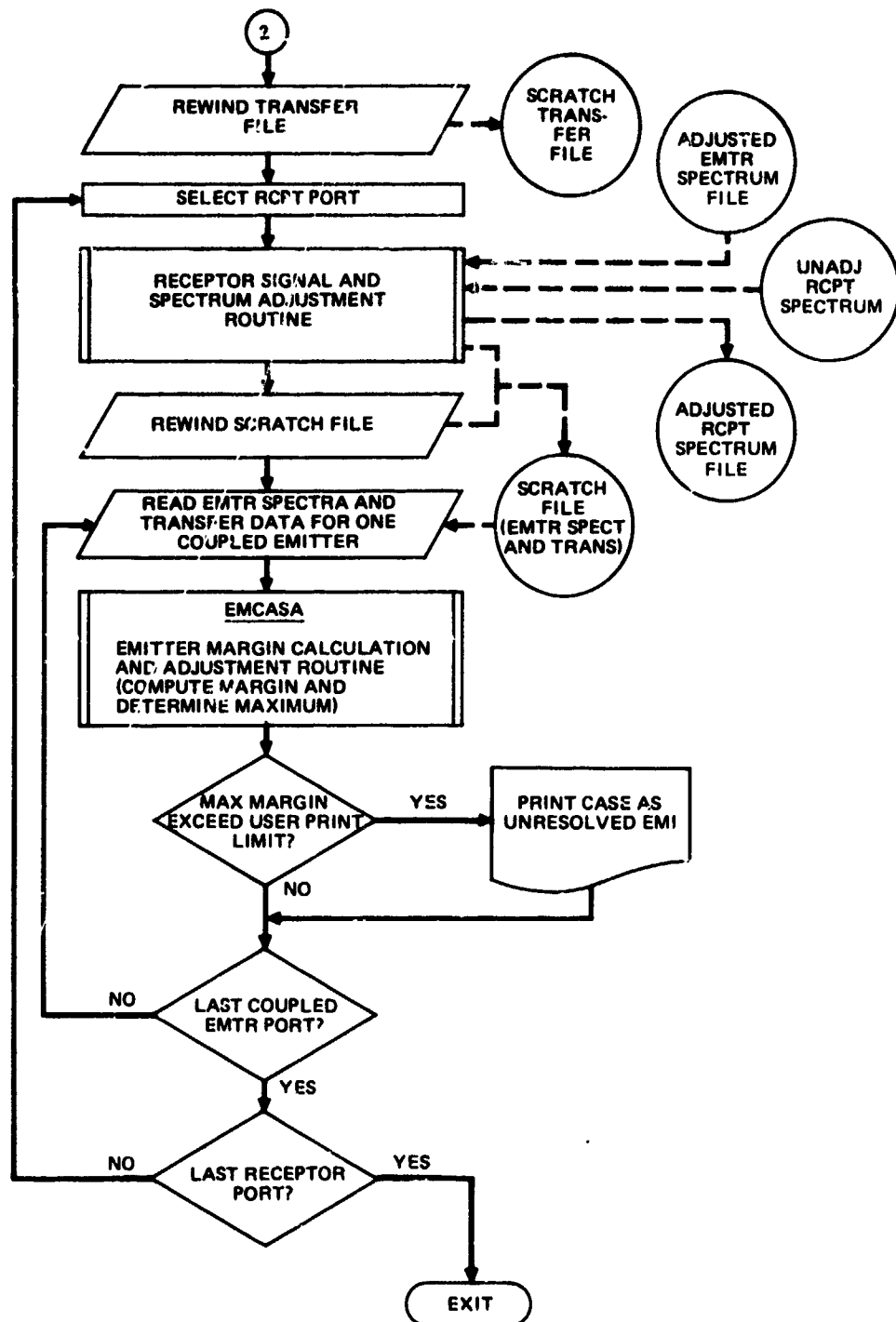


FIGURE 19
SPECIFICATION GENERATION ROUTINE FUNCTIONAL FLOW DIAGRAM

GP74 0267 18



GP74 0267 79

FIGURE 19 (Continued)
SPECIFICATION GENERATION ROUTINE FUNCTIONAL FLOW DIAGRAM

After each receptor spectrum is adjusted, the information stored on this second scratch file is used to compute the EMI margins from each coupled emitter to the adjusted receptor. If the maximum of this margin exceeds empl, the case is printed as unresolved EMI. The next receptor is then selected, the total signal to it is computed, its spectrum is adjusted, and the coupled emitters tested for unresolved EMI. This is repeated until all receptor ports have been processed. The routine then returns control to the main program.

The finally adjusted emitter and receptor port spectra are printed and used to generate an ISF for use in future runs. Also, during the above process, a BTF is generated containing the transfer ratios and EMI margins for future trade-off and waiver analyses.

5.1.2.1 Coupling Path Routine (COUPLE) - This routine tests a port pair for a coupling path between them. If a path exists, COUPLE identifies the path type, determines the common frequency range, and calls the appropriate transfer routine which computes the transfer ratio at the emitter and receptor frequencies within the common range. If the emitter and/or receptor have filters associated, COUPLE calls the filter model routine and includes the filter factors in the transfer ratios.

A flow diagram of the routine is given in Figure 20. Upon entry into COUPLE, it first tests for common equipment. If both emitter and receptor ports are within the same equipment, they are assumed compatible, and no path exists. If they are not in the same equipment, the port types are tested for one of the paths shown in Table 5.

If there is a path, further culling may be necessary. For antenna-to-antenna, the port pair is rejected if they share the same antenna. The coordinates are checked, and if the same there is no path. For wire-to-wire a series of tests are made. To have a path, the wires of the two ports must be in the same bundle. If in the same bundle, they must not be connected to the same wire except a power wire. If these requirements are not met, there is no path. For case to case, the locations of the two boxes are checked. If they are in different compartments, there is no path. In any of the above if there is no path, COUPLE returns to the calling routine and indicates no path.

If there is a path, the frequency ranges of the two ports are examined to determine the common range. If there is no overlap, the routine indicates no path and returns. If there is, the range is determined, and the appropriate transfer model routine is called to compute the transfer ratio at each emitter and receptor frequency over the common range. These are the Antenna Coupled Transfer Evaluation Routine (ACTFER) for antenna-to-antenna and antenna-to-wire coupling, the Wire-to-Wire Transfer Function Routine (WTWTFR), and the Case-to-Case Transfer Function Routine (CTCTFR). If COUPLE is called with the emitter designated as an environmental field, the Environmental Field Routine (ENVIRN) is called. If either or both ports have associated filters the Filter Model Routine (FILTER) is called, and the filter factors are added

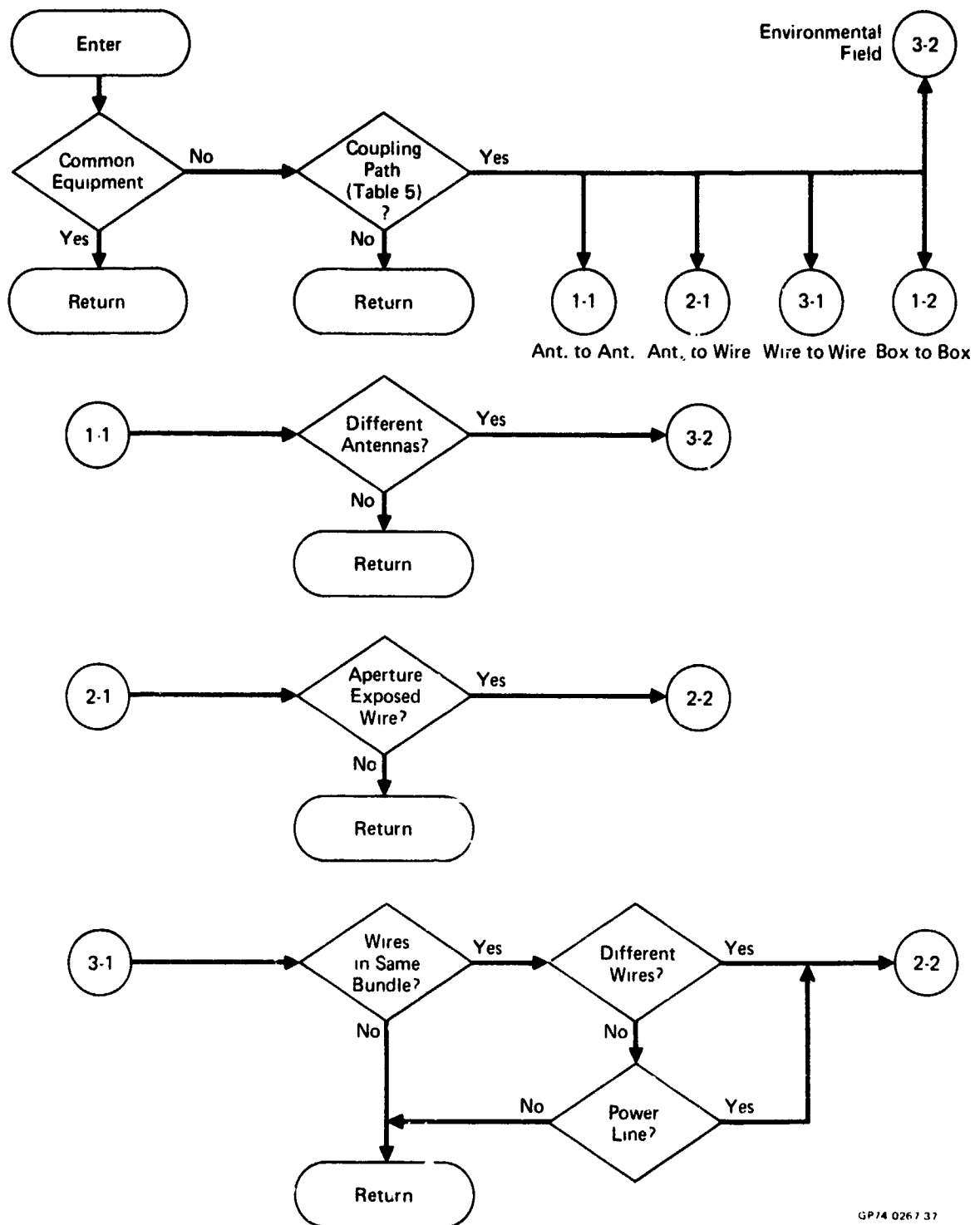
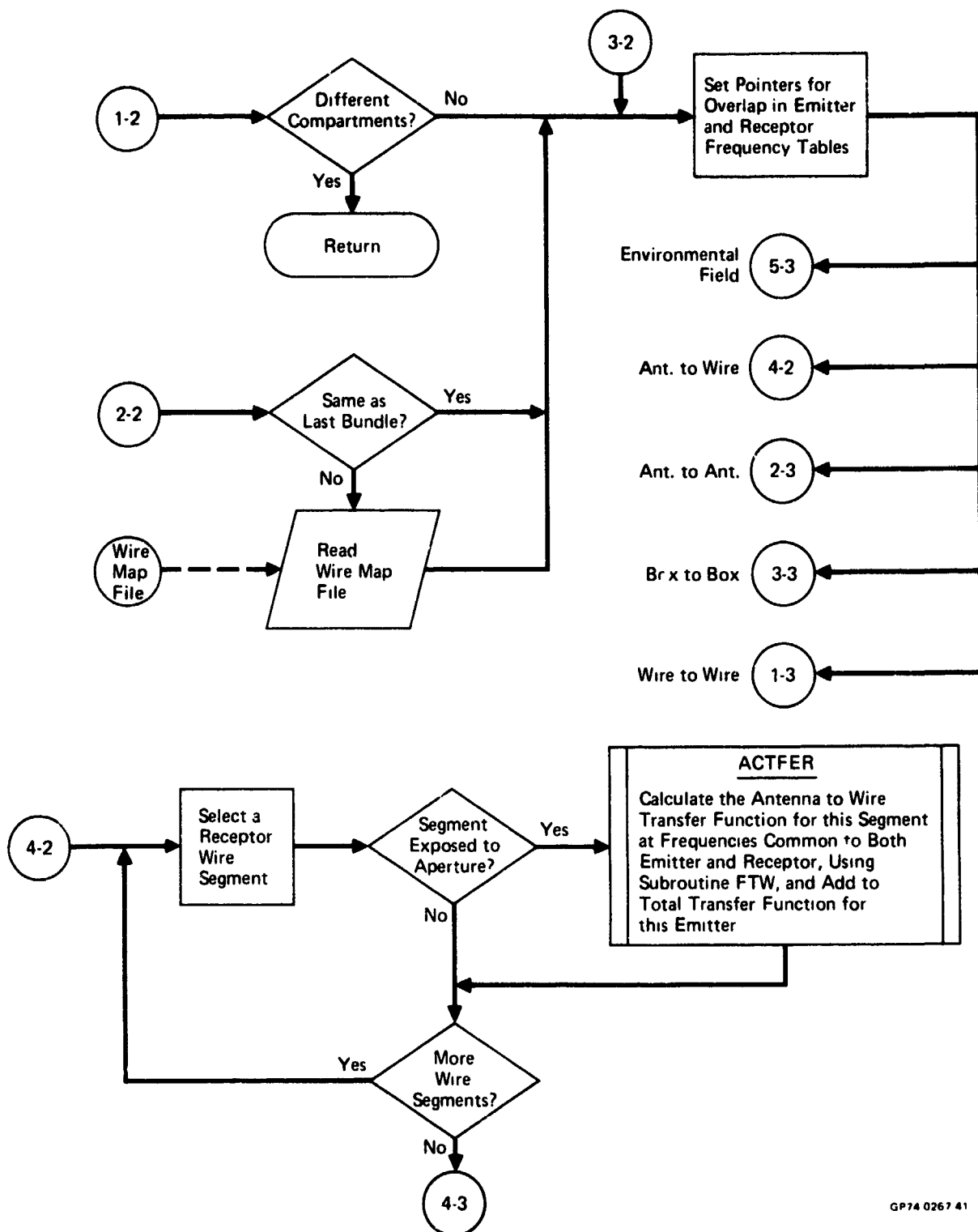
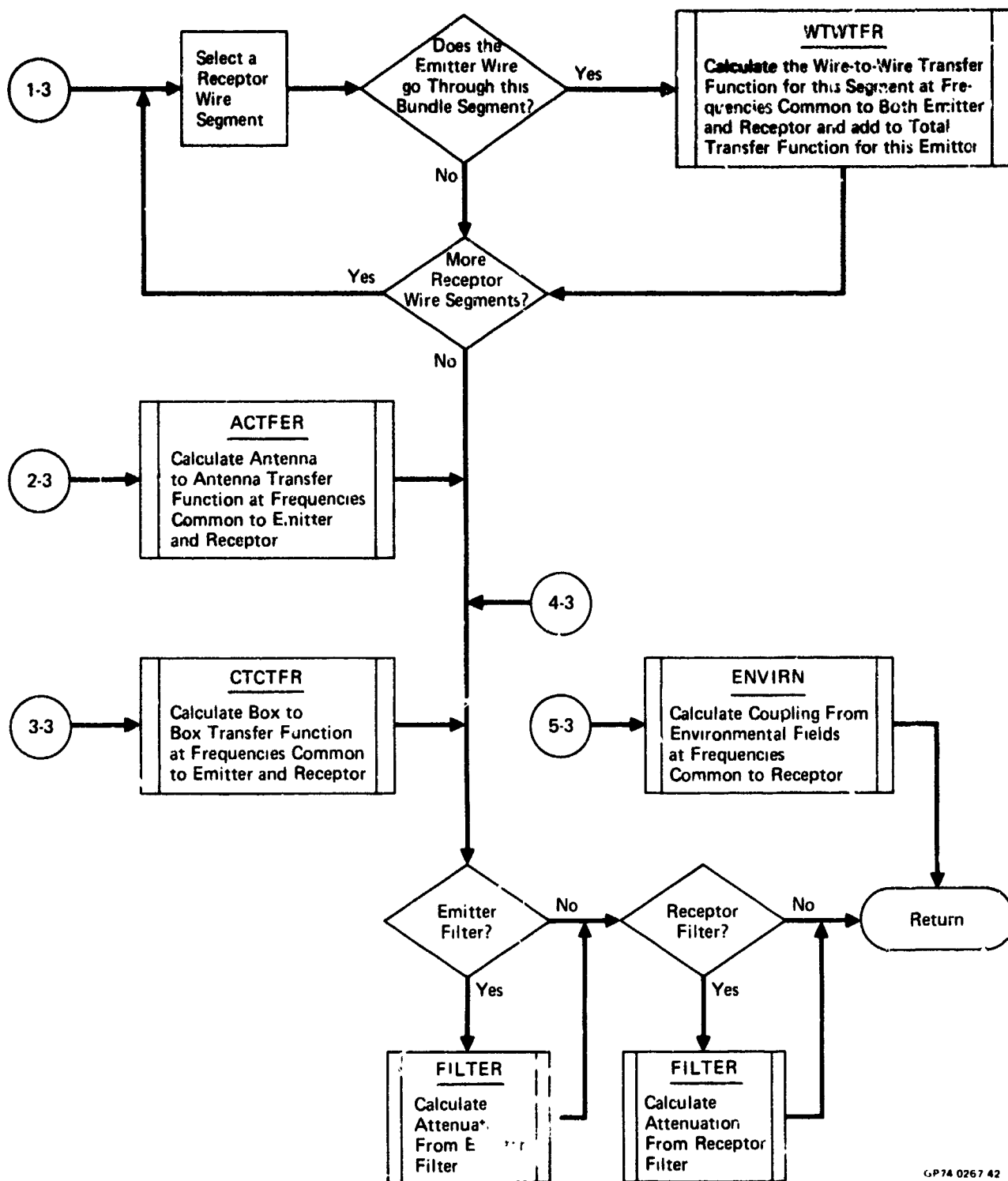


FIGURE 20
COUPLE SUBROUTINE
 Called by SGR and CEAR
 (Part 1 of 3)



GP74 0267 41

FIGURE 20 (Continued)
COUPLE SUBROUTINE
(Part 2 of 3)



GP74 0267 42

FIGURE 2G (Continued)
COUPLE SUBROUTINE
(Part 3 of 3)

Emitter Port Connection	Receptor Port Connection			
	Antenna	Nonexposed Wire	Aperture-Exposed Wire	Equipment Case
Antenna	1	0	2	0
Nonexposed Wire	0	3	3	0
Aperture-Exposed Wire	0	3	3	0
Equipment Case	0	0	0	4
Codes 0 = No Path 3 = Wire-to-Wire 1 = Antenna-to-Antenna 4 = Case-to-Case 2 = Antenna-to-Wire				

GP74 0267 121

TABLE 5
PORT COUPLING PATH CODES

to the transfer ratio. (Detailed descriptions of these models are given in Section 6, and the above routines are described in Section 5.3.) COUPLE then returns to the calling routine.

5.1.2.2 Emitter Margin Calculation and Spectrum Adjustment Routine

(EMCASA) - This routine computes the received signal and EMI margins for port pairs and performs the emitter spectrum adjustment. A functional flow diagram of EMCASA is presented in Figure 21 along with the basic analysis equations; the symbols used are defined in Table 6.

EMCASA can be used to compute EMI margins with or without the spectrum adjustment. SGR uses this routine to adjust the emitter spectrum amplitude where incompatibilities are found (i.e., positive EMI margins) for compatibility (zero margin) minus the user-specified safety factor (asm). SGR also uses EMCASA to compute EMI margins and received signals without adjustment for the receptor total signal and unresolved EMI computations. CEAR uses EMCASA for received signal and margin computations without adjustment.

EMCASA utilizes the emitter port broadband and narrowband spectra, the emitter frequency table for these spectra, the receptor susceptibility spectrum, the receptor frequency table, and the transfer ratios completed by COUPLE at emitter and receptor frequencies. Since the emitter and receptor frequency tables may differ, EMCASA uses a double-point frequency scan technique in which two emitter spectrum points are selected, and the receptor frequencies are scanned for inclusion between them. Log-linear interpolation is used to obtain the emitter amplitudes at receptor frequencies and vice versa.

The routine uses four frequency pointers in the double-point frequency scan. The present and previous emitter table search frequencies are f_{es} and f_{ep} , respectively; and the present and previous receptor table search frequencies are f_{rs} and f_{rp} , respectively. Upon entry into EMCASA (Figure 21), f_{es} and f_{rs} are set to the lowest common values in their respective frequency ranges. The broadband and narrowband spectrum levels (P_{SN} and P_{SB}) and adjustment limit levels (L_{SN} and L_{SB}) at f_{es} are extracted from storage and held. The receptor susceptibility level (S_S) at f_{rs} is similarly extracted. For the first pass, the receptor search frequency is advanced to the next with the present values designated as the previous values. Initially, therefore, f_{rs} is at the second to lowest common table frequency and f_{rp} is at the lowest.

EMCASA then advances f_{rs} and f_{rp} until they straddle f_{es} . The receptor susceptibility (S_{es}) at the emitter frequency f_{es} is obtained by interpolation between f_{rp} and f_{rs} using the equation shown. The received signal levels, both narrowband and broadband, are then computed at f_{es} and used to compute the EMI margins. If EMCASA is being used to compute margins only or f_{es} is in the emitter's required range, the routine branches to the back-search section discussed below. If not, adjustment at f_{es} begins by testing for compatibility at f_{es} , computing the broadband and narrowband required adjustment amounts (A_{SN} and A_{SB}). These are computed by subtracting asm from the margins. If both A_{SN} and A_{SB} are below zero, compatibility exists at f_{es} . If

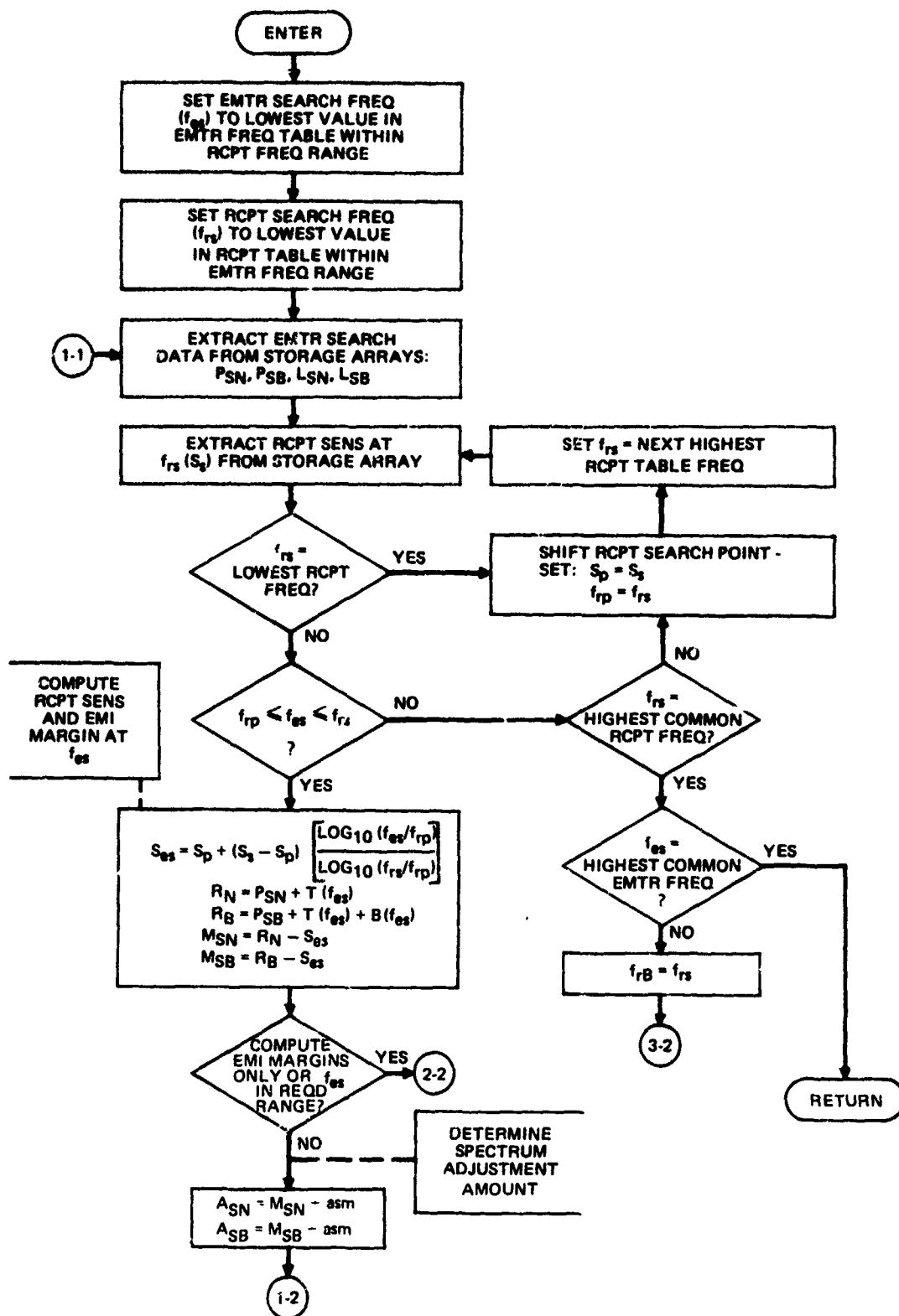


FIGURE 21
EMITTER MARGIN CALCULATION AND SPECTRUM ADJUSTMENT ROUTINE –
FUNCTIONAL FLOW DIAGRAM (Part 1 of 4)

GP74 0267 80

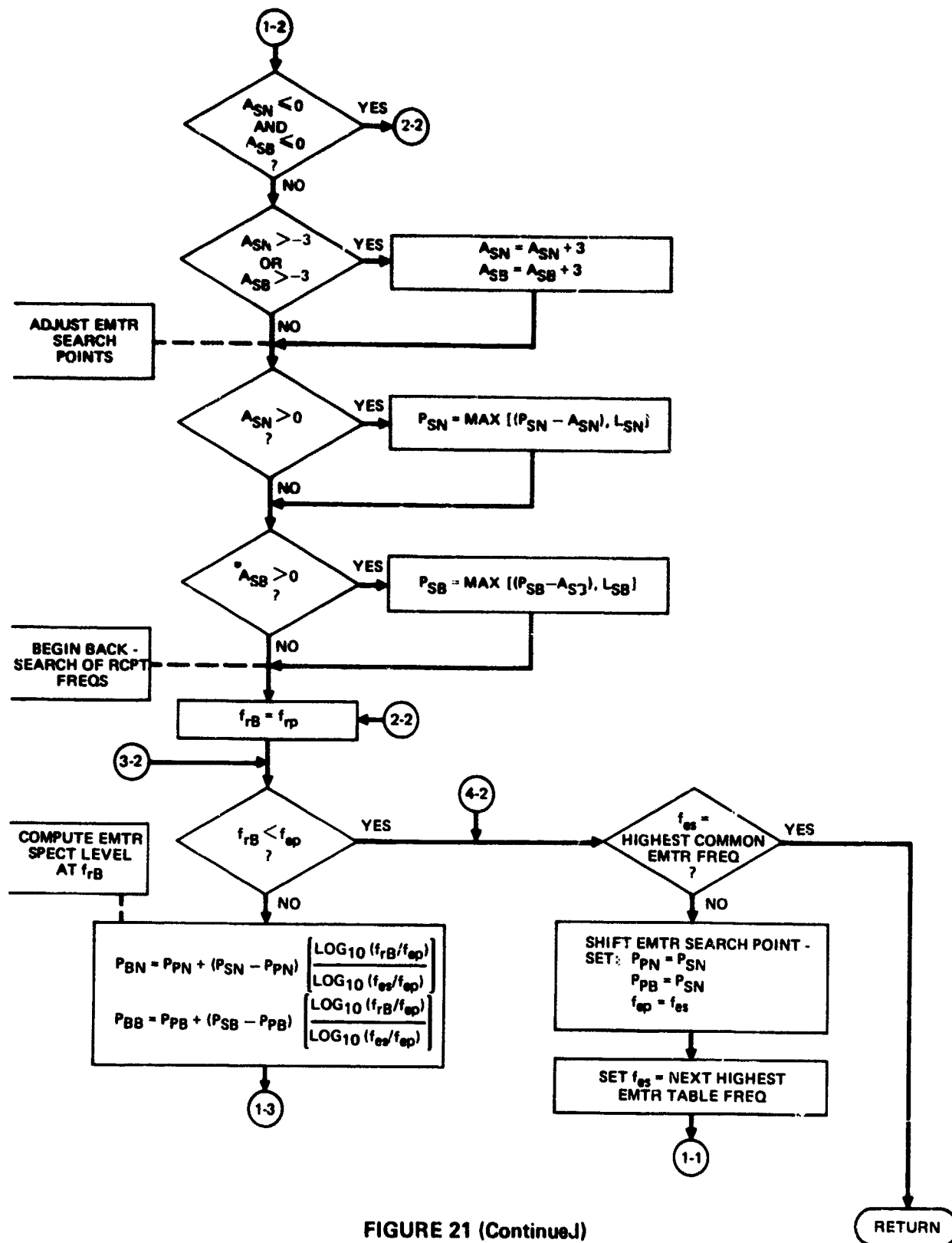


FIGURE 21 (ContinueJ)
EMITTER MARGIN CALCULATION AND SPECTRUM ADJUSTMENT ROUTINE -
FUNCTIONAL FLOW DIAGRAM (Part 2 of 4)

GP74 0267 81

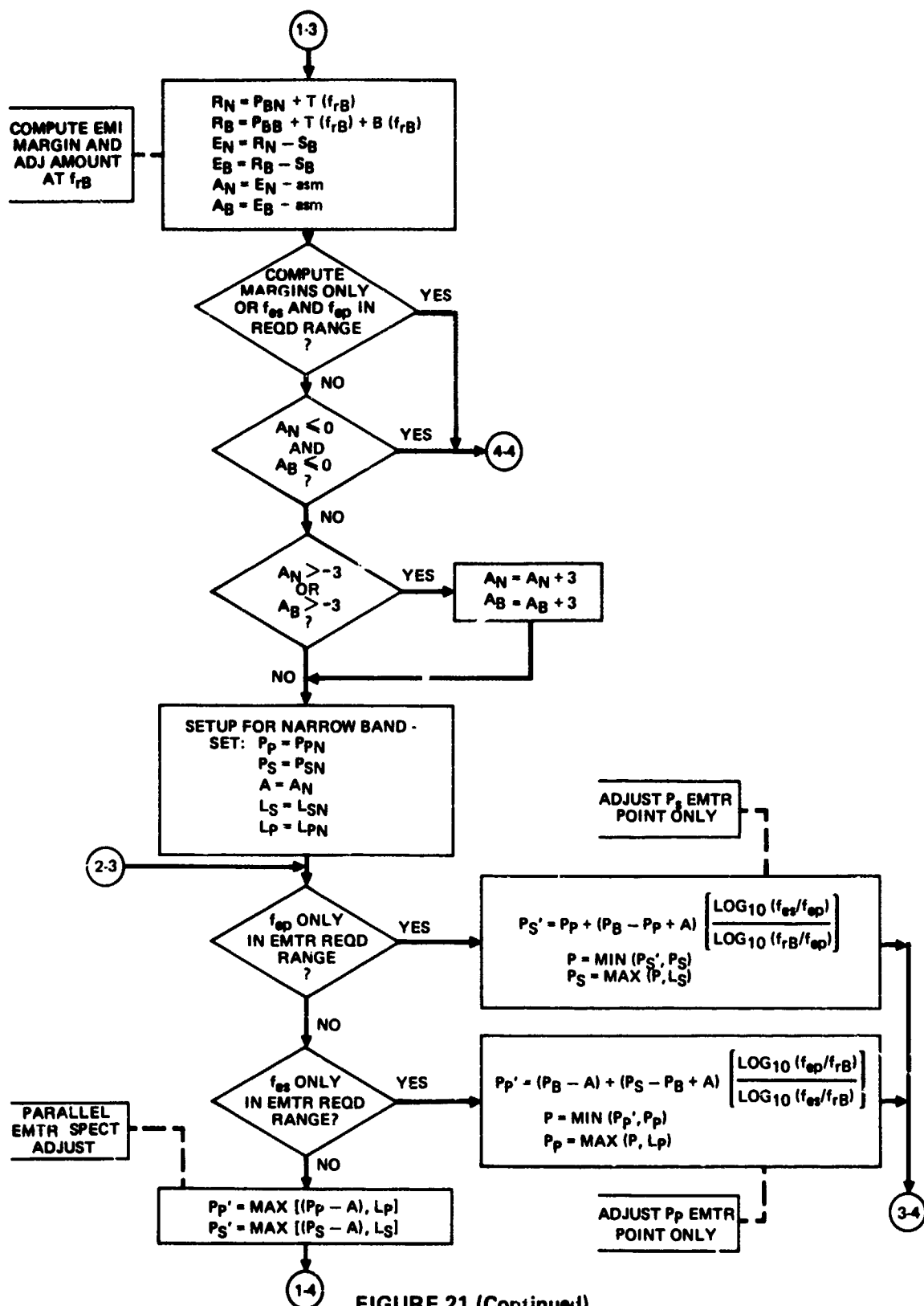


FIGURE 21 (Continued)
EMITTER MARGIN CALCULATION AND SPECTRUM ADJUSTMENT ROUTINE -
FUNCTIONAL FLOW DIAGRAM (Part 3 of 4)

GP74 0267 82

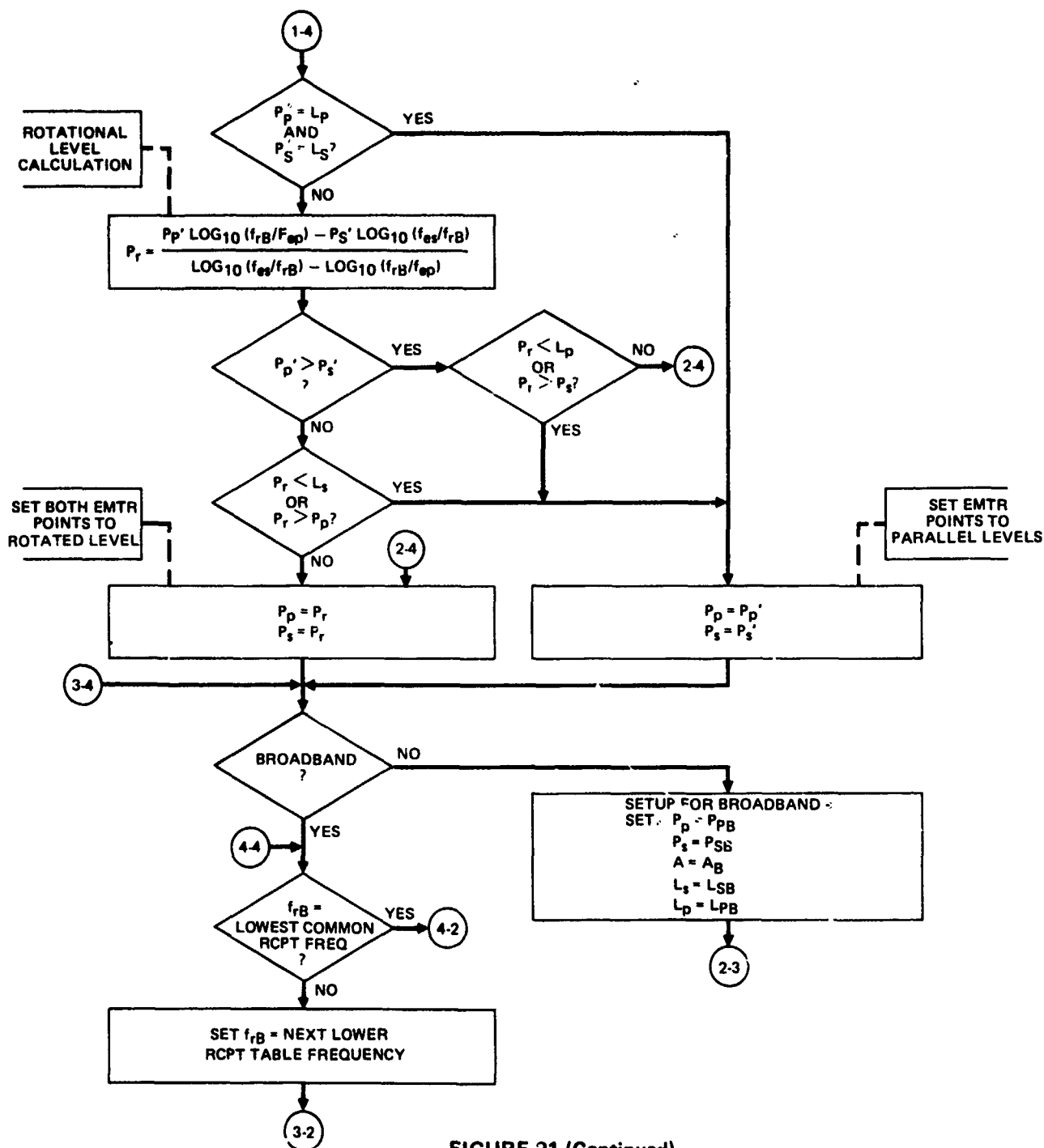


FIGURE 21 (Continued)
EMITTER MARGIN CALCULATION AND SPECTRUM ADJUSTMENT ROUTINE -
FUNCTIONAL FLOW DIAGRAM (Part 4 of 4)

GP74 0267 83

TABLE 6

FLOW SYMBOLS USED IN EMITTER MARGIN CALCULATION AND SPECTRUM ADJUST FLOW

MATH FLOW SYMBOL	SYMBOL DEFINITION
f_{es}	EMTR SEARCH FREQ
f_{ep}	PREVIOUS EMTR SEARCH FREQ
f_{rs}	RCPT SEARCH FREQ
f_{rp}	PREVIOUS RCPT SEARCH FREQ
P_{SN}	EMTR NARROWBAND SPECTRUM LEVEL AT f_{es}
P_{SB}	EMTR BROADBAND SPECTRUM LEVEL AT f_{es}
S_S	RCPT SPECTRUM (SENSITIVITY) LEVEL AT f_{rs}
S_P	RCPT SPECTRUM LEVEL AT f_{rp}
R_N	RECEIVED SIGNAL (NARROWBAND)
R_B	RECEIVED SIGNAL (BROADBAND)
M_S	EMI MARGIN (NARROWBAND)
M_{SB}	EMI MARGIN (BROADBAND)
$T(f_{es})$	TRANSFER RATIO AT f_{es}
$B(f_{es})$	BANDWIDTH FACTOR
S_{es}	RCPT SPECTRUM LEVEL AT f_{es}
A_N	ADJUSTMENT AMOUNT (NARROWBAND)
A_B	ADJUSTMENT AMOUNT (BROADBAND)
asm	ADJUSTMENT SAFETY MARGIN
L_{SN}	EMTR SPECTRUM ADJUSTMENT LIMIT LEVEL (NB)
L_{SB}	EMTR SPECTRUM ADJUSTMENT LIMIT LEVEL (BB)
f_{rB}	RCPT BACK-SEARCH FREQ
P_{BN}	EMTR SPECTRUM LEVEL AT f_{rB} (NARROWBAND)
P_{BB}	EMTR SPECTRUM LEVEL AT f_{rB} (BROADBAND)

TABLE 6 (Concluded)

MATH FLOW SYMBOL	SYMBOL DEFINITION
$T(f_{rB})$	TRANSFER RATIO AT f_{rB}
$B(f_{rB})$	BANDWIDTH FACTOR AT f_{rB}
S_B	RCPT SPECTRUM LEVEL AT f_{rB}
P_{pB}	BROADBAND EMTR SPECTRUM LEVEL AT f_{ep}
P_{pN}	NARROWBAND EMTR SPECTRUM LEVEL AT f_{ep}
L_{pN}	NARROWBAND EMTR SPECTRUM LIMIT AT f_{ep}
L_{pB}	BROADBAND EMTR SPECTRUM LIMIT AT f_{ep}

not, either or both the narrowband or broadband signals are causing interference and must be adjusted. Since the broadband and narrowband are signal components from the same source and add, A_{SN} and A_{SB} are tested to determine if they are both greater than -3 dB. If they are, the composite signal will be incompatible if each component is reduced only to the susceptibility level. Hence, each received signal component is adjusted an additional 3 dB below the susceptibility level by adding 3 dB to A_{SN} and A_{SB} . If A_{SN} is greater than zero, the narrowband emission spectrum level at f_{es} is reduced by A_{SN} or to the limit L_{SN} , whichever is greater. Likewise, the broadband level is reduced by A_{SB} or to L_{SB} , whichever is greater.

The back-search section of EMCASA is then entered. During the preceding, compatibility was established at f_{es} and, during a previous pass, at f_{ep} . However, there may be receptor frequencies between f_{es} and f_{ep} where incompatibilities exist. The back-search routine scans them and adjusts the amplitude at f_{es} and f_{ep} assuming log-linear line segments between them in the emission spectra. The receptor back-search frequency, f_{rB} , is initially set to f_{rp} (which is the first receptor frequency below f_{es} since f_{rp} and f_{rs} straddle f_{es}). The emitter spectrum narrowband and broadband emission levels (P_{BN} and P_{BB}) are computed by interpolation between f_{es} and f_{ep} using the equations shown. The transfer ratio, previously computed at f_{rB} via COUPLE, is used to compute the received signal levels (R_N and R_B). The EMI margins and adjustment amount at f_{rB} are then computed in the same manner as the foregoing adjustment at f_{es} . The 3 dB factor is added as before.

The following adjustment procedure is then entered unless f_{es} and f_{ep} are required or EMCASA is being used to compute margins only. The routine passes through this procedure twice, once for the narrowband and once for the broadband component. To get to this point in the routine, either f_{ep} or f_{es} or both are non-required. But one may be required, and the routine tests for this. If so, the emission level at the non-required frequency is adjusted such that the received signal level at f_{rB} is reduced by the adjustment amount or to its limit.

If both f_{ep} and f_{es} are non-required, both levels are adjustable. The routine adjusts these for compatibility at f_{rB} by, first, a parallel adjustment equal to the adjustment amount or to the limit and, second, rotating the line segment about the f_{rB} level such that the received signals at f_{ep} and f_{es} are equal. The rotation prevents an unduly stringent adjustment at either f_{ep} or f_{es} . However, the routine ensures during rotation that the amplitude at either frequency is not raised above its original level.

When the above procedure has been applied to both narrowband and broadband emission spectrum components, the next lower receptor frequency is selected. The back-search process is repeated until f_{rB} is below f_{ep} . At that time, the emission amplitudes at f_{ep} are stored, the values presently at f_{es} are transferred to f_{ep} , and f_{es} is advanced to the next emitter frequency. The routine then branches to the f_{es} adjustment procedure, and repeats all of the above. This continues until the highest common emitter

or receptor frequency is reached, at which point EMCASA returns to the calling routine.

The following example of the EMCASA emitter spectrum adjustment procedure is presented to illustrate the above. For simplicity, all frequencies are assumed non-required, and there is no adjustment limit. Also the broadband and narrowband signal components are treated as one. Assume receptor susceptibility levels and received signal (emission level less the transfer loss) upon entry into EMCASA as shown in Figure 22.

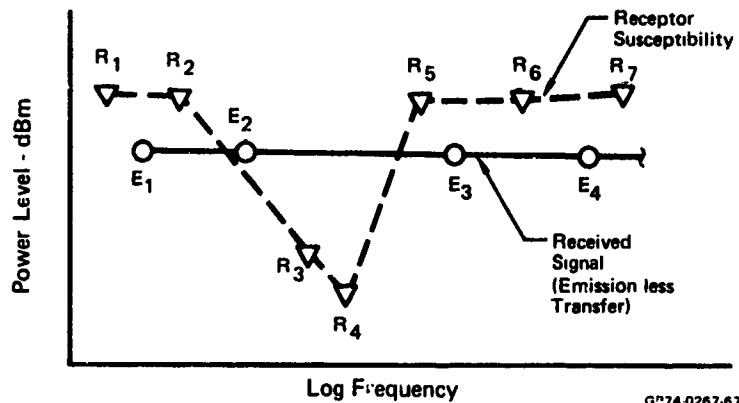


FIGURE 22
INITIAL EMITTER SPECTRUM DIAGRAM

Initially, the emitter search frequency pointer, f_{es} , is set to the frequency of point E_1 . Receptor frequency pointers f_{rp} and f_{rs} are advanced until they straddle E_1 , which places f_{rp} at the frequency of R_1 and f_{rs} at R_2 . The routine then interpolates between the frequencies of R_1 and R_2 to obtain the susceptibility at the frequency of E_1 . The received signal at E_1 is compared to the interpolated susceptibility level; and, since it is below, there is compatibility at E_1 . Then, f_{es} is moved to the next frequency (E_2); and f_{rp} and f_{rs} are moved to straddle it. They thus point to the frequency of R_2 and R_3 , respectively, as shown in Figure 23. Interpolating between R_2 and R_3 to obtain the susceptibility at the frequency of E_2 and comparing the signal level to it shows an incompatibility. Hence, the amplitude of the emission spectrum at E_2 must be reduced to E_2' such that the received signal is below the susceptibility level by-asm. The level at E_2' then replaces E_2 , and the back-search is entered. A check of R_2 shows compatibility, so f_{es} is advanced to the next frequency, that of E_3 , as shown in Figure 24. The amplitude at E_1 is stored.

Since, compatibility exists at E_3 , no adjustment is made, and the back-search routine is entered. The back-search frequency, f_{rb} , is initially set to R_5 . By interpolation between the present amplitudes of E_2 and E_3 , the emission level at the frequency of R_5 is obtained. This less the transfer loss gives the received signal level at R_5 . It is compared to the susceptibility at R_5 to obtain the EMI margin, at which there is compatibility.

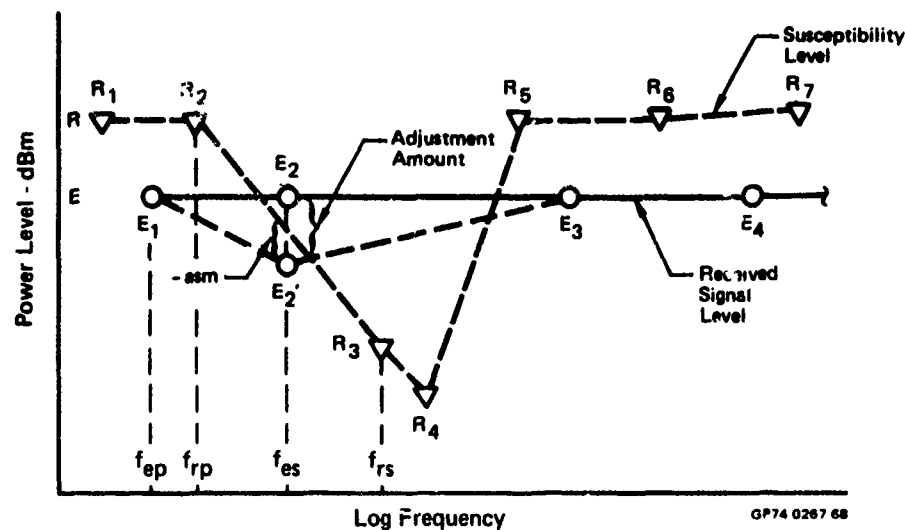


FIGURE 23
ADJUSTMENT OF EMITTER POINT FOR COMPATIBILITY AT E_2

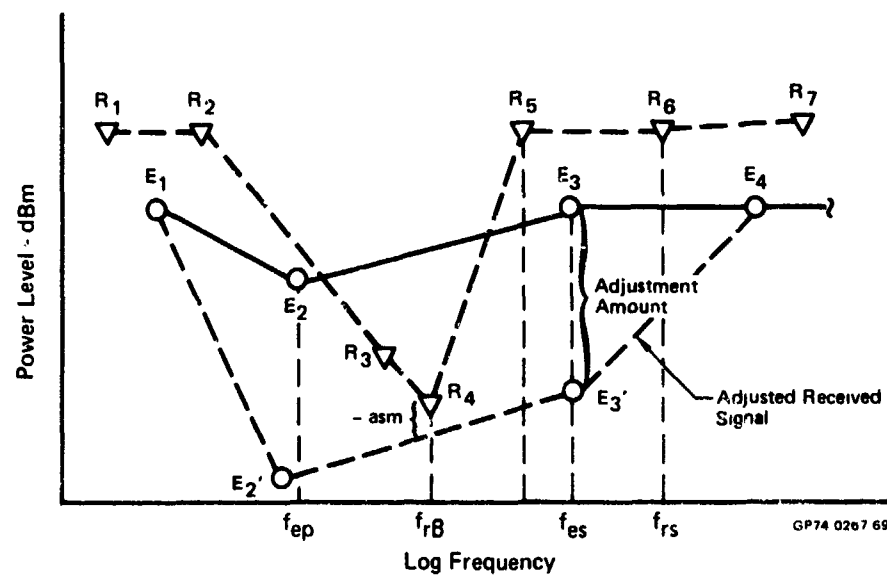


FIGURE 24
PARALLEL ADJUSTMENT OF EMITTER LINE SEGMENT
 E_2 - E_3 FOR COMPATIBILITY AT R_4

Pointer f_{rB} is then moved to the next lower receptor frequency which, as shown in Figure 24, is R_4 . Interpolation between E_2 and E_3 provides the emission level of f_{rB} which is used to compute the received signal level and the EMI margin. Since there is incompatibility, the line segment $E_2 - E_3$ is adjusted. First, E_2 and E_3 are reduced by the same amount such that compatibility exists at f_{rB} . This amounts to a parallel adjustment of the line segment, as shown. Next, as shown in Figure 25, E_2 is raised and E_3 is lowered to equalize the received signal at both frequencies so that neither emitter point is reduced to an undue level. This amounts to rotating the line segment about the compatible amplitude at f_{rB} . E_2' and E_3' replace the values of E_2 and E_3 , and the back-search continues.

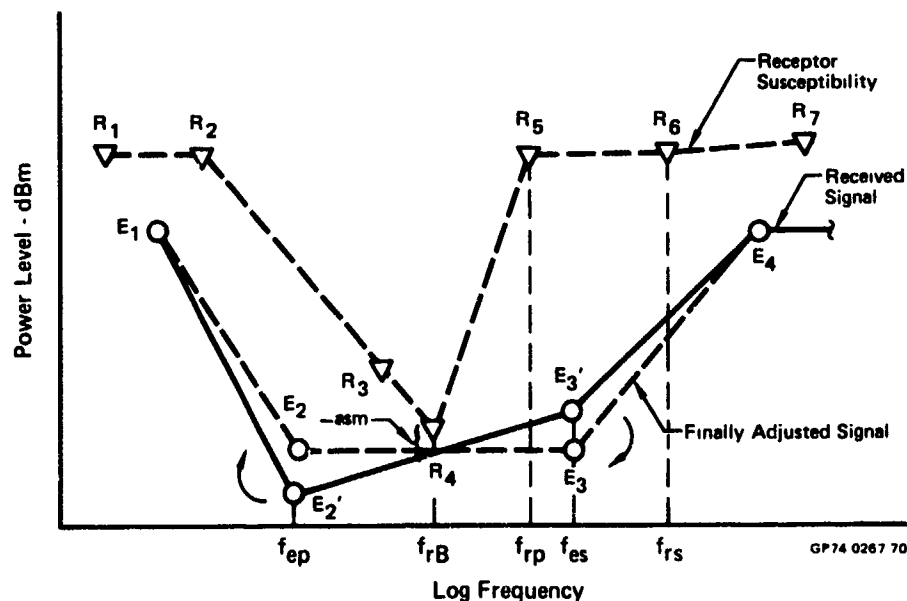


FIGURE 25
ROTATION OF EMITTER LINE SEGMENT $E_2'-E_3'$

With f_{RB} at R_3 frequency, there is compatibility and no further adjustment is made. The next lower receptor frequency, at R_2 , is below f_{ep} so the back-search terminates. The finally adjusted amplitude at E_2 is stored, the values at f_{es} are transferred to f_{ep} , f_{es} is moved to E_4 , and the process continues. When f_{es} exceeds the highest common frequency between the emitter and receptor ports, the routine returns to the calling routine.

5.1.2.3 Total Signal Calculation and Receptor Spectrum Adjustment - After all emitters have been adjusted in conjunction with all receptors, this routine computes the total received signal into each receptor using the adjusted emission spectra and adjusts its susceptibility spectrum for compatibility to this signal. Physically, the controlling routine is contained in SGR and calls three other routines. The Total Received Signal Routine (TORS) computes the total signal and in turn calls the Integrated EMI Margin Routine (EMINTS). It also uses EMCASA. A flow diagram of the controlling routine is shown in Figure 26, and the symbols used are defined in Table 7.

Two scratch files are used. One contains the transfer data from the emitter adjustment phase, and the second is used for the unresolved interference phase. These are used within SGR only and are released after the run.

After a receptor is selected, the routine is entered, and all pointers and arrays initialized. Data for the first coupled emitter is read from the scratch transfer file, and the Adjusted Emitter Spectrum File is then scanned to obtain its spectra. The received signal is computed using EMCASA in the EMI margin only mode. TORS is then called. In TORS, each receptor frequency is selected, and its sample boundary frequencies are determined. Within the interval, TORS searches for emitter frequencies, and if there are any, the received signal level at each is examined and the maximum of the narrowband and broadband components are separately determined. The levels at the receptor sample frequency are also examined, and the maximum narrowband and broadband levels of all those examined are selected. The antilog is taken of these selected signals, to obtain normalized power, and these are added to the total signal array element for the receptor sample frequency. Both the narrowband and broadband signals are included so that the maximum composite signal from the selected emitter within the sample interval is determined and added to the total. Thus, any narrow peaks near the receptor frequency are included.

Note that interpolation of the emission spectrum cannot be used to obtain the signal at the sample interval boundaries. The transfer ratio is known only at emitter and receptor frequencies, and the transfer cannot be assumed to be log-linear between sample frequencies. Hence, only signal levels at sample frequencies are considered. The transfer ratio and emitter spectra are saved on a second scratch file.

After the above has been performed for all receptor frequencies common to the emitter, TORS returns control to SGR. SGR then reads the data for the next coupled emitter and repeats the above until the total signal has been accumulated from all coupled emitters. It then scans through the receptor frequencies. At each frequency, it converts the total signal back to dB

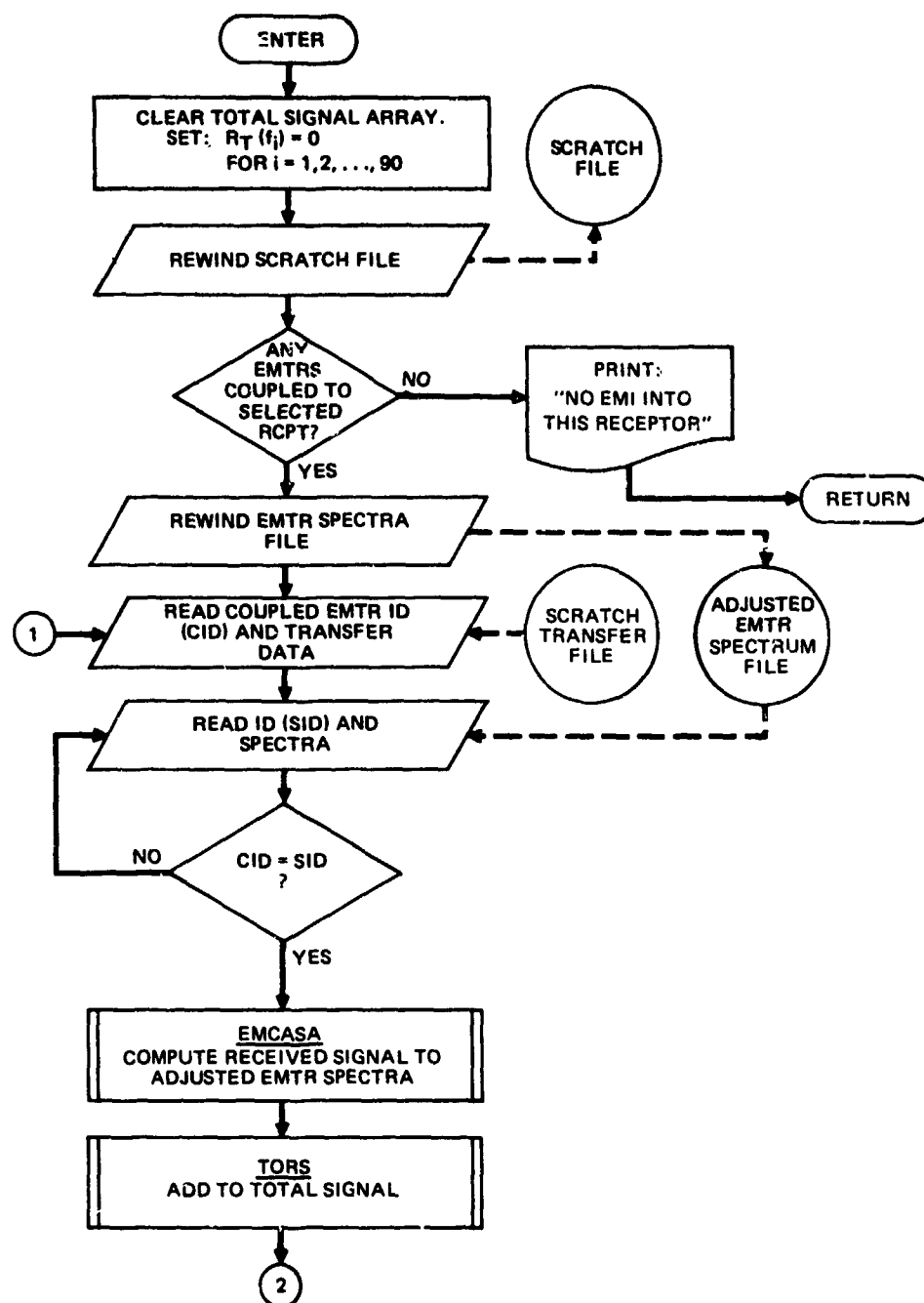


FIGURE 26
RECEPTOR SIGNAL AND SPECTRUM ADJUSTMENT ROUTINE –
FUNCTIONAL FLOW DIAGRAM

GP74 0267 84

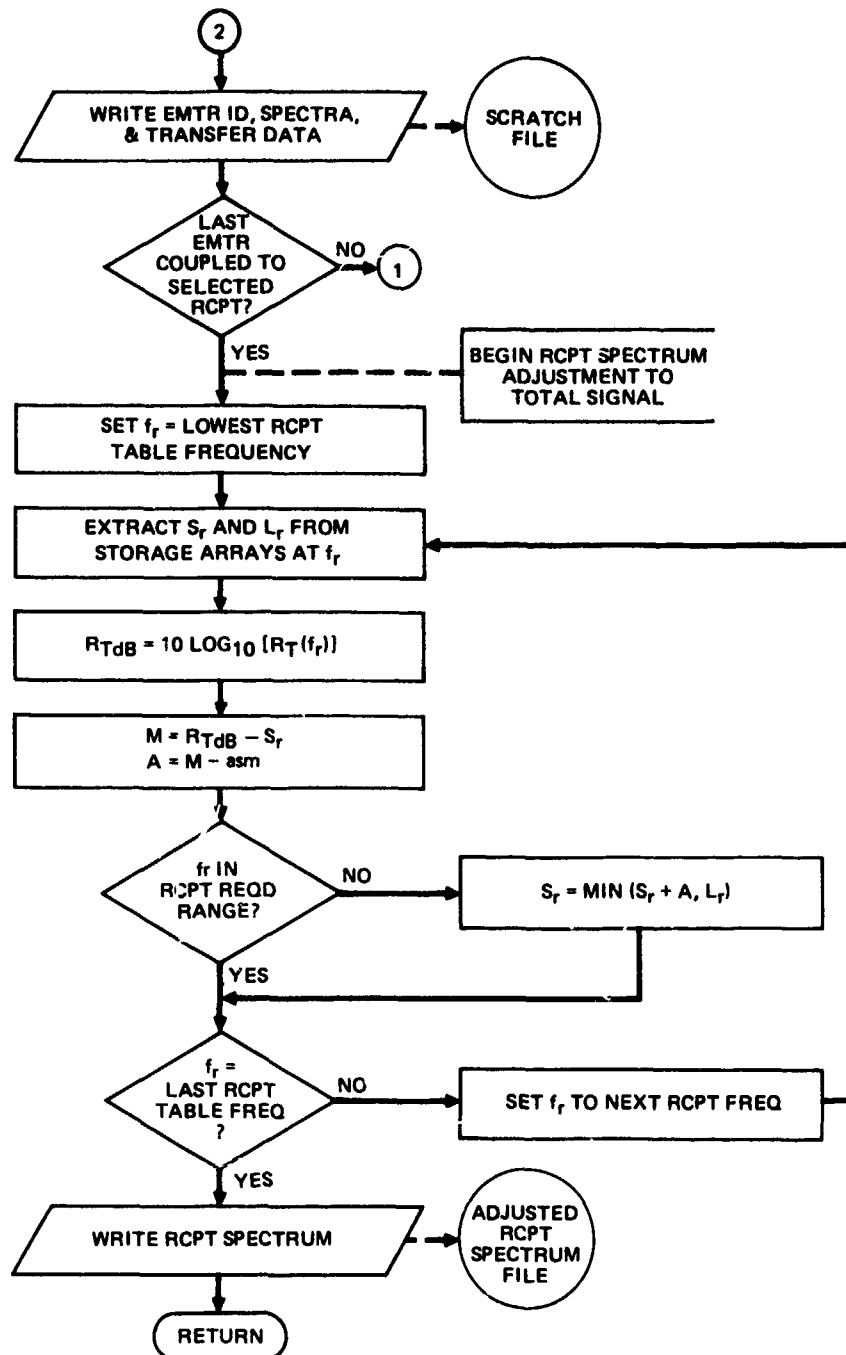


FIGURE 26
RECEPTOR SIGNAL AND SPECTRUM ADJUSTMENT ROUTINE -
FUNCTIONAL FLOW DIAGRAM (Continued)

GP74 0267 85

TABLE 7

SYMBOLS USED IN RECEPTOR SPECTRUM ADJUSTMENT FLOW

MATH FLOW SYMBOL	SYMBOL DEFINITION
$R_T(F)$	TOTAL RECEIVED SIGNAL LEVEL
f_r	RCPT ADJUSTMENT FREQ
S_r	RCPT SPECTRUM LEVEL AT f_r
L_r	RCPT SPECTRUM ADJUSTMENT LIMIT AT f_r
M	EMI MARGIN
A	ADJUSTMENT AMOUNT
asm	SAFETY MARGIN (USER-SPECIFIED)

and computes the EMI margin to the susceptibility level. If the margin at a given frequency is greater than *asm* and the frequency is outside the receptor required range, the susceptibility level is raised by an amount equal to the margin minus *asm* or to the limit, whichever is lower. The adjusted receptor spectrum is saved on the Adjusted Receptor Spectrum File.

SGR then rewinds the second scratch file and reads the transfer ratio and spectra for each coupled emitter. In each case, it calls EMCASA to compute the EMI margin. If the maximum margin exceeds *empl* for a given emitter, the case is unresolved EMI; and a summary of the margins, signal and spectrum levels, etc. is printed.

5.1.2.4 Integrated EMI Margin Computation - TORS scans through the received signal levels at emitter and receptor frequencies as it computes the total signal. During this, it calls the Integrated EMI Margin Routine (EMINTS), which computes the narrowband and broadband components of the Integrated EMI margin. The scan frequencies are supplied to EMINTS in numerical order regardless of whether they are emitter or receptor frequencies. TORS adds the narrowband and broadband components together to obtain the composite integral between the scan frequencies. These composite integrals are summed so that the integrated margin over the entire frequency range common to the emitter and receptor is computed. This is converted to dB and printed in the emitter adjustment, unresolved EMI, and other emitter-receptor pair EMI summaries. The integrated margins are also added for all coupled emitters to each receptor to determine the total integrated EMI margin, converted to dB, and printed with the receptor spectrum adjustment and total signal EMI summaries. The computational methods used in EMINTS are discussed in Section 2.2.3.3.

5.2 COMPARATIVE EMI ANALYSIS ROUTINE

5.2.1 Description

Unlike SGR, which has one specific purpose, the Comparative EMI Analysis Routine (CEAR) is a multi-purpose analytical tool and EMC design aid. With this routine, the user can determine EMI in the original (baseline) system design, determine the effect of design changes as they are made, and obtain aid in making trade-off decisions. It can be used independently or in conjunction with SGR to provide a variety of analyses, as discussed in Section 3.2.2. The only restrictions on changes for comparative analyses (trade-off and waiver) are:

- o No ports may be deleted
- o The frequency table for an existing equipment may not be changed.

5.2.2 Routine Operation

CEAR is divided into two basic sections, as shown in Figure 27. The first section performs the baseline EMI survey and trade-off analyses involving changes which affect the transfer. The second performs the specification waiver analyses and trade-off analyses involving spectrum changes only. Consequently, the first test in CEAR determines which section is to be used, as shown. The flow through Figure 27 will depend on this test and the specified analysis task. The flow for each of these is discussed below.

5.2.2.1 Baseline EMI Survey Analysis - If the baseline system is being surveyed for EMI, CEAR selects a receptor, and scans through the emitters using RCPTRD and EMTRD, as discussed for SGR (Section 5.1.2), except the spectrum files are not swapped in EMTRD. COUPLE (Section 5.1.2.1) is used to determine if a path exists and to call the appropriate transfer model routines if it does. If a path exists, EMCASA (Section 5.1.2.2) is called to compute the received signal and EMI margins at all common frequencies, and if the maximum margin exceeds empl, the EMI summary is printed. Also, the emitter ID, transfer ratio, and EMI margins are written on the BTF. The EMI from the total signal and the environmental fields are also computed and stored on the BTF. The routine selects the next emitter and continues until all emitters have been examined in conjunction with all receptors and returns to the main program.

5.2.2.2 Trade-Off Analysis with Transfer Changes - During the IDIPR portion of a trade-off analysis, the modifications to system, port, wire, etc. parameters are incorporated into the data written on the working files. IDIPR also generates a code for each port indicating whether it is unchanged or modified. If modified, the code indicates if changes are in the spectra and/or port parameters. EMI is computed between the ports in the modified system and compared to that stored on a previously generated BTF (from either an SGR or survey run).

As shown in Figure 27, a receptor is selected in the modified system, and its data is read from the working files. The first emitter is selected, its data read, and the change codes of both ports are checked to determine if either was added to the system (i.e., not in the baseline). If so, the routine proceeds as in the survey analysis to check for a path, and call EMCASA to compute the EMI margins.

If neither port was added the routine checks the BTF to determine if a path existed in the baseline system. The file match flag, initialized to "true," is used to indicate a match between the emitter ID on the BTF and that selected from the working files by EMTRD. The next test is of the emitter and receptor change codes to determine if both are unchanged. If so and a match exists between working file and BTF emitter subsystem, equipment, and port ID's, the transfer and EMI margins are read from the BTF to position it to the next coupled emitter and the file match flag is reset to "true." The next emitter is then selected.

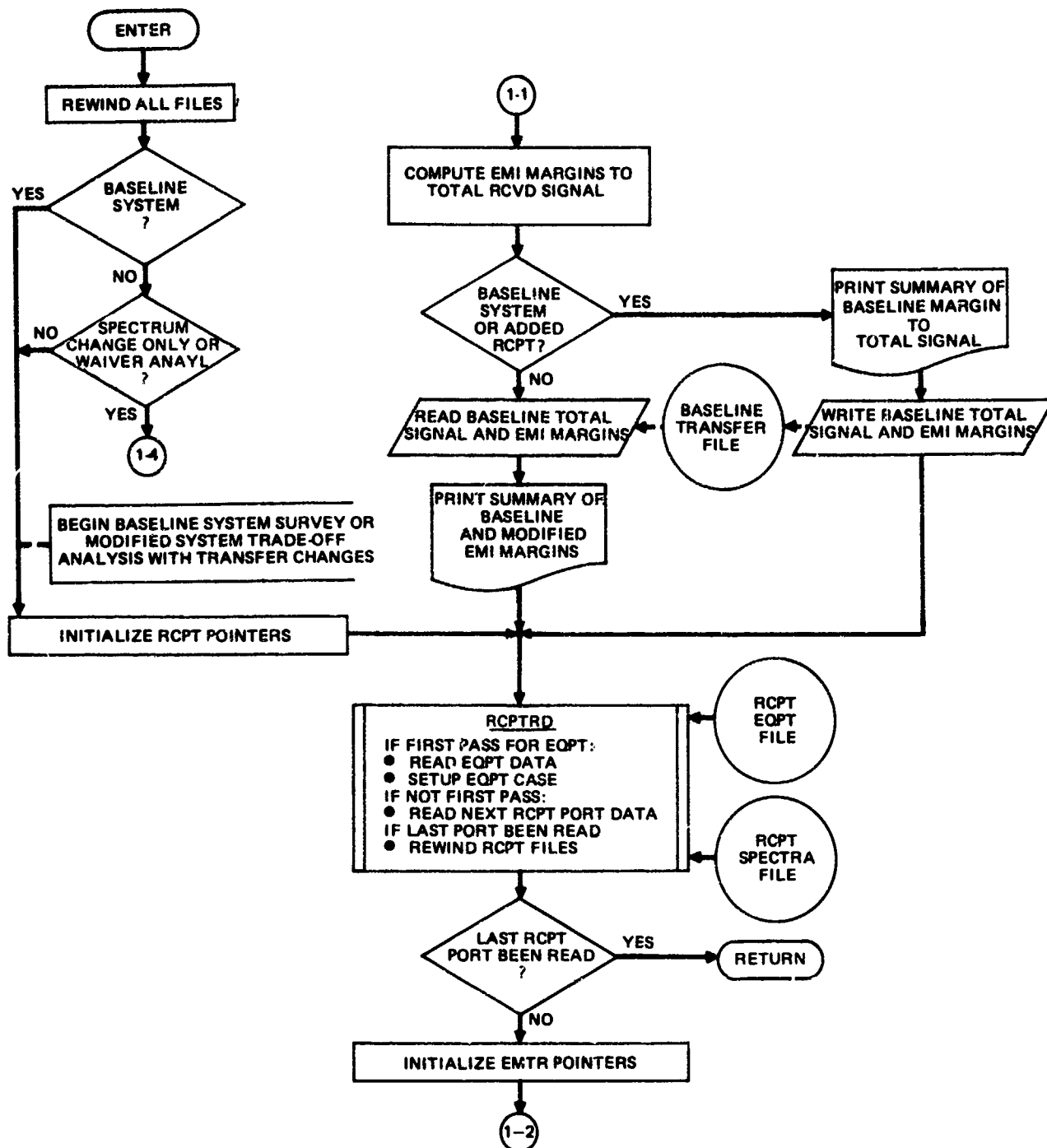
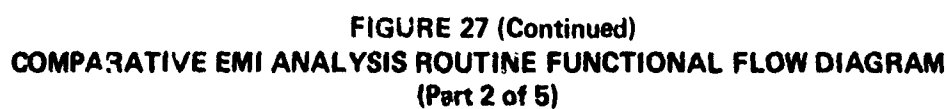
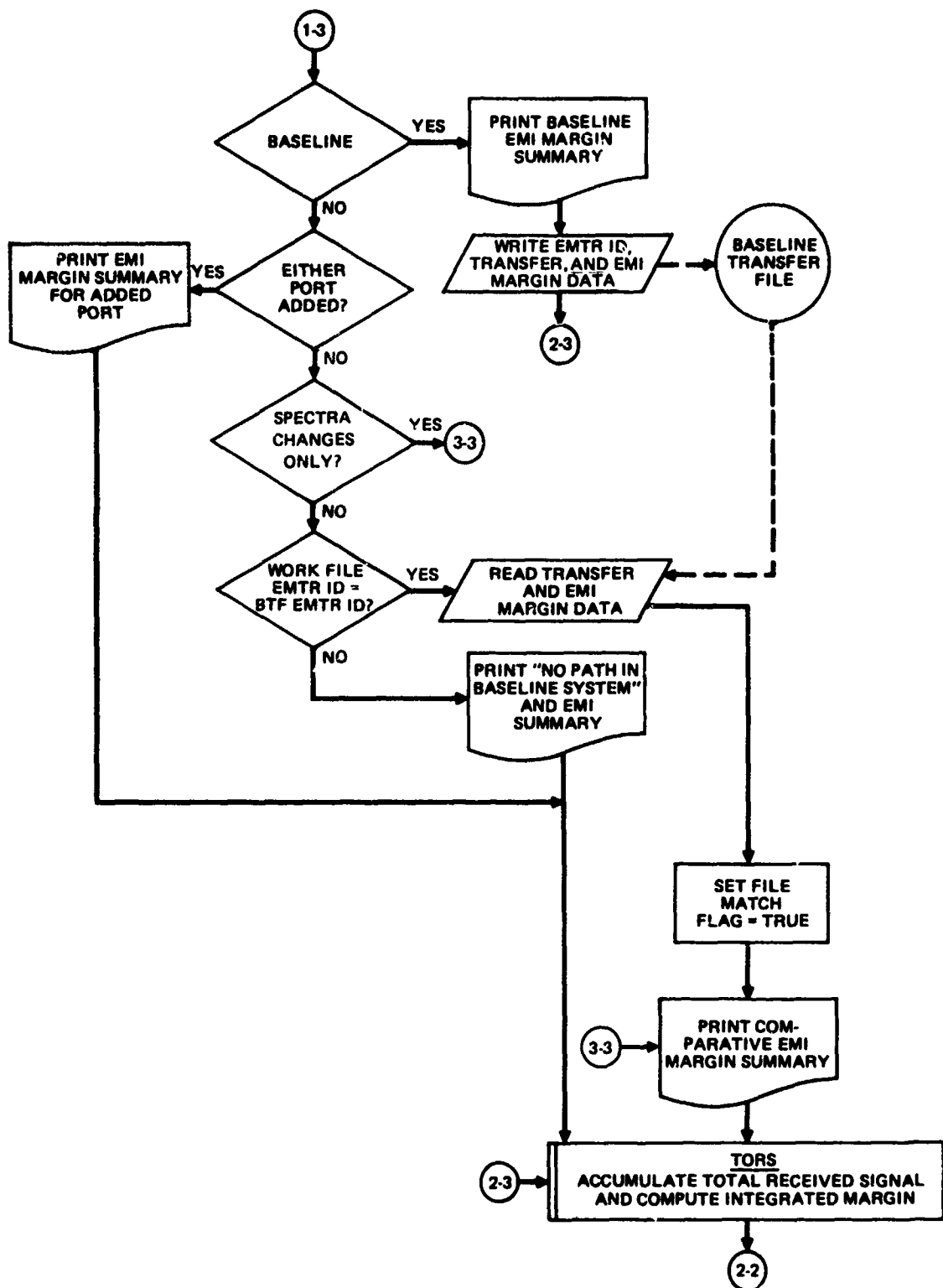


FIGURE 27
COMPARATIVE EMI ANALYSIS ROUTINE FUNCTIONAL FLOW DIAGRAM
(Part 1 of 5)

674 3267 86





GP74 0267-00

FIGURE 27 (Continued)
COMPARATIVE EMI ANALYSIS ROUTINE FUNCTIONAL FLOW DIAGRAM
(Part 3 of 5)

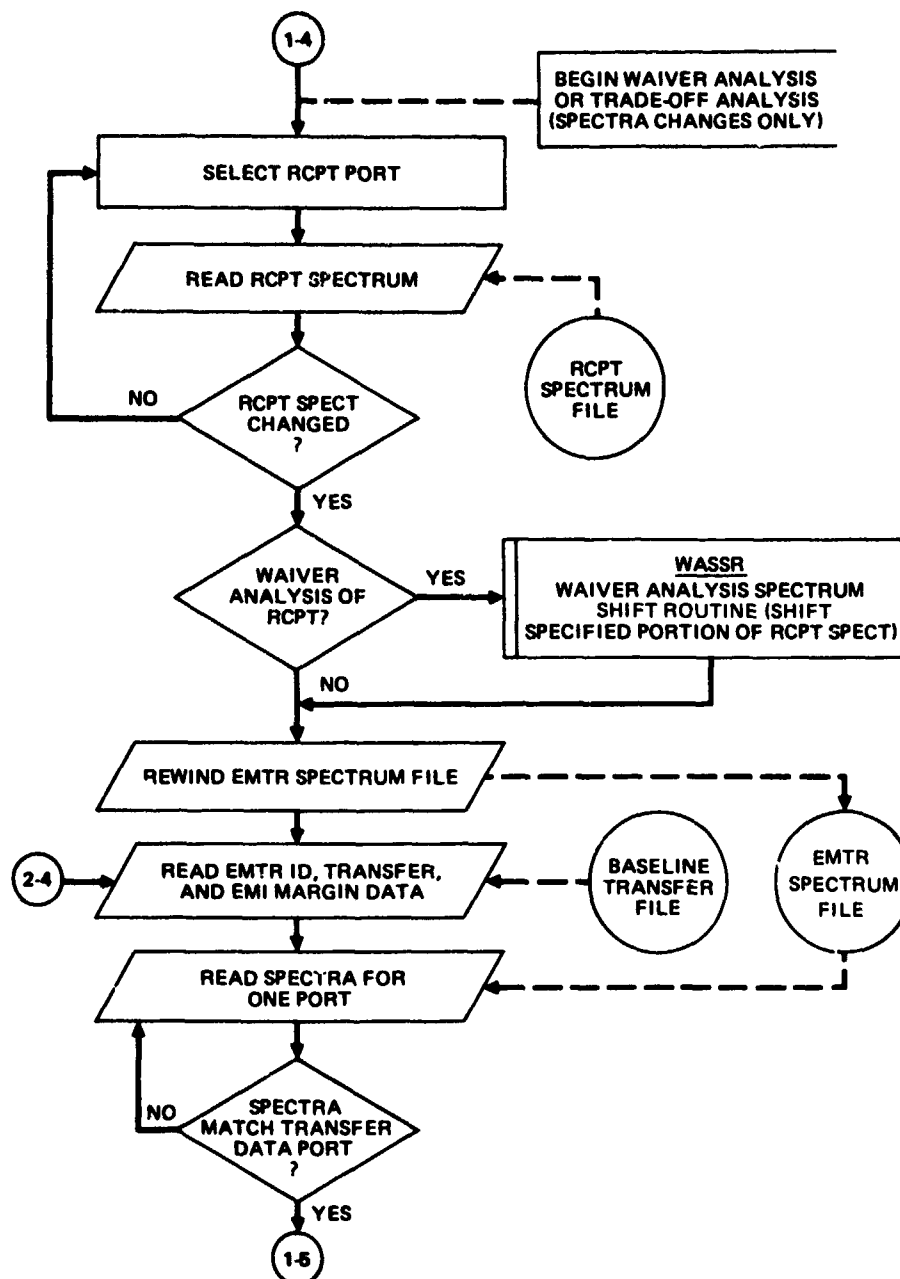


FIGURE 27 (Continued)
COMPARATIVE EMI ANALYSIS ROUTINE FUNCTIONAL FLOW DIAGRAM
(Part 4 of 5)

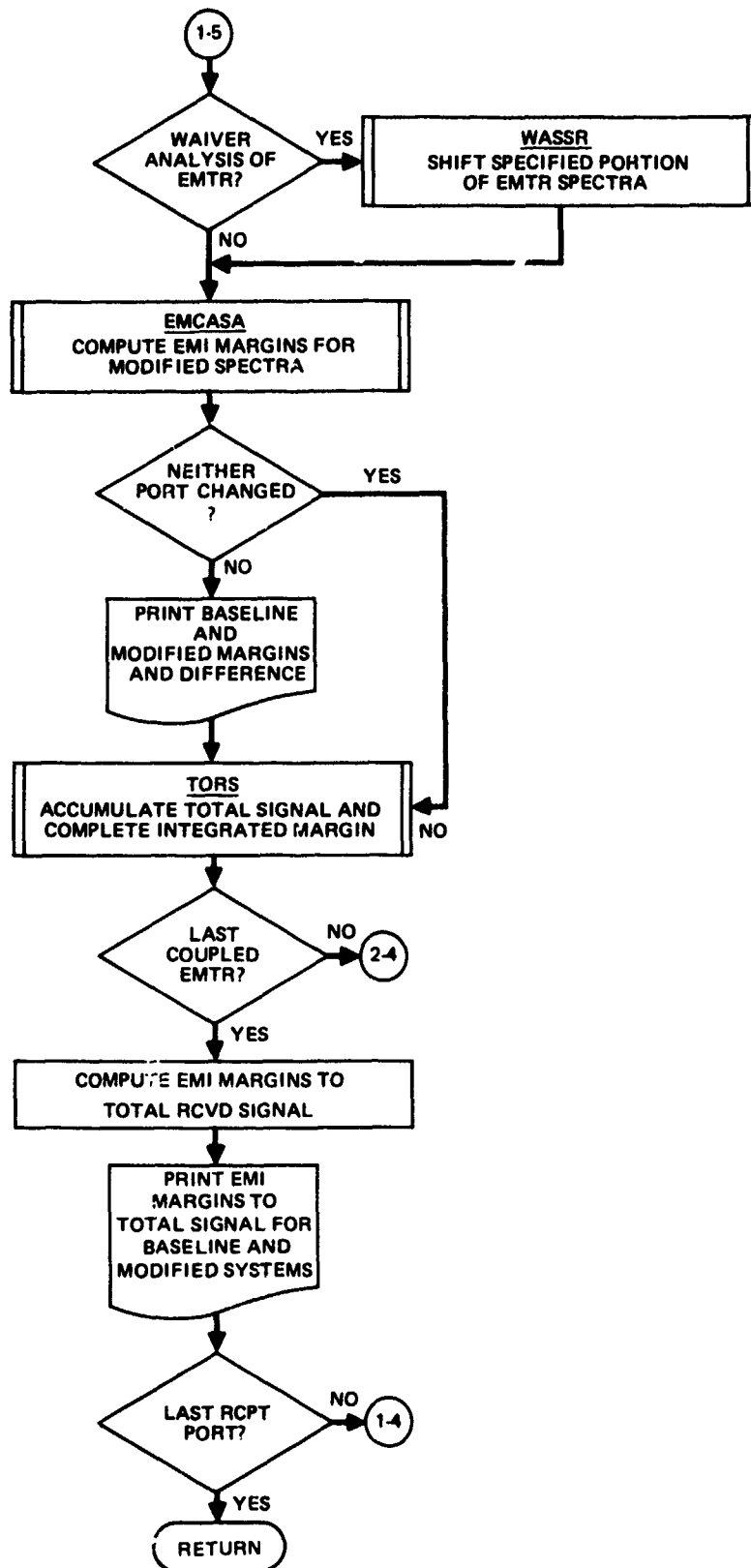


FIGURE 27 (Continued)
COMPARATIVE EMI ANALYSIS ROUTINE FUNCTIONAL FLOW DIAGRAM
(Part 5 of 5)

GP74 0267 90

If either or both ports were changed, their change codes are tested to determine if the changes involve spectra only, indicating that there is no change in the transfer ratio. If so, the baseline transfer and EMI margins are read from the BTF, and this transfer is used by EMCASA to compute the EMI margins for the modified ports. If there is a change in the path, COUPLE is called to compute modified transfer ratio, and this is used by EMCASA.

Upon return from EMCASA, if either port was added a summary of the EMI margins is printed for the ports as in the survey analysis. If neither port was added and the changes are of spectra only, a comparative summary is printed showing the EMI margins in the baseline and modified systems and the change. If there were path changes, the emitter subsystem, equipment and port ID's from the working files are tested for match with those of the BTF. If there is no match, there was no path between these ports in the baseline system. A message so indicating is printed along with a summary of the EMI margins of the modified ports. If the ID's match, there was a path in the baseline system, the transfer and EMI margins are read from the BTF, the file match flag is reset to "true," and a comparative EMI summary is printed. TORS (Section 5.1.2.3) is called to accumulate the total signal and compute the integrated margin.

The next emitter is selected, and the above is repeated until all emitters have been selected including the environmental field, if present. A summary of the total signal EMI is then printed. The entire process is repeated until all receptors have been selected, and CEAR returns to the main program.

5.2.2.3 Trade-Off Analysis With Spectrum Changes Only - If a trade-off analysis is specified and a scan of all port change codes shows no changes other than to spectra, CEAR branches to a different section of the routine (Part 4 of Figure 27). Since there are no path changes or added ports, the transfer models are not needed. For each coupled emitter-receptor pair, the transfer and EMI margin data is read from the BTF. This transfer data is used by EMCASA to compute the modified EMI margins, and a comparative EMI margin summary is printed. The environmental field and total signal EMI are also compared to baseline and printed, as shown.

5.2.2.4 Specification Waiver Analysis - This is the same procedure as described above in Section 5.2.2.3 except the spectra from the working files are shifted before analysis. The Waiver Analysis Spectrum Shift Routine (WASSR) searches the waiver data supplied by the user for a match between subsystem, equipment, and port ID's with the receptor and emitter being analyzed. If there is a match, the port spectra are shifted (i.e., the amplitudes are raised or lowered) as specified over the designated frequencies. For example, a spectrum may be shifted +10 dB from 20 kHz to 1 MHz. The EMI margins are computed between the shifted spectra, and a comparative EMI summary is printed. Environmental field and total signal EMI are also compared to baseline and printed.

5.3 TRANSFER MODEL ROUTINES

This section describes the implementation into TART of the transfer math models. (The models themselves are discussed in Section 6.) Flow charts and the basic routines are presented and described. These are the routines called by COUPLE, as discussed in Section 5.1.2.1.

5.3.1 Antenna Coupled Transfer Function Evaluation Routine (ACTFER)

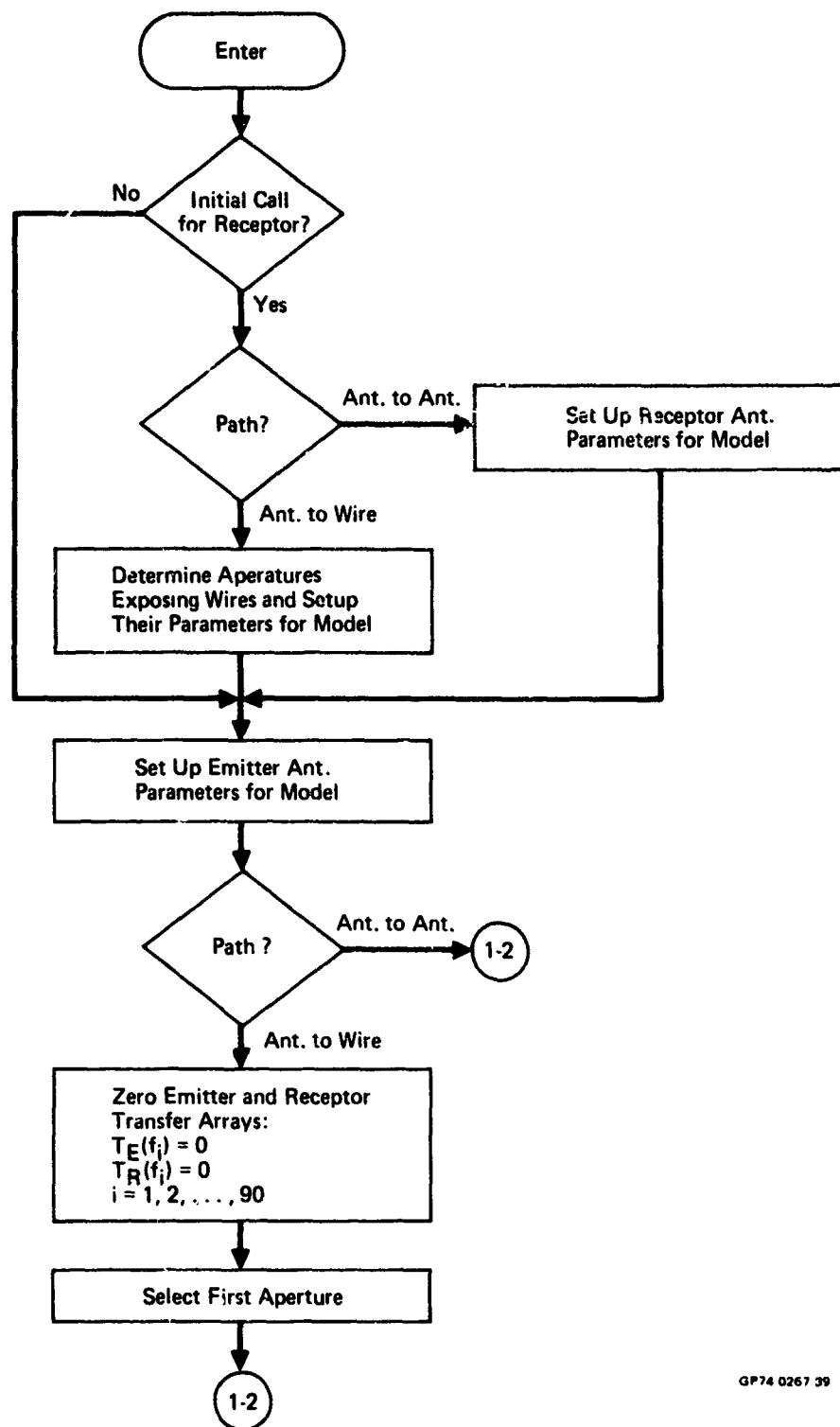
This routine uses the models discussed in Section 6.4.2.2 to compute transfer between two antennas over a finitely conducting ground plane for ground stations and a cylindrical body (with and without wings) for aircraft and spacecraft. It also uses Section 6.4.2.3 models to compute coupling between antennas and receptor ports connected to aperture-exposed wire segments. The flow through ACTFER is shown in Figure 28, and the symbols are in Table 8.

Upon entry into ACTFER, a test is made to determine if this is the initial call for this receptor. If it is, and the path is antenna-to-antenna (ATA), the appropriate parameters are extracted from storage, converted to the proper units, and other model setup computations are performed. If antenna-to-wire (ATW), this is done for all apertures exposing the wire connected to the receptor port. The emitter antenna parameters are then set up for the models.

5.3.1.1 Antenna-to-Antenna Coupling - If the path is ATA, the routine sets up the normalized frequency (1 GHz) at which all the coupling is initially computed using the models. The normalized coupling is then used to compute the coupling at other frequencies without the need of re-computing non-frequency dependent parameters. If the system is a ground station, the separation between antennas is computed, and the vehicle separation and shading models are bypassed. If it is a spacecraft (wingless cylinder), the cylindrical/conical body model (CYLMDL) routine is called which uses the procedures discussed in Section 6.4.2.2.1 to compute the antenna separation and shading over the body. If an aircraft, the AIRCFT routine is called which interfaces with the Wing Shading Routine (WINGSH) and CYLMDL to compute the path loss at the normalized frequency. Next the antenna look-angles are computed and used by the Antenna Gain Routine, GAIN (Section 6.3.3). This is done for both emitter and receptor antennas.

The transfer ratio at all emitter and receptor frequencies common to the two ports is then computed using the normalized transfer computed above.

5.3.1.2 Antenna-to-Wire Coupling - For ATW coupling, the procedure above is followed for each aperture exposing the receptor wire. The transfer between the emitter antenna and the electric field intensity at the aperture is computed using the above models. The transfer from the aperture E-field to the receptor port load is then computed by the field-to-wire subroutine FTW using the model discussed in Section 6.4.2.3. The flow through FTW is shown in Figure 29 and the symbols in Table 9. The total signal level at the receptor load from all apertures exposing the receptor wire is computed using superposition.



GP74 0267 39

FIGURE 28
ANTENNA-COUPLED TRANSFER FUNCTION EVALUATION ROUTINE
 (ACTFER) Called by COUPLE
 Part 1 of 5

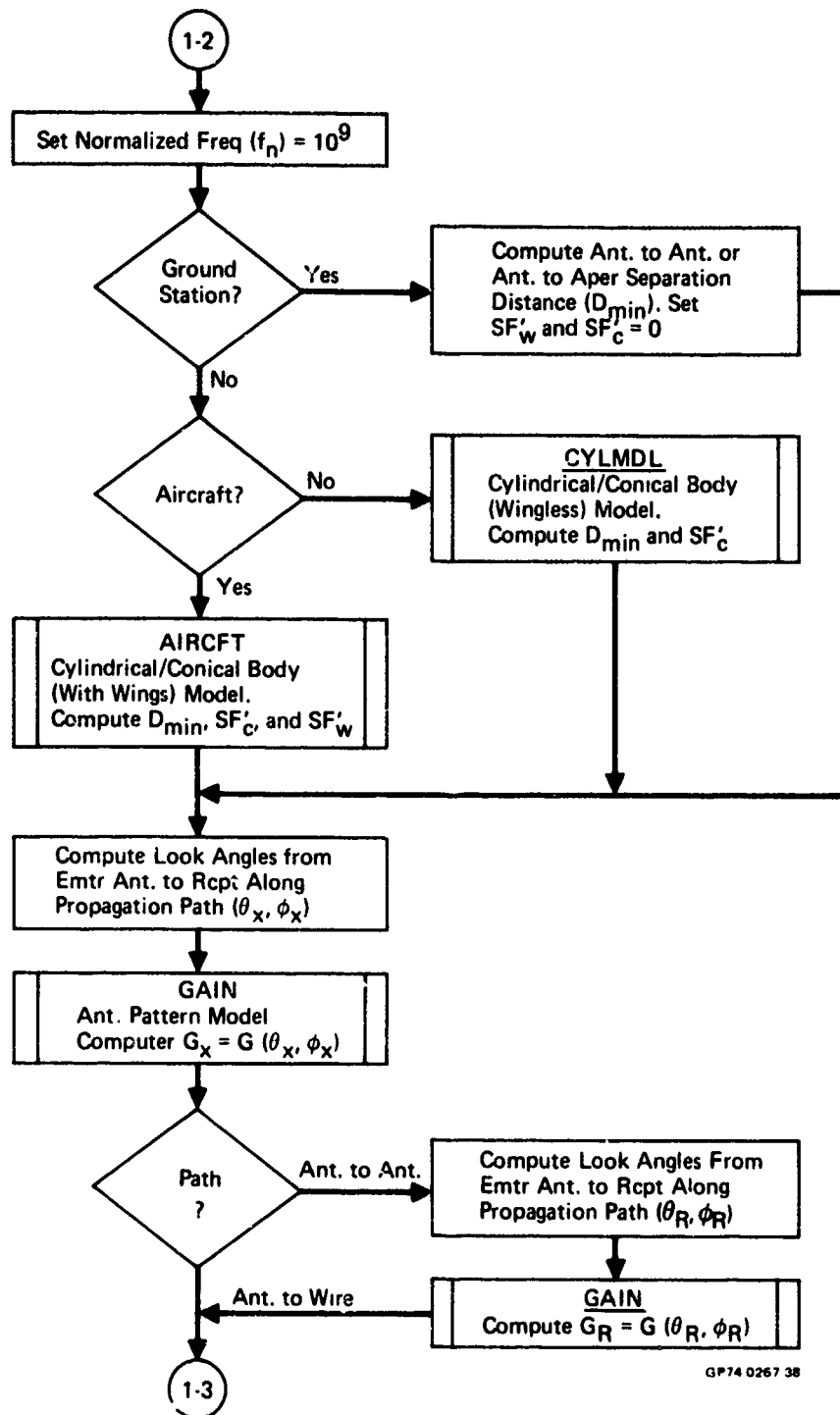
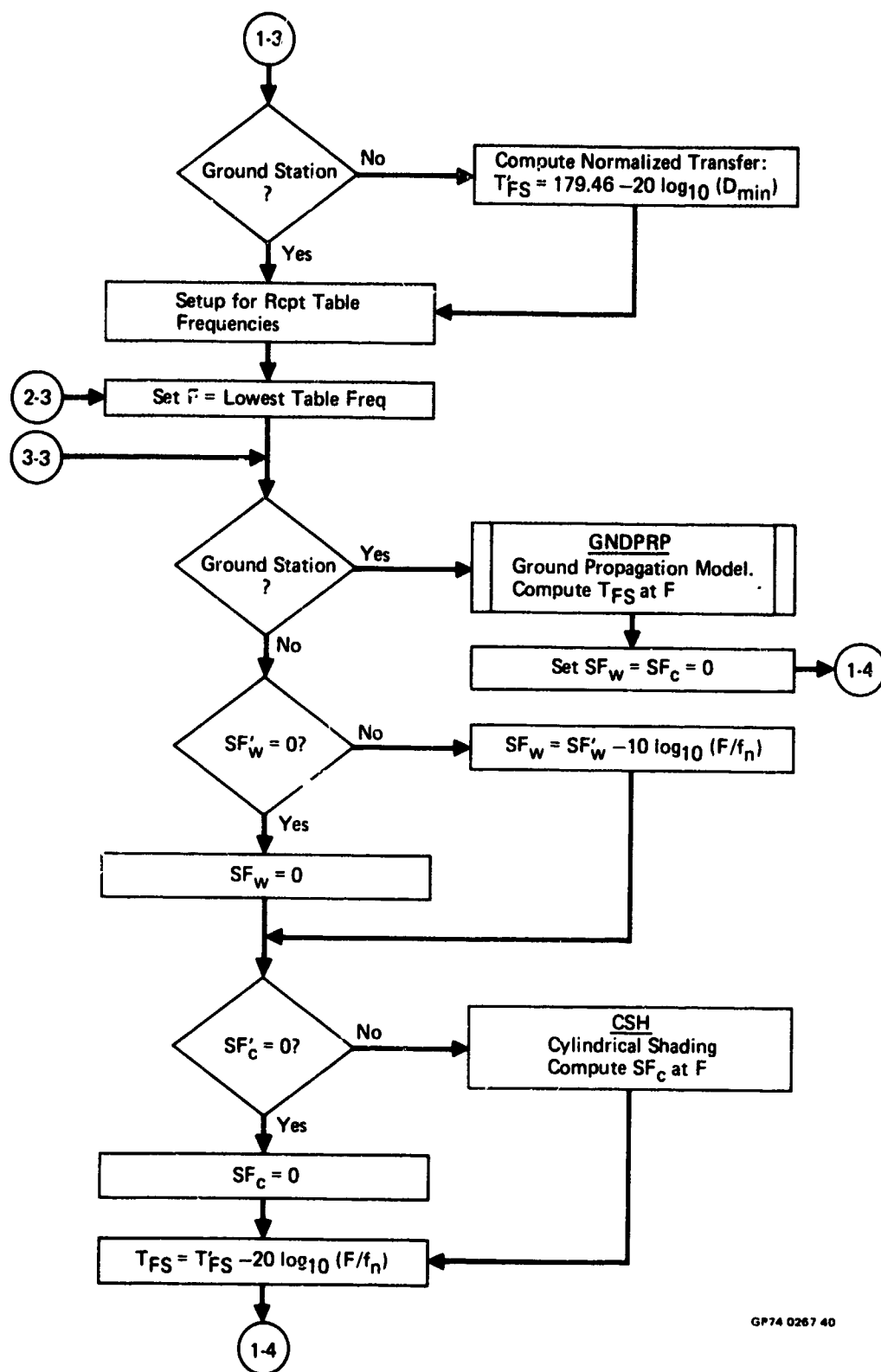
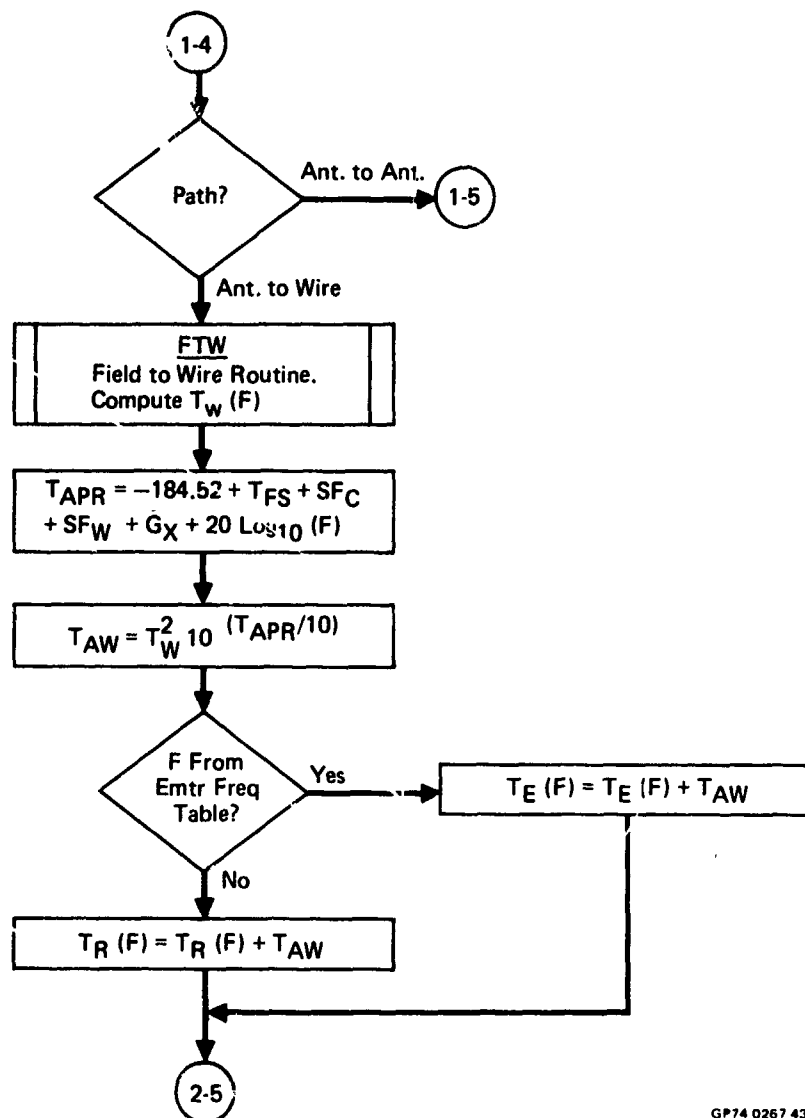


FIGURE 28 (Continued)
ANTENNA-COUPLED TRANSFER FUNCTION EVALUATION ROUTINE
Part 2 of 5



GP74 0267 40

FIGURE 28 (Continued)
ANTENNA-COUPLED TRANSFER FUNCTION EVALUATION ROUTINE
Part 3 of 5



GP74 0267 43

FIGURE 28 (Continued)
ANTENNA-COUPLED TRANSFER FUNCTION EVALUATION ROUTINE
Part 4 of 5

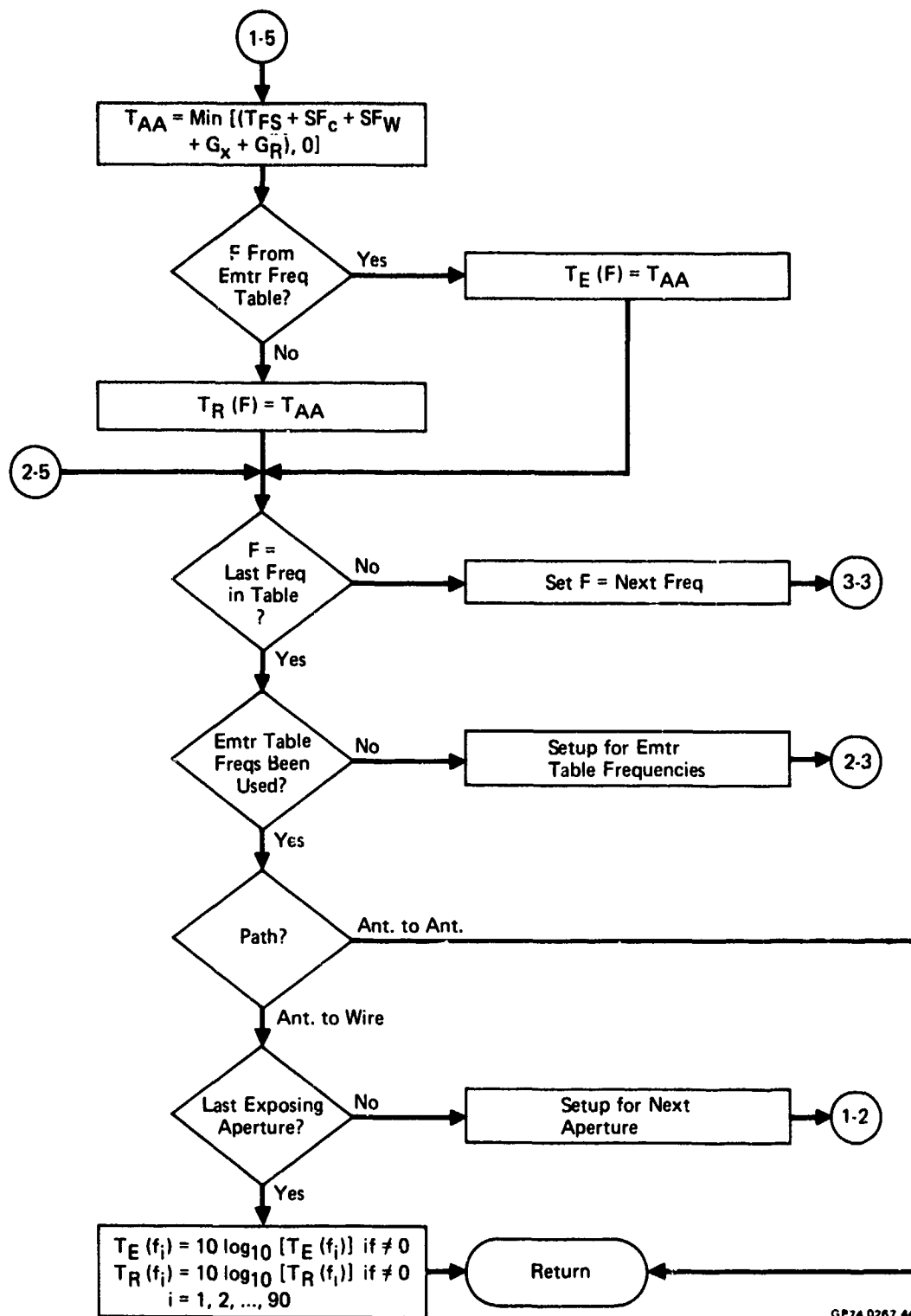


FIGURE 28 (Continued)
ANTENNA-COUPLED TRANSFER FUNCTION EVALUATION ROUTINE
 Part 5 of 5

TABLE 8 FLOW SYMBOLS IN ACTFER SUBROUTINE

MATH FLOW SYMBOL	SYMBOL DEFINITION
$T_E(f)$	TRANSFER RATIO (DB) FOR EMTR TABLE FREQS
$T_R(f)$	TRANSFER RATIO (DB) FOR RCPT TABLE FREQS
SF'_w	WING SHADING FACTOR (DB) NORMALIZED AT f_n
SF'_c	CYLINDRICAL SHADING (DB) NORMALIZED AT f_n
T'_{FS}	FREE SPACE TRANSFER (DB) NORMALIZED AT f_n
f_n	NORMALIZATION FREQUENCY
D_{min}	ANTENNA-ANTENNA OR ANTENNA-APERTURE MIN DISTANCE OVER SURFACE OR VEHICLE
θ_x	ELEVATION ANGLE FROM VERT FOR EMTR ANT
ϕ_x	AZIMUTH ANGLE FOR EMTR ANT
θ_r	ELEVATION ANGLE FOR RCPT ANT
ϕ_r	AZIMUTH ANGLE FOR RCPT ANT
G_x	GAIN (DB) OF EMTR ANT
G_R	GAIN (DB) OF RCPT ANT
F	FREQ BEING EVALUATED
T_{FS}	FREE SPACE TRANSFER AT F
SF_w	WING SHADING FACTOR AT F
SF_c	CYLINDRICAL SHADING FACTOR AT F
T_W	TRANSFER FROM APERTURE FIELD TO WIRE LOAD (NUMERIC) AT F
T_{APR}	TRANSFER FROM EMTR ANT TO APERTURE FIELD (DB) AT F
T_{AW}	TRANSFER FROM ANTENNA TO WIRE LOAD (NUMERIC) AT F
T_{AA}	TRANSFER FROM EMTR ANT TO RCPT ANT (DB) AT F

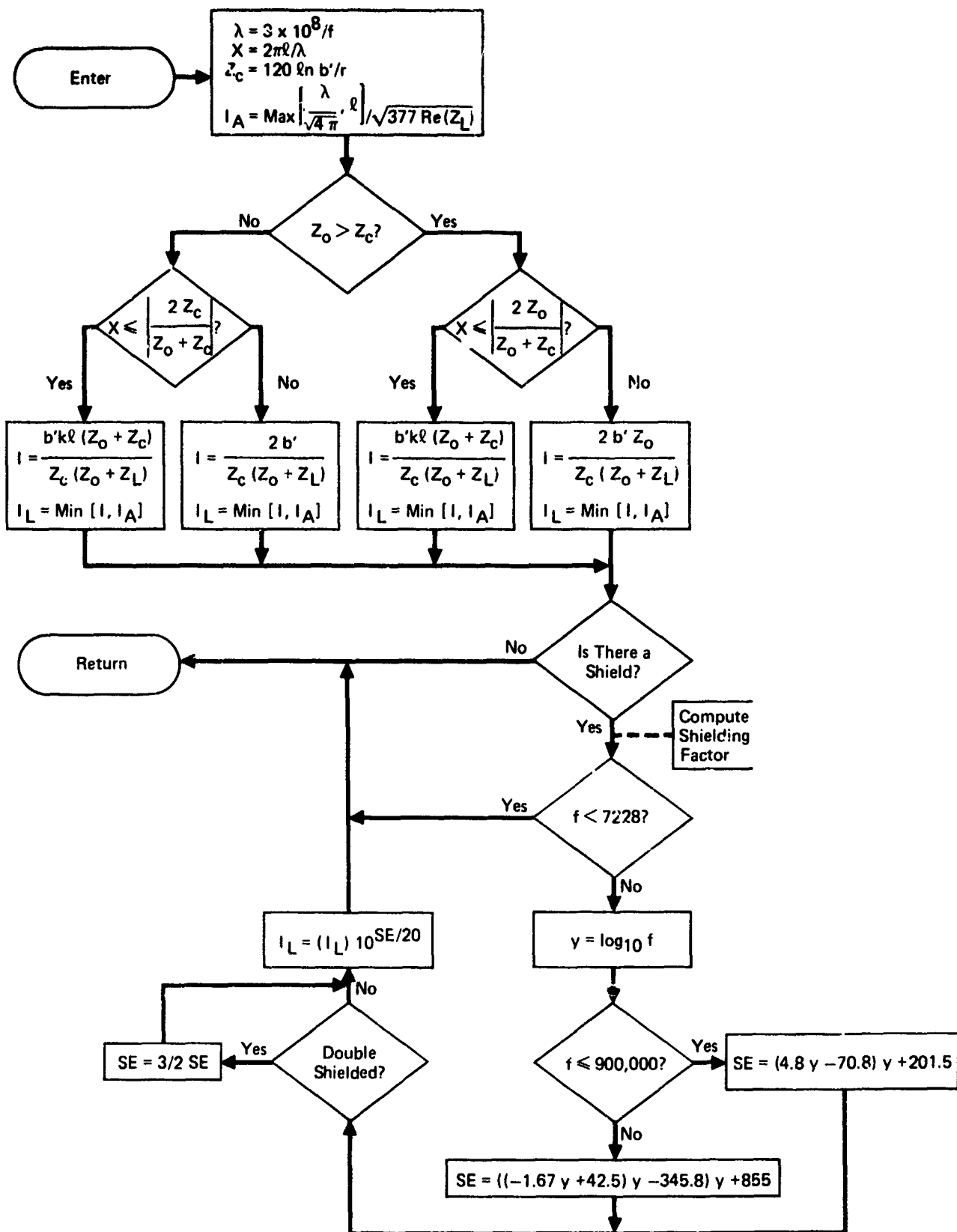


FIGURE 29
FIELD TO WIRE (FTW) SUBROUTINE
 Called by ACTFER and ENVIRN

GP74 0267 45

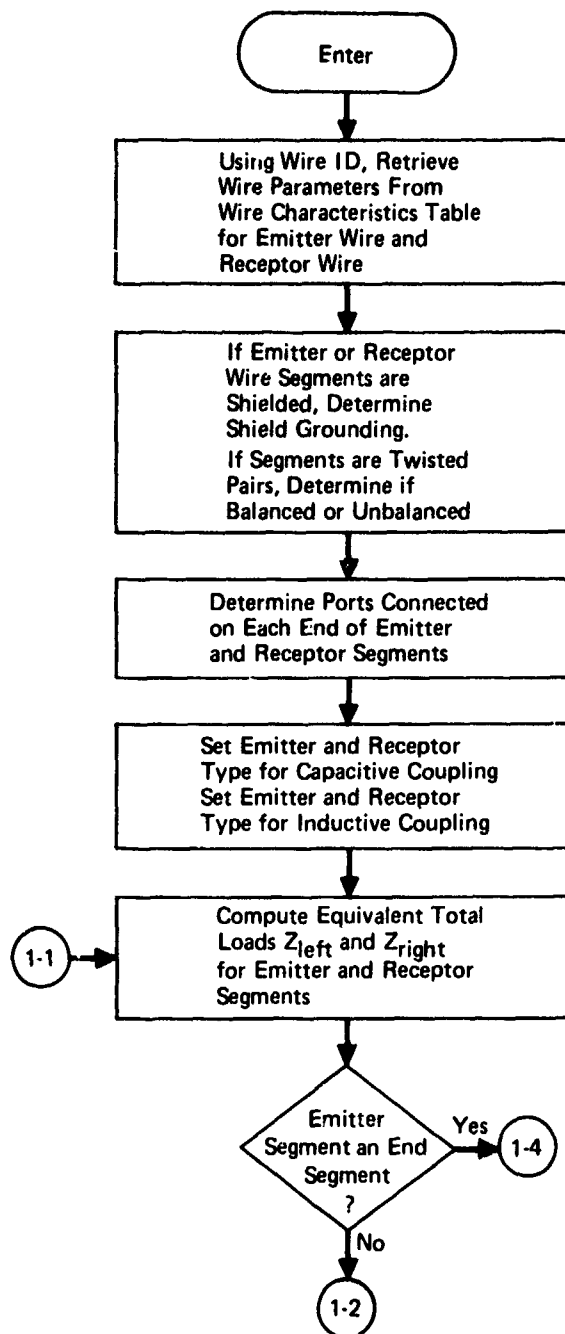
TABLE 9 FLOW SYMBOLS IN FTW SUBROUTINE

MATH FLOW SYMBOL	SYMBOL DEFINITION
b'	SEPARATION BETWEEN WIRE AND ITS RETURN OR IMAGE
r	WIRE RADIUS
λ	WAVELENGTH OF INCIDENT FIELD
f	FREQUENCY OF INCIDENT FIELD
ℓ	LENGTH OF WIRE SEGMENT
Z_L	"RECEPTOR SIDE" IMPEDANCE
Z_O	"SOURCE SIDE" IMPEDANCE
X	ELECTRICAL LENGTH OF WIRE SEGMENT
Z_c	CHARACTERISTIC IMPEDANCE OF WIRE
I_A	UPPER BOUND ON CURRENT, BASED ON "EFFECTIVE AREA" OF WIRE SEGMENT AS AN ANTENNA
I_L	CURRENT INDUCED AT "RECEPTOR SIDE" OF WIRE SEGMENT DUE TO A UNIT INCIDENT FIELD
SE	SHIELDING EFFECTIVENESS (DB)

5.3.2 Wire-to-Wire Transfer Function Routine (WTWTFR)

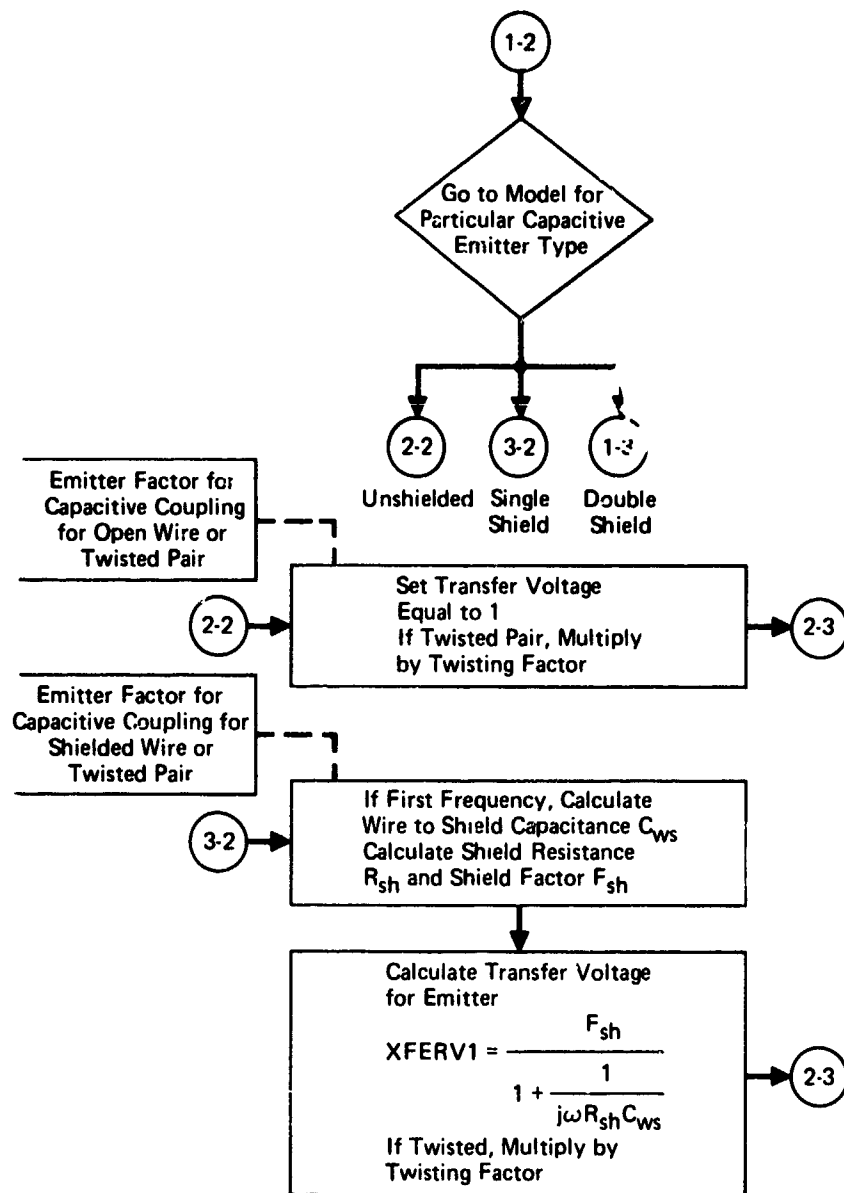
The wire-to-wire transfer routine, called by COUPLE, calculates the transfer ratio between an emitter wire and a receptor wire which are within the same bundle and have a common run length using the models described in Section 6.4.2.4. This is accomplished by use of data from the wire characteristics table and previously computed information on the branching, terminations, and common run length for the emitter and receptor wires. The flow through WTWTFR is shown in Figure 30, and the symbols are defined in Table 10.

The routine initially calculates the values of capacitance and inductance to be used for calculation of the transfer ratios (for all desired frequencies). At this point, it also sets program flags according to the type and configuration of the emitter and receptor segments.



GP74 0267 48

FIGURE 30
WIRE TO WIRE TRANSFER ROUTINE (WTWTFR)
 Called by Couple
 (Part 1 of 11)



GP74 0267 49

FIGURE 30 (Continued)
WIRE TO WIRE TRANSFER ROUTINE (WTWTFR)
 (Part 2 of 11)

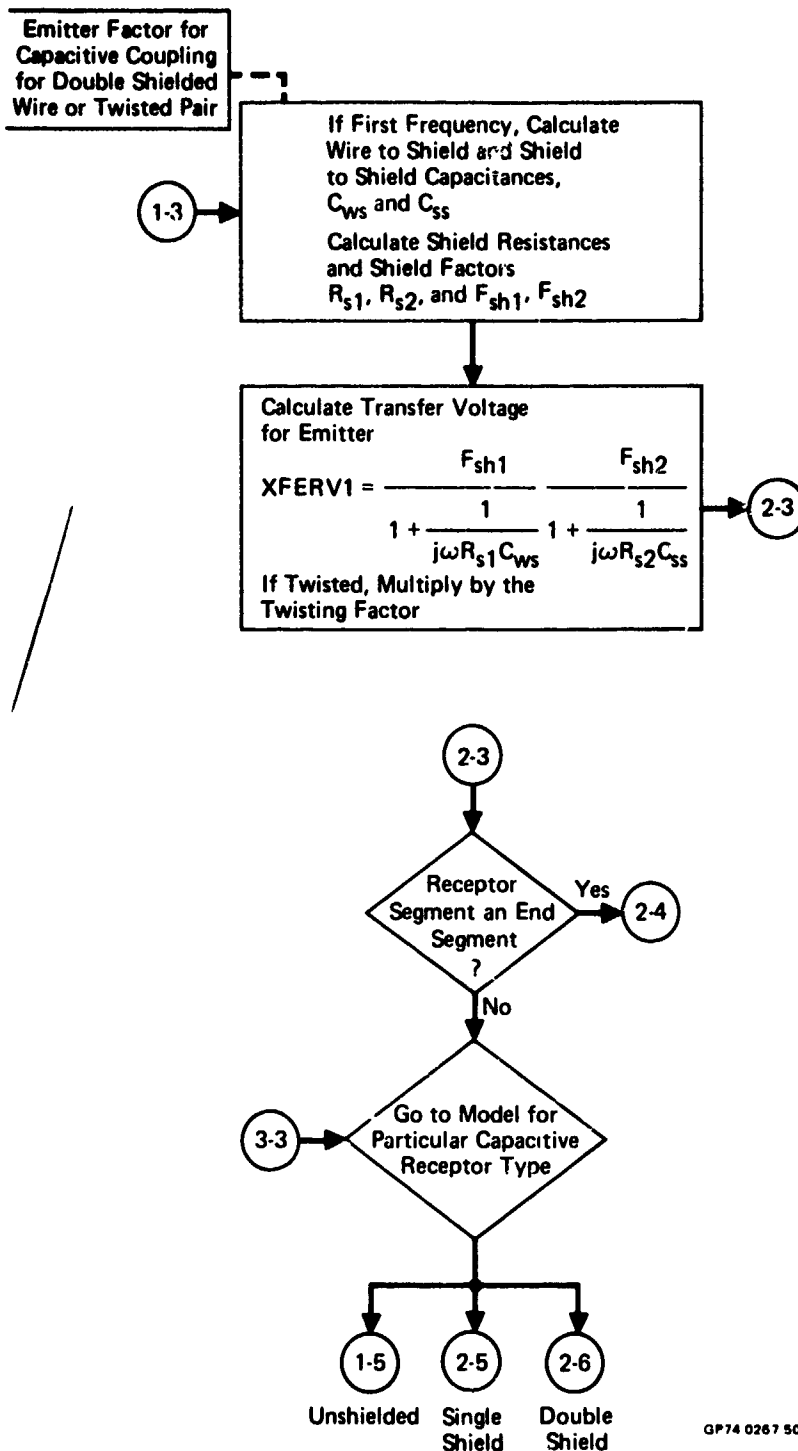
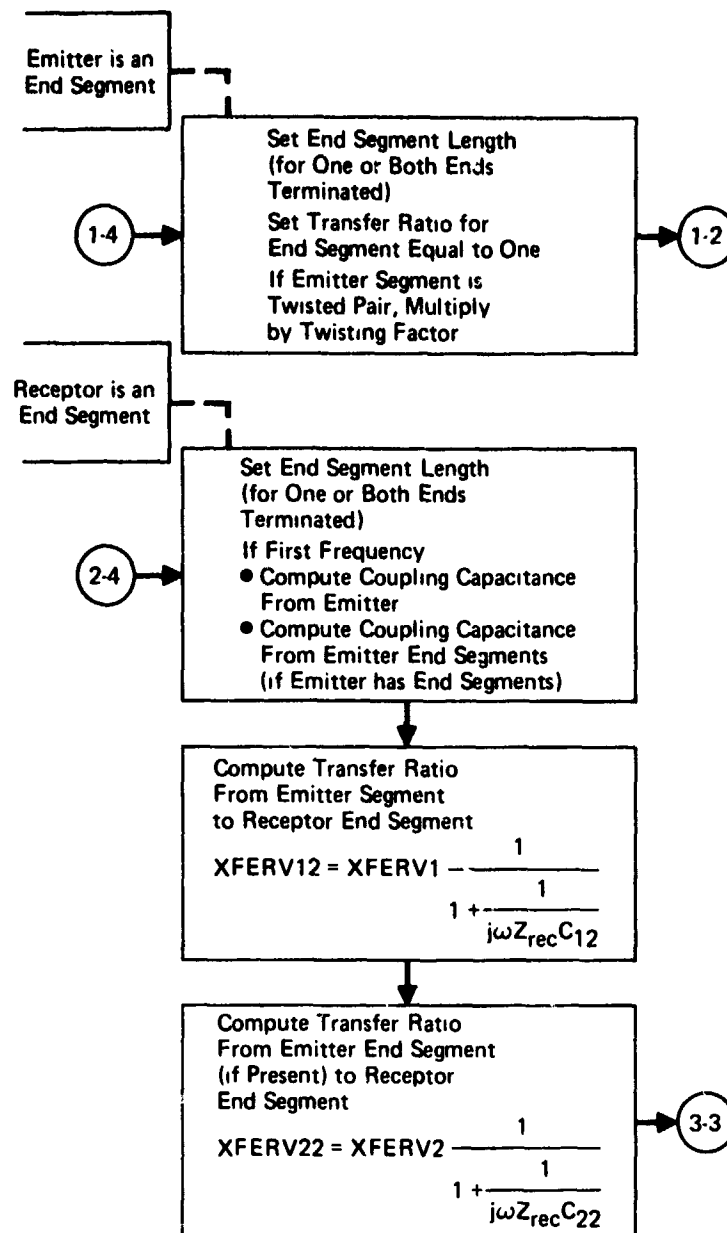
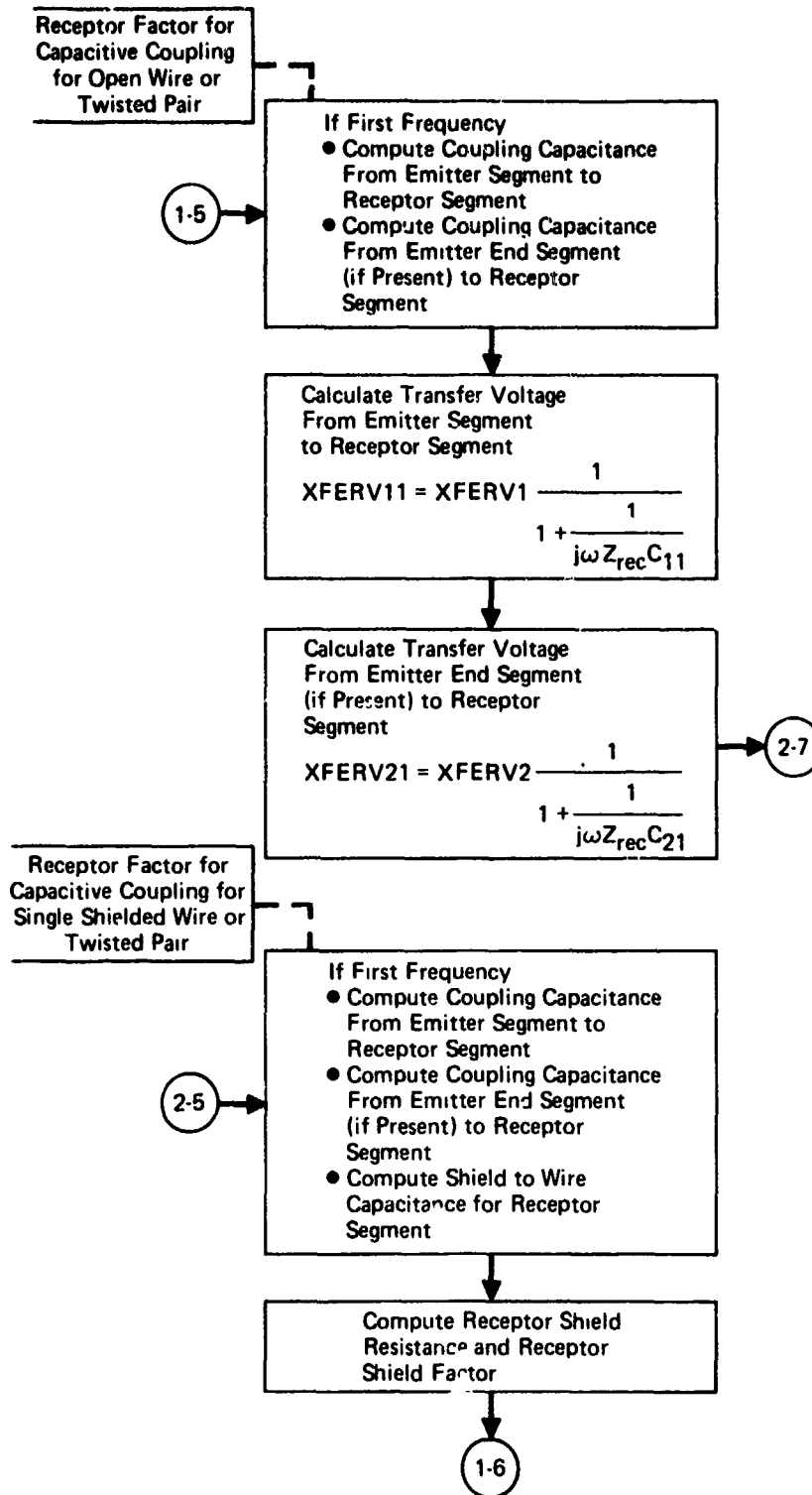


FIGURE 30 (Continued)
WIRE TO WIRE TRANSFER ROUTINE (WTWTFR)
(Part 3 of 11)



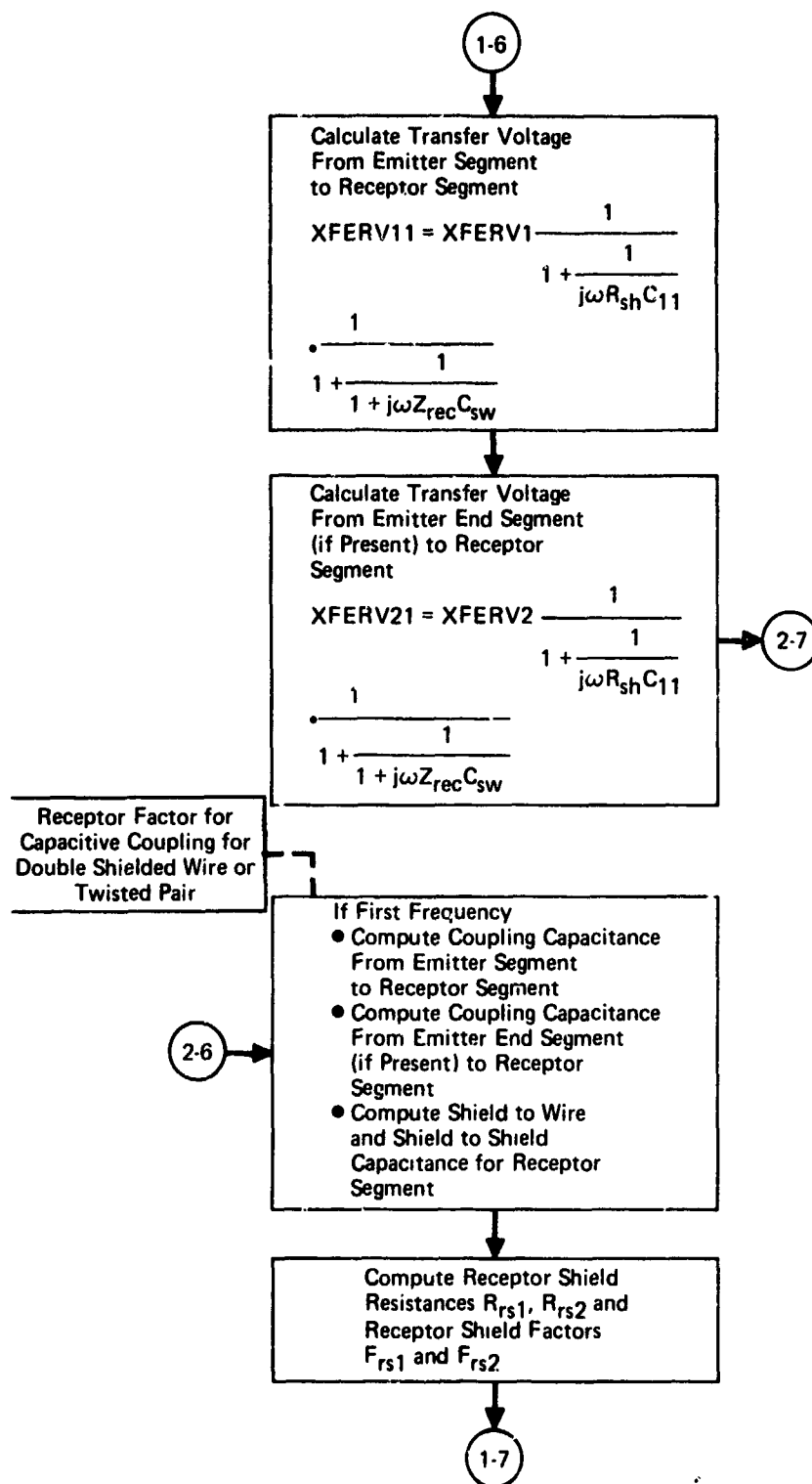
GP74 0267 51

FIGURE 30 (Continued)
WIRE TO WIRE TRANSFER ROUTINE (WTWTFR)
 (Part 4 of 11)



GP74 0267 52

FIGURE 30 (Continued).
WIRE TO WIRE TRANSFER ROUTINE (WTWTR)
 (Part 5 of 11)



GP74 0267 53

FIGURE 30 (Continued)
WIRE TO WIRE TRANSFER ROUTINE (WTWTFR)
 (Part 6 of 11)

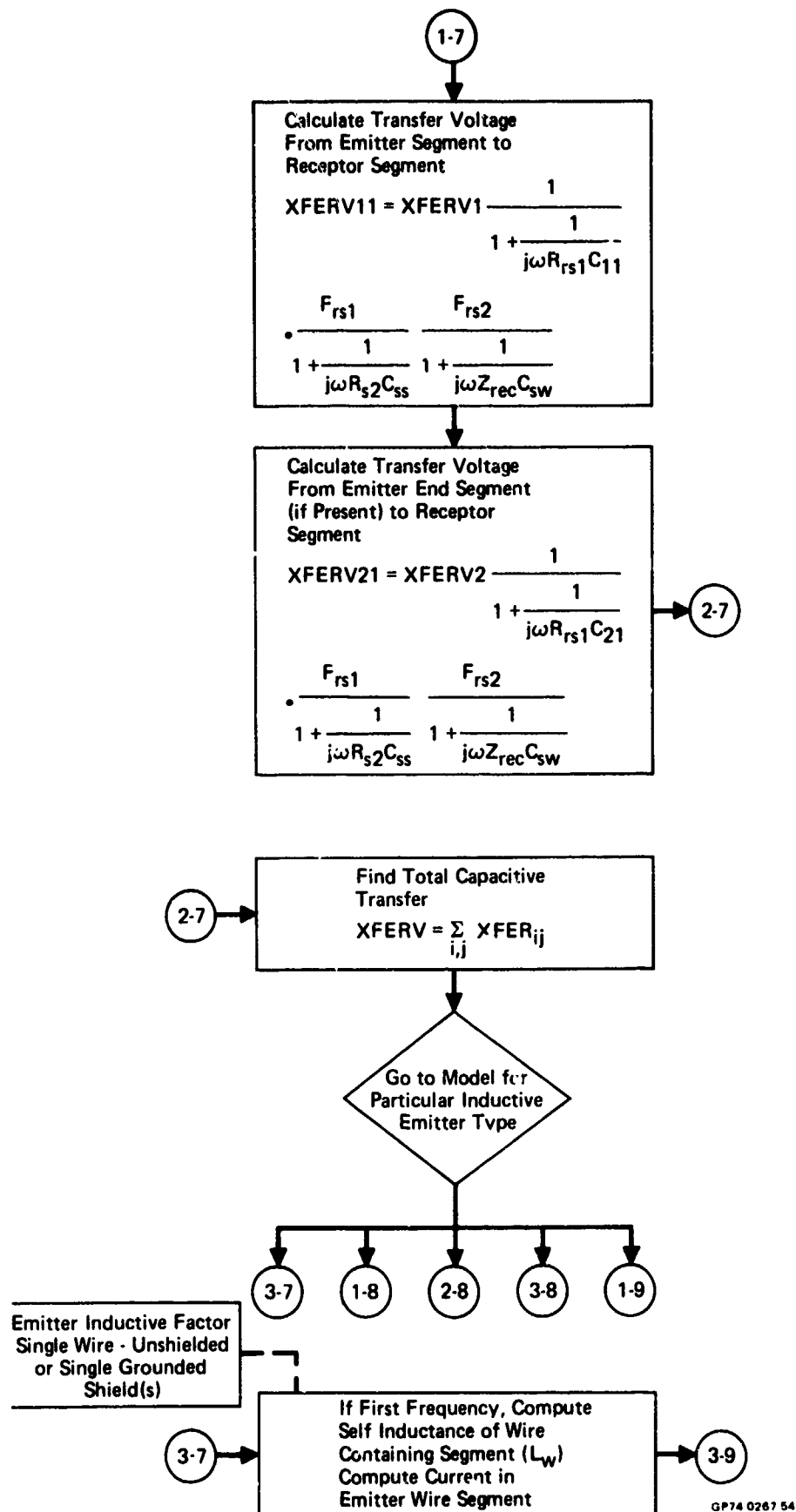


FIGURE 30 (Continued)
WIRE TO WIRE TRANSFER ROUTINE (WTWTFR)
(Part 7 of 11)

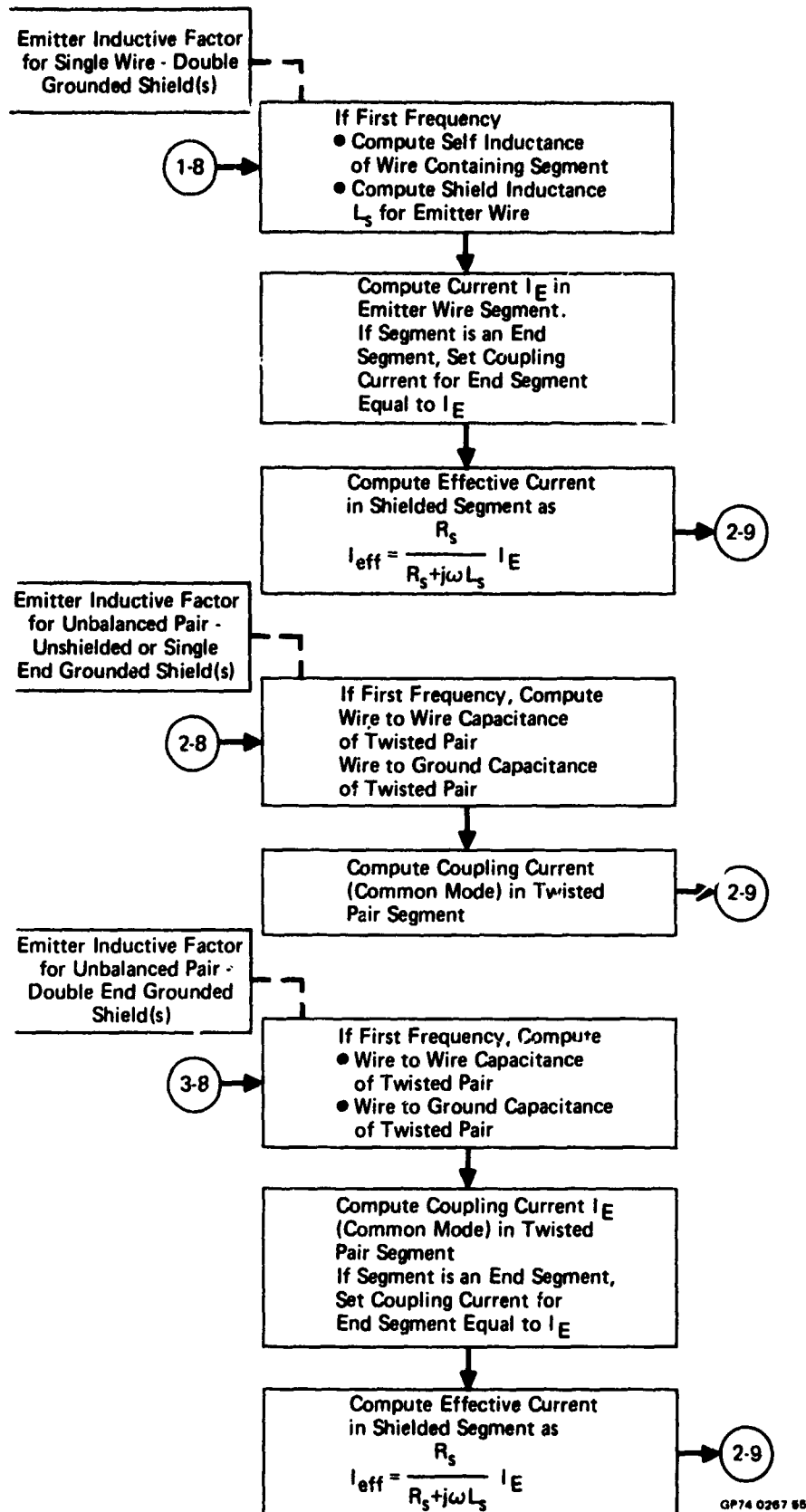
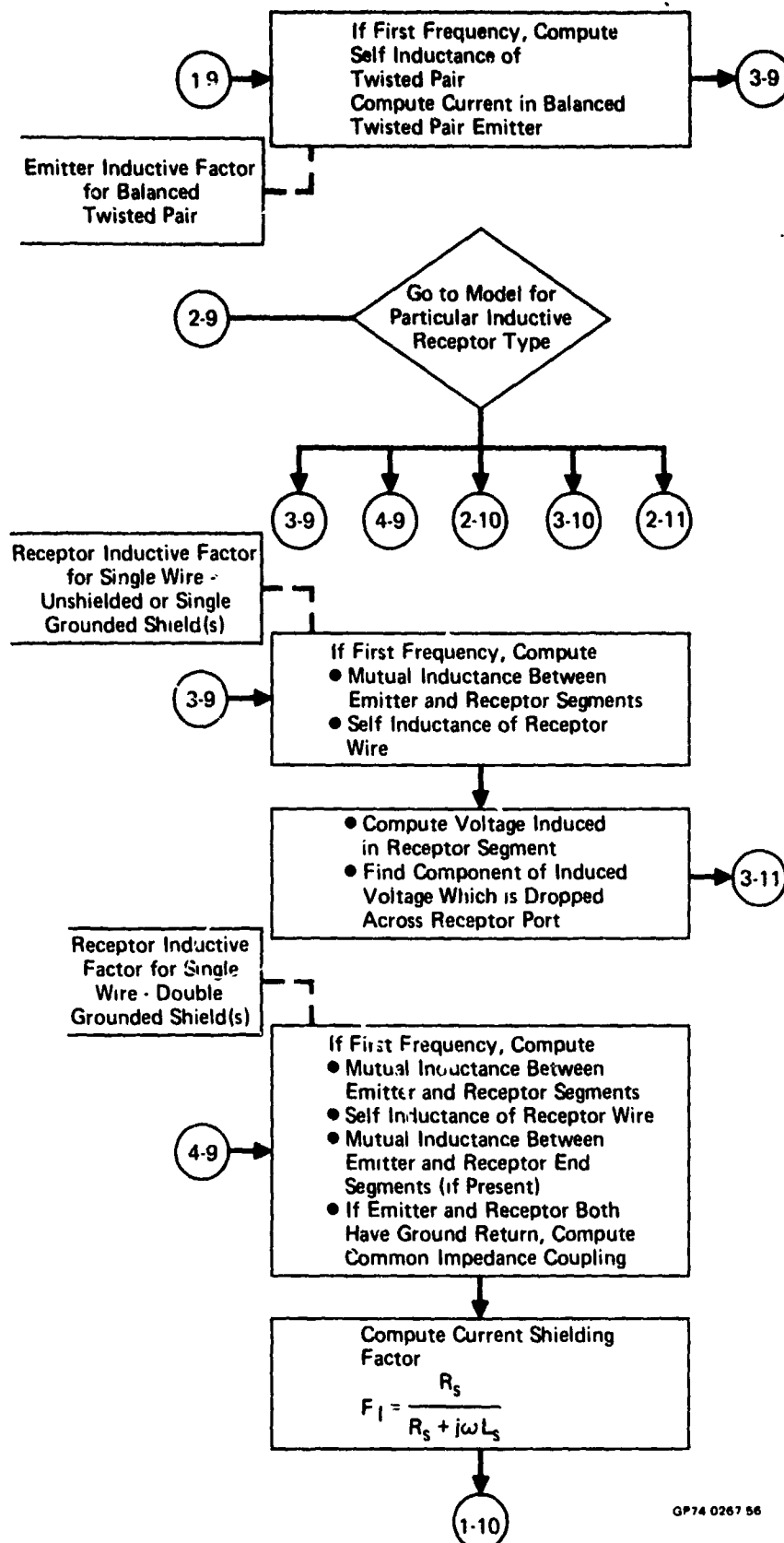


FIGURE 30 (Continued)
WIRE TO WIRE TRANSFER ROUTINE (WTWTFR)
(PART 8 of 11)



GP74 0267 56

FIGURE 30 (Continued)
WIRE TO WIRE TRANSFER ROUTINE (WTWTR)
 (Part 9 of 11)

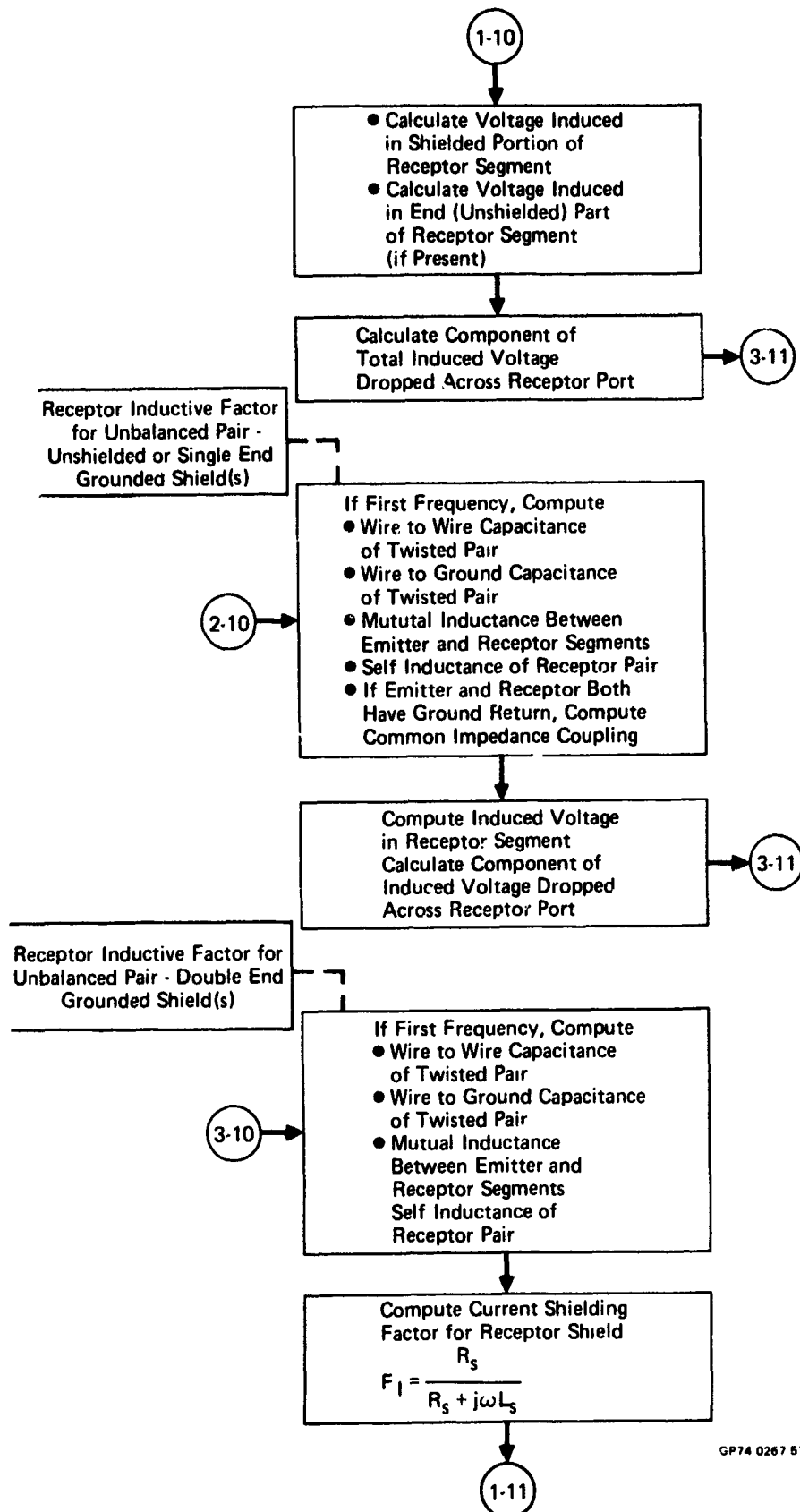
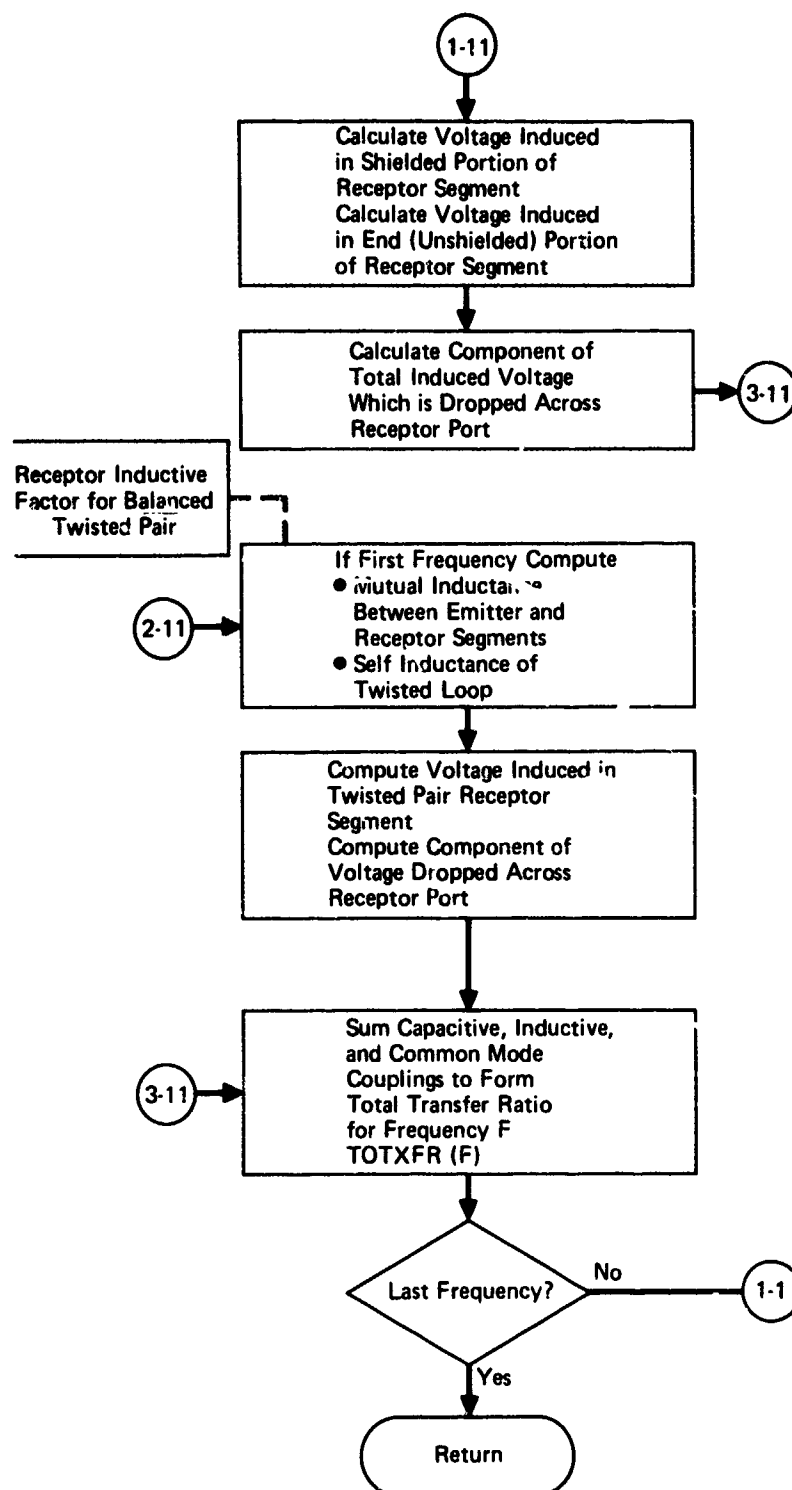


FIGURE 30 (Continued)
WIRE TO WIRE TRANSFER ROUTINE (WTWTFR)
 (Part 10 of 11)
 135



GP74 0267 58

FIGURE 30 (Continued)
WIRE TO WIRE TRANSFER ROUTINE (WTWTFR)
 (Part 11 of 11)

TABLE 10 FLOW SYMBOLS IN WTWTER SUBROUTINE

MATH FLOW SYMBOL	SYMBOL DEFINITION
Z_{left}	TOTAL IMPEDANCE CONNECTED TO LEFT SIDE OF WIRE SEGMENT
Z_{right}	TOTAL IMPEDANCE CONNECTED TO RIGHT SIDE OF WIRE SEGMENT
R_{sh}	SHIELD RESISTANCE OF SINGLE SHIELDED CONDUCTOR
F_{sh}	SHIELD FACTOR FOR SINGLE SHIELDED CONDUCTOR
ω	RADIAN FREQUENCY
C_{ws}	WIRE TO SHIELD CAPACITANCE FOR WIRE SEGMENT
C_{ss}	SHIELD TO SHIELD CAPACITANCE FOR DOUBLE SHIELDED SEGMENT
XFERV1	VOLTAGE ON OUTSIDE OF SHIELD OF EMITTER WIRE SEGMENT
R_{s1}	SHIELD RESISTANCE OF INSIDE SHIELD OF DOUBLE SHIELDED EMITTER
R_{s2}	SHIELD RESISTANCE OF OUTSIDE SHIELD OF DOUBLE SHIELDED EMITTER
F_{sh1}	SHIELD FACTOR FOR INSIDE SHIELD OF DOUBLE SHIELDED EMITTER
F_{sh2}	SHIELD FACTOR FOR OUTSIDE SHIELD OF DOUBLE SHIELDED EMITTER
C_{11}	COUPLING CAPACITANCE BETWEEN EMITTER SEGMENT AND RECEPTOR SEGMENT
C_{12}	COUPLING CAPACITANCE BETWEEN EMITTER SEGMENT AND RECEPTOR END
C_{21}	COUPLING CAPACITANCE BETWEEN EMITTER END AND RECEPTOR SEGMENT
C_{22}	COUPLING CAPACITANCE BETWEEN EMITTER SEGMENT AND RECEPTOR END
Z_{rec}	PARALLEL COMBINATION OF Z_{left} AND Z_{right} FOR RECEPTOR SEGMENT
XFERV2	VOLTAGE ON EMITTER WIRE SEGMENT

TABLE 10 FLOW SYMBOLS IN WTWTER SUBROUTINE (CONTINUED)

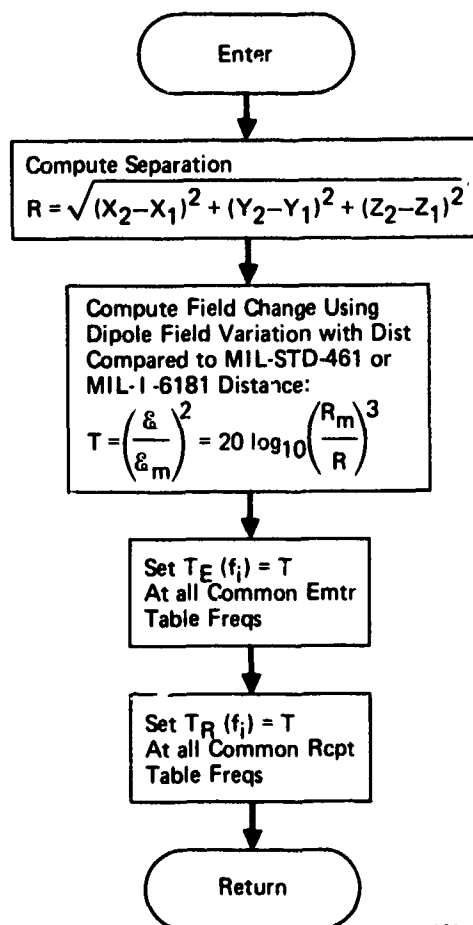
MATH FLOW SYMBOL	SYMBOL DEFINITION
XFERV11	VOLTAGE TRANSFER RATIO FROM EMITTER SEGMENT TO RECEPTOR SEGMENT
XFERV12	VOLTAGE TRANSFER RATIO FROM EMITTER SEGMENT TO RECEPTOR END
XFERV21	VOLTAGE TRANSFER RATIO FROM EMITTER END TO RECEPTOR SEGMENT
XFERV22	VOLTAGE TRANSFER RATIO FROM EMITTER SEGMENT TO RECEPTOR END
R_{rs1}	SHIELD RESISTANCE OF INSIDE SHIELD OF DOUBLE SHIELDED RECEPTOR
R_{rs2}	SHIELD RESISTANCE OF OUTSIDE SHIELD OF DOUBLE SHIELDED RECEPTOR
F_{rs1}	SHIELD FACTOR FOR INSIDE SHIELD OF DOUBLE SHIELDED RECEPTOR
F_{rs2}	SHIELD FACTOR FOR OUTSIDE SHIELD OF DOUBLE SHIELDED RECEPTOR
XFERV	TOTAL VOLTAGE TRANSFER RATIO FOR CAPACITIVE COUPLING
L_w	SELF INDUCTANCE OF EMITTER WIRE
L_s	SELF INDUCTANCE OF EMITTER SHIELD
I_E	CURRENT IN EMITTER WIRE
I_{eff}	EFFECTIVE CURRENT IN EMITTER SEGMENT
M	MUTUAL INDUCTANCE BETWEEN EMITTER AND RECEPTOR SEGMENTS
M'	MUTUAL INDUCTANCE BETWEEN EMITTER END AND RECEPTOR END
L_r	SELF INDUCTANCE OF RECEPTOR WIRE
L_{sr}	SELF INDUCTANCE OF RECEPTOR SHIELD
F_I	SHIELD FACTOR FOR INDUCTIVE SHIELDING
TOTXFR	TOTAL TRANSFER RATIO FOR CAPACITIVE AND INDUCTIVE COUPLING
R_s	EFFECTIVE RESISTANCE OF EMITTER SHIELD

It then calculates the capacitive and inductive coupling factors of the emitter segment (for the first frequency). Modifications are made to these factors according to the configuration (shielding, twisting, etc.) of the segment according to the setting of the program flags. This procedure is then repeated for the receptor segment after which the emitter and receptor factors are multiplied together to find the capacitive and inductive coupling between segments. The capacitive and inductive coupling components are then added together to form the transfer ratio (for the first frequency).

These calculations are repeated at every emitter and receptor sample frequency contained within the frequency range common to both emitter and receptor equipments (common frequencies).

5.3.3 Case-to-Case Coupled Transfer Function Routine (CTCTFR)

This routine uses the case-to-case dipole model discussed in Section 6.4.2.5 to evaluate the electromagnetic transfer function between two equipment cases in the same compartment. The flow through CTCTFR is shown in Figure 31, and the symbols are defined in Table 11.



GP74 0267 46

FIGURE 31
CASE TO CASE TRANSFER
Called by COUPLE

TABLE 11 FLOW SYMBOLS IN CTCTFR SUBROUTINE

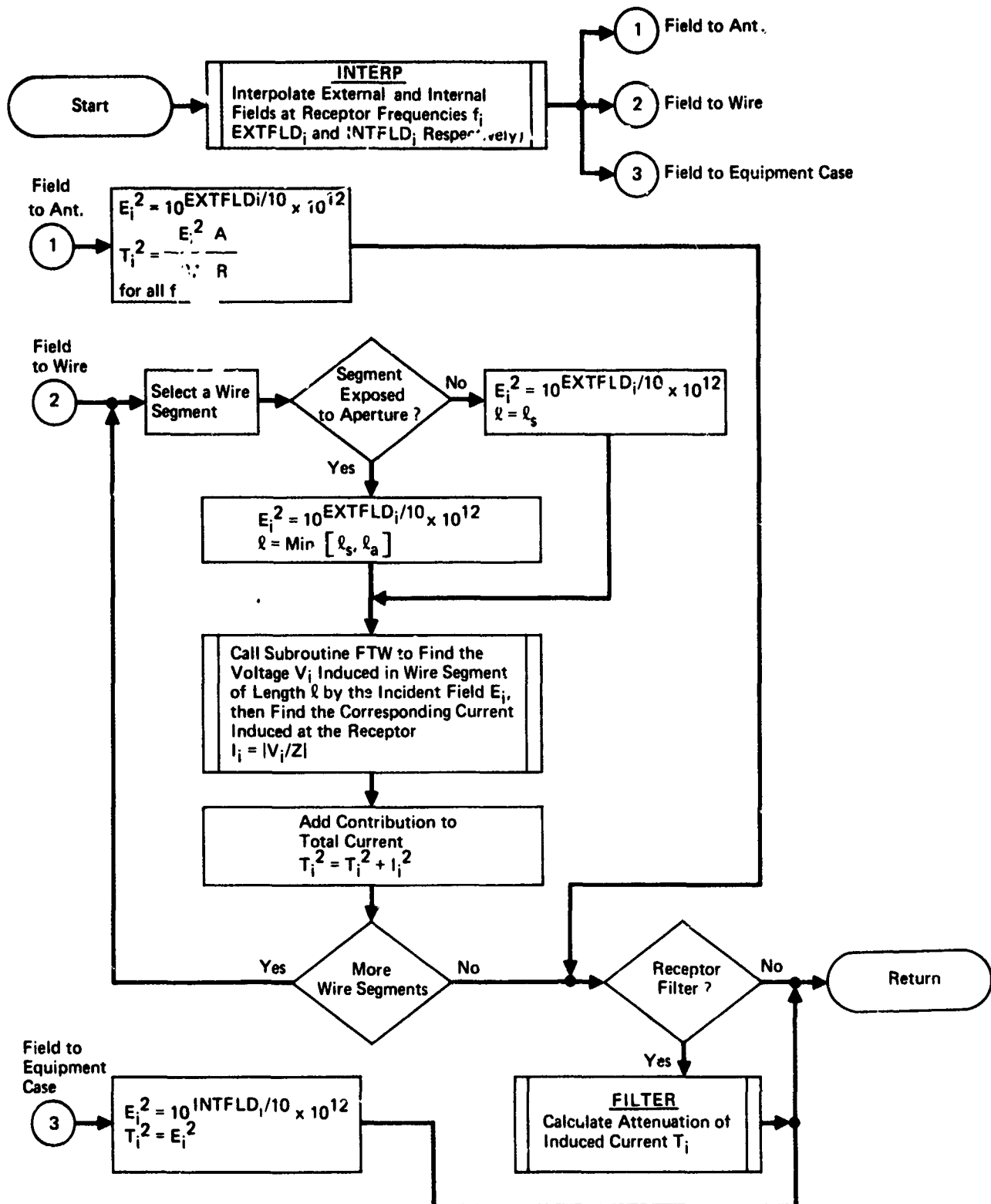
MATH FLOW SYMBOL	SYMBOL DEFINITION
x_1, y_1, z_1	COORDINATES OF EQUIPMENT CASE EMITTER
x_2, y_2, z_2	COORDINATES OF EQUIPMENT CASE RECEPTOR
ϵ	ELECTRIC FIELD INTENSITY AT RECEPTOR
ϵ_m	ELECTRIC FIELD INTENSITY A DISTANCE R_m FROM EMITTER
R_m	MIL-STD-461 OR MIL-STD-6181 DISTANCE (ONE METER)
R	SEPARATION BETWEEN EMITTER AND RECEPTOR
T	CASE-TO-CASE TRANSFER FUNCTION

5.3.4 Filter Routine (FILTER)

The routine calculates the attenuation provided by a filter placed in an emitter or receptor circuit to reduce interference. It uses the various filter models discussed in Section 6.4.2.1.

5.3.5 Environmental Field Routine (ENVIRN)

The environmental field routine calculates the interference at a receptor port due to ambient electromagnetic radiation, external to the system and, as attenuated by the skin, internal to it. Induced current is calculated for antenna and wire ports, while only the incident field is calculated for an equipment case. A flow diagram of ENVIRN is given in Figure 32, and the symbols used are given in Table 12.



GP74 0267 60

FIGURE 32
ENVIRONMENTAL FIELD ROUTINE
Flow Diagram

TABLE 12
MATH FLOW SYMBOLS IN ENVIRN

Math Flow Symbol	Definition
$EXTFLD_1$	external electric field interpolated at receptor frequency f_1
$INTFLD_1$	internal electric field interpolated at receptor frequency f_1
E_1	electric field $\mu V/M$
T_1	current induced by environmental field (unless receptor is an equipment case, where T_1 is set equal to E_1)
A_1	effective cross section of antenna
l_s	wire segment length
l_a	aperture length
R	real part of receptor impedance
Z	receptor impedance
V_1	voltage induced in wire segment
I_1	current induced in receptor by environmental field coupling to a wire segment
f_1	receptor frequencies

First, the user-supplied electric field levels are interpolated at receptor frequencies. If the receptor is an antenna port, the energy density associated with an incident plane wave at its antenna is calculated and multiplied by the effective cross section of the antenna to get the total received power. It is then converted to the value of induced current at each receptor frequency.

For a wire-connected port, the field-to-wire routine (FTW) (Section 5.3.1.2) is called for each wire segment. The field incident on aperture-exposed segments is assumed to be the external value, and on non-exposed segments it is assumed to be the internal level. The contribution of each segment is added to the total induced current at the receptor.

If a filter is connected to a wire or antenna-connected port, the FILTER subroutine (Section 5.3.4) calculates the attenuation of the induced current at each receptor frequency.

Section 6

MODELS

The mathematical models used by the program can be divided into the general classifications of emitter models, receptor models, transfer models, and the system model. The emitter models relate the parameters of the equipment and port data to the power spectral density output by the emitter port. These emitter models are incorporated in the program for most common emitter types and provision is made for user input of spectral densities for those types not modeled. The transfer models are used to compute the ratio between the energy output at an emitter port and that present at the input to a receptor port. For example, the antenna to antenna transfer model computes the ratio of the energy output of a transmitter to the energy at the input of the receiver. Receiver models relate the energy spectrum at the receptor port to the response produced by that spectrum. This calculation is based on the sensitivity of the receptor versus frequency.

The system model is used to relate the manner in which the emitter, transfer and receptor models are combined to account for simultaneous operation of all equipments. This enables calculations for compatibility and specification generation to be performed not only between pairs of equipments, but also among all equipments when all are operating simultaneously. The system formulas are given in Section 2.2.3; their mathematical basis is given in Section 2.2.1.

This section contains a description of the models incorporated in the program. This description consists of the mathematical formulation of the models in the cases where a concise formulation of this kind exists, and a general description for the cases where a concise mathematical formulation does not exist. At the conclusion of this section the formulas applicable to the IEMCAP program are expressed in tabular form along with pictorial representations shown in terms of the program input parameters.

6.1 EMITTER MODELS

6.1.1 Power Spectrum of Binary Frequency - Shift Keying

The mathematical model presented herein to represent binary frequency - shift keying is a sinusoidal wave of constant amplitude whose instantaneous frequency can assume either of two values, f_1 or f_2 . The instantaneous frequency is constant over periods of duration T , and either of the two values of frequency can be assumed at the start of each period with equal probability. The transition between the two values of frequency, when it occurs, takes place in such a way that the wave is continuous at the transition. This latter restriction is necessary to distinguish between equipments where the frequency of a single oscillator is changed back and forth between the two values of the instantaneous frequency, which is the case under consideration, and equipment where the output is obtained by switching back and forth between two free-running oscillators. It has been shown elsewhere that this latter case results

in a power spectrum of each oscillator consisting of a discrete line at the oscillator frequency and a continuous spectrum of the form $\sin^2(\pi f T)/(\pi f T)^2$, where f is the frequency and T is the inverse of the bit rate, centered on this line.

The model is used to obtain an envelope of the exact spectrum output of an FSK system. The validity of the envelope representation can be determined by going back through the derivation of the exact spectral density and then justifying the assumptions presented herein.

The general approach taken in deriving the exact spectral density (See Pelchat) is conventional and consists of computing the autocorrelation function from which the power spectrum is obtained by application of the Wiener-Khinchine theorem.

Some of the gross characteristics of the power spectrum of FSK are as follows. If the deviation ratio D , the difference between the two possible values of the instantaneous frequency divided by the bit rate, is much smaller than unity, the bulk of the power is contained in a bandwidth small compared to the bit rate and centered on the average frequency. Also, if D is equal to an integer, the power spectrum contains two discrete spectral lines.

The output of a frequency modulated output can be expressed as

$$e(t) = \text{Re} \left[\exp [j\omega_c t + \Delta\omega \int_{t_0}^t V(t') dt' + \theta] \right]$$

where

ω_c = carrier frequency

$V(t)$ = modulating wave form

$\Delta\omega$ = constant determining degree of modulation

t = time referenced to t_0

θ = phase angle

$V(t)$ is a binary wave form which can assume $+1$ or -1 , both with probability 0.5 . Transitions in $V(t)$ are instantaneous and are separated in time by an amount qT , q being an integer and T being the bit length.

The autocorrelation function $k(\tau)$ of $e(t)$ can be written as

$$\begin{aligned} k(\tau) &= E[e(t) \cdot e(t + \tau)] \\ &= \text{Re} \left[\exp(j\omega_c \tau) E[\exp(j\{\psi(\tau) - \psi(0)\})] \right] \end{aligned}$$

provided $[\psi(t + \tau) - \psi(t)]$ is stationary. $\psi(t)$ as used above is defined as $\Delta\omega \int_{t_0}^t V(t') dt' + \theta$. For the purpose of evaluating $k(\tau)$, it is convenient to define a new random process $\phi(t)$ as

$$\phi(t + \delta) = \psi(t)$$

with δ denoting the value of t in the interval $-T \leq t \leq 0$ at which a bit transition is possible. δ is a random variable with uniform probability density $p(\delta)$.

$$\begin{aligned} p(\delta) &= 1/T & 0 \leq \delta \leq T \\ p(\delta) &= 0 & \delta < 0, \delta > T \end{aligned}$$

$k(\tau)$ can be re-expressed as

$$\begin{aligned} k(\tau) &= \cos \omega_c \tau \cdot E \{ \exp (j[\phi(\tau+\delta) - \phi(\delta)]) \} \\ k(\tau) &= \cos \omega_c \tau \cdot R(\tau) \end{aligned}$$

The determination of $R(\tau)$ is carried out in two steps: for $0 \leq \tau \leq T$ and for $nT \leq \tau \leq (n+1)T$, $n = 1, 2, 3, \dots$. The results of this determination of $R(\tau)$ results in the following expression for $k(\tau)$.

$$\begin{aligned} k(\tau) &= \cos \omega_c \tau \left[\frac{2T-\tau}{2T} \cos \Delta\omega\tau + \frac{\tau}{2T} \frac{\sin \Delta\omega\tau}{\Delta\omega\tau} \right] \text{ for } 0 \leq \tau \leq T \\ \text{and} \\ k(\tau) &= \cos \omega_c \tau \left[\frac{\cos^{n-1} \Delta\omega T}{2} \left[\left(\cos \Delta\omega T + \frac{\sin \Delta\omega T}{T} \right) \cos \Delta\omega\tau_s \right. \right. \\ &\quad \left. \left. - \frac{T-\tau_s}{T} \sin \Delta\omega T \sin \Delta\omega\tau_s \right] \right] \\ &\text{for } nT \leq \tau < (n+1)T \end{aligned}$$

where τ_s is defined as $\tau - nT$.

The desired power spectrum $P(f)$ is given by the Fourier transform of $k(\tau)$

$$\begin{aligned} P(f) &= \int_{-\infty}^{\infty} \cos \omega_c \tau R(\tau) \exp (-j\omega\tau) d\tau \\ &= \frac{1}{2} [\delta(f_c) + \delta(-f_c)] * G(f) \end{aligned}$$

where

$$G(f) = \sum_{n=0}^{\infty} G_n(f) = 2 \sum_{n=0}^{\infty} \int_{nT}^{(n+1)T} R_n(\tau) \cos \omega\tau d\tau$$

The resulting spectrum is

$$P(f) = \frac{4\bar{P}}{\pi^2 f_B} \left[\frac{D}{D^2 - X^2} \right]^2 \frac{(\cos \pi D - \cos \pi X)^2}{1 - 2 \cos \pi D \cos \pi X + \cos^2 \pi D}$$

$$f_B = \text{Bit rate} = 1/T$$

$$f_c = (f_1 + f_2)/2$$

$$f_1, f_2 = \text{lower and upper instantaneous frequencies}$$

$$X = \frac{2(f - f_c)}{f_B} = \text{normalized frequency}$$

$$D = (f_1 - f_2)/f_B = \text{deviation ratio}$$

$$\bar{P} = \text{average power emitted}$$

$$G(f) = \text{power spectrum (watts/Hz)}$$

This exact analysis is assumed to be a valid representation since it is mathematically correct and has been experimentally proven to give the correct power spectrum, as presented in Pelchat's paper.¹

There are two distasteful aspects of the last expression which make it unreasonable for EMC analysis. The first is that it is highly oscillatory so that in a systems analysis the sampling rate of the spectrum would have to be recomputed for every new FSK system. The second problem arises when the deviation ratio D equals an integer, for then the resulting spectrum contains two discrete spectral lines. In broad band terminology, the result is a spectrum of infinite height and infinitesimal width.

Since power spectral density is only an intermediate step between power emitted and power received and most receptors have a certain amount of bandwidth, this last fault can be remedied by representing the discrete spectral lines by a power spectral density whose integrated power was equal to that contained in the discrete spectral line.

The model consists of the envelope function

$$P(f) = \frac{4\bar{P}}{\pi^2 f_B} \left[\frac{D}{D^2 - X^2} \right]^2$$

truncated in the vicinity of $X = \pm D$ by a fixed value dependent on the particular value of D .

The truncated value is selected with a view, not of approximating $P(f)$ as given by the exact expression in this region, but rather with the intention of having the same area under the model as lies under the exact expression in this region.

The exact form of the model, where $X = 2 \frac{\Delta f}{f_B}$ and $D = \frac{f_1 - f_2}{f_B}$, is

$$P_{BB}(f) = P_0 \quad \text{for } X \leq X_M$$

$$P_{BB}(f) = \frac{4P}{2f_B} \left(\frac{D}{D^2 - X^2} \right)^2 \quad \text{for } X > X_M$$

The bandwidth is the sum of the bit rate, f_B , and the frequency difference between the two oscillators, $f_1 - f_2$.

(both P_0 and X_M depend on the value of D as shown below)

$$\text{For } D < \frac{4}{\pi^2}$$

$$P_0 = \left(\frac{\pi}{2D} \right)^2 \frac{P}{f_B}$$

$$X_M = \sqrt{D^2 + (2D/\pi)^{2/3}}$$

$$\text{For } D > \frac{4}{\pi^2}$$

$$P_0 = \frac{\pi^2}{4} \frac{P}{f_B}$$

$$X_M = \sqrt{D^2 + 4/\pi^2 D}$$

These formulas may be related to the program input parameters by identifying the following:

P = transmitter average power (watts)

f_B = bit rate

diff = $f_1 - f_2 = Df_B$

f_c = center frequency (carrier) = $\frac{1}{2} (f_1 + f_2)$

This model depends on easily obtainable data, is physically sound, is reasonably efficient in run times and provides all the information about the FSK spectrum required to assess its effects on possible unintentional receptors.

6.1.2 Spectrum Model for Amplitude Modulation with Stochastic Process

The equation for an amplitude modulated waveform is

$$x(t) = K[1 + mS(t)] \cos(\omega_c t + \theta)$$

where $S(t)$ is the random modulating signal waveform

θ is the random phase between $(0, 2\pi)$
 ω_c is the carrier frequency
 m is the modulation index
 K is the amplitude

This waveform when put into the defining equation for the autocorrelation

$$R(\tau) = \lim_{T \rightarrow \infty} \frac{1}{T} \int_{-T/2}^{T/2} f(t) f(t + \tau) dt$$

leads to

$$R(\tau) = K^2 [1 + m^2 R_s(\tau)] \frac{1}{2} \cos \omega_c \tau$$

where the modulating waveform $S(t)$ is such that $\overline{S(t)} = 0$ and $R_s(\tau)$ is the autocorrelation function of the signal process.³

The Fourier transform of $R(\tau)$ results in the power spectral density

$$P(f) = \frac{1}{4} K^2 [\delta(f - f_c) + \delta(f + f_c) + m^2 P_s(f - f_c) + m^2 P_s(f + f_c)]$$

where

$$P_s(f) = F[R_s(\tau)]$$

The AM model used in IEMCAP assumes the modulation process to be voice, clipped voice, or non-voice.⁴ These modulation models are shown in the programmed formula section. Identifying these modulations as g_1 , g_2 and g_3 respectively the following formulas are applicable to IEMCAP:

$$P_{BB}(f) = \frac{m^2}{2} P_{g_i}(|\Delta f|) \quad i = 1, 2, 3$$

$$P_{NB} = P \delta(\Delta f)$$

The bandwidth used is twice the modulating signal bandwidth as determined by 81.

These formulas may be related to the program input parameters by making the following identifications:

P = carrier average power in (watts)

m = modulation index

$\Delta f = f - f_{\text{carrier}}$

This AM model provides a sufficient characterization of amplitude modulation for interference analysis with regard to unintentional receptors. It uses easily obtainable data in an efficiently running form that is physically sound.

6.1.3 Spectrum Model for Angle Modulation with Stochastic Process

Angle modulation can be represented as

$$Y(t) = \cos [\omega_c t + M(t) + \theta]$$

ω_c = carrier frequency

$M(t)$ = stochastic process

θ = random variable, independent of $M(t)$ with uniform distribution over $(0, 2\pi)$

For phase modulation the modulating signal is $M(t)$ while for FM the modulating signal is $d/dt M(t)$.

Since the modulating signal is a random process, it is necessary to determine the autocorrelation function of $Y(t)$ in terms of the autocorrelation function of $M(t)$ and from it the output spectrum by use of the Wiener-Khintchine Theorem.

The autocorrelation function of the output can be obtained as follows:⁵

$$R_Y(t_1, t_2) = E[Y_1 Y_2]$$

where

$$Y_1 = Y(t_1), Y_2 = Y(t_2)$$

$$M_1 = M(t_1), M_2 = M(t_2)$$

and

$$\rho(\theta) = 1/2\pi \quad (0, 2\pi)$$

$$= 0 \text{ elsewhere}$$

$$R_Y(t_1, t_2) = 1/2 \operatorname{Re} [\exp(j\omega(t_1 - t_2)) E(\exp(j(M_1 - M_2)))]$$

$M(t)$ is assumed to be slowly varying with respect to ω_c .

This expression is applicable to all random modulating signals regardless of their distribution but the normal (Gaussian) process is the only random process that permits explicit solution to the problem. Therefore, a Gaussian process is assumed and the calculation completed, resulting in:

$$R_y(\tau) = 1/2 \exp(-\sigma_M^2) \exp(R_M(\tau)) \cos \omega_c \tau$$

where

$M(t)$ = a stationary random process

$\sigma_M^2 = \sigma_{M_1}^2 = \sigma_{M_2}^2$ = mean square value of modulating signal

and $R_M(\tau = t_1 - t_2)$ = the autocorrelation function of $M(t)$.

The output spectrum is now obtained by Fourier transforming $R_y(\tau)$.

An approximation to the frequency modulated signal for a known bandwidth stochastic process is used in IEMCAP. The equations are:

$$P(f) = \frac{P}{2.062 B_{FM}} \quad ; |\Delta f| \leq B_{FM}$$

$$P(f) = \frac{P}{2.062 B_{FM}} \left(\frac{B_{FM}}{f} \right)^{33.219} \quad ; B_{FM} < \Delta f \leq 2 B_{FM}$$

$$P(f) = \frac{P}{2.062 B_{FM}} \times 10^{-10} \quad ; |\Delta f| > 2 B_{FM}$$

where $B_{FM} = f_{DEV} + B$

f_{DEV} = peak frequency deviation

B = bandwidth of modulation process and

P = transmitter power (peak in watts)

This model is mathematically consistent with the stochastic characterization of received signal power into an unintentional receptor. The input data is easily obtainable.

6.1.4 Spectral Characteristics of Single Sideband Amplitude, Phase and Frequency Modulation with a Stochastic Process

Consider a real function of $g(t)$ whose Fourier transform is

$$P(f) = \int_{-\infty}^{\infty} g(t) \exp(-j2\pi ft) dt$$

$g(t)$ can be represented as ⁶

$$g(t) = \int_{-\infty}^0 G(f) \exp(j2\pi ft) dt + \int_0^{\infty} G(f) \exp(j2\pi ft) dt$$

or

$$g(t) = 1/2 \int_{-\infty}^{\infty} (1 + \operatorname{sgn} f) G(f) \exp(-j2\pi ft) dt + 1/2 \int_{-\infty}^{\infty} (1 - \operatorname{sgn} f) G(f) \exp(-j2\pi ft) dt$$

where

$$\operatorname{sgn} f = \begin{cases} 1 & f > 0 \\ -1 & f < 0 \end{cases}$$

and its inverse Fourier transform is

$$F^{-1}[\operatorname{sgn} f] = j / \pi t$$

Thus $g(t)$ can be expressed as

$$g(t) = g_+(t) + g_-(t)$$

where

$$g_+(t) = 1/2 g(t) + 1/2 j \frac{1}{\pi t} * g(t)$$

$$g_-(t) = 1/2 g(t) - 1/2 j \frac{1}{\pi t} * g(t)$$

and $*$ denotes convolution.

The Hilbert transform of $g(t)$ is defined as

$$\hat{g}(t) = 1/\pi * g(t) = 1/\pi \int_{-\infty}^{\infty} \frac{g(\tau)}{t-\tau} d\tau$$

and the Hilbert transform of $\hat{g}(t)$ is

$$\hat{\hat{g}}(t) = 1/\pi \int_{-\infty}^{\infty} \frac{\hat{g}(\tau)}{t-\tau} d\tau = -g(t)$$

Therefore

$$g_+(t) = 1/2 [g(t) + j \hat{g}(t)]$$

and

$$g_-(t) = 1/2 [g(t) - j \hat{g}(t)]$$

Although these previous mathematical steps are correct, the logic is not too appealing to a purist. A somewhat more complete treatment may be obtained from Morse & Feshbach.

The same theorems apply to analytic signals as to other standard signals. The Wiener-Khintchine Theorem can be used to calculate the power contained in single sideband signals.

It can be shown that

$$P_{g-}(f) = 1/2 [1 - \text{sgn } f] P_g(f)$$

$$P_{g+}(f) = 1/2 [1 + \text{sgn } f] P_g(f)$$

and

$$P_{g+g-}(f) = 0$$

where

$P_g(f)$ is the power spectrum of $g(t)$

$P_{g-}(f)$ is the power spectrum of $g_-(t)$

$P_{g+}(f)$ is the power spectrum of $g_+(t)$

and

$P_{g+g-}(f)$ is the cross spectral density

The last expression shows that $g_+(t)$ and $g_-(t)$ are uncorrelated.

Consider now an AM single sideband signal analysis. There are several methods of generating AM single sideband signals including the filter method and the phase shift method. Using the filter method, the output power can be expressed in terms of the filtered input

$$P_o(f) = |H(f)|^2 P_i(f)$$

where

$$H(f) = -j \text{sgn } f$$

Consider a double sideband suppressed carrier amplitude modulated signal

$$g_D(t) = 2 \operatorname{Re} \{g(t) \exp(j2\pi f_c t)\}$$

Its spectrum is

$$P_D(f) = P(f-f_c) + P(f+f_c)$$

This may be decomposed into upper and lower sidebands

$$P_D(f) = P_U(f-f_c) + P_L(f+f_c)$$

where

$$P_U(f) = P_+(f-f_c) + P_-(f+f_c)$$

and

$$P_L(f) = P_+(f+f_c) + P_-(f-f_c)$$

where G_+ and G_- are the Fourier transformation of $g_+(t)$ and $g_-(t)$. The upper and lower sideband signals can then be represented as

$$g_U(t) = \operatorname{Re} \{[g(t) + j g(t)] \exp(j2\pi f_c t)\}$$

and

$$g_L(t) = \operatorname{Re} \{[g(t) - j g(t)] \exp(j2\pi f_c t)\}$$

The power spectrum of, for example, an (upper) SSB-AM waveform using the analysis tools presented previously is obtained using

$$\begin{aligned} g_U(t) &= 2 \operatorname{Re} [g_+(t) \exp(j2\pi f_c t) \exp(j\theta)] \\ &= g_+(t) j2\pi f_c t \exp(j\theta) + g_-(t) \exp(-j2\pi f_c t) \exp(-j\theta) \end{aligned}$$

where θ is a random variable with uniform distribution

$$p(\theta) = \begin{cases} 1/2\pi & 0 \leq \theta < 2\pi \\ 0 & \text{elsewhere} \end{cases}$$

and $g(t)$ is an independent stationary random process.

Using the Wiener-Khintchine Theorem, the power density for the (upper) AM-SSB is

$$P_U(f) = P_{g+}(f-f_c) + P_{g-}(f+f_c)$$

Similarly for the (lower) sideband

$$P_L(f) = P_{g+}(f+f_c) + P_{g-}(f-f_c)$$

Three models in IEMCAP are contained in this discussion. They are double sideband suppressed carrier, AM-DSB/SC, upper single sideband suppressed carrier, SSB-upper and lower single sideband suppressed carrier, SSB-lower. As in the amplitude modulation model there are three modulation forms assumed, g_i , where $i = 1, 2, 3$.

- $i = 1 = \text{voice}$
- $i = 2 = \text{clipped voice}$
- $i = 3 = \text{non-voice}$

The model for AM-DSB/SC is

$$P_{BB}(f) = P/2 \quad g_i(|\Delta f|) \quad i = 1, 2, 3$$

Bandwidth equals twice modulation bandwidth

The model for SSB-upper is

$$P_{BB}(f) = P \quad g_i(\Delta f) \quad i = 1, 2, 3$$

Bandwidth equals modulation bandwidth

The model for SSB-lower is

$$P_{BB}(f) = P \quad g_i(-\Delta f) \quad i = 1, 2, 3$$

Bandwidth equals modulation bandwidth

In all three models described herein P is the transmitter peak envelope power in watts.

These sideband models provide sufficient frequency and amplitude description for the assessment of the interference effects on non intentional receptors.

6.1.5 A Simplified Method For Calculating The Bounds On The Emission Spectra Of Chirp Radars ECAC TN-002-27

The model used in IEMCAP to represent the emission spectrum of chirp radars consists of an envelope approximation encompassing all the significant aspects of this form of emission.

The form of the spectrum envelope approximation is as shown in Figure 33.

$$P_{dB}(f) = P_0 \quad 0 \leq |\Delta f| \leq \Delta f_{aa}$$

$$P_{dB}(f) = P_0 - M \log \left| \frac{\Delta f}{\Delta f_{aa}} \right| \quad \Delta f_{aa} < |\Delta f| \leq \Delta f_b$$

If $\Delta f_2 \geq \Delta f_b$:

$$P_{dB}(f) = P_0 - 20 \log \left| \frac{\Delta f}{\Delta f_1} \right| \quad \Delta f_b < |\Delta f| \leq \Delta f_2$$

$$P_{dB}(f) = P_0 - 20 \log \left| \frac{\Delta f_2}{\Delta f_1} \right| - 40 \log \left| \frac{\Delta f}{\Delta f_2} \right| \quad |\Delta f| > \Delta f_2$$

If $\Delta f_2 < \Delta f_b$:

$$P_{dB}(f) = P_0 - 20 \log \left| \frac{\Delta f_2}{\Delta f_1} \right| - 40 \log \left| \frac{\Delta f}{\Delta f_2} \right| \quad |\Delta f| > \Delta f_2$$

where

$$P_0 = 10 \log \left[P \left(\tau + \frac{\tau_r}{2} + \frac{\tau_f}{2} \right)^2 f_B / D \right]$$

f_c = carrier frequency

f_0 = function of f_c , τ , τ_r , τ_f , D

Δf = $f - f_0$

Δf_{aa} , Δf_b = functions of τ , τ_r , τ_f , D , $\text{sgn}(f - f_0)$

P = RF power (peak)

τ = pulse width

τ_r = pulse rise time

τ_f = pulse fall time

D = pulse compression ratio (negative of frequency decreases during pulse)

f_B = pulse repetition rate

$$\Delta f_1 = \frac{\sqrt{|D|}}{\pi (\tau + \tau_r/2 + \tau_f/2)}$$

$$\Delta f_2 = \frac{1/\tau_r + 1/\tau_f}{2\pi}$$

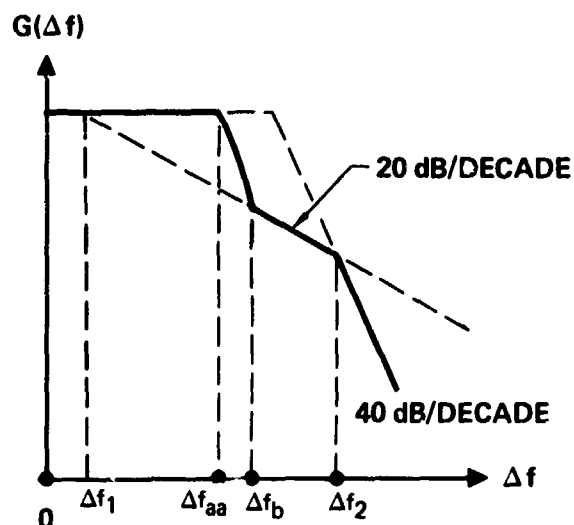


FIGURE 33
SPECTRUM ENVELOPE OF CHIRP RADAR

Note that the frequency break points Δf_{aa} and Δf_b are functions of the sign of $(f - f_0)$. The spectrum is not necessarily symmetric about f_0 but may be skewed in one direction or the other. The spectrum of a chirp radar pulse would be symmetric about f_0 only if the fall time and rise time of the pulse were the same.

An algorithm for the power spectral density of a chirp radar pulse is given in Figure 34.

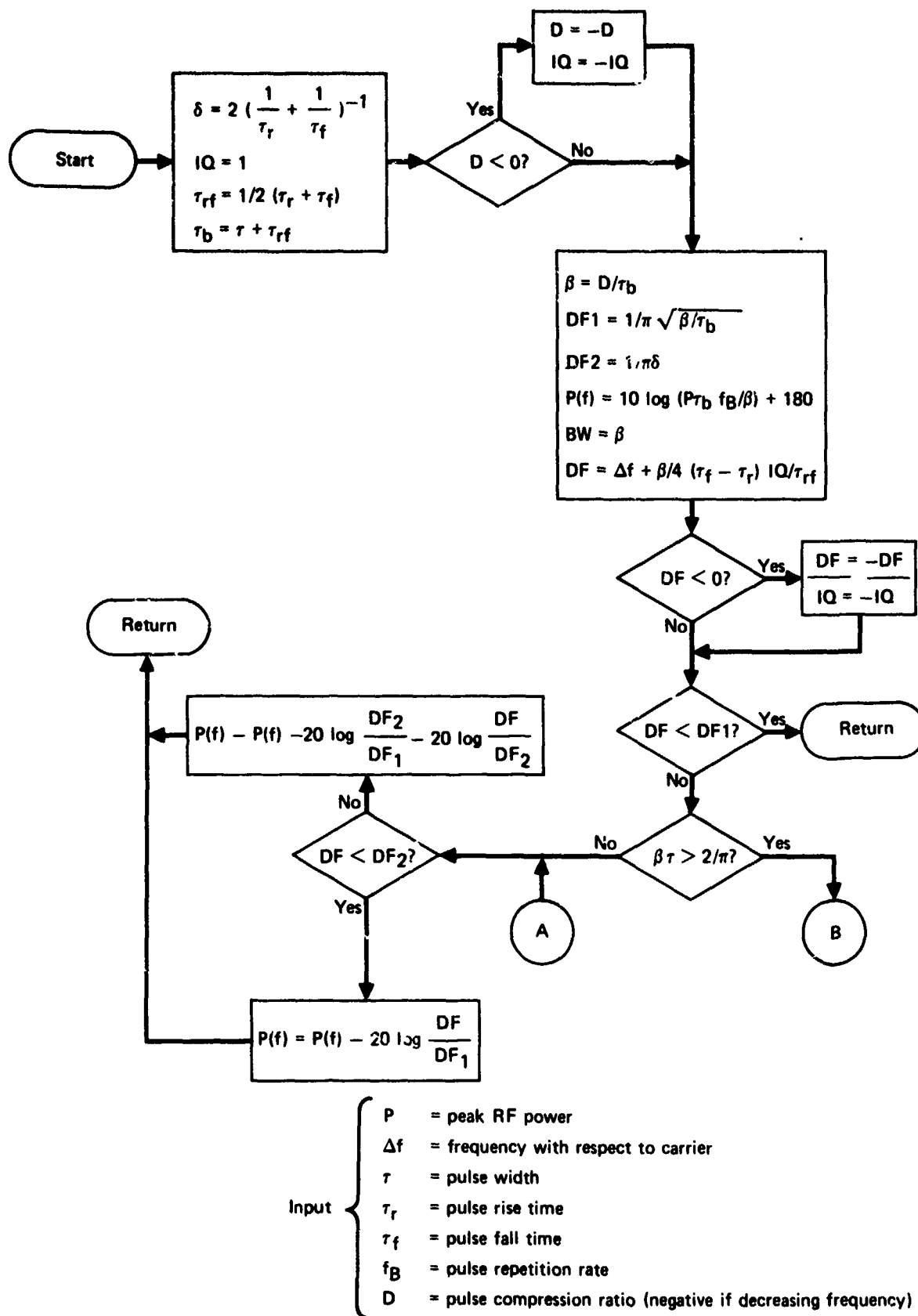


FIGURE 34
FLOW DIAGRAM OF CHIRP RADAR ALGORITHM

GP74 0267 1

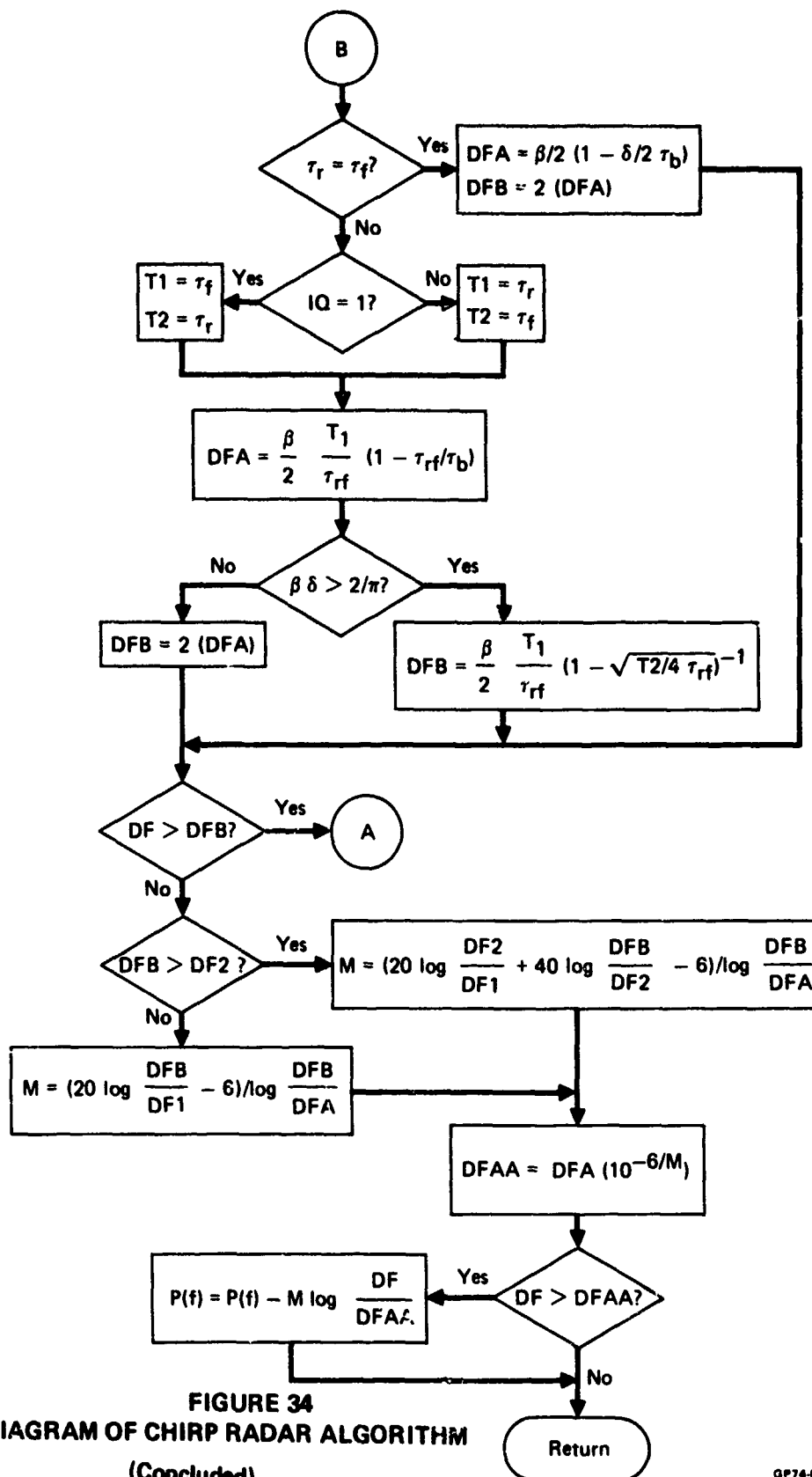


FIGURE 34
FLOW DIAGRAM OF CHIRP RADAR ALGORITHM
(Concluded)

GP74-0267 2

6.1.6 PCM/AM-NRZ

In PCM/AM-NRZ modulation, a PCM-NRZ waveform is used to modulate an RF carrier. Basically, there are two types of PCM-NRZ coding, the most familiar being a representation of one binary state by one voltage level and the other binary state by the other level. In the alternative coding scheme, one binary state is represented by a change in voltage level at the beginning of the bit interval, and the other binary state is represented by no change in level. Assuming the two binary states carry the same information value, both states are equally probable. Consequently, regardless of which coding scheme is used, the a priori probability of a given voltage level occurring in an interval is exactly one-half, and the two coding schemes are characterized by the same stochastic process. Choosing the two voltage levels of 0 and V_0 , the PCM waveform may be expressed:

$$v(t) = \frac{V_0}{2} [1 + m(t)]$$

where $m(t)$ is a stochastic process, $m(t) = \pm 1$ with equal probabilities in the interval $n\tau < t < (n+1)\tau$.

The autocorrelation function of $v(t)$ is then:

$$R_v(\tau) = \overline{v(t) v(t+\tau)} = \frac{V_0^2}{4} \overline{[1+m(t)] [1+m(t+\tau)]}$$

$$R_v(\tau) = \frac{V_0^2}{4} \overline{[1+m(t)+m(t+\tau) + m(t) m(t+\tau)]}$$

Since the expected value of $m(t)$ or $m(t+\tau)$ is zero,

$$R_v(\tau) = \frac{V_0^2}{4} \overline{[1 + m(t) m(t+\tau)]}$$

The expected value of $m(t)m(t+\tau)$ can be thought of as the average of the product of the original waveform and an identical waveform delayed in time by τ seconds.

For $\tau < T$ the two waveforms will be identical in every interval $nT < t < (n+1)T$ for a total time of $T - \tau$. For the rest of the interval, $m(t+\tau)$ and $m(t)$ are independent of each other.

$$\overline{m(t) m(t+\tau)} = \overline{m^2(t)} = 1 \quad nT < t < (n+1)T - \tau$$

$$\overline{m(t) m(t+\tau)} = \overline{m(t) m(t+\tau)} = 0 \quad [(n+1)T - \tau] < t < (n+1)T$$

The expected value of the product $m(t) m(t+\tau)$ will then be the weighted average:

$$\overline{m(t) m(t+\tau)} = \frac{T - |\tau|}{T} \quad |\tau| < T$$

Of course, for $\tau > T$, $m(t)$ and $m(t+\tau)$ are completely independent in any interval and $m(t)m(t+\tau) = 0$. The autocorrelation function can therefore be expressed as

$$R_V(\tau) = \begin{cases} \frac{V_o^2}{4} + \frac{V_o^2}{4} \left(1 - \frac{|\tau|}{T}\right) & |\tau| < T \\ \frac{V_o^2}{4} & |\tau| > T \end{cases}$$

From the Wiener-Khintchine Theorem, the power spectral density of a stationary stochastic process is equal to the Fourier Transform of its autocorrelation function.

$$P_V(f) = \frac{V_o^2}{4} \delta(f) + \frac{V_o^2}{4} \frac{\sin^2(\pi f T)}{(\pi f T)^2}$$

So the power spectral density is a DC spike plus a continuous spectrum with a bandwidth corresponding to the reciprocal of the bit period, centered about $f = 0$.

When the PCM signal is used to modulate an RF carrier,

$$e(t) = v(t) \cos(2\pi f_c t)$$

$$R_v(\tau) = \overline{e(t) e(t+\tau)} = \overline{v(t) \cos(2\pi f_c t) v(t+\tau) \cos[2\pi f_c(t+\tau)]}$$

Assuming that the sinusoidal term is independent of the stochastic process,

$$R_v(\tau) = \overline{v(t) v(t+\tau)} \cos(2\pi f_c t) \cos[2\pi f_c(t+\tau)]$$

Taking the Fourier Transform,

$$P_v(f) = \int_{-\infty}^{\infty} R_v(\tau) \exp[-j2\pi f_c \tau] d\tau$$

Considering the positive sided spectrum only, $f > 0$,

$$P_v(f) = \frac{P_T}{4} \delta(f - f_c) + \frac{P_T}{4} \frac{\sin^2[\pi(f - f_c) T]}{[\pi(f - f_c) T]^2}$$

where P_T is $\frac{V_0^2}{2}$, the peak transmitter power. The power in the carrier component is $\frac{P_T}{4}$, and the integrated power in the random component is also $\frac{P_T}{4}$, with a total of $\frac{P_T}{2}$. The average power is indeed $\frac{P_T}{2}$, since the transmitter would be "on" only half of the time.

The envelope of the spectral density has skirts which fall off at 20 dB/decade.

The PCM-NRZ model discussed herein is used, in IEMCAP, as both an RF modulation waveform and as a signal/control baseband spectrum.

The RF model consists of

$$P_{BB}(f) = \frac{1}{4} \frac{P}{f_B} \quad \text{for } |\Delta f| < \Delta f_M$$

$$P_{BB}(f) = \frac{1}{4} \frac{P}{f_B} \left(\frac{\Delta f_M}{\Delta f} \right)^2 \quad \text{for } |\Delta f| > \Delta f_M$$

$$P_{NB}(f) = \frac{1}{4} P \delta(\Delta f)$$

where

$$\Delta f = f - f_c$$

$$\text{bandwidth} = f_B = \text{bit rate}$$

$$\Delta f_M = \frac{1}{\pi} f_B$$

P = peak transmitter power

The signal/control model consists of

$$P_{BB}(f) = \frac{1}{2} \frac{A^2}{f_B} \quad 0 < f \leq f_M$$

$$P_{BB}(f) = \frac{1}{2} \frac{A^2}{f_B} \left(\frac{f_M}{f} \right)^2 \quad f > f_M$$

where

$$\text{bandwidth} = \frac{1}{2} f_B = \frac{1}{2} (\text{bit rate})$$

$$f_M = \frac{f_B}{\pi}$$

A = peak voltage/current into 1 ohm

This model provides a sufficient representation of PCM-NRZ modulation to be used for both a baseband and RF model. The routine inputs are easily obtainable and the model is physically sound.

6.1.7 Pulse Position Modulation

Pulse position modulation is constituted by the position of a fixed width pulse being used to convey sampled analog information. It is similar to pulse duration modulation (PDM), with a variable trailing edge being replaced by a short pulse. A PPM waveform can be generated from a PDM waveform by triggering off the trailing edge of each pulse.

The advantage of PPM is that less power is transmitted in the waveform. For a sampling period "T" and pulse width "δ", the average power is $E_0^2 \frac{\delta}{T}$.

The power spectral density of a PPM waveform can be determined from its autocorrelation function $R(\tau)$ by means of the Wiener-Khintchine Theorem.

The autocorrelation function $R(\tau)$ is defined:

$$R(\tau) = \overline{e(t) e(t + \tau)}$$

To derive the autocorrelation function of a PPM waveform, it is convenient to express $e(t)$ as the sum of two waveforms $e_a(t) + e_b(t)$, each sampled at intervals $2T$.

Then

$$R(\tau) = \overline{[e_a(t) + e_b(t)] [e_a(t + \tau) + e_b(t + \tau)]}$$

$$R(\tau) = \overline{e_a(t) e_a(t + \tau)} + \overline{e_b(t) e_b(t + \tau)} + \overline{e_a(t) e_b(t + \tau)} + \overline{e_b(t) e_a(t + \tau)}$$

$$R(\tau) = R_{aa}(\tau) + R_{bb}(\tau) + R_{ab}(\tau) + R_{ba}(\tau)$$

As in PDM, the simplifying assumption is made that the samples are independent of each other. This component $R_{aa}(\tau)$ is the autocorrelation function of a PPM wave sampled every $2T$ seconds, and is equal to E_0^2 times the expected value of the overlap between the function $e_a(t)$ and $\overline{e_a(t + \tau)}$.

The average overlap can be considered as the average pulse width of a pulse train equal to the product $e_a(t)e_a(t + \tau)$, which takes on values of 0 or E_0^2 .

For $0 < \tau < \delta$, the average overlap is $\delta - \tau$, so

$$R_{aa}(\tau) = \begin{cases} \frac{E_0^2 (\delta - \tau)}{2T} & 0 < \tau < \delta \\ 0 & \delta < \tau < T \end{cases}$$

For values of τ between δ and T , no overlapping is possible, and the correlation function $R_{aa}(\tau)$ is zero. For values of τ between T and $2T$, there is a possibility of overlap between each pulse and the following pulse advanced by time τ .

The expected value of the overlap, $\langle \xi \rangle$, can be evaluated

$$\langle \xi \rangle = \int_0^T \int \int dx dy \phi(x, y) \xi(x, y, \tau)$$

where $\phi(x, y)$ is the mutual probability density of \tilde{x} , \tilde{y} pulse positions.

Assuming a uniform, independent pulse position between zero and $T - \delta$, $\phi(x, y) \equiv \left(\frac{1}{T - \delta}\right)^2$.

The overlap $\xi(x, y, \tau)$ is equal to

$$\xi(x, y, \tau) = \text{Sup} [\delta - |x - T + \tau' - y|, 0] \quad 0 < \tau' < T \quad \text{where } \tau' = \tau - T$$

where Sup means supremum.

The integral is evaluated over the area in the x - y plane where $\xi \geq 0$. The area must be broken up into regions where $x - T + \tau' - y$ is positive and regions where it is negative.

The result of the integration is:

$$R(T + \tau') = \begin{cases} \frac{E_0^2}{4T(T - \delta)^2} \frac{\tau'^3}{3} & \tau' \leq \delta \\ \frac{E_0^2}{4T(T - \delta)^2} \left[2\delta^2(\tau' - \delta) + \frac{(2\delta - \tau')^3}{3} \right] & \delta \leq \tau' \leq 2\delta \\ \frac{E_0^2}{4T(T - \delta)^2} 2\delta^2(\tau' - \delta) & 2\delta \leq \tau' \leq T \end{cases}$$

Defining the function $f(x)$, $0 < x < T$, as

$$f(x) = \begin{cases} x^3/3 & 0 < x < \delta \\ 2\delta^2(x-\delta) + \frac{(2\delta-x)^3}{3} & \delta < x < 2\delta \\ 2\delta^2(x-\delta) & 2\delta < x < T \end{cases}$$

we can write

$$R_{aa}(\tau) = R_{bb}(\tau) = \begin{cases} \frac{E_o^2(\delta-\tau)}{2T} & 0 < \tau < \delta \\ 0 & \delta < \tau < T \\ \frac{E_o^2}{2T(T-\delta)^2} & T < \tau < 2T \\ \frac{E_o^2}{2T(T-\delta)^2} f(3T-\tau) & 2T < \tau < 3T \end{cases}$$

The cross-correlation function $R_{ab}(\tau)$ can be obtained more easily. For $\tau > 0$, it is obvious that $R_{ab}(\tau)$ is equal to the same integral as $R_{aa}(\tau + T)$ for $\tau > 0$.

$$R_{ab}(\tau) = R_{ba}(\tau) = \begin{cases} \frac{E_o^2}{2T(T-\delta)^2} f(\tau) & 0 < \tau < T \\ \frac{E_o^2}{2T(T-\delta)^2} f(2T-\tau) & T < \tau < 2T \end{cases}$$

Combining $R(\tau) = 2 \times R_{ab}(\tau) + 2 \times R_{ab}(\tau)$, we obtain an expression with periodic and non-periodic components

$$R(\tau) = R(\tau)|_{\text{per}} + R(\tau)|_{\text{ran}}$$

$$R(\tau)|_{\text{per}} = \frac{E_o^2}{T(T-\delta)^2} [f(\tau) + f(T-\tau)] \quad 0 < \tau < T$$

$$R(\tau)|_{\text{ran}} = \begin{cases} \frac{E_o^2(\delta-\tau)}{T} - \frac{E_o^2}{T(T-\delta)^2} f(T-\tau) & 0 < \tau < \delta \\ -\frac{E_o^2}{T(T-\delta)^2} f(T-\tau) & \delta < \tau < T \end{cases}$$

The periodic component repeats itself after a period T seconds, oscillating between $\frac{2E_o^2\delta^2(T-2\delta)}{T(T-\delta)^2}$ and $\frac{2E_o^2\delta^2}{T(T-\delta)}$.

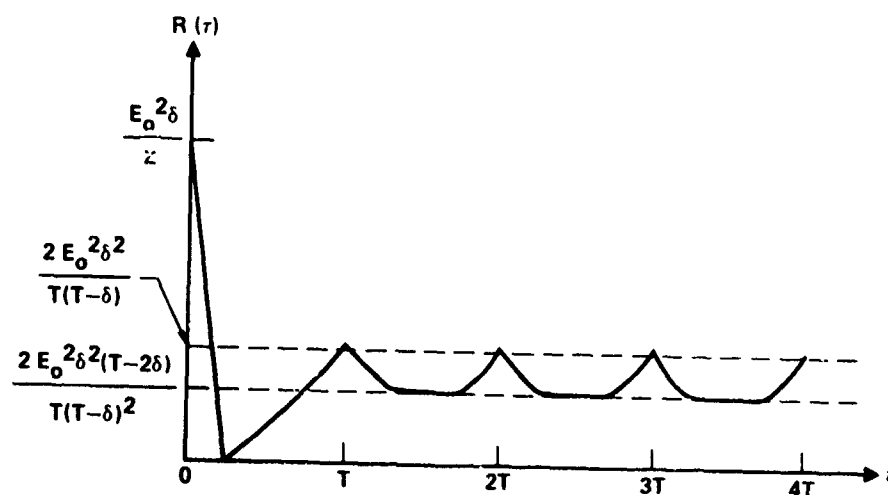


FIGURE 35
AUTOCORRELATION FUNCTION OF TOTAL PPM WAVEFORM

The "random" autocorrelation component, $R_r(\tau)$, Fourier transforms into a continuous spectral density component $G_r(f)$, and the periodic autocorrelation component $R_p(\tau)$ transforms into a discrete spectral density at frequency intervals $\frac{1}{T}$.

For $\delta \ll T$, the probability of independent pulses overlapping becomes negligible, and the power spectral density becomes that of a rectangular pulse train of period T and width δ , as will be demonstrated.

$$R(\tau) \approx \begin{cases} \frac{E_o^2}{T} (\delta - \tau) & 0 < \tau < \delta \\ 0 & \tau > \delta \end{cases}$$

$$G(f) = \int_{-\infty}^{\infty} R(\tau) \exp(-j\omega\tau) d\tau$$

$$G(f) = 2 \int_0^{\delta} \frac{E_o^2}{T} (\delta - \tau) \cos(\omega\tau) d\tau$$

$$G(f) = \frac{E_o^2 \delta^2 \sin^2(\pi f \delta)}{(\pi f \delta)^2 T} \quad -\infty < f < \infty$$

This $\frac{\sin x}{x}$ expression is identical to the spectral density of the rectangular pulse train, except that it is a continuous rather than discrete spectrum. The periodic component becomes negligible.

Such a result is consistent with an intuitive approach to the problem, in which the pulse train is viewed as a succession of non-interacting individual pulses and the power spectral density obtained by multiplying the energy density times the "average" pulse repetition rate $\frac{1}{T}$.

If the PPM waveform is used to modulate an RF carrier $e(t) = v(t) \cos(2\pi f_c t + \phi)$, the power spectral density is shifted about the carrier frequency in the usual way.

The PPM model discussed herein is used in IEMCAP as both an RF modulation waveform and as a signal/control baseband spectrum.

The RF model consists of

$$P_{BB}(f) = P \tau^2 f_B \quad |\Delta f| \leq \Delta f_M$$

$$P_{BB}(f) = P \tau^2 f_B \left(\frac{\Delta f_M}{\Delta f} \right)^2 \quad |\Delta f| > \Delta f_M$$

where

$$\text{bandwidth} = \frac{1}{\tau}$$

P = peak transmitter power

f_B = bit rate

τ = pulse width (sec)

$$\Delta f = f - f_c$$

$$\Delta f_M = \frac{1}{\pi \tau}$$

The signal/control model consists of

$$P_{BB}(f) = 2A^2 \tau^2 f_B \quad 0 < f < f_M$$

$$P_{BB}(f) = 2A^2 \tau^2 f_B \left(\frac{f_M}{f} \right)^2 \quad f > f_M$$

where

A = peak voltage/current into 1 ohm

f_B = bit rate

τ = pulse width (sec)

$$f_M = \frac{1}{\pi \tau}$$

This PPM model is a mathematically correct representation of pulse position modulation and yields frequency and amplitude information sufficient to characterize the interference into unintentional receptors. It is used for both a baseband spectrum and an RF spectrum.

6.1.8 PCM/AM - Biphase

In biphase PCM, one binary state is represented by a voltage pulse which remains at one level for the first half of the interval and switches to the other level for the remaining half of the interval. The other binary state is represented by the opposite pulse form.

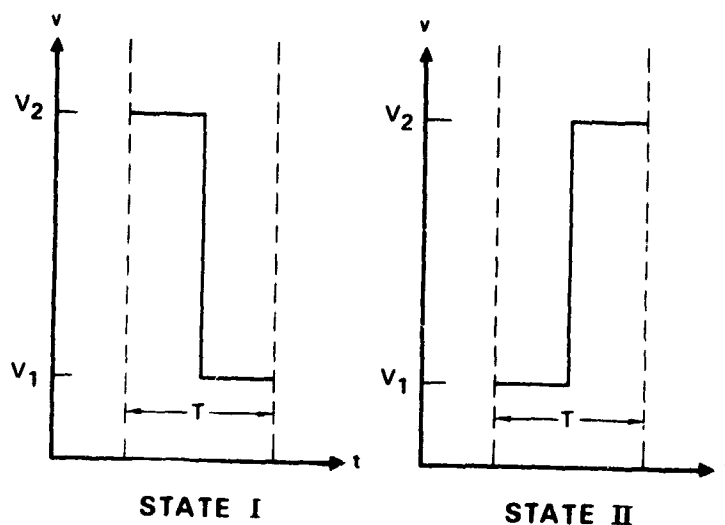


FIGURE 36
TWO BIPHASE STATES

Assuming the two binary states convey the same information value, each state has an equal probability of occurrence in the interval $nT < t < (n+1)T$. Mathematically, the biphase PCM waveform may be expressed:

$$v(t) = V_0 [1 + \beta m(t) s(t)]$$

where $s(t)$ is a normalized square wave of period T , $m(t)$ is a stochastic process taking on the value $+1$ or -1 in the interval $nT < t < (n+1)T$ with equal probabilities, and β is the modulation index, $0 \leq \beta \leq 1$.

The autocorrelation function of the PCM waveform is:

$$R_V(\tau) = \overline{v(t) v(t+\tau)} = V_0^2 \overline{[1 + \beta m(t) s(t)] [1 + \beta m(t+\tau) s(t+\tau)]}$$

$$R_V(\tau) = V_0^2 \overline{[1 + \beta m(t) s(t) + \beta m(t+\tau) s(t+\tau) + \beta^2 m(t) m(t+\tau) s(t) s(t+\tau)]}$$

Since $m(t)$ is a stochastic process and $s(t)$ is a deterministic squarewave, they are mutually independent, and

$$\overline{m(t) s(t)} = \overline{m(t)} \overline{s(t)} = 0$$

$$\overline{m(t+\tau) s(t+\tau)} = \overline{m(t+\tau)} \overline{s(t+\tau)} = 0$$

so that

$$R_V(\tau) = V_0^2 \overline{[1 + \beta^2 m(t) m(t+\tau) s(t) s(t+\tau)]}$$

The expected value $\overline{m(t) m(t + \tau)}$ was shown in the discussion of PCM/AM-NRZ to be equal to $1 - \frac{|\tau|}{T}$ for $|\tau| > T$.

The expected value of the product of the square wave $s(t)$ times an identical wave shifted in time $s(t + \tau)$ may be calculated by expressing both waves in a Fourier series:

$$\overline{s(t) s(t+\tau)} = \sum_{n \text{ odd}} \frac{4}{n\pi} \sin \frac{2n\pi t}{T} \sum_{m \text{ odd}} \frac{4}{m\pi} \sin \frac{m\pi (t+\tau)}{T}$$

All products where $m \neq n$ are zero due to orthogonality, so:

$$\overline{s(t) s(t+\tau)} = \frac{1}{2} \sum_{n \text{ odd}} \left(\frac{4}{n\pi} \right)^2 \cos \frac{2n\pi\tau}{T}$$

Substituting into the autocorrelation function,

$$R_V(\tau) = V_o^2 \left[1 + \frac{\beta^2}{2} \sum_{n \text{ odd}} \left(\frac{4}{n\pi} \right)^2 \cos \left(\frac{2n\pi\tau}{T} \right) \left(1 - \frac{|\tau|}{T} \right) \right]$$

The power spectral density from the Wiener-Khintchine theorem, is equal to the Fourier transform of the autocorrelation function

$$G_V(f) = \int_{-\infty}^{\infty} R_V(\tau) \exp(-j\omega\tau) d\tau$$

The transform of the factor $1 - \frac{|\tau|}{T}$ is simply $T \frac{(\sin \pi f T)^2}{(\pi f T)^2}$, so the transform of that factor times an infinite series of exponentials is merely a series of similar spectra translated in frequency:

$$G_V(f) = V_o^2 \delta(f) + \frac{4T\beta^2 V_o^2}{\pi^2} \left[\sum_{n \text{ odd}} \frac{1}{n^2} \left\{ \frac{\sin \left[\pi \left(f - \frac{n}{T} \right) T \right]}{\pi \left(f - \frac{n}{T} \right) T} \right\}^2 + \sum_{n \text{ odd}} \frac{1}{n^2} \left\{ \frac{\sin \left[\pi \left(f + \frac{n}{T} \right) T \right]}{\pi \left(f + \frac{n}{T} \right) T} \right\}^2 \right]$$

This is the power spectral density of the PCM-Biphase waveform. If a waveform is used to modulate an RF carrier, $e(t) = v(t) \cos(2f_c t + \emptyset)$, then

$$G_V(f) = \frac{1}{4} G(f-f_c) + \frac{1}{4} G(f+f_c)$$

Taking the one-sided spectrum for positive frequencies only the following expression for the PCM/AM-Biphase waveform is obtained, after substituting $P_c = \frac{V_o^2}{2}$:

$$G_V(f) = P_c \delta(f-f_c) + \frac{4\beta^2 P_c T}{\pi^2} \sum_{n \text{ odd}} \frac{1}{n^2} \left[\left\{ \frac{\sin \left[\pi \left(f-f_c - \frac{n}{T} \right) T \right]}{\pi \left(f-f_c - \frac{n}{T} \right) T} \right\}^2 + \left\{ \frac{\sin \left[\pi \left(f-f_c + \frac{n}{T} \right) T \right]}{\pi \left(f-f_c + \frac{n}{T} \right) T} \right\}^2 \right]$$

This function has local maxima for frequencies displaced from the carrier by an odd multiple of $\frac{1}{T}$. The maximum occurring at $f-f_c = \frac{n}{T}$, where n is odd, has the value $\frac{4\beta^2 P_c T}{\pi^2 n^2}$:

A derivation for the power spectral density of the PCM/AM-Biphase waveform was published by N.M. Shehadeh⁸ in 1970. Shehadeh stated that the total power spectral density was equal to $\frac{1}{T} |H(f)|^2$ where $H(f)$ is the Fourier transform of a single biphase pulse which holds at one voltage level for half the T interval and the other level for the remainder. Shehadeh is incorrect, because his method does not take into account the stochastic properties of the wave. The exact error incurred with such a method for a generalized pulse shape is given by N. Solat in a letter to IEEE, Proc. in April 1964.⁹

The PCM-Biphase model discussed herein is used in IEMCAP as both an RF modulation waveform and as a signal/control baseband spectrum.

The RF model consists of

$$P_{BB}(f) = \frac{4m^2 P}{\pi^2 f_B} \quad |\Delta f| \leq \Delta f_M$$

$$P_{BB}(f) = \frac{4m^2 P}{\pi^2 f_B} \left(\frac{\Delta f_M}{\Delta f} \right)^2 \quad |\Delta f| > \Delta f_M$$

$$P_{NB}(f) = P \delta(\Delta f)$$

where

$$\text{bandwidth} = \frac{\pi^2}{16} f_B$$

$$\Delta f = f - f_c$$

P = carrier average power (watts)

f_B = bit rate

m = modulation index

The signal/control model consists of

$$P_{BB}(f) = \frac{8 m^2 A^2}{\pi^2 f_B} \quad 0 < f < f_M$$

$$P_{BB}(f) = \frac{8 m^2 A^2}{\pi^2 f_B} \left(\frac{f_M}{f} \right)^2 \quad f > f_M$$

where

$$\text{bandwidth} = \frac{\pi^2}{32} f_B$$

A = peak voltage/current into 1 ohm

$f_M = f_B$ = bit rate

m = modulation index

The PCM-Biphase model used in IEMCAP is consistent with the previous correct mathematical details representing this form of modulation. From generally available input data, the model can be used to generate either a baseband or RF spectrum.

6.1.9 Spectral Analysis of PAM-FM Signal

This model¹⁰ presents both a Pulse Amplitude Signal and the resulting spectrum of modulating an FM system with this signal. An elementary system of this type would simultaneously monitor a number of data sources, each of which is a band-limited stochastic process. The signal of each channel source is sampled in regular sequence by a commutator. Instantaneous sampling results in pulses with magnitudes equal to the signal magnitude at the center of each pulse, and further assume that each channel source is a stationary Gaussian random process with flat low-pass band-limited spectra. The resulting time-division multiplexed signal is then transmitted by frequency modulation. The analysis herein describes the spectral distribution of the transmitter output under various conditions of baseband signal level and sampling pulsewidth.

For clarity, this discussion will be divided into a discussion of the composite PAM signal and then the PAM-FM signal i.e., the output of the transmitter.

The PAM Multiplexed Signal - Consider N stationary Gaussian Random Process sensor outputs $[s_1(t), \dots, s_N(t)]$. Each of the sensor outputs is band-limited with a maximum frequency f_m Hertz and sampled instantaneously by a commutator at the optimum sampling rate of $2 f_m$ Hertz or every $1/(2f_m)$ seconds as dictated by the Nyquist sampling criteria. If each sampling pulse has a waveform $x_n(t)$, then the resulting PAM signals $[x_1(t), \dots, x_N(t), x_N(t)]$ created by such sampling are small width rectangles resulting in the PAM multiplexed signal at the commutator of

$$m(t) = \sum_{n=1}^N x_n(t)$$

If each sampling pulse is time limited to α seconds, the maximum number of sampled signals that may be accommodated is

$$N = \frac{1}{2f_m} \cdot 1/\alpha$$

As long as the number of sampled signals does not exceed this limit, the multiplexed signal is also a Gaussian Random Process.

Consider now the cumulative output at any time, t , where the measurements are made over a time T divided into $2N$ periods each of length T_0 seconds. We can therefore represent the output of the multiplexed signal as

$$y_N = \sum_{n=-N}^N y_n u(t - nT_0)$$

where y_n is the constant output of the n - th sample and $u(t - nT_0)$ is the unit impulse function defined by

$$u(t - nT_0) = \begin{cases} 1 & \text{for } nT_0 < t < (n+1)T_0 \\ 0 & \text{elsewhere} \end{cases}$$

The autocorrelation of the sampled process is defined in the limit as $T \rightarrow \infty$,

$$R_y(t) = \lim_{T \rightarrow \infty} \frac{1}{T} \int_{-T/2}^{T/2} y_N(t_0) y_N(t_0+t) dt_0$$

Since the sampling is discrete and y_n equals zero for times greater than $T/2$, T can be replaced by $(2N + 1) T_0$ and the limits of the integral can be extended over an infinite domain.

$$R_{ys}(t) = \lim_{N \rightarrow \infty} \left[\frac{1}{(2N+1)T_0} \sum_{m, n=-N}^N y_m y_n \int_{-\infty}^{\infty} u(t_0 - mT_0) u(t_0 + t - nT_0) dt_0 \right]$$

where the subscript s implies sampled function. Replacing the unit impulse functions by the following integral representation

$$u(t) = \int_{-\infty}^{\infty} S_u(f) \exp[j2\pi ft] df$$

yields

$$R_{ys} = \lim_{N \rightarrow \infty} \left[\frac{1}{(2N+1)T_0} \sum_{m, n=-N}^N y_n y_m \int_{-\infty}^{\infty} dt_0 \int_{-\infty}^{\infty} df \int_{-\infty}^{\infty} df' S_n(f) S_n(f') \right. \\ \left. \cdot \exp[j2\pi f(t_0 - mT_0)] \exp[j2\pi f'(t_0 + t - nT_0)] \right]$$

Carrying out the integrations, first over t_0 and over f' , and using the integral form of a delta function leads to

$$R_{ys}(t) = \frac{1}{T_0} \int_{-\infty}^{\infty} |S_u(f)|^2 \exp[-j2\pi ft] \left[\lim_{N \rightarrow \infty} \frac{1}{2N+1} \cdot \sum_{m, n=-N}^N y_m y_n \exp[j2\pi f(n-m)T_0] \right] df$$

Now consider the definition of an autocorrelation function for a discrete process.

$$R_y(k) = \lim_{N \rightarrow \infty} \left[\frac{1}{2N+1} \sum_{n=-N}^N y_n y_{n+k} \right]$$

where $y_n = y(t_n)$

The trick now is to transform a portion of $R_{ys}(t)$ to obtain a term which is comparable to $R_y(k)$.

Look at

$$\sum_{m=-N}^N \sum_{n=-N}^N y_m y_n \exp[j\omega(n-m)T_0]$$

and let $n-m = k$, recalling that for the truncated wave y_n or y_m vanishes for $|n|, |m| > N$, this double sum can be expressed as

$$\sum_{k=-\infty}^{\infty} \exp[j\omega k T_0] \sum_{m=-N}^N y_m y_{m+k}$$

where the limits on k have been extended to plus and minus infinity, since these additional terms are each equal to zero.

Therefore the limit and summation can be interchanged yielding

$$R_{ys}(t) = \frac{1}{T_0} \int_{-\infty}^{\infty} df |S_n(f)|^2 \exp[-j2\pi ft] \left\{ \sum_{k=-\infty}^{\infty} \exp[j2\pi f k T_0] \left[\lim_{N \rightarrow \infty} \frac{1}{2N+1} \sum_{m=-N}^N y_m y_{m+k} \right] \right\}$$

Using the definition of the autocorrelation function of a discrete process leads to

$$R_{ys}(t) = \frac{1}{T_0} \int_{-\infty}^{\infty} \sum_{k=-\infty}^{\infty} R_y(k)_d |S(f)|^2 \exp[-j2\pi f(t-kT_0)] df$$

The integral over f is by definition the autocorrelation function of the unit impulse evaluated at $t = t-kT_0$

$$R_{ys}(t) = \frac{1}{T_0} \sum_{k=-\infty}^{\infty} R_y(k)_d R_u(t-kT_0)$$

For possible positive and negative pulses in each successive interval

$$R_y(k)_d = \begin{cases} \sigma^2 & k=0 \\ 0 & k=\pm 1, \pm 2, \dots \end{cases}$$

where σ^2 is the average pulse height squared.

The autocorrelation function for the unit pulse is calculated as follows:

$$R_u(t_0 - kT_0) = \frac{1}{T_0} \int_{-t_0 - kT_0}^{\alpha - t_0 - kT_0} 1 dt = \frac{1}{T_0} (\alpha - |r|) \quad |r| \leq \alpha$$

where T_0 is the total time between successive pulses. Maximum correlation is achieved when $\alpha = T_0$, its upper limit as explained in the beginning of the article. Therefore

$$R_y(t)_d = \begin{cases} \sigma^2 \left[1 - \frac{|t|}{\alpha} \right] & |t| \leq \alpha \\ 0 & |t| > \alpha \end{cases}$$

The PAM multiplexed signal spectrum is obtained by Fourier transforming the autocorrelation function yielding

$$P(f) = \alpha \sigma^2 \left[\frac{\sin(\pi f \alpha)}{\pi f \alpha} \right]^2$$

The PAM-FM Signal - Consider the multiplexed signal, $m(t)$, to be the input modulating signal of an FM transmission system that is given by

$$v(t) = \cos \left[2\pi f_c t + \int_{-\infty}^t m(\tau) d\tau \right]$$

where f_c is the carrier frequency.

Consider the expectation value of process $T_g(y)$ where y is the input and T_g is an operator resulting in $g(y)$.

$$E \left\{ T_g(y_1) T_g(y_2) \right\} = E \left\{ g(v(t_1)) g(v(t_2)) \right\}$$

This equals

$$E \left\{ T_g(y_1) T_g(y_2) \right\} = \iint_{-\infty}^{\infty} g(y_1) g(y_2) W_2(y_1, y_2, t) dy_1 dy_2$$

where W_2 is the joint probability distribution function.

Introduce the Laplace inverse transform of $g(y)$

$$g(y) = \int_{-\infty-jc}^{\infty-jc} f(j\xi) \exp[j\xi y] \frac{d\xi}{2\pi} = \frac{1}{2\pi} \int_c f(j\xi) \exp[j\xi y] d\xi$$

Interchanging the ζ and y integrations leads to

$$E \left\{ g(y_1) g(y_2) \right\} = \frac{1}{(2\pi)^2} \int_{-\infty-jc}^{\infty+jc} \int_{-\infty-jc}^{\infty+jc} f(j\xi_1) f(j\xi_2) \overline{\exp[j(\xi_1 y_1 + \xi_2 y_2)]} d\xi_1 d\xi_2$$

where the over bar denotes the expectation of y_1 and y_2 .

Since in general ζ_1, ζ_2 are complex the averaging is not the joint characteristic function of random variables y_1, y_2 which is defined for real ζ_1, ζ_2 but by analytical continuation it has the same functional form therefore we still write $F_{y_1, y_2}(j\zeta_1, j\zeta_2; \tau)$ remembering

$$\overline{\exp[j(\xi_1 y_1 + \xi_2 y_2)]} = \int_{-\infty}^{\infty} \int_{-\infty}^{\infty} \exp[j(\xi_1 y_1 + \xi_2 y_2)] W_2(y_1, y_2; \tau) dy_1 dy_2$$

Therefore

$$E \left\{ g(y_1) g(y_2) \right\} = \frac{1}{(2\pi)^2} \int_{-\infty-jc}^{\infty+jc} \int_{-\infty-jc}^{\infty+jc} f(j\xi_1) f(j\xi_2) F_{y_1 y_2}(j\xi_1, j\xi_2; \tau) d\xi_1 d\xi_2$$

Considered now that

$$V(t) = A_0 \cos [\omega_c t + \Phi_{FM}(t)]$$

is the FM output where

$$\Phi_{FM}(t) = \int_{-\infty}^t m(\tau) d\tau$$

The expectation value of $V(t)$ is

$$K_V(t) = \frac{A_0^2}{2} \operatorname{Re} \left[\exp[-j\omega_c t] E \left\{ \exp[j\Phi(t_1+t) - j\Phi(t_1)] \right\} \right]$$

$$K_V(t) = \frac{A_0^2}{2} \operatorname{Re} \left[\exp[-j\omega_c t] F_2(-1, 1; t) \right]$$

Define

$$\psi = \phi(t_1 + t) - \phi(t_1), \text{ yielding}$$

$$E \left\{ \exp[j\psi(t, t_1)] \right\} = F_1(1; t)$$

according to the notation used herein. This is the characteristic function of $e^{j\psi}$ since there are no problems necessitating analytic continuation. In general terms we can define ψ as a FM functional

$$\Psi(t) = \int_{a(t)}^{b(t)} A(t, \tau) \chi(\tau) d\tau$$

Expanding the exponential leads to

$$F_Y(j\xi) = \sum_{m=0}^{\infty} \frac{(j\xi)^{2m}}{m!} \int_a^b \dots \int_a^b E \left\{ \chi(\tau_1) \dots \chi(\tau_m) \right\} \prod_{j=1}^{2m} A(t, \tau_j) d\tau_j$$

Assuming x to be normal

$$E \left\{ x_1, x_2, \dots, x_{2m} \right\} = \sum_{\text{all pairs}} \left(\prod_{j \neq k}^{2m} x_j x_k \right)$$

$$E \left\{ x_1, x_2, \dots, x_{2m+1} \right\} = 0$$

Now the number of possible pairings of $2m$ distinct objects is easily calculated. Pick any one object leaving $(2m-1)$ other possible pairing candidates. Pick one leaving $(2m-2)$. Pick one of the $(2m-2)$ objects left leaving $(2m-3)$ possible pairing candidates. Continuing this process results in

$$(2m-1) (2m-3) \dots 1$$

possible combinations. This can be re-expressed as

$$\frac{(2m)!}{2^m m!}$$

Therefore

$$F_Y(j\xi) = \sum_{m=0}^{\infty} \frac{(-1)^m (\xi)^{2m}}{(2m)!} \int_a^b \dots \int_a^b \prod_{j=1}^{2m} A(t, \tau_j) d\tau_j \sum_{\text{all pairs}} E \left\{ x_k x_l \right\}$$

$$F_Y(j\xi) = \sum_{m=0}^{\infty} \frac{(-1)^m}{(2m)!} \xi^{2m} \frac{(2m)!}{2^m m!} \left[\int_a^b \int_a^b A(t, \tau) K_X(\tau_1, \tau_2) A(t, \tau_2) d\tau_1 d\tau_2 \right]^m$$

Summing the series leads to

$$F_Y(j\xi) = \exp \left[-\frac{\xi^2}{2} K_Y(t_1, t_2) \right]$$

where

$$K_Y(t_1, t_2) = \int_a^b \int_a^b A(t_1, \tau_1) K_X(\tau_1, \tau_2) A(t_2, \tau_2) d\tau_1 d\tau_2$$

In the case considered here $\xi = \pm 1$. It further can be shown $K_Y(t_1, t_2)$ depends only on the difference between t_1 and t_2 so that

$$K_Y = \int_0^t \int_0^t K_X(\tau_1 - \tau_2) d\tau_1 d\tau_2 = 2 \int_0^t (t - \tau) K_X(\tau) d\tau$$

Therefore

$$F_Y(j1) = \exp \left[-\int_0^t (t - \tau) K_X(\tau) d\tau \right]$$

remembering that according to the W-K theorem that the K , covariance function and the R , autocorrelation function are interchangeable.

Now denoting a change in notation of y from the FM function to y the output PAM FM signal.

$$y(t) = \cos \left[2\pi f_c t + \int_{-\infty}^t m(\tau) d\tau \right]$$

$$R_y(\tau) = 1/2 \exp \left(- \int_0^\tau (\tau - \chi) R_m(\chi) d\chi \right) \cos(2\pi f_c \tau)$$

Cast this into

$$R_y(\tau) = 2R_1(\tau) \cos(2\pi f_c \tau)$$

where

$$R_1(\tau) = 1/4 \exp \left[- \int_0^\tau (\tau - \chi) R_m(\chi) d\chi \right]$$

Substituting $R_m(x)$ in the above leads to

$$R_1(\tau) = \begin{cases} 1/4 \exp \left[- \frac{\sigma^2}{\alpha} \left(- \frac{|\tau|^3}{6} + \frac{\alpha \tau^2}{2} \right) \right] & 0 \leq |\tau| \leq \alpha \\ 1/4 \exp \left[- \frac{\sigma^2}{\alpha} \left(\frac{\alpha^2 |\tau|}{2} - \frac{\alpha^3}{6} \right) \right] & |\tau| > \alpha \end{cases}$$

The resulting spectrum is

$$P_y(f) = P_1(f - f_c) + P_1(f + f_c)$$

where $P_1(f)$ is the Fourier transform of $R_1(y)$.

Some interesting conclusion will be noted. The maximum value of the spectral distribution always occurs at the carrier, f_c . Increasing the input modulating signal strength as measured by the mean value σ^2 causes the spectrum to continually broaden about the carrier frequency and approach a Gaussian shape.

For small values of α , the pulse width, the output spectrum is narrow and in the limit

$$\lim_{\alpha \rightarrow 0} P_y(f) = \int_{-\infty}^{\infty} \lim_{\alpha \rightarrow 0} R_y(\tau) \exp(-j2\pi f \tau) d\tau$$

$$\lim_{\alpha \rightarrow 0} P_y(f) = 1/4 \delta(f - f_c) + 1/4 \delta(f + f_c)$$

since $R_y(T)$ goes to $1/2$ in this limit. Decreasing the sampling pulse width increases the baseband spectrum width, and, if the input signal mean square value is maintained constant, the maxima of the baseband spectrum decreases. Increasing the sampling pulse width causes the output spectrum to broaden and approach a fixed Gaussian shape for a fixed mean square value of $R_m(0)$, i.e.,

$$\lim_{\alpha \rightarrow \infty} R_Y(\tau) = 1/2 \exp \left[-\frac{\sigma^2 \tau}{2} \right] \cos(2\pi f_c \tau)$$

This section has discussed the PAM-FM signal as applied to time multiplexed signals. The results are limiting forms of the spectra wherein maximum transmission capability is assumed. The resulting limits are from a delta function form to a Gaussian form whose standard deviation is determined for the variance of the signals being multiplexed. In addition to the PAM-FM model, a PAM system has been modeled, as required to fulfill the stated objective. The models are mathematically correct and use easily obtainable data.¹¹

The PAM model discussed herein is used in IEMCAP as both an RF model, PAM-FM, and a signal/control baseband spectrum model, PAM.

The RF model consists of

$$P_{BB}(f) = P/\sigma \sqrt{2\pi} \exp \left\{ -1/2 \left(\frac{\Delta f}{\sigma} \right)^2 \right\}$$

where

P = transmitter average power, watts

$\Delta f = f - f_c$

$\sigma = 1/3$ of peak frequency deviation

bandwidth = $\sigma \sqrt{2\pi}$

The PAM model consists of

$$P_{BB}(f) = 2 A^2 \tau^2 f_B \quad f \leq f_M$$

$$P_{BB}(f) = 2 A^2 \tau^2 f_B \left(\frac{f_M}{f} \right)^2 \quad f > f_M$$

where

$$\text{bandwidth} = \frac{1}{2\tau}$$

τ = pulse width

$$f_M = \frac{1}{\pi \tau}$$

f_B = bit rate

A = peak voltage/current r. to 1 ohm

6.1.10 Pulse Duration Modulation

Pulse duration modulation is a form of pulse modulation in which the information resides in the width of each successive pulse. Analog information, such as speech, can be sampled at regular intervals and the instantaneous amplitude at the time of sampling can be converted to a pulse of proportional width.

The PDM waveform is thus a binary signal taking on only values of zero or E_0 at a given time. The analog information can be recovered by an integration-detection circuit.

One would expect the spectrum of such a waveform to have a bandwidth comparable to $1/T$, where T is the sampling interval. The power spectral density must be derived from the autocorrelation function of the PDM wave, however, because the width of each successive pulse is derived from a stochastic process. If it were not, and the waveform were determinate, no information would be conveyed.

The autocorrelation function $R(\tau)$ is the expected value or time average of the product $e(t) \times e(t + \tau)$.

$$R(\tau) = \lim_{D \rightarrow \infty} \frac{1}{D} \int_{-D/2}^{D/2} e(t) e(t + \tau) dt$$

This can be integrated geometrically as the time average of a pulse train consisting of the original pulse train multiplied by itself shifted " τ " in time. The new pulse train takes on the value E_0^2 whenever two pulses overlap and zero when they do not.

Y. W. Lee¹² calculates the autocorrelation function for a PDM wave with a sampling period $2T$ with each pulse width varying from 0 to τ (uniform probability density), under the assumption that each pulse width is independent of the others. This does not give the correct autocorrelation for the waveform previously described, but it is possible to derive the autocorrelation function of the complete waveform sampled at intervals T , as the autocorrelation of two independent waveforms as follows:

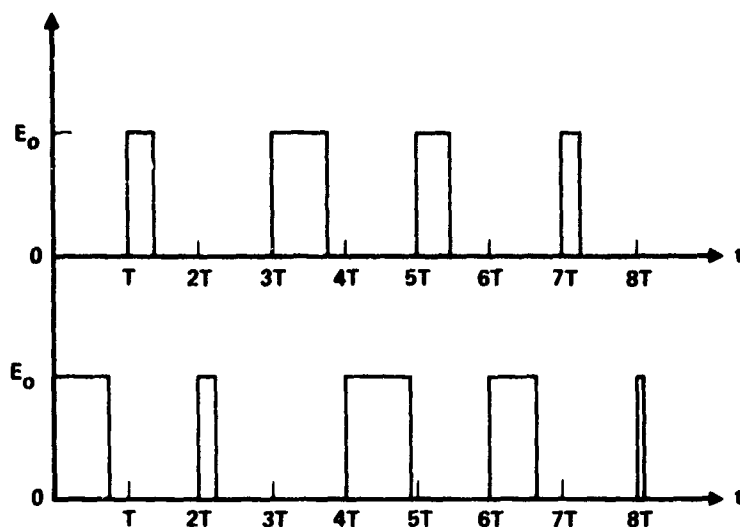


FIGURE 37
TWO INDEPENDENT PDM WAVEFORMS

$$e(t) = e_a(t) + e_b(t)$$

The autocorrelation function for $e_a(t)$ or $e_b(t)$ can be expressed as a combination of a periodic component with a period $2T$, and a random component which is non-zero only for $-T < \tau < T$.

$$R_{aa}(\tau) = R_{bb}(\tau) = R_{aa}(\tau)|_{\text{per}} + R_{aa}(\tau)|_{\text{ran}}$$

$$R_{aa}(\tau)|_{\text{per}} = \frac{E_0^2}{12T^3} [3T(T - |\tau|)^2 - (T - |\tau|)^3]$$

for $-T < \tau < T$

$$R_{aa}(\tau)|_{\text{ran}} = \frac{E_0^2}{12T^3} [T - |\tau|]^3$$

The autocorrelation function $\overline{e(t)e(t+\tau)}$ can then be expressed as

$$R(\tau) = \overline{e(t)e(t+\tau)} = \overline{[e_a(t) + e_b(t)][e_a(t+\tau) + e_b(t+\tau)]}$$

$$R(\tau) = \overline{e_a(t)e_a(t+\tau)} + \overline{e_b(t)e_b(t+\tau)} + \overline{e_a(t)e_b(t+\tau)} + \overline{e_b(t)e_a(t+\tau)}$$

$$R(\tau) = R_{aa}(\tau) + R_{bb}(\tau) + R_{ab}(\tau) + R_{ba}(\tau)$$

It can be shown that the cross-correlation functions $R_{ab}(\tau)$ and $R_{ba}(\tau)$ are equal to the periodic component of $R_{aa}(\tau)$ shifted by an amount T , or half the period.

The total autocorrelation function is then expressible in a random and a periodic component, $R(\tau) = R_{\text{random}} + R_{\text{periodic}}$:

$$R(\tau)|_{\text{ran}} = \frac{E_o^2}{6} \left(1 - \left|\frac{\tau}{T}\right|\right)^3 \quad -T < \tau < T$$

$$R(\tau)|_{\text{per}} = \frac{E_o^2}{6} \left| 2 + 3\left|\frac{\tau}{T}\right| - 3\left|\frac{\tau}{T}\right|^2 \right| \quad -\frac{T}{2} < \tau < \frac{T}{2}$$

The periodicity is now of length T rather than $2T$.

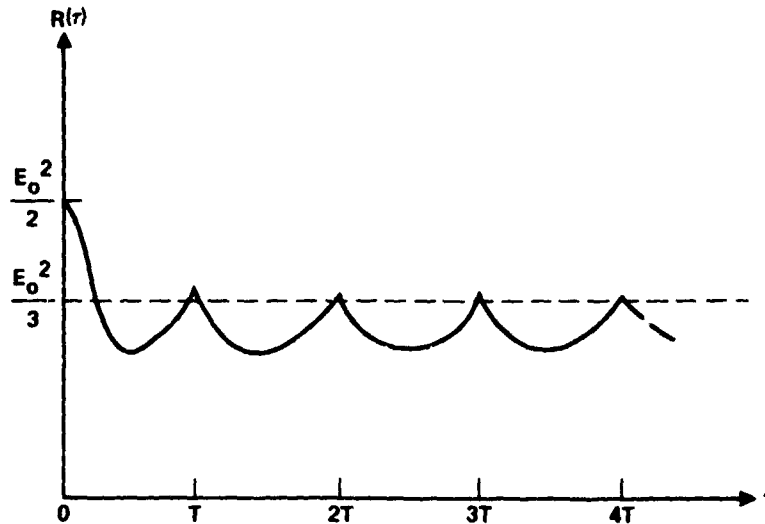


FIGURE 38
AUTOCORRELATION FUNCTION OF TOTAL PDM WAVEFORM

The spectral density is just the Fourier Transform of the autocorrelation function.

$$G(f) = \int_{-\infty}^{\infty} R(\tau) \exp[-j\omega\tau] d\tau = G_r(f) + G_p(f)$$

$$G(f) = \frac{E_o^2 T}{4(\pi f T)^2} \left[1 - \frac{\sin^2(\pi f T)}{(\pi f T)^2} \right] + \left[\frac{E_o^2}{4} \delta(f) + \frac{E_o^2}{4\pi^2} \sum_{n=1}^{\infty} \delta\left(f - \frac{n}{T}\right) \frac{1}{n^2} \right]$$

If the PDM coded signal is used to modulate an AM system, the spectrum would be shifted by an amount f_0 , where f_0 is the carrier frequency.

However, if the PDM signal is used to modulate an FSK or PSK system, where "mark" and "space" correspond to distinct frequencies or opposite phases, then the calculation of the RF power spectral density becomes very difficult.

The average power in the PDM waveform is equal to $R(0)$,

$$P_{AVG} = R(0) = \frac{E_o^2}{2} = \frac{P_{MAX}}{2}$$

This result is intuitively satisfying, since the average pulse width is $T/2$, and the signal is "on" half the time. Looking at the power in the random and periodic components,

$$P_{ran} = R_r(0) = \frac{E_o^2}{6} = \frac{P_{MAX}}{6}$$

$$P_{per} = R_p(0) = \frac{E_o^2}{3} = \frac{P_{MAX}}{3}$$

The PDM model described herein is used in IEMCAP as both an RF modulation and as a signal/control baseband spectrum.

The RF model is

$$P_{BB}(f) = 1/6 \ P/f_B \quad |\Delta f| \leq \Delta f_M$$

$$P_{BB}(f) = 1/6 \ P/f_B \left(\frac{\Delta f_M}{\Delta f} \right)^2 \quad |\Delta f| > \Delta f_M$$

$$P_{NB}(f) = 1/3 \ P \ \delta(\Delta f)$$

where

$$\text{bandwidth} = 2 f_B$$

$$f_B = \text{bit rate}$$

$$\Delta f = f - f_c$$

$$P = \text{peak RF power, watts}$$

$$\Delta f_M = \frac{\sqrt{3}}{\pi} f_B$$

The signal control model consists of

$$P_{BB}(f) \approx 1/3 A^2/f_B \quad 0 < f < f_M$$

$$P_{BB}(f) = 1/3 A^2/f_B \left(\frac{f_M}{f}\right)^2 \quad f > f_M$$

where

A = peak voltage/current into 1 ohm

f_B = bit rate

$$f_M = \frac{\sqrt{3}}{\pi} f_B$$

bandwidth = f_B

The PDM models presented herein and used in IFMCA are mathematically correct, usable from generally known data and yield the needed spectral distribution and amplitude information.

6.1.11 Control and Signal Waveform Analysis

Herein is presented a complete analysis of various signal waveforms which do not modulate a carrier. The analysis is presented for the sake of completeness, since it can be applied to any waveform and therefore is usable for additional signals not presently part of the Intra System EMC Analysis Program.

Analysis of Single Pulse - Consider a single voltage pulse as shown in Figure 22, where A is the amplitude in volts and the pulse exists T seconds beginning at time $-\tau/2$ and ending at $\tau/2$. If one wishes the power into a one ohm load you merely integrate the voltage squared over the duration and average this energy over the duration, i.e., in this instance

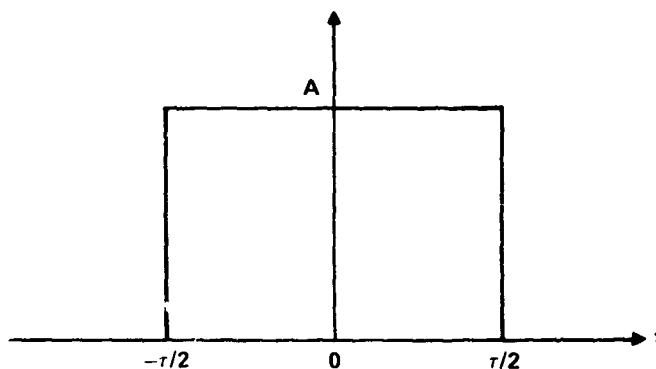


FIGURE 39
SINGLE VOLTAGE PULSE

$$\text{Power} = \frac{1}{\tau} \int_{-\tau/2}^{\tau/2} A^2 d\tau = A^2 \text{ watts}$$

Now if the spectral density is required, both voltage and power, these should be determined commensurate with the total power being A^2 watts.

Let us begin with this calculation. The Fourier transform of the pulse in Figure 39 is calculated as

$$V(f) = \int_{-\tau/2}^{\tau/2} A \exp [-j2\pi ft] dt$$

$$V(f) = A\tau \frac{\sin (\pi f\tau)}{\pi f\tau}$$

Now using some theorems from spectral analysis we can express the power spectral density as

$$P(f) = \frac{1}{\tau} V(f) V^*(f)$$

where the * denotes complex conjugation, and using the definition of $V(f)$ it can be seen that

$$V^*(f) = V(-f) = V(f)$$

Therefore

$$P(f) = \frac{1}{\tau} V(f) V(f)$$

Now solving for the power spectral density,

$$P(f) = \frac{1}{\tau} (2A\tau)^2 \frac{\sin(\pi f\tau)^2}{\pi f\tau}$$

At this point it should be pointed out that power spectral density was not obtained as a Fourier transform of the power but is a density in the strictest sense of the word, i.e.,

$$\text{Power} = \int_{f_1}^{f_2} P(f) df$$

Now resorting to another communication theory theorem, note that the Fourier transform of $V(f) V^*(f)$ is the autocorrelation function and the autocorrelation function evaluated at zero is the power in the pulse, therefore

$$R(\tau) = \frac{1}{\tau} \int_{-\infty}^{\infty} V(f) V^*(f) \exp[j\omega\tau] df \quad \text{Power} = R(0)$$

Using this approach, the autocorrelation function is expressed as

$$R(t) = \frac{(2A\tau)^2}{\tau} \int_{-\infty}^{\infty} \frac{2 \exp[j2\pi ft] - \exp[j2\pi f(t+\tau)] - \exp[+j2\pi f(t-\tau)]}{(2\pi f\tau)^2} df$$

This is a familiar form of integral which occurs in complex variables and is usually evaluated by the use of the Cauchy Integral Theorem. The integrand appears to be finite along the real axis except possibly at the origin, $f = 0$. Letting f go to zero in the integrand and using L'Hospital's Rule twice shows that indeed the function is not singular. Different contours are required to evaluate the complete function, one that is counterclockwise in the upper half plane and one that is clockwise in the lower half plane. This is due to the relative values of t and τ . The lower clockwise contour term can be transformed into an upper counterclockwise term and the inversion proceeded for cases of $|\tau|$ greater than $|t|$. Since we are interested in the value of the integral for all times, t , the above described contours must be inverted and the integrals evaluated again.

Note the slight change in the definition of power spectral density. This has only meaning over the duration of the pulse.

Analysis of Pulse Train - Consider now the following pulse train of Figure 40, where A is the amplitude in volts, τ is the duration and T is the period. As before the voltage spectral density will be calculated and then the resulting power spectral density determined.

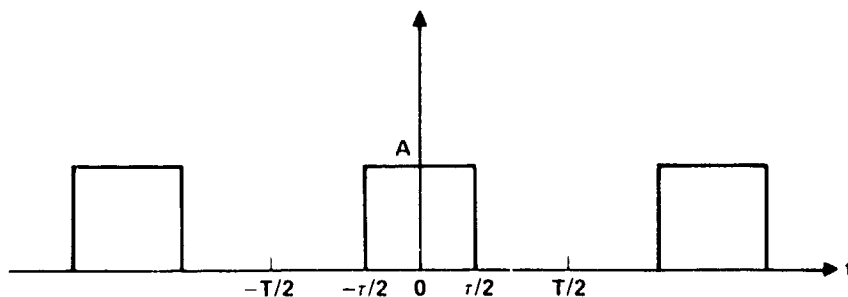


FIGURE 40
PULSE TRAIN

In this case since we have a periodic signal, $v(t)$ can be expressed in a Fourier series

$$V(t) = \sum_{n=-\infty}^{\infty} C_n \exp\left[j2\pi n \frac{t}{T}\right]$$

of period T seconds.

Solving for c_n yields

$$C_n = A \frac{\tau}{T} \frac{\sin\left(n\pi \frac{\tau}{T}\right)}{n\pi \frac{\tau}{T}}$$

The voltage signal can therefore be expressed as

$$V(t) = \sum_{n=-\infty}^{\infty} A \frac{\tau}{T} \frac{\sin\left(n\pi \frac{\tau}{T}\right)}{n\pi \frac{\tau}{T}} \exp\left[j2\pi n \frac{t}{T}\right]$$

Since $v(t)$ is periodic the power spectral density can be determined by way of the transform of the autocorrelation function.

$$R(\tau) = \lim_{T \rightarrow \infty} \frac{1}{T} \int_{-T/2}^{T/2} V(t) V(t+\tau) d\tau$$

And using the fact that $v(t)$ is periodic $R(\tau)$ can be expressed as

$$R(\tau) = \frac{1}{T} \int_{-T/2}^{T/2} \sum_{n=-\infty}^{\infty} \sum_{m=-\infty}^{\infty} \left(A \frac{\tau}{T}\right)^2 \frac{\sin\left(m\pi \frac{\tau}{T}\right)}{m\pi \frac{\tau}{T}} \exp\left[j2\pi m \frac{\tau}{T}\right] \exp\left[j2\pi(m+n) \frac{\tau}{T}\right] d\tau$$

Using

$$\int_{-T/2}^{T/2} \exp \left[2\pi(m+n) \frac{t}{T} \right] dt = T \delta_{n,-m}$$

and carrying out the summation over n results in

$$R(\tau) = \sum_{m=-\infty}^{\infty} \left(A \frac{\tau}{T} \right)^2 \frac{\sin^2 \left(m\pi \frac{\tau}{T} \right)}{\left(m\pi \frac{\tau}{T} \right)^2} \exp \left[j2\pi m \frac{\tau}{T} \right]$$

The Fourier transform of this expression leads to

$$P(f) = \int_{-\infty}^{\infty} R(\tau) \exp[j2\pi f\tau] d\tau$$

$$P(f) = \left(A \frac{\tau}{T} \right)^2 + \sum_{m=1}^{\infty} 2 \left(A \frac{\tau}{T} \right)^2 \frac{\sin^2 \left(m\pi \frac{\tau}{T} \right)}{\left(m\pi \frac{\tau}{T} \right)^2} \delta \left(f - \frac{m}{T} \right)$$

All of the signal waveforms contained herein can be obtained by the preceding methods.

1) Rectangular Pulse Train

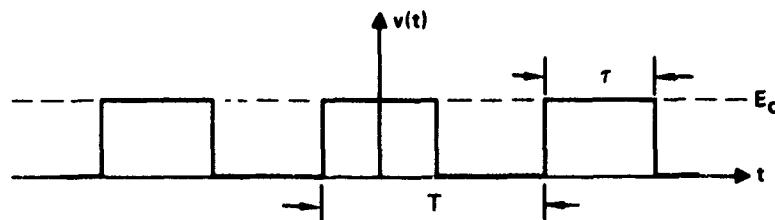


FIGURE 41
RECTANGULAR PULSE TRAIN

Discrete Spectrum

$$P(f) = E_0^2 \frac{\tau^2}{T^2} \delta(f) + \sum_{n=1}^{\infty} \frac{2 E_0^2 \tau^2}{T^2} \frac{\sin^2\left(n\pi \frac{\tau}{T}\right)}{\left(n\pi \frac{\tau}{T}\right)^2} \delta\left(f - \frac{n}{T}\right)$$

Analog Representation

$$P(f) = \frac{2 E_0^2 \tau^2}{T} \frac{\sin^2(\pi f \tau)}{(\pi f \tau)^2} \quad f > 0$$

The formula used in IEMCAP for the rectangular pulse train is

$$P_{BB}(f) = 2A^2 \tau^2 f_B \quad 0 < f < f_M$$

$$P_{BB}(f) = 2A^2 \tau^2 f_B \left(\frac{f_M}{f}\right)^2 \quad f > f_M$$

where

$$\text{bandwidth} = \frac{1}{2\tau}$$

τ = pulse width

f_B = bit rate

$$f_M = \frac{1}{\pi\tau}$$

A = peak current/voltage into 1 ohm

2) Trapezoidal Pulse Train (Equal rise and fall times)

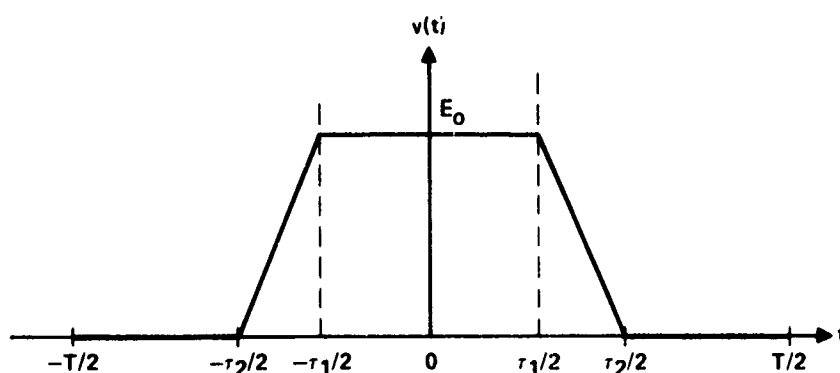


FIGURE 42

TRAPEZOIDAL PULSE TRAIN

Discrete Spectrum

$$P(f) = \frac{E_0^2 \tau^2}{T^2} \delta(f) + \sum_{n=1}^{\infty} \frac{2 E_0^2 \tau^2}{T^2} \frac{\sin^2\left(n\pi \frac{\tau}{T}\right)}{\left(n\pi \frac{\tau}{T}\right)^2} \frac{\sin^2\left(n\pi \frac{\delta}{T}\right)}{\left(n\pi \frac{\delta}{T}\right)^2} \delta\left(f - \frac{n}{T}\right)$$

Analog Representation

$$P(f) = \frac{2 E_0^2 \tau^2}{T} \frac{\sin^2(\pi f \tau)}{(\pi f \tau)^2} \frac{\sin^2(\pi f \delta)}{(\pi f \delta)^2} \quad f > 0$$

$$\tau_{1,2} = \tau \mp \delta$$

where τ = pulse width = $1/2(\tau_1 + \tau_2)$

δ = pulse rise/fall time = $1/2(\tau_2 - \tau_1)$

The formula used in IEMCAP for the trapezoidal pulse train is

$$P_{BB}(f) = 2A^2 \tau^2 f_B \quad 0 < f < f_{M1}$$

$$P_{BB}(f) = 2A^2 \tau^2 f_B \left(\frac{f_{M1}}{f} \right)^2 \quad f_{M1} < f < f_{M2}$$

$$P_{BB}(f) = 2A^2 \tau^2 f_B \left(\frac{f_{M1}}{f_{M2}} \right)^2 \left(\frac{f_{M2}}{f} \right)^4 \quad f > f_{M2}$$

where

$$\text{bandwidth} = \frac{1}{2\tau}$$

τ = pulse width

τ_r = rise time = full time

A = peak current/voltage into 1 ohm

f_B = bit rate

$$f_{M1} = \frac{1}{\pi \tau}$$

$$f_{M2} = \frac{1}{\pi \tau_r}$$

3) Triangular Pulse Train

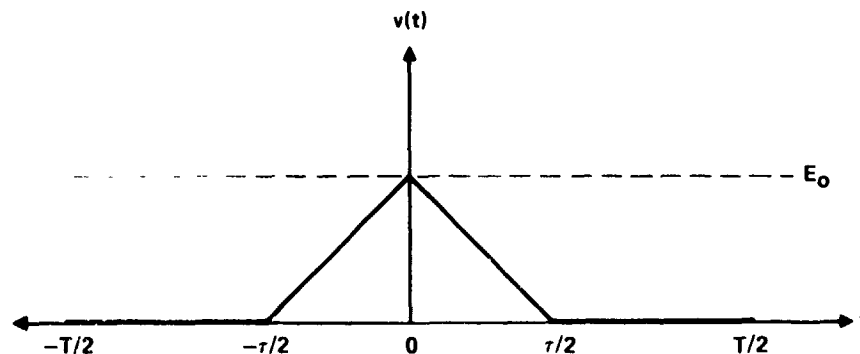


FIGURE 43
TRIANGULAR PULSE TRAIN

Discrete Spectrum

$$G(f) = \frac{E_0^2 \tau^2}{T^2} \delta(f) + \sum_{n=1}^{\infty} \frac{2 E_0^2 \tau^2}{T^2} \frac{\sin^4 \left(n\pi \frac{\tau}{T} \right)}{\left(n\pi \frac{\tau}{T} \right)^4} \delta \left(f - \frac{n}{T} \right)$$

Analog Representation

$$G(f) = 2 E_0^2 \frac{\tau^2}{T} \frac{\sin^4(\pi f \tau)}{(\pi f \tau)^4}$$

The formula used in IEMCAP to represent the triangular pulse train is

$$P_{BB}(f) = 2A^2 \tau^2 f_B \quad 0 < f < f_M$$

$$P_{BB}(f) = 2A^2 \tau^2 f_B \left(\frac{f_M}{f} \right)^4 \quad f > f_M$$

where

A = peak current/voltage into 1 ohm

f_B = bit rate

$$f_M = \frac{1}{\pi \tau}$$

τ = pulse duration

$$\text{bandwidth} = \frac{1}{2\tau}$$

4) Sawtooth Pulse Train

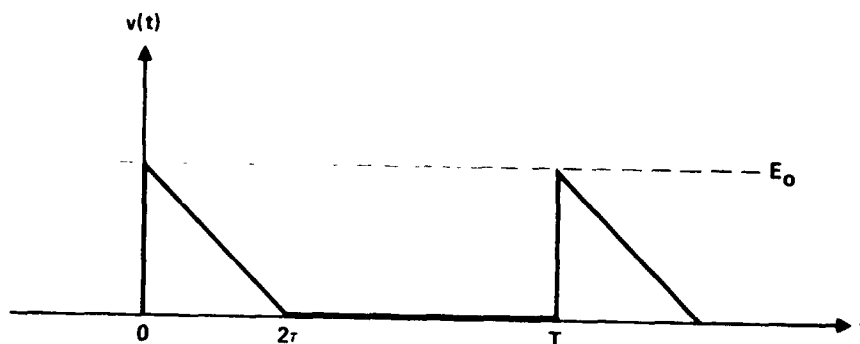


FIGURE 44
SAWTOOTH PULSE TRAIN

Discrete Spectrum

$$P(f) = \frac{E_0^2 \tau^2}{T^2} \delta(f) + \sum_{n=1}^{\infty} \frac{2 E_0^2 \tau^2}{\left(2\pi n \frac{\tau}{T}\right)^4} \left[\sin^2\left(2\pi n \frac{\tau}{T}\right) + \left(2\pi n \frac{\tau}{T}\right)^2 - \left(2\pi n \frac{\tau}{T}\right) \sin\left(4\pi n \frac{\tau}{T}\right) \right] \delta\left(f - \frac{n}{T}\right)$$

Analog Representation

$$P(f) = \frac{2 E_0^2 \tau^2}{T(2\pi f\tau)^4} \left[\sin^2(2\pi f\tau) + (2\pi f\tau)^2 - (2\pi f\tau) \sin(4\pi f\tau) \right] \text{ for } f > 0$$

The formula used in IEMCAP to represent the sawtooth pulse train is

$$P_{BB}(f) = \frac{2A^2 \tau^2 f_B}{(2\pi f\tau)^4} [\sin^2(2\pi f\tau) + (2\pi f\tau)^2 - (2\pi f\tau) \sin 4\pi f\tau]$$

where

A = peak current/voltage into 1 ohm

$$\text{bandwidth} = \frac{1}{2\tau}$$

$$\tau = \text{pulse width at } \frac{1}{2} A$$

5) High-frequency Exponential Pulse Train

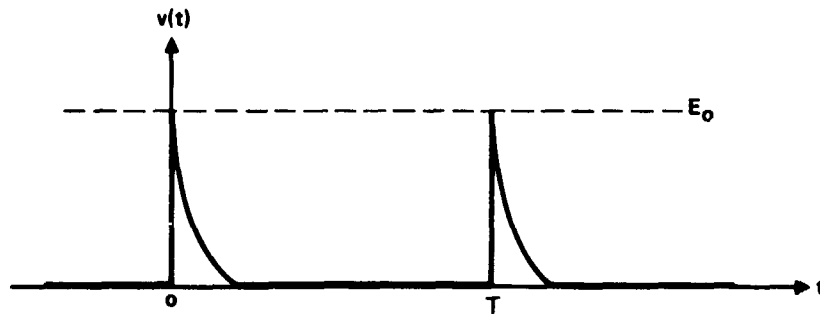


FIGURE 45
HIGH-FREQUENCY EXPONENTIAL PULSE TRAIN

Discrete Spectrum

$$P(f) = \frac{E_0^2}{\alpha T} \delta(f) + \sum_{n=1}^{\infty} \frac{2 E_0^2}{(2\pi n)^2 + \alpha^2 T^2} \delta\left(f - \frac{n}{T}\right)$$

$$\alpha = \frac{1}{\tau}$$

Continuous

$$P(f) = \frac{2 E_0^2}{T[(2\pi f)^2 + \alpha^2]} \quad f > 0$$

The formula used in IEMCAP to represent the exponential pulse train (high-frequency) is

$$P_{BB}(f) = 2A^2 f_B \left[(2\pi f)^2 + \left(\frac{1}{\tau}\right)^2 \right]^{-1}$$

where

τ = decay time constant (time required for voltage to decay to E_0/e)

$$\text{bandwidth} = \frac{1}{4\tau}$$

A = peak current/voltage into 1 ohm

f_B = bit rate

6) Damped Sinusoid

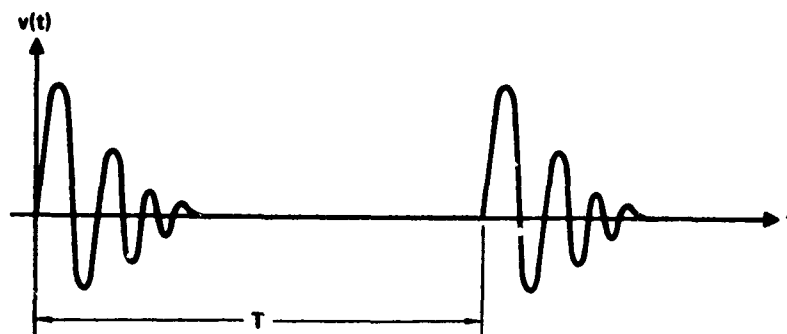


FIGURE 46
DAMPED SINUSOID

$$V(t) = E_0 \exp\left[-\frac{t}{\tau}\right] \sin \omega_0 t$$

where τ is the time required for the pulse to reach $1/e$ times the peak, E_0 .

Discrete Spectrum

$$G(f) = \sum_{n=1}^{\infty} \frac{2 E_0^2 f_0^2}{(2\pi)^2 \tau^2} \frac{1}{\left[\alpha^2 + f_0^2 - \left(\frac{n}{\tau}\right)^2 \right]^2 + \left(\frac{2n}{\tau}\right)^2 \alpha^2} \delta\left(f - \frac{n}{\tau}\right)$$

Continuous Spectrum

$$G(f) = \frac{2 E_0^2 f_0^2}{(2\pi)^2 \tau} \frac{1}{(\alpha^2 + f_0^2 - f^2)^2 + (2\alpha f)^2}$$

where $\alpha = \frac{1}{\tau}$

The formula in IEMCAP to represent a damped sinusoid pulse train is

$$P_{BB}(f) \approx \frac{2A^2 f_o f_B}{(2\pi)^2 [(\alpha^2 + f_o^2 - f^2)^2 + (2\alpha f)^2]}$$

where

f_o = frequency of sinusoid

f_B = bit rate

A = peak current/voltage into 1 ohm

bandwidth = $2\pi^2\alpha$

α = reciprocal of decay constant

6.2 RECEPTOR MODELING

In the course of the development of IEMCAP the literature was researched for methods of representing a receiver's (RF or signal/control) in-band sensitivity curve and its relative rejection of electromagnetic interference. No models were found that were capable, with any reasonable economy, of describing quantitatively the rejection capability of a given receiver to an arbitrary interference signal. Some interesting methods were found to be under development at the time of the IEMCAP development; however, these potentially promising techniques were not sufficiently developed to enable their inclusion in IEMCAP. In particular, a method under investigation at the Electromagnetic Compatibility Analysis Center using empirical test data for receiver characterization and a second effort on non-linear receiver analysis at Rome Air Development Center may become valuable tools for receptor modeling in the future.

Because of the scarcity of accurate and economical receptor modeling techniques the IEMCAP approach to this aspect of interference analysis is to make use of the user's knowledge of the specific receptor susceptibility characteristics. The basic approach for receptors employed in IEMCAP is to accept input data on in-band sensitivity, along with a bandwidth parameter, and to then form a rectangular shaped susceptibility function in the required spectral region that connects to non-required spectra defined by user-adjusted military specification interference limits. An RF receiver representation in the program will, in general, actually have a trapezoidal shaped susceptibility function (in-band) due to the skirt slopes of the normal selectivity curve. Specifically, the susceptibility of an RF port is assumed to be equal to the tuned sensitivity of the receiver, as provided in the input data, over the entire frequency range defined by the user-specified bandwidth. The susceptibility of a signal or control port is assumed to be equal to the operating level (in dBμA) less 20 dB. This is a somewhat arbitrary susceptibility level, based on characteristics of common avionics equipments. If the user wants a higher or lower susceptibility level in the required range of a signal or control port, he need only specify a higher or lower operating level, respectively.

In the case of receivers where more is known about the details of its response curve than just the flat response discussed above, the user can specify the known response curve by a discrete spectrum of up to ten frequencies with associated levels. Interference calculations using either the specified spectrum or the flat response function are conducted by weighting the received interference signal power by the ratio of the receptor to emitter bandwidths, when the former is the smaller value of the two.

The user has an additional option of augmenting either of the two preceding receptor models with certain filter functions as described in this manual under the heading of Transfer Models. When employed, the filter models relate the susceptibility level of a given receptor to the level at the filter input terminals for compatibility assessment.

The combination of user-supplied receptor spectrums with the filter models in the program provide the user considerable flexibility in receptor modeling.

6.3 TRANSFER MODELS

6.3.1 Filter Models

The filter models used in IEMCAP are discussed in the following.

There are seven filter models used in IEMCAP: single tuned, transformer coupled, Butterworth tuned, low pass, high pass, band pass and band reject filter models. The models represent filters as ideal, lossless networks, made up of only reactive elements (capacitors and inductors). When a filter is used in a circuit, however, it "sees" an input impedance at the source end and an output impedance at the load end, both of which contribute to the overall transfer function between source and load. In the absence of a filter, the maximum power is delivered to the load when the load impedance matches the source impedance. For equal source and load resistances, the maximum power delivered to the load is half the total power, the other half being dissipated in the source resistance. The insertion of a filter between the source and load selectively attenuates the signal delivered to the load at a given frequency. The single tuned filter consisting of a parallel LC combination (Figure 47), for example, attenuates signals at all frequencies other than the resonant frequency $\frac{1}{2\pi\sqrt{LC}}$ where it presents an infinite parallel

impedance that allows the maximum power to be delivered to the load.

The filter transfer models calculate the "insertion loss" in dB provided by a filter at a given frequency, i.e., the reduction in delivered power due to insertion of a filter. Thus the insertion loss of the single tuned filter at the resonant frequency is 0 dB, i.e., the insertion of the filter does not attenuate the signal delivered to the load at that frequency.

Practical filters are not ideal, lossless networks; there are always dissipative elements which affect filter performance. Consequently the filter models provide for a minimum insertion loss, γ , to represent actual dissipation at the tuned frequency or in the pass band. The filter models also provide a maximum insertion loss or isolation, $isol$, to represent the departure from the ideal rejection in the rejection band. The minimum and maximum insertion loss provide lower and upper bounds for the filter transfer function.

The filter transfer functions derived in this section are given in terms of T^2 (the ratio of V_2^2/V_1^2 with a filter to V_2^2/V_1^2 without the filter, where V_2 is the voltage delivered to the load and V_1 is the source voltage).

The filter models calculate T^2 as shown for the seven filter types. Then they bound T^2 by the minimum insertion loss γ and maximum isolation isol :

$$\text{If } T^2 < 10^{\frac{\text{isol}}{10}}, T^2 = 10^{\frac{\text{isol}}{10}}$$

$$\text{If } T^2 > 10^{\frac{\gamma}{10}}, T^2 = 10^{\frac{\gamma}{10}}$$

If, for example, the minimum insertion loss is -1 dB and the maximum isolation is -80 dB, then $10^{-8} \leq T^2 \leq .794$

1. Single Tuned Filter

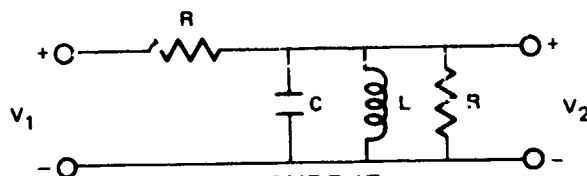


FIGURE 47
SINGLE TUNED FILTER

The transfer function of the above general single tuned filter is the ratio of the general output signal voltage to the input voltage. Note the resistances are equal so as to provide a match for the pass band of the receptor.

$$\frac{V_2}{V_1} = \frac{1/2}{1 + j \frac{R}{2} \sqrt{C/L} (\omega \sqrt{LC} - \frac{1}{\omega \sqrt{LC}})}$$

The square of the magnitude of transfer function is

$$\left| \frac{V_2}{V_1} \right|^2 = \frac{\frac{1}{4}}{1 + \left[\frac{R}{2} \sqrt{C/L} \left(\omega \sqrt{LC} - \frac{1}{\omega \sqrt{LC}} \right) \right]^2}$$

Defining $f_o = \frac{1}{2\pi\sqrt{LC}}$ tuned frequency in radians

and $B = \frac{1}{\pi RC}$ bandwidth in radians and inserting in the above leads to:

$$\left| \frac{V_2}{V_1} \right|^2 = \frac{\frac{1}{4}}{1 + \left[\frac{f_o}{B} \left(\frac{f}{f_o} - \frac{f_o}{f} \right) \right]^2}$$

This expression can be simplified as

$$\left| \frac{V_2}{V_1} \right|^2 = \frac{\frac{1}{4}}{1 + X^2} \quad X = \frac{f_o}{B} \left(\frac{f}{f_o} - \frac{f_o}{f} \right)$$

Defining filter "gain" as $T^2 = \frac{(V_2/V_1)^2 \text{ with filter}}{(V_2/V_1)^2 \text{ without filter}}$

$$T^2 = \frac{\left(\frac{\frac{1}{4}}{1 + X^2} \right)}{\left(\frac{R}{R+R} \right)^2} = \frac{1}{1 + X^2}$$

2. Transformer Coupled Filter

Consider the following circuit, representative of a transformer coupled filter.

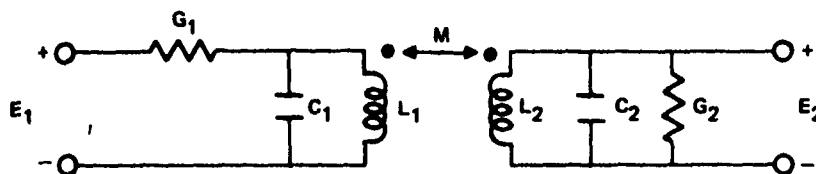


FIGURE 48
TRANSFORMER COUPLED FILTER

Solving the loop equations for the ratio between the output and input voltages yields

$$\frac{E_2}{E_1} = \frac{\frac{s M G_1}{L_1 L_2 C_1 C_2}}{\left(s^2 + \frac{G_1}{C_1} s + \frac{1}{L_1 C_1}\right) \left(s^2 + \frac{G_2}{C_2} s + \frac{1}{L_2 C_2}\right) - (sk)^2 \left(s + \frac{G_1}{C_1}\right) \left(s + \frac{G_2}{C_2}\right)}$$

$$\text{where } k = M / \sqrt{L_1 L_2}$$

Assume both tuned circuits have the same resonant frequency

$$\omega_c = 1/\sqrt{L_1 C_1} = 1/\sqrt{L_2 C_2}$$

and both tuned circuits have the same resonant Q

$$Q = \omega_c C_1 / G_1 = \omega_c C_2 / G_2 \gg 1$$

$$\text{In the passband of the filter, let } |j\omega| \cong \omega_c \gg \frac{G_1}{C_1}$$

Then

$$\begin{aligned} \frac{E_2}{E_1} &\cong \frac{j\omega_c M G_1}{L_1 L_2 C_1 C_2} \frac{1}{(2j\omega_c)^2 \left(j\omega - j\omega_c + \frac{\omega_c}{2Q}\right)^2 - k^2 \omega_c^4} \\ &= \frac{jM G_1}{4\omega_c L_1 L_2 C_1 C_2} \frac{-1}{(j\omega - j\omega_c)^2 + \left(\frac{\omega_c}{2Q}\right)^2 + 2j(\omega - \omega_c) \frac{\omega_c}{Q} + \frac{k^2 \omega_c^2}{4}} \end{aligned}$$

Defining $\delta = \frac{\omega - \omega_c}{\omega_c}$

yields

$$\frac{E_2}{E_1} = \frac{j M G_1}{4 \omega_c^3 L_1 L_2 C_1 C_2} \frac{1}{\delta^2 - \frac{1}{4Q^2} - \frac{k^2}{4} - j \frac{\delta}{Q}}$$

The magnitude of this expression is

$$\left| \frac{E_2}{E_1} \right| = \frac{k \sqrt{L_1 L_2} G_1}{4 \omega_c^3 L_1 L_2 C_1 C_2} \sqrt{\frac{1}{\left(\delta^2 - \frac{1}{4Q^2} - \frac{k^2}{4} \right)^2 + \left(\frac{\delta}{Q} \right)^2}}$$

Substituting $L_1 L_2 C_1 C_2 = \frac{1}{\omega_c^2}$

and $\omega_c \sqrt{L_1 L_2} G_1 \cong \frac{G_1}{\omega_c C_1} = \frac{1}{Q}$

in the above yields

$$\left| \frac{E_2}{E_1} \right| = \frac{k}{4Q} \sqrt{\frac{1}{\left(\delta - \frac{1}{4Q^2} - \frac{k^2}{4} \right)^2 + \left(\frac{\delta}{Q} \right)^2}}$$

This expression is valid in the passband. However, at frequencies far from the tuned frequency, the original expression becomes:

$$\left| \frac{E_2}{E_1} \right| \cong \frac{k}{Q} \frac{1}{\delta^3} \quad ; \quad \omega \gg \omega_c$$

The two approximations are equal at $\delta = 4$. For $\delta < 4$, the more complicated expression is used and for $\delta > 4$, the asymptotic expression is used:

The filter gain for the transformer coupled filter is defined as

$$T^2 = \frac{\left(\frac{E_2}{E_1}\right)^2 \text{ with filter}}{\left(\frac{E_2}{E_1}\right)^2 \text{ without filter}}$$

$$T^2 = \begin{cases} \frac{k^2}{Q^2} \frac{1}{\left(\delta^2 - \frac{1}{4Q^2} - \frac{k^2}{4}\right)^2 + \left(\frac{\delta}{Q}\right)^2} & ; \delta < 4 \\ \frac{4k^2}{Q^2 \delta^3} & ; \delta \geq 4 \end{cases}$$

3. Butterworth Tuned Filter

A Butterworth tuned filter is defined as a filter having a filter gain of

$$T^2 = \frac{1}{1 + x^{2n}}$$

$$x = \frac{f_o}{\beta} \left(\frac{f}{f_o} - \frac{f_o}{f} \right)$$

β = bandwidth

f_o = tuned frequency

n = order of filter

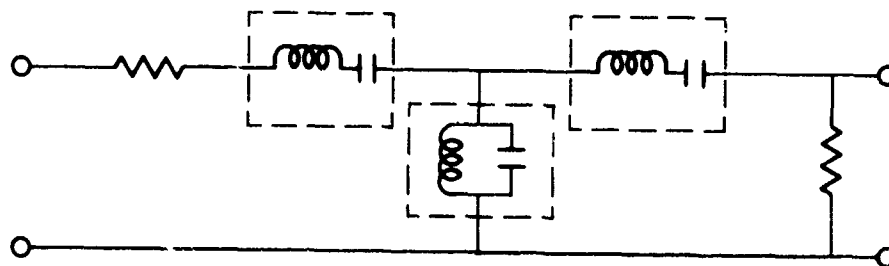


FIGURE 49
EXAMPLE OF THIRD ORDER
BUTTERWORTH FILTER

4. Low Pass Filter

An nth order low pass filter has a filter "gain" of:

$$T^2 \approx 1 \quad ; \quad f \ll f_U$$

$$T^2 \approx (f_U/f)^{2n} \quad ; \quad f \gg f_U$$

These asymptotic values are equal at $f = f_U$, so an envelope approximation is used:

$$T^2 = 1 \quad ; \quad f \leq f_U$$

$$T^2 = (f_U/f)^{2n} \quad , \quad f > f_U$$

5. High Pass Filter

An nth order high pass filter has a filter "gain" of:

$$T^2 \approx 1 \quad ; \quad f \gg f_L$$

$$T^2 \approx (f/f_L)^{2n} \quad ; \quad f \ll f_L$$

These asymptotic values are equal at $f = f_L$ so an envelope approximation is used.

$$T^2 = 1 \quad ; \quad f \geq f_L$$

$$T^2 = (f/f_L)^{2n} \quad ; \quad f < f_L$$

6. Band Pass Filter

The following formulas are used to represent a bandpass filter.

$$T^2 = (f/f_L)^{2n} ; f < f_L$$

$$T^2 = 1 ; f_L < f < f_U$$

$$T^2 = (f_U/f)^{2n} ; f > f_U$$

7. Band Reject Filter

The band reject filter is assumed to accept all frequencies less than f_L and all frequencies higher than f_U , but to attenuate frequencies in between. Assuming a minimum gain T_{\min} (The antilogarithm of the negative of the insertion loss divided by ten).

$$T^2 = 1 ; f \leq f_L$$

$$T^2 = (f_L/f)^{2n} ; f_L < f < f_1$$

$$T^2 = T_{\min} ; f_1 \leq f \leq f_2$$

$$T^2 = (f/f_U)^{2n} ; f_2 < f < f_U$$

$$T^2 = 1 ; f \geq f_U$$

$$f_1 = f_L (T_{\min})^{-1/2n}$$

$$f_2 = f_U (T_{\min})^{1/2n}$$

Implicit in this model is the assumption that $T_{\min} > \left(\frac{f_U}{f_L}\right)^{2n}$. In case this is not so, the model takes the maximum of $\left(\frac{f_U}{f}\right)^{2n}$, $\left(\frac{f}{f_L}\right)^{2n}$ and T_{\min} when $f_L < f < f_U$.

6.3.2 Simplified Theoretical Ground Wave Model (STGW) ECAC TN-003-315

A smooth earth surface is assumed, with a $4/3$ earth radius accounting for atmospheric refraction.¹³ The model is valid for frequencies greater than 1 MHz and less than 1 GHz, and moderate antenna height. The limitation on antenna height is a consequence of a plane earth approximation for distances up to $d = \frac{h_1 h_2}{79.6\lambda}$ where $h_{1,2}$ = antenna heights in meters and λ is the wavelength in meters. The plane earth approximation makes possible a two-ray optics solution, neglecting the "surface" wave for the moment.

The electric field at point B at height " h_2 " above the plane due to radiation from point A at height " h_1 ", is the superposition of a direct ray and a reflected ray (Figure 50).

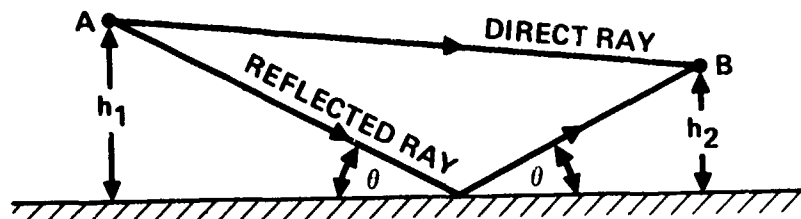


FIGURE 50
TWO RAY OPTICS REPRESENTATION

For far field distances much larger than the antenna heights, the reflected ray is nearly horizontal, and the difference between path lengths becomes very small. The plane wave propagation loss due to path length, proportional to $\frac{1}{d^2}$, is virtually identical for the two rays, but the small difference in path length can affect the phase difference if it is comparable to a wavelength.

$$\text{Let } E = (E_0 e^{-jkS_d} + \rho E_0 e^{-jkS_r}) e^{j\omega t}$$

$$E_0 = \text{free space field} \sim \frac{1}{d}$$

$$\rho = \text{complex reflection coefficient of earth}$$

$$S_d = \text{path length along direct ray}$$

$$S_r = \text{path length along reflected ray}$$

$$\text{So } \frac{E}{E_0} = e^{-jkS_d} + \rho e^{-jkS_r}$$

$$\left| \frac{E}{E_0} \right| = \left| 1 + \rho e^{jk(S_d - S_r)} \right|$$

$$\left| \frac{E}{E_0} \right| = \sqrt{\left(1 + \rho \cos \frac{2\pi \Delta S}{\lambda}\right)^2 + \rho^2 \sin^2 \left(\frac{2\pi \Delta S}{\lambda}\right)}$$

For a strongly conducting earth $\rho \approx -1$, so

$$\left| \frac{E}{E_0} \right| \cong \sqrt{2\left(1 - \cos \frac{2\pi \Delta S}{\lambda}\right)}$$

From the geometry, the difference in path length $S \approx \frac{2h_1 h_2}{d}$, and for $\Delta S \ll \lambda$,

$$\left| \frac{E}{E_0} \right| = \sqrt{2\left(1 - \left[1 - \frac{1}{2} \left(\frac{2\pi \Delta S}{\lambda}\right)^2\right]\right)} = \frac{2\pi \Delta S}{\lambda}$$

$$\left| \frac{E}{E_0} \right| = \frac{4\pi h_1 h_2}{\lambda d} = \frac{d_{FSM}}{d}; \quad d_{FSM} = \frac{4\pi h_1 h_2}{\lambda}$$

At a value of d equal to d_{FSM} , the electric field would be equal to the space field, beyond which it would decrease linearly as d increased until the plane earth assumption is no longer valid at $d = d_c$. At values of d less than d_{FSM} , the electric field would oscillate with a maximum of twice the free space field at points where the two fields are exactly in phase (Figure 51).

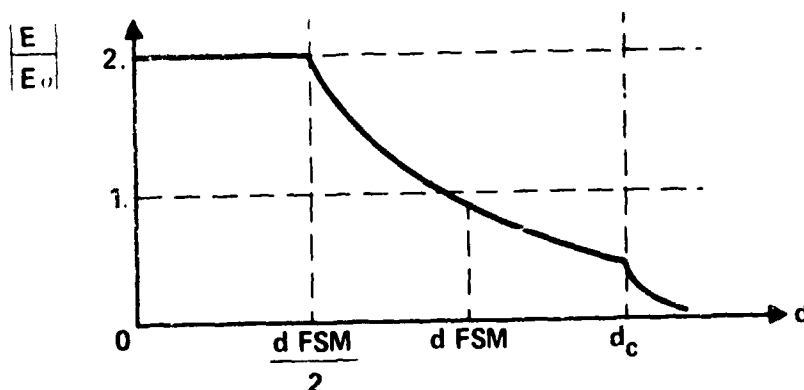


FIGURE 51
GAIN OVER FREE SPACE vs DISTANCE

For equal antenna heights, the model is valid only when

$$d_{FSM} = \frac{4\pi h_1 h_2}{\lambda} = \frac{4\pi h_1^2}{\lambda} < d_c$$

Thus
$$h_{MAX} = \sqrt{\frac{\lambda d_c}{4\pi}}$$

For heights greater than h_{MAX} , the point d_{FSM} , where the electric field is equal to the free space field, would occur beyond the plane earth distance d_c , invalidating the model.

When the effect of the "surface wave" is included, the simplified theoretical ground wave model is as follows:

$$A_{dB} = 20 \log \left| \frac{E}{E_0} \right| = -6 \quad d < \frac{d_{FSM}}{2}$$

$$A_{dB} = 20 \log \frac{d}{d_{FSM}} \quad \frac{d_{FSM}}{2} < d$$

where

$$d_{FSM} = \frac{4 h_1' h_2'}{\lambda}$$

and

$$h_1' = \text{Maximum } [h_1, h_0]$$

= Effective Antenna Height of A

$$h_2' = \text{Maximum } [h_2, h_0]$$

= Effective Antenna Height of B

$$h_0 = \frac{\lambda [c_r^2 + (0.06 \lambda \sigma)^2]^{1/2}}{2 \pi [(\epsilon_r - 1)^2 + (0.06 \lambda \sigma)^2]^{1/4}}$$

= Minimum Effective Antenna Height for Vertical Polarization

$$h_0 = \frac{\lambda}{2 \pi [(\epsilon_r - 1)^2 + (0.06 \lambda \sigma)^2]^{1/4}}$$

= Minimum Effective Antenna Height for Horizontal Polarization

where

σ = ground conductivity in mmhos/meter

ϵ_r = relative dielectric constant of ground

The propagation loss does not vary with antenna height for heights between zero and the minimum effective antenna height h_0 . This phenomenon is a consequence of the surface wave which follows the contour of the earth and is most significant at the lower frequencies. The quantity $\sqrt{h_1 h_2}$ must not exceed the maximum h_{MAX} if the model is to be valid.

The minimum effective antenna height increases with increasing wavelength. For vertical polarization it also increases with increasing ground conductivity σ . The ground conductivity is 27.8 mmhos/m for average land and varies from 0.03 mmhos/m for tundra up to 11 mmhos/m for marsh land.

The maximum antenna height h_{MAX} and maximum distance the earth is considered as a plane are shown as a function of frequency (Figures 52 and 53).

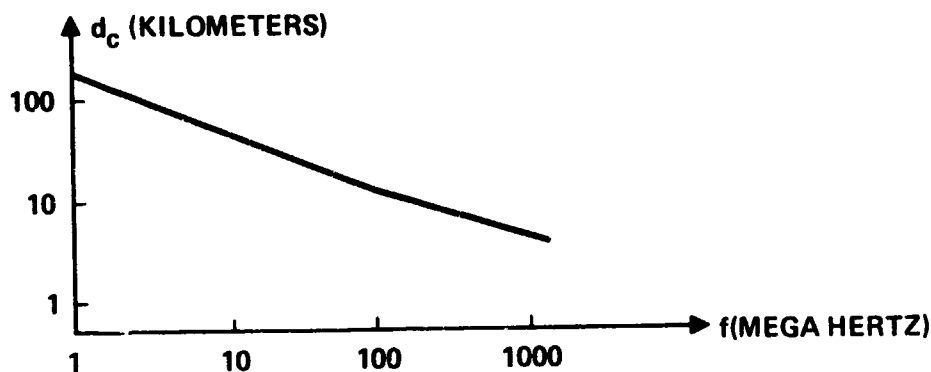


FIGURE 52
MAXIMUM PLANE EARTH DISTANCE vs FREQUENCY

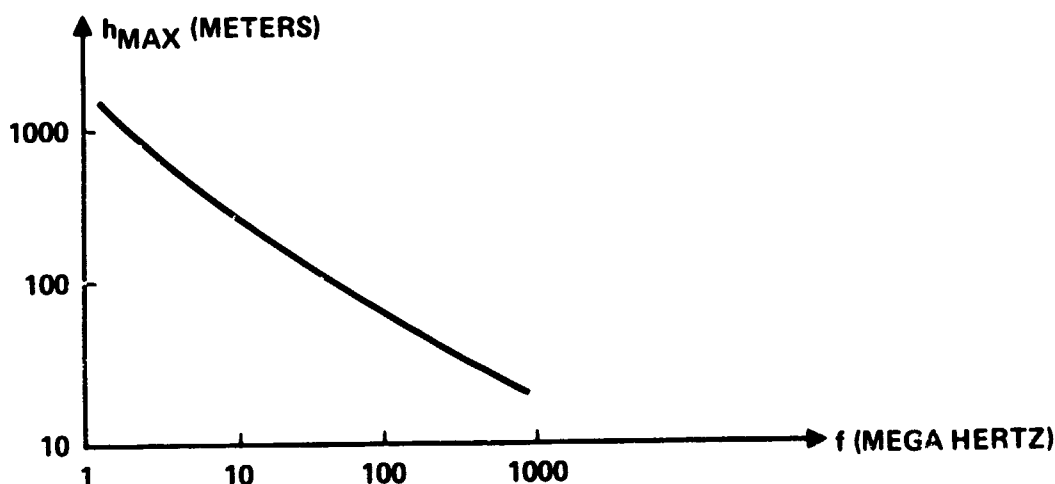


FIGURE 53
MAXIMUM ALLOWABLE ANTENNA HEIGHT vs FREQUENCY

The model is only valid when $h_1' h_2' < \frac{\lambda^2}{4\pi} = h_{MAX}^2$. For unequal antenna heights, one antenna may exceed h_{MAX} as long as the inequality is satisfied.

For equal antenna heights the constraint is

$$h' < h_{MAX}$$

and since $h' = \text{Max} [h_1 h_0]$, and $h_0 < h_{MAX}$ for all cases except vertical polarization over sea water, the restriction will always be satisfied for equal antenna heights if:

$$h < h_{MAX}$$

The units used throughout this model discussion are in terms of the MKS system. The user input data is converted to the MKS system from the user input form.

EXAMPLE

At 250 MHz, $h_{MAX} = 30$ meters, and the model is valid when each antenna height is 30 meters or about 100 feet. At that frequency, the maximum effective antenna height is $h_0 = 0.8$ meters for vertical polarization over average land and $h_0 = 0.05$ meters for horizontal polarization. For an antenna combination of 1 meter and 900 meters,

$$h_1' h_2' = \text{Max} (0.8, 1) \times \text{Max} (0.8, 900) = 900 = h_{MAX}^2$$

and the model is still valid for vertical or horizontal polarization over average land at 250 MHz.

The model for ground propagation is physically correct and has been empirically proven. The input data required is normally available.

6.3.3 Antenna Model

In the antenna model, antennas are categorized into two groups. Antennas included in the first group are low gain antenna types such as a monopole, dipole, slot or loop. Antennas included in the second group are medium to high gain antenna types, such as horn or parabolic reflector.

All antennas in the first group are modeled analytically by trigonometric expressions. A dipole, for example, has a directive gain $G = 1.6 \sin^2 \theta$, where θ is the angle of an arbitrary direction with respect to the dipole axis.

All antennas in the second group are modeled by a three dimensional three-sector representation. Each sector subtends a solid angle in the unit sphere and has an associated quantized antenna gain.

The three sectors are intended to correspond to a main beam, major side-lobe and backlobe. A four sector model had been considered, but it was decided that the three sector representation would be sufficient to characterize most medium to high gain antennas, and that even two sectors would be sufficient in many cases.

Since antenna measurements are rarely available at frequencies other than the design frequency or the first few harmonics thereof, the representation is considered frequency independent as a worst case condition.

The three-sector model is pictured in Figure No. 54.

To use the three-sector representation, the sector parameters θ_{MB} , ϕ_{SL} , G_{SL} , and G_{BL} are drawn from the antenna data file, where:

- θ_{MB} = Vertical half-beamwidth of main beam
- ϕ_{MB} = Horizontal half-beamwidth of main beam
- G_{MB} = Main beam gain
- ϕ_{SL} = Sidelobe half-beamwidth
- G_{SL} = Sidelobe gain
- G_{BL} = Backlobe gain

The gain in an arbitrary direction θ , ϕ in the coordinate system of the antenna is found by determining the sector in which that direction falls and choosing the gain associated with that particular sector.

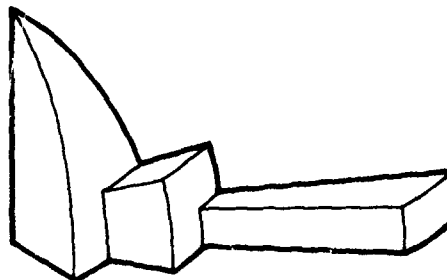
If the antenna coordinate system is rotated with respect to the system reference frame, an orthogonal transformation must be used to calculate the "look angle" with respect to the antenna coordinate system.

If the look angle in the system frame is given by (ϕ_D, θ_D) where θ_D is the angle to the Z-axis and ϕ_D is the azimuthal angle, and the antenna is rotated by angle ϕ_R about its Z-axis and θ_R about its Y-axis, respectively, then the look angle in the antenna coordinate system (ϕ, θ) is defined by the Euler transformation:

$$\sin \theta \cos \phi = \cos \theta_R \cos \phi_R \sin \theta_D \cos \phi_D + \cos \theta_R \sin \phi_R \sin \theta_D \sin \phi_D + \sin \theta_R \cos \theta_D$$

$$\sin \theta \sin \phi = -\sin \phi_R \sin \theta_D \cos \phi_D + \cos \phi_R \sin \theta_D \sin \phi_D$$

$$\cos \theta = -\sin \theta_R \cos \phi_R \sin \theta_D \cos \phi_D - \sin \theta_R \sin \phi_R \sin \theta_D \sin \phi_D + \cos \theta_R \cos \theta_D$$



GP73 0495 24

FIGURE 54
ANTENNA PATTERN BEAM ANGLES

6.3.4 Intravehicular Propagation Model

This model¹⁴ calculates the propagation loss associated with an electromagnetic coupling path when both source and receptor are located on the same aircraft or spacecraft. The power received is related to the power transmitted in the following way:

$$P_R = P_T + TFS + SF$$

where

P_T = transmitter power in dBm

TFS = free space transmission factor in dB

SF = shading factor in dB

The free space transmission factor is derived from the Friis transmission equation and is given by:

$$TFS = G_T + G_R + 20 \log_{10} \left(\frac{\lambda}{4\pi D} \right)$$

where

G_T = gain of transmitting antenna in dB

G_R = gain of receiving antenna in dB

λ = wavelength in meters

D = distance between two antennas in meters

The shading factor SF is the adjustment to the free space transmission factor due to the presence of the aircraft or spacecraft, whose bulk may be interposed in the region between transmitter and receiver.

Vehicular Geometry

The antenna separation, D, is determined using the aircraft model shown in Figure 55. Antenna locations are specified in the usual fuselage station (FS), waterline (WL) and butt-line (BL) system used for aircraft. For analysis, these locations are converted by the computer into cylindrical coordinates (ρ , θ , Z) (ρ and Z are in inches, θ is in radians). The Z-axis of the cylindrical coordinate system is the centroid of the aircraft and is displaced vertically from the WL = 0 line, a distance denoted as WLC. The base of the conical nose section is specified by FSN.

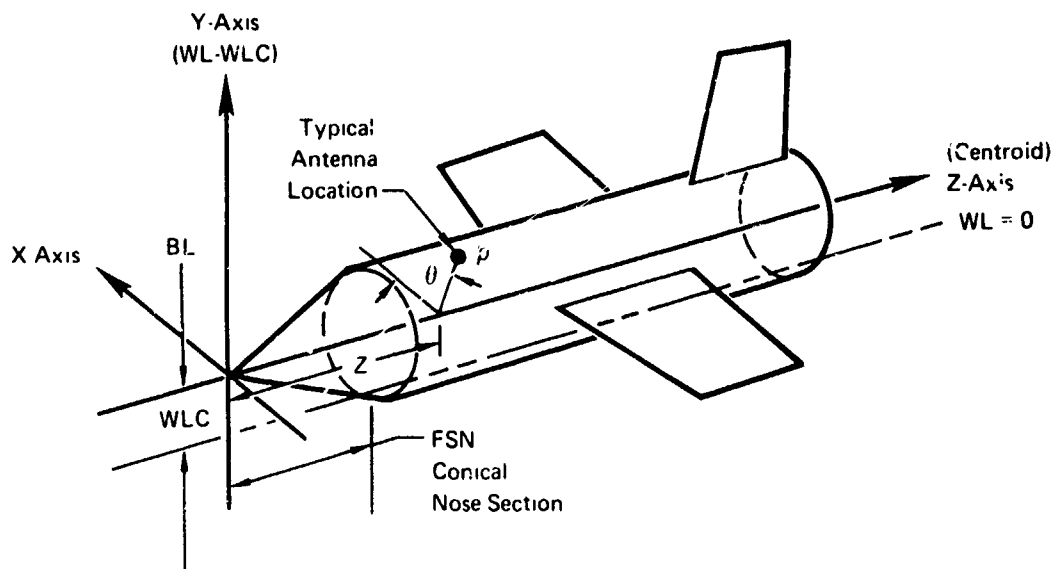


FIGURE 55
MODEL USED TO APPROXIMATE AIRCRAFT

GP73 0495 22

D is determined by using the combination of straight lines, conical spirals, and/or cylindrical spirals that gives the shortest distance between the two antennas over the aircraft surface. The combination used depends on the relationship of the two antennas to the fuselage and wings. With both antennas on the fuselage, a conical spiral is used when one or both antennas are forward of FSN, and a cylindrical spiral is used when both are aft of FSN.

For the conical spiral, the distance between two points, $P_1(\rho_1, \theta_1, Z_1)$ and $P_2(\rho_2, \theta_2, Z_2)$ is

$$D_{\text{con}} = \left| \frac{\rho_1 c - \rho_2 d}{2a} + \frac{a^2 + b^2}{2a} \ln \left| \frac{\rho_1 + c}{\rho_2 + d} \right| \right|$$

where $a = \frac{\rho_2 - \rho_1}{\theta_2 - \theta_1}$

$$b = \frac{Z_2 - Z_1}{\theta_2 - \theta_1}$$

$$c = \sqrt{a^2 + b^2 + \rho_1^2}$$

$$d = \sqrt{a^2 + b^2 + \rho_2^2}$$

For the cylindrical spiral ($\rho_1 = \rho_2 = \rho_f$), the distance between two points is

$$D_{cy1} = \sqrt{\rho_f^2 (\theta_2 - \theta_1)^2 + (Z_2 - Z_1)^2}$$

Straight line distances are found using

$$D_{sl} = \sqrt{\rho_1^2 + \rho_2^2 - 2\rho_1\rho_2 \cos(\theta_2 - \theta_1) + (Z_2 - Z_1)^2}$$

When one antenna is off the fuselage but the other is on, as illustrated in Figure 56, D is a combination of straight line and cylindrical spiral segments.

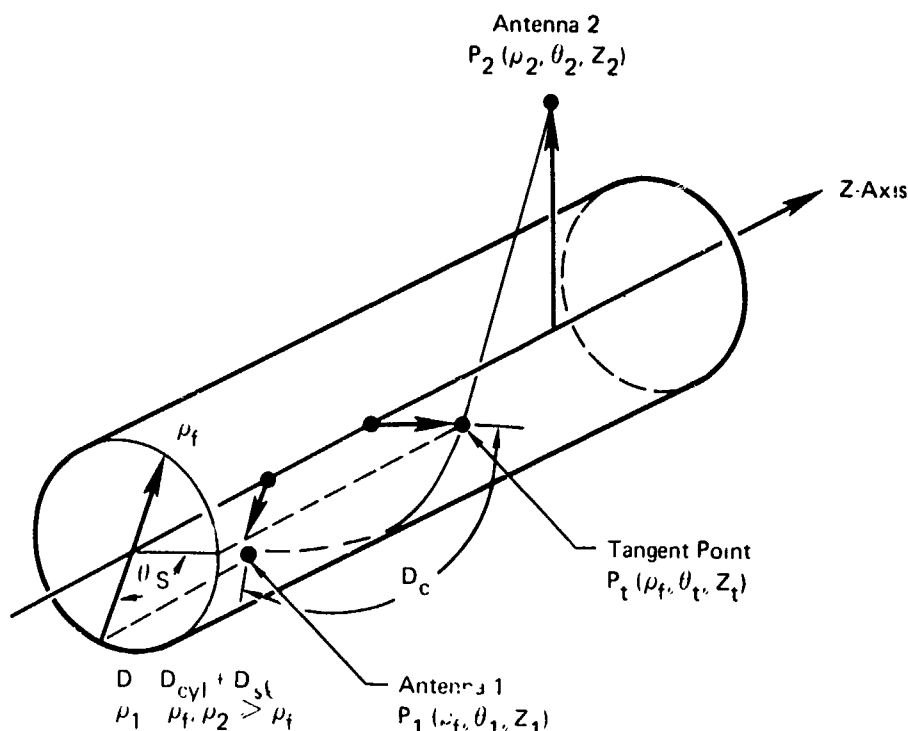
The tangent point on the fuselage for which D is minimum has a coordinate (assuming ρ_2, θ_2, Z_2 is the point off the fuselage)

$$\theta_t = \theta_2 \pm \tan^{-1} \left[\frac{\sqrt{\rho_2^2 - \rho_1^2}}{\rho_1} \right]$$

(The appropriate sign is used that produces minimum D.) The Z coordinate of the tangent point is

$$Z_t = \frac{\rho_1 |\theta_1 - \theta_t| Z_2 + Z_1 \sqrt{\rho_2^2 - \rho_1^2}}{\rho_1 |\theta_1 - \theta_t| + \sqrt{\rho_2^2 - \rho_1^2}}$$

ρ_1 now becomes ρ_f in the previous equations and (θ_1, Z_1) become (θ_t, Z_t) respectively when calculating the straight line segment.

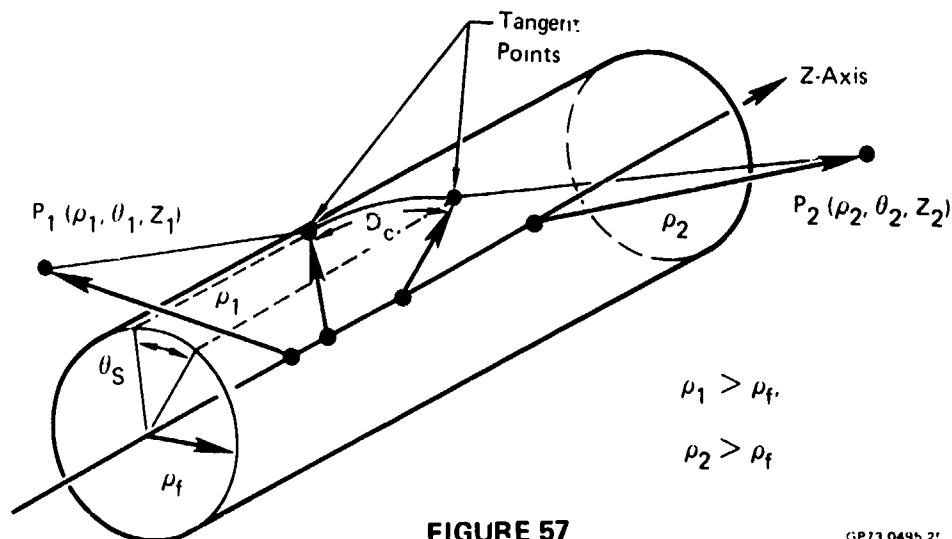


GP73-0495 26

FIGURE 56

DISTANCE BETWEEN TWO ANTENNAS WHEN ONE IS LOCATED OFF FUSELAGE AND A PORTION OF THE PATH IS AROUND THE FUSELAGE

When both antennas are off the fuselage and the shortest path between them is around the fuselage, D consists of two straight line segments and one cylindrical spiral segment as shown in Figure 57. In this case, there are two tangent points. The θ coordinate for the tangent points, θ_{t1} and θ_{t2} , are computed using the above angle equation, and the Z coordinates are

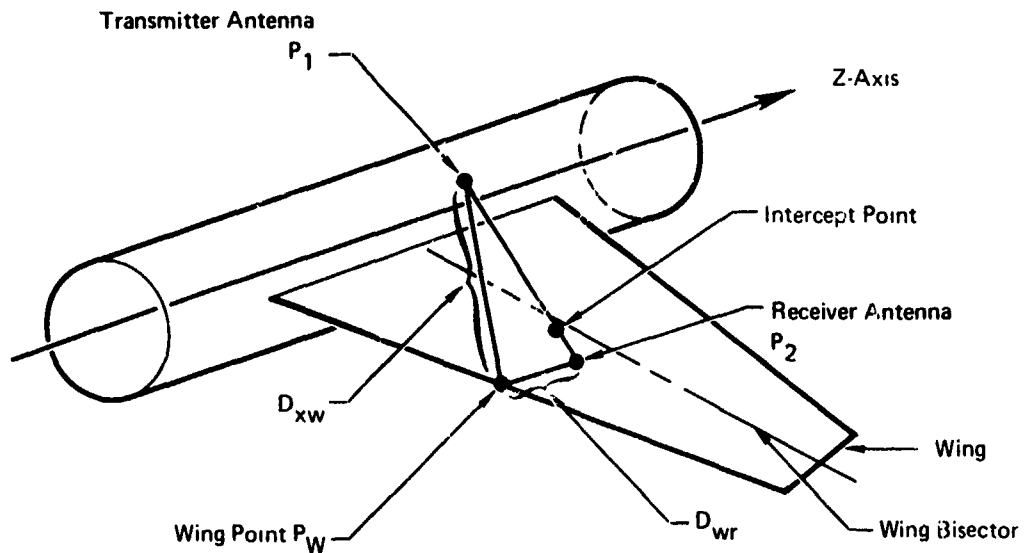


GP73-0495 27

FIGURE 57

DISTANCE BETWEEN TWO ANTENNAS WHEN BOTH ARE OFF THE FUSELAGE AND THE PATH IS AROUND THE FUSELAGE

In the event that a wing intersects the propagation path, the wing must be included in the distance calculation as well as the shading calculation. The propagation path around the wing edge must be determined such that its total length D , is a minimum. First, the forward or aft wing edge is selected, depending on which path will have the shortest total distance. This is determined by calculating the intersection of the wing and a straight line between the two antennas. Once the wing edge is determined, an iterative technique is used to find the point on that edge such that the propagation path is a minimum. A typical example, with both antennas off the fuselage is shown in Figure 58. For this, the distances are determined from the wing point to each antenna using the techniques described above. The result is the minimum distance D .



GP73-1495-19

FIGURE 58
TYPICAL PROPAGATION PATH WITH WING SHADING

Shading and Diffraction

Where a portion of the propagation path is around any curved surface, allowance must be made for shading effects. An equation for the fuselage shading, as a portion of the shading factor SF was derived from Hasserjian and Ishimaru.¹⁵ In their work, a function was given relating propagation around an infinite conducting cylinder to that over a flat plane. The function can be reasonably approximated by

$$SF_C = \frac{-A}{(\eta A + \xi)}$$

where $A = \rho_f \theta_s^2 \sqrt{\frac{2\pi}{\lambda D_c}}$

$$\eta = \begin{cases} 5.478 \times 10^{-3}, & \text{for } A < 26 \\ 3.340 \times 10^{-3}, & \text{for } A \geq 26 \end{cases}$$

$$\xi = \begin{cases} 0.5083, & \text{for } A < 26 \\ 0.5621, & \text{for } A \geq 26 \end{cases}$$

and SF_C = fuselage (cylindrical) shading factor (dB)

ρ_f = radius of cylinder (meters)

θ_s = angle around cylinder of propagation path (radians)

λ = wavelength (meters)

D_c = distance of cylindrical segment of propagation path (meters)

When a portion of the propagation path is around the wing, or any surface edge, allowance must be made for diffraction effects. An incident electric field can be related to a diffracted electric field using optic theory and lowering the frequency range to radio frequency. From Figure 59, the diffraction attenuation function for the wing can be calculated using

$$SF_w = 20 \log_{10} \left| \frac{\mathcal{E}_r}{\mathcal{E}_x} \right|$$

where $\left| \frac{\mathcal{E}_r}{\mathcal{E}_x} \right| = \frac{\max \left| \sec \frac{1}{2} (\alpha_x - \alpha_r) \pm \csc \frac{1}{2} (\alpha_x + \alpha_r) \right| \cos \beta}{\sqrt{8\pi k D_{wr}}}$

and SF_w = Wing shading factor (dB)

\mathcal{E}_x = Incident electric field from transmitter at wing point

\mathcal{E}_r = Received electric field at receiver antenna

α_x = Angle between Z_2 axis and incident wave propagation vector projected onto $Y_2 - Z_2$ plane

α_r = Angle between Z_2 axis and receptor wave propagation vector projected onto $Y_2 - Z_2$ plane

β = Angle of incident wave propagation vector to $Y_2 - Z_2$ plane

k = $2\pi/c$ = Propagation constant

c = Velocity of Light (3×10^8 m/sec)

D_{wr} = Distance from wing point to receptor point (meters)

The total shading factor is then the sum of the edge and cylindrical surface factors.

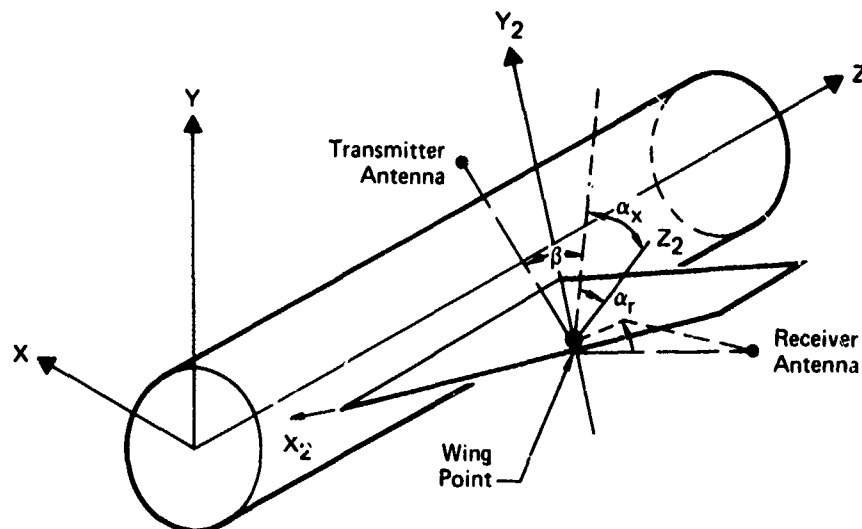


FIGURE 59

GP73 0495 21

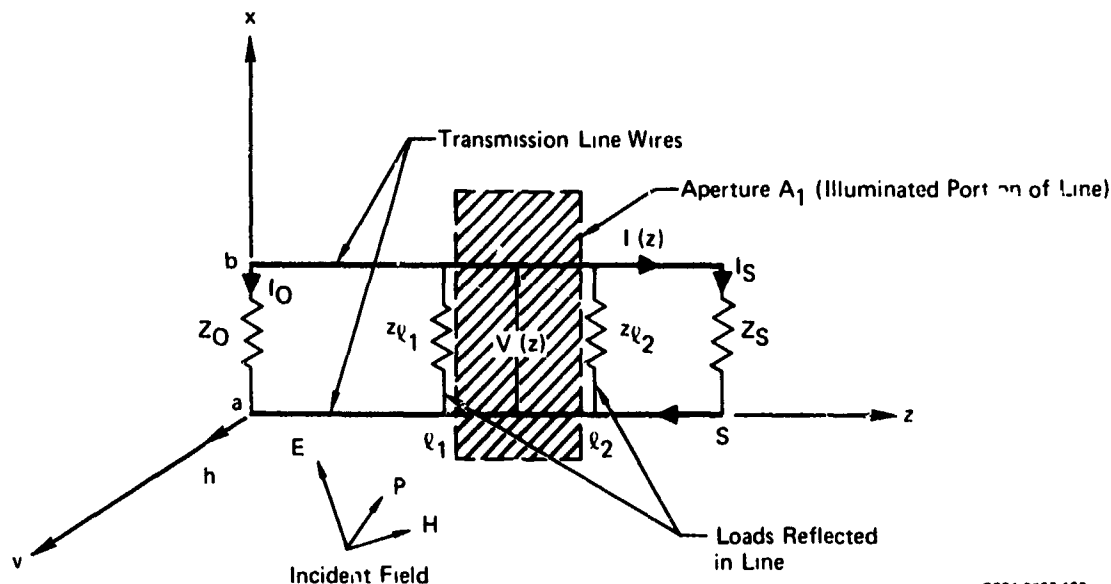
DIFFRACTION COORDINATE SYSTEM WHEN THE PROPAGATION PATH IS AROUND THE WING EDGE. ATTENUATION FUNCTION IS CALCULATED USING ANGLES IN THIS COORDINATE SYSTEM

6.3.5 Field to Wire Compatibility Analysis

The coupling from environmental electromagnetic fields onto wiring is important in the design of USAF systems. Usually, the fields enter the vehicle through dielectric apertures in the systems skin and couple onto wires immediately adjacent. These apertures include radomes, canopies, landing gear doors, camera windows and air intakes, on aircraft and space vehicles and doors and windows in ground systems.

Exposed wires are assumed to be adjacent to the aperture, and the amount of RF energy coupled depends on the aperture size and location. A transmission line model is then used to compute the currents induced in the wire loads. Worst-case electromagnetic field vector orientation is determined and used for the calculation.

Figure 60 shows a transmission line exposed to an electromagnetic field.



GP74 0267 123

FIGURE 60
TRANSMISSION LINE ILLUMINATED BY ELECTROMAGNETIC FIELD

Integration of Faraday's law over the surface of the transmission line results in

$$\int_{A_1} (\nabla \times \vec{E}) \cdot \hat{n} dS = - \frac{\partial}{\partial t} \int \vec{B} \cdot \hat{n} dS$$

Defining the voltage across the wires at a given z as

$$V(z) = - \int_a^b E_x(x,z) dx$$

leads to the following transmission line partial differential equations with voltage and current sources included:

$$\frac{\partial V(z)}{\partial z} + Z I(z) = j \omega \int_a^b B_y^i(x,z) dx$$

and

$$\frac{\partial I(z)}{\partial z} + Y V(z) = j\omega Y \int_0^b E_x^i(x, z) dx$$

where a sinusoidal time dependence is assumed, E^i and B^i are the incident fields, and Y and Z are the transmission line admittance and impedance, respectively. 16

The two previous equations can then be used to derive two inhomogeneous second order differential equations for the transmission line currents and voltages. These equations are solved using the method of variation of parameters.

When the entire transmission line is not exposed to the incident field, expressions for the equivalent impedance of the unexposed transmission line and the physical loads replace Z_0 and Z_S in Figure 60 and the equations. The resulting current in Z_0 is then

$$I_0 = \frac{Z_c}{D [Z_c \cosh(\gamma \ell_1) + Z_{\ell_1} \sinh(\gamma \ell_1)]} \left[\int_{\ell_1}^{\ell_2} [E_z^i(b, z) - E_z^i(a, z)] [Z_c \cosh \gamma(\ell_2 - z) + Z_{\ell_2} \sinh \gamma(\ell_2 - z)] dz \right. \\ \left. + [Z_c \cosh \gamma(\ell_2 - \ell_1) + Z_{\ell_2} \sinh \gamma(\ell_2 - \ell_1)] \int_0^b E_x^i(x, \ell_1) dx \right. \\ \left. - Z_c \int_0^b E_x^i(x, \ell_2) dx \right]$$

Likewise, the current in Z_S is given by

$$I_s = \frac{Z_c}{D [Z_c \cos \gamma (s - \ell_2) + Z_{\ell_2} \sinh \gamma (s - \ell_2)]} \left[\int_{\ell_1}^{\ell_2} [E_z^i(b, z) - E_z^i(0, z)] [Z_c \cosh \gamma (z - \ell_1) + Z_{\ell_1} \sinh \gamma (z - \ell_1)] dz - [Z_c \cosh (\gamma \ell_2) + Z_{\ell_1} \sinh (\gamma \ell_2)] \int_0^b E_x^i(x, \ell_2) dx + Z_c \int_0^b E_x^i(x, \ell_1) dx \right]$$

where

Z_c = transmission line characteristic impedance
 γ = complex propagation constant
 b = separation between wires
 s = total length of transmission line
 ℓ_1 and ℓ_2 = define exposed portion of line

and

$$D = (Z_c Z_{\ell_1} + Z_{\ell_2} Z_c) \cosh \gamma (\ell_2 - \ell_1) + (Z_c^2 + Z_{\ell_2} Z_{\ell_1}) \sinh \gamma (\ell_2 - \ell_1)$$

Z_{ℓ_1} and Z_{ℓ_2} are the termination impedances as seen at the aperture edges.

They are given by

$$Z_{\ell_1} = Z_c \frac{Z_0 + Z_c \tanh \gamma \ell_1}{Z_c + Z_0 \tanh \gamma \ell_1}$$

and

$$Z_{\ell_2} = Z_c \frac{Z_s + Z_c \tanh \gamma (s - \ell_2)}{Z_c + Z_s \tanh \gamma (s - \ell_2)}$$

These equations are dependent only on the incident electric fields, since the scattered fields have been accounted for in the induced transmission line currents.

For a transmission line that is electrically short, $[\gamma(\ell_2 - \ell_1)] \ll 1$, the equations for the currents generated in the transmission line by an incident electromagnetic field take on an asymptotic form.

If the incident wave is propagating along the direction of the line, with the electric field in the plane of the wires, the current generated at l_2 is approximately:

$$I_{l_2} = -Eb(l_2 - l_1) \frac{\gamma Z_{l_1} + \gamma Z_c}{Z_c(Z_{l_1} + Z_{l_2})}$$

where E is the electric field intensity and b is the separation between the two wires (or double the distance above a ground station)

For a transmission line that is not electrically short, the expression for the current is more complex. However, if the line is almost lossless, i.e., $\gamma \approx j\kappa$, the current at l_2 is approximately:

$$I_{l_2} = \frac{-E(l_2 - l_1)}{D} j(Z_{l_1} + Z_c) \sin \kappa(l_2 - l_1)$$

where

$$D = Z_c(Z_{l_1} + Z_{l_2}) \cos \kappa(l_2 - l_1) + j[Z_c^2 + Z_{l_1}Z_{l_2}] \sin \kappa(l_2 - l_1)$$

An envelope expression was developed for this case and implemented in IEMCAP.

Assuming Z_L is the load in question the programmed formulas are

$$\text{if } Z_o > Z_c \text{ and } X \leq \left| \frac{2Z_o}{Z_c + Z_o} \right|$$

$$|I'_L| = bX \left| \frac{Z_o + Z_c}{Z_c(Z_o + Z_L)} \right|$$

$$\text{if } Z_o > Z_c \text{ and } X > \left| \frac{2Z_o}{Z_c + Z_o} \right|$$

$$|I'_L| = 2b \left| \frac{Z_o}{Z_c (Z_o + Z_L)} \right|$$

$$\text{if } Z_o < Z_c \text{ and } X \leq \left| \frac{2 Z_c}{Z_c + Z_o} \right|$$

$$|I'_L| = bX \left| \frac{Z_o + Z_c}{Z_c (Z_o + Z_L)} \right|$$

$$\text{if } Z_o < Z_c \text{ and } X > \left| \frac{2 Z_c}{Z_c + Z_o} \right|$$

$$|I'_L| = 2b \left| \frac{1}{Z_o + Z_L} \right|$$

The induced current is

$$|I_L| = \text{Min} [|I'_L|, I_{\text{Bound}}]$$

$$I_{\text{Bound}} = \frac{\frac{\lambda}{\text{Max} [\sqrt{4\pi}, 1]}}{\sqrt{377 \times R_e (Z_L)}}$$

If a shield is present and the frequency is greater than 7228 Hz but less than 9×10^5 Hz

$$I_L = I_L \times 10^{[4.8 \log_{10} f - 70.8] \log_{10} f + 201.5}$$

If the frequency is greater than 9×10^5 Hz

$$I_L = I_L \times 10^{[(-67 \log_{10} f + 42.5) \log_{10} f - 345.8] \log_{10} f + 855}$$

If a double shield is present, the above powers of ten are multiplied by $\frac{3}{2}$.

The above analysis can be easily extended to wires routed close to more than one aperture. Using superposition, the analysis is used to calculate the currents from each exposure, and the resulting complex currents are summed.

Ground Plane Effects

This analysis can also be applied to circuits with a ground plane return. In this case, the transmission line is formed by using the ground plane image of the primary wire. The above equations are applied using twice the height above ground for the wire separation.

6.3.6 Wire to Wire Coupling

During the calculation of the coupling from emitter ports to a particular receptor port, a check is made to determine if any wires connected to any of the emitter ports are in the same bundle and run as wires connected to the receptor port. If there are such wires, the wire to wire coupling routine is called. This routine computes the spectral voltages induced in the receptor circuit by the emitter circuit. These calculations are performed on a pair basis (only one emitter circuit considered to couple with the receptor circuit for each calculation) with the effects of all other circuits neglected during this calculation. Each possible pair coupling is computed in turn and the total coupling is calculated by summing all of the pair couplings without regard to phase. It should be noted that the validity of this wire-to-wire coupling model has been verified by experimental data.

In order to make this applicable to general systems, it is necessary to have models available for computing the coupling between the circuit pairs even when the connecting wires have a relatively complex configuration (such as shielded, twisted pairs). For this program, the circuits for which models have been developed include

- (a) Single (unshielded) wires with ground return
- (b) Twisted pair circuits (balanced or unbalanced)
- (c) Shielded wires (single or double shield) with single or multiply grounded shields
- (d) Shielded twisted pair circuits (balanced or unbalanced, single or double shield) with single or multiply grounded shields.

These models are valid for both emitter and receptor circuits and any type of emitter circuit may be analyzed with any type receptor circuit.

For frequencies where the wire length is short compared to a wavelength, the models provide an accurate representation of the actual coupling situations. However, for the frequencies where the wire lengths are comparable to or greater than the wavelength, the actual coupling is very sensitive to line length and no simple model is available for modeling the exact coupling. In this frequency range, the models approximate the envelope of the coupling curve so that the predicted coupling is never less than the actual.

The basic model for wire to wire coupling considers capacitive coupling due to the interwire capacitance and inductive coupling due to the mutual inductance between the wires.¹⁷⁻²¹ This model uses the approximation that the total coupling can be computed as the sum of the capacitive and inductive coupling computed separately.

The analysis of circuits which are more complex than a single wire with ground return is accomplished by finding an equivalent (in terms of coupling) single wire representation for the circuit. Although the single wire equivalents for these circuits are different for capacitive and inductive coupling, this technique allows the same routines to be used for all circuits considered.

The calculation procedure must be modified somewhat for emitter and receptor circuits which have several branches, discontinuities, pigtail shield terminations, etc. This is necessary because the emitter current and equivalent circuit change from segment to segment for circuits with these discontinuities. In this case the emitter current (and the summation of voltages coupled to the receptor port) is computed on the basis of the entire emitter (receptor) configuration but the coupling is computed on a segment by segment basis. This is accomplished by first computing the current and the single wire equivalent for each segment of the emitter circuit which has a common segment with the receptor port circuit. The proper equivalent receptor circuit segment is paired with the correct emitter segment for computation of the coupling on a segment by segment basis. All of the coupling components are then summed (according to the wire map for the receptor circuit) to determine the total coupling. This is done for both capacitive and inductive coupling at all frequencies for which the coupling is required (these frequencies are supplied by COUPLE).

This method of segmenting the wires allows the calculation of the effects of environmental fields on the complete receptor circuit at the same time the first emitter circuit is being analyzed. This is accomplished by using asymptotic expressions for field to wire coupling on internal circuits.

Data for calculation of the coupling parameters and the wire map for ascertaining how the components of coupling must be combined is supplied from port data, bundle data, and from the wire characteristics table. In all parameter calculations, the wire spacing is taken as one-fourth of a bundle diameter. This value was picked as a reasonable compromise between the worst case situation (where wires are separated only by their insulation) and the average value of separation of wires in a bundle (assuming random placement of wires during bundle construction).

Capacitive Coupling - For the calculation of the capacitive coupling between an emitter circuit segment and a receptor circuit segment, the wire to wire capacitance between the segments is computed for the length which the segments have in common. The basic configuration for this calculation is two wires above a ground plane as shown in Figure 61.

The circuit representation of the capacitive coupling for this configuration is shown in Figure 62.

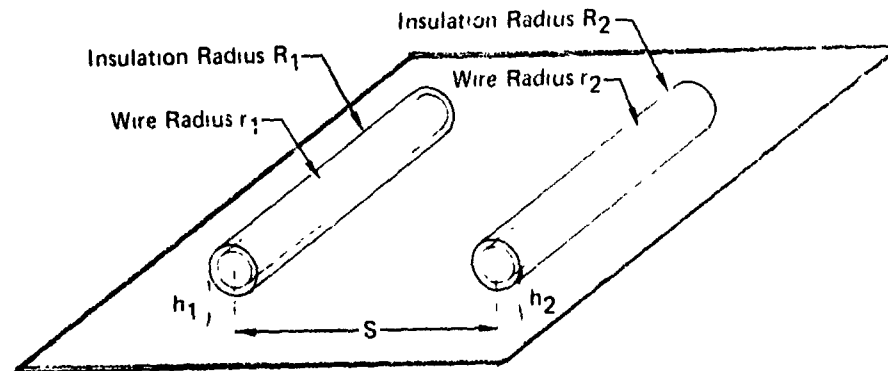


FIGURE 61
PARALLEL WIRES OVER A GROUND PLANE

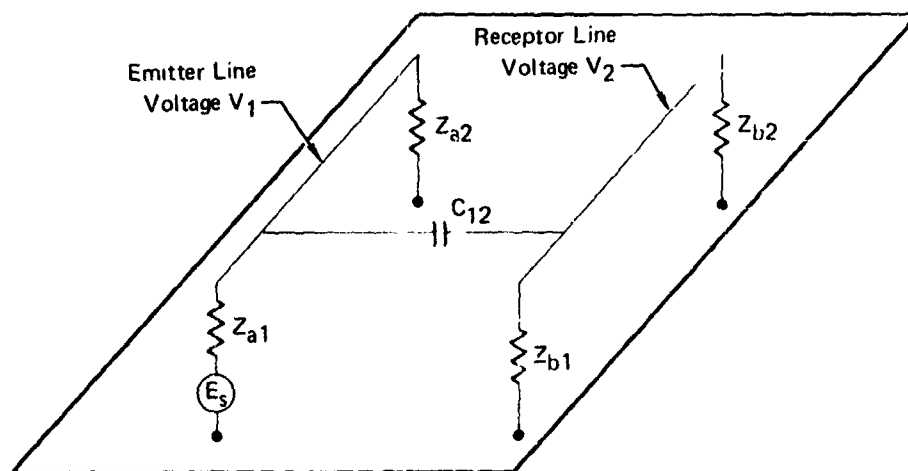


FIGURE 62
CIRCUIT REPRESENTATIVE OF CAPACITIVE COUPLING BETWEEN
PARALLEL WIRES OVER A GROUND PLANE

In this case the capacitance per unit length between the two wires is given by

$$C_{12} = - \frac{2\pi \epsilon_{\text{eff}} P_{12}}{\det}$$

where

$$P_{12} = 1/2 \left[\cosh^{-1} \left(\frac{s^2 + (r_1^2 - r_2^2)}{2sr_1} \right) + \cosh^{-1} \left(\frac{s^2 - (r_1^2 - r_2^2)}{2sr_2} \right) \right. \\ \left. - \cosh^{-1} \left(\frac{s'^2 + (r_1^2 - r_2^2)}{2s'r_1} \right) - \cosh^{-1} \left(\frac{s'^2 - (r_1^2 - r_2^2)}{2s'r_2} \right) \right]$$

$$s' = \sqrt{4h_1h_2 + s^2}$$

$$\det = \cosh^{-1} \left(\frac{h_1}{r_1} \right) \cosh^{-1} \left(\frac{h_2}{r_2} \right) - P_{12}^2$$

and

$$\epsilon_{\text{eff}} = \epsilon_0 + \frac{\left(\frac{R_1 + R_2}{r_1 + r_2} \right)^2 - 1}{1/2 \left(\frac{2s + R_1 + R_2}{r_1 + r_2} \right)^2} [\epsilon - \epsilon_0]$$

This capacitance is used to calculate the capacitive coupling of the emitter segment to the receptor segment according to the relation

$$\frac{V_2}{V_1} = \frac{1}{1 + \frac{1}{j\omega Z C_{12} \ell_s}}$$

where

$$Z = \frac{Z_{b1} Z_{b2}}{Z_{b1} + Z_{b2}}$$

and ℓ_s is the segment length.

In a case where the emitter wire is shielded, the above equation is used to find the capacitive coupling but C_{12} is computed using r_1 equal to the outside radius of the emitter shield. This gives

$$\frac{V_2}{V_{eso}} = \frac{1}{1 + \frac{1}{j\omega Z C_{12} l_s}}$$

where the emitter voltage, V_{eso} , is the voltage on the outside of the emitter shield rather than the emitter wire voltage. It is computed by a two step procedure where the capacitive coupling from the emitter wire to its shield determines the potential on the inner surface of the shield, and the shield factor for the shield determines V_{eso} .

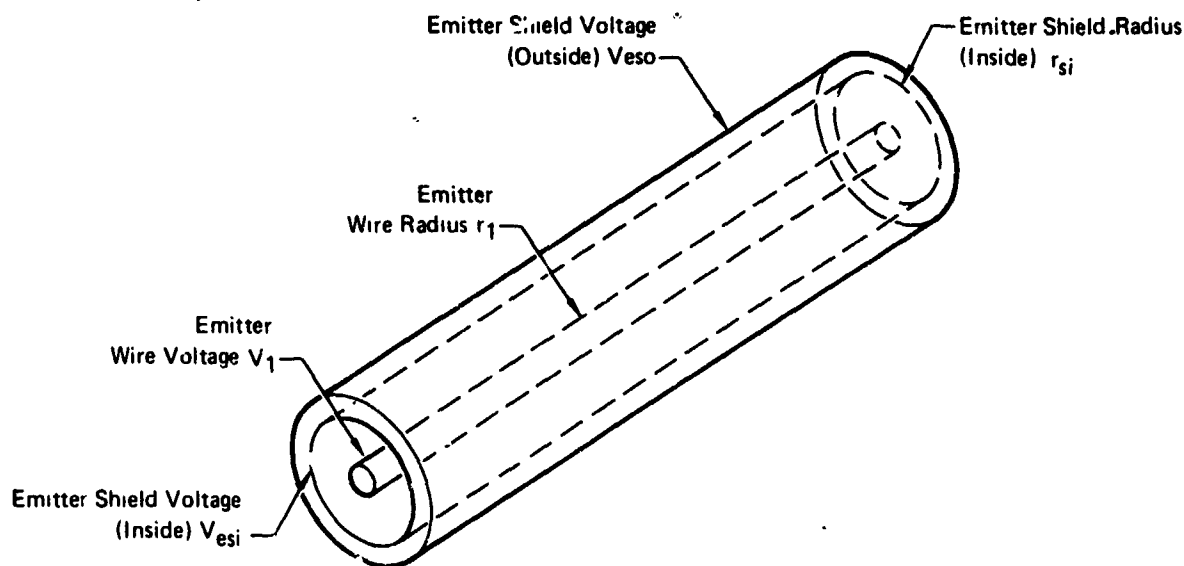


FIGURE 63
SHIELDED EMITTER WIRE SEGMENT

GP73-0485-13

The wire to shield capacitance per unit length for this configuration is

$$C_{ws} = \frac{2\pi \epsilon}{\ln \left(\frac{r_{si}}{r_1} \right)}$$

where ϵ is the permittivity of the material between wire and shield and r_{si} and r_1 are as shown in Figure 63.

The voltage V_{esi} on the inner shield surface can then be written as

$$\frac{V_{esi}}{V_1} = \frac{1}{1 + \frac{1}{j\omega R_s C_{ws} \ell_s}}$$

where V_1 is the voltage on the emitter wire and R_s is the frequency dependent shield resistance to ground. Since the number of shield terminations to ground has been found to have only a minor effect on shield resistance, R_s is computed as the resistance from the middle of the emitter segment to its nearest ground termination. It is given by the equation

$$R_s = R_0 \left(\frac{t_e}{\delta_e} \right) \left(\frac{\sinh \frac{2t_e}{\delta_e} + \sin \frac{2t_e}{\delta_e}}{\cosh \frac{2t_e}{\delta_e} - \cos \frac{2t_e}{\delta_e}} \right)$$

where t_e is the emitter shield thickness, and δ_e is the emitter skin depth. R_0 is the total dc shield resistance given by

$$R_0 = \frac{\ell_{es}}{2\pi r_{si} \sigma t}$$

where ℓ_{es} is the shield length (measured from the middle of the segment to the nearest termination), σ is shield conductivity and t is shield thickness. The voltage V_{eso} on the outside of the shield can be written in terms of V_{esi} as

$$\frac{V_{eso}}{V_{esi}} = \exp \left[-\frac{t_e}{\delta_e} \right] + F_e$$

The factor $e^{-\frac{t_e}{\delta_e}}$ models the penetration of the field through the shield metal while the factor F_e accounts for the penetration of the field through the shield weave. It has been found that F_e can be approximated as .02 for shields which have an optical coverage of 80-90% and this is the value used for calculations. For shields with better optical coverage, the coupling due to F_e will be slightly overpredicted.

The voltage coupled to the receptor segment is given by the product of these factors as

$$\left(\frac{V_2}{V_1}\right) = \left(\frac{1}{1 + \frac{1}{j\omega R_s C_{ws} \ell_s}}\right) \left(\exp -\left(\frac{t_e}{\delta_e}\right) + F_e\right) \left(\frac{1}{1 + \frac{1}{j\omega Z C_{12} \ell_s}}\right)$$

where all symbols are as given previously.

When the emitter wire is double shielded, it is necessary to insert two more multiplicative factors into the above equation for capacitive coupling. These factors are

$$\frac{1}{1 + \frac{1}{j\omega C_{s1s2} \ell_s R_{s2}}}$$

and

$$\exp\left(-\frac{t_{e2}}{\delta_{e2}}\right) + F_{e2}$$

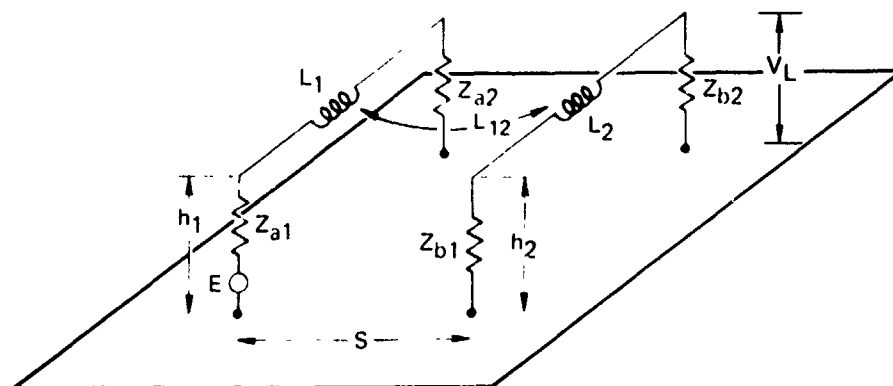
The first factor computes the capacitive coupling from the first shield to the second and the second factor models the penetration of the field through the second shield. In these factors, C_{s1s2} is the capacitance per unit length from the inside shield to the outside shield, R_{s2} is the resistance of the outside shield and t_{e2} , δ_{e2} , and F_{e2} are the thickness, skin depth, and weave penetration factor respectively for the outside shield.

For cases where the receptor wire is shielded, the same factors are used to compute the field penetration through the receptor shield(s) and the capacitive coupling from shield to wire (or shield to shield to wire).

An additional factor has been put into all shielding formulas in the program to account for the exposed portion of a shielded wire due to the pigtail shield termination. The program assumes that all circuits have three inches of exposed wire between the shield and the wire termination. So as not to be unrealistic in the amount of coupling resulting from the circuit exposure this effect is only accounted for when an emitter wire segment is in common with this portion of the receptor circuit and vice versa for an emitter pigtail segment.

When either the emitter wire or the receptor wire is twisted, the capacitive coupling is altered by the presence of the second wire in the twisted pair. The exact effect of this alteration is dependent on several factors such as twist, insulation thickness, degree of balance, etc. These effects are difficult to model accurately, however, a worst case situation can be modeled by assuming that the second wire provides no reduction in the amount of coupling. To enable the use of a simple model which will never underpredict the coupling, this worst case model is used. That is, the capacitive coupling of a twisted pair circuit with another circuit is treated the same as the coupling of a single wire with another circuit.

Inductive Coupling - The calculation of inductive coupling between the emitter and the receptor circuits is computed using the mutual inductance between the circuits. The circuit representation of the basic configuration of two open wires with ground return as shown in Figure 64.



ADP 710495 10

FIGURE 64
CIRCUIT REPRESENTATIVE OF INDUCTIVE COUPLING BETWEEN
PARALLEL WIRES OVER A GROUND PLANE

For this configuration, the voltage induced in the receptor segment is given by

$$V_i = j\omega L_{12} I_1 \ell_s$$

where I_1 is the current in the emitter circuit and ℓ_s is the length of the receptor segment. The mutual inductance per unit length, L_{12} , is given by

$$L_{12} = \frac{\mu_0}{4\pi} \ln \left[\frac{(h_1 + h_2)^2 + s^2}{(h_1 - h_2)^2 + s^2} \right]$$

where μ_0 is the permeability of free space and the other symbols are as shown in Figure 48. The component of the voltage V_1 which appears at the receptor port in the receptor circuit is

$$V_L = \frac{Z_{b2}}{Z_{b1} + Z_{b2} + j\omega L_2 \ell_s} V_i$$

where the impedances are as shown in Figure 64. L_2 is the self inductance per unit length of the receptor wire and is given by

$$L_2 = \frac{\mu_0}{2\pi} \ln \left[\frac{2h_2}{r_2} - 1 \right]$$

where h_2 and r_2 are as shown in Figure 61. The current I_1 may be written as

$$I_1 = \frac{V_1}{Z_{a2} + j\omega L_1 \ell_s}$$

where V_1 is the voltage on the emitter wire (voltage is approximated as constant at all points along the wire) and L_1 is the self inductance per unit length of the emitter wire as given by

$$L_1 = \frac{\mu_0}{2\pi} \ln \left[\frac{2h_1}{r_1} - 1 \right]$$

The symbols h_1 and r_1 are height and radius respectively for the emitter wire (see Figure 61).

For a configuration consisting of single wire emitter and receptor with ground return, the above equations can be combined to give the voltage at the receptor port

$$V_L = \left(\frac{Z_{b2}}{Z_{b1} + Z_{b2} + j\omega L_2 \ell_s} \right) j\omega L_{12} \ell_s \left(\frac{V_1}{Z_{a2} + j\omega L_1 \ell_s} \right)$$

When the emitter (or receptor) circuit is shielded and/or twisted, the same procedure is used with the composite circuits replaced by their single wire models. It is, of course, necessary to compute the parameter values for these single wire equivalents in terms of the actual circuit parameter values. This procedure is used for any circuit which consists of twisted pairs or which has multiple grounded shields (whether a twisted pair or not). In cases where the shield(s) is(are) single grounded or ungrounded the shield current is taken as zero and the inductive coupling is unaffected by shielding.

When the emitter wire has a multiple grounded shield, its single wire equivalent is found by computing the net current in the wire and its shield. The single wire equivalent is then taken as a wire of radius equal to the outside shield radius which carries a current equal to the net current on the wire and its shield.

The current induced on the shield can be written as

$$I_{sh} = \frac{V_s}{R_s + j\omega L_{sw} \ell_s}$$

where R_s is the total shield resistance (as given previously) and L_{sw} is the shield to wire inductance per unit length which can be approximated as

$$L_{sw} = \frac{\mu_0}{2\pi} \ln \left(\frac{2h_1}{r_s} - 1 \right)$$

In this case, h_1 is the height (above ground) of the emitter wire and r_s is the shield radius. The voltage, V_s , induced in the shield is given by

$$V_s = j\omega L_{sw} I_1 \ell_s$$

and the net emitter current I_{eff} is

$$I_{eff} = I_1 - I_{sh}$$

or

$$I_{eff} = \frac{R_s}{R_s + j\omega L_{sw} \ell_s} I_1$$

This effective current is used with the shield radius r_s to form the single wire equivalent emitter for the calculation of inductive coupling.

If the emitter segment is double shielded (with multiple grounds on both shields), the effective current is computed as the net current flowing on the emitter wire and both shields. This is computed using the same equation as above with the same value for ℓ_s and the parallel combination of the shield resistances for R_s .

When the receptor circuit has a multiple grounded shield, the current in the shield can be calculated as

$$I_{rs} = \frac{V_{rs}}{R_{rs} + j\omega L_{rs} \ell_s} = \frac{j\omega L_{es2} \ell_s I_1}{R_{rs} + j\omega L_{rs} \ell_s}$$

where L_{rs} and R_{rs} are the self inductance per unit length and total resistance of the receptor shield. In this case, L_{es2} is the mutual inductance per unit length between the emitter circuit and the receptor shield. The total voltage induced on the receptor wire is given by the sum of the voltages induced by the emitter current and by the receptor shield current. It can be written as

$$V_2 = j\omega L_{ew2} \ell_s I_1 - j\omega L_{s2w2} \ell_s I_{rs}$$

or

$$V_2 = j\omega L_{ew2} \ell_s I_1 - j\omega L_{s2w2} \ell_s \left(\frac{j\omega L_{es2} \ell_s I_1}{R_{rs} + j\omega L_{rs} \ell_s} \right)$$

where L_{ew2} is the mutual inductance per unit length between the emitter circuit and receptor wire, L_{s2w2} is the mutual inductance per unit length between the receptor wire and its shield, and L_{es2} is the mutual inductance between the emitter circuit and the receptor shield. Since the emitter and receptor are taken to be one-fourth bundle diameter apart, this can be approximated as

$$V_2 = (j\omega L_{es2} - j\omega L_{s2w2} \frac{j\omega L_{es2}}{R_{rs} + j\omega L_{rs} \ell_s}) \ell_s I_1$$

or

$$V_2 = j\omega L_{es2} \left(\frac{R_{rs} \ell_s I_1}{R_{rs} + j\omega L_{rs} \ell_s} \right)$$

For cases where the emitter circuit is shielded, I_1 is replaced by I_{eff} . If the receptor circuit is double shielded with multiple grounds, the same equations are used with R_{RS} being computed as the parallel combination of the two shield resistances.

For circuits composed of twisted pairs, two components of inductive coupling are considered. First, for unbalanced twisted pairs, there is a coupling caused by the common mode currents flowing in the twisted pair. This coupling is found by computing the common mode current and calculating coupling based on a single wire carrying this current. Second, a component of inductive coupling exists due to the differential mode current flowing in the twisted pair irrespective of whether the circuit is balanced. This coupling is computed by using the mutual inductance of the loop formed by the twisted pair emitter (receptor) circuit and the receptor (emitter) circuit.

For an unbalanced twisted pair emitter circuit such as shown below, the common mode current can be calculated as

$$I_c = j\omega C_s V_1$$

$$\text{where } C_s = \frac{2\pi \epsilon_0 \ell_s}{\ln(2h/r_w)}$$

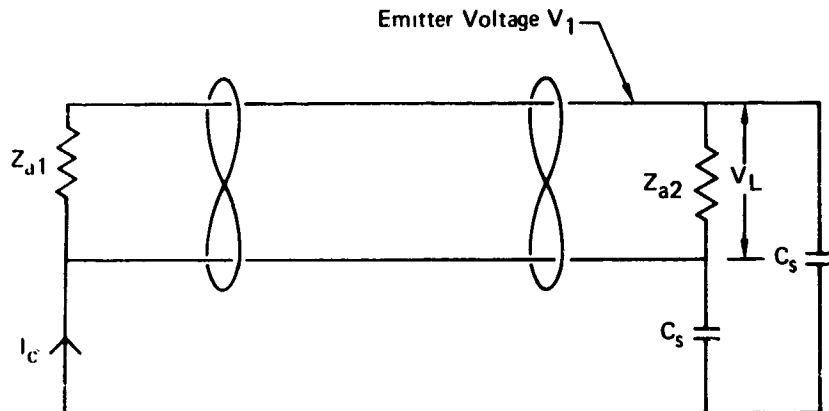


FIGURE 65
INDUCTIVE MODEL FOR UNBALANCED, TWISTED EMITTER WIRE PAIR

for a shunt capacitance C_s as shown. This common mode current can then be used as the single wire equivalent emitter current. If the twisted pair emitter circuit is perfectly balanced, there is no common mode current and only the differential mode coupling need be considered. For this case the maximum coupling will exist when there is no twisting or only a small amount. This worst case model where the wires are considered as parallel and separated only by their insulation is used for calculation of differential mode coupling.

The voltage induced in the receptor circuit by this differential mode current is

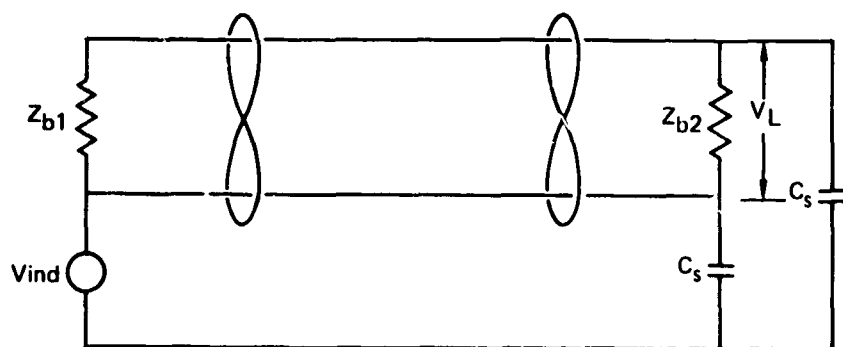
$$V_L = j\omega L'_{12} I_d$$

In this equation, the mutual inductance L'_{12} of the twisted pair loop and the receptor circuit is

$$L'_{12} = \frac{\mu_0}{4\pi} \ell \ln \left[\left(\frac{d}{s} \right)^2 + 1 \right]$$

where d is the separation of the twisted pair and s is the average separation between the emitter wire and receptor pair. The differential mode current, I_d , is the current which flows around the loop formed by the twisted pair. For a twisted pair emitter circuit which is shielded, the common mode current coupling is handled in exactly the same way as a single wire carrying the common mode current while the differential coupling is unaffected by the shielding.

The twisted pair receptor circuit is modeled in a similar way. The load voltage produced by the common mode currents for an unbalanced twisted receptor are found by considering the loop formed by the twisted pair and the ground plane as shown below.



GP73-0495 12

FIGURE 66
INDUCTIVE MODEL FOR UNBALANCED, TWISTED RECEPTOR WIRE PAIR

The load voltage V_L can be written in terms of the induced voltage V_{ind} as

$$V_L = \frac{j\omega Z_{eq} C_s}{1 + j\omega Z_{eq} C_s} V_{ind}$$

where

$$Z_{eq} = \frac{Z_{b1} Z_{b2}}{Z_{b1} + Z_{b2}}$$

and

$$V_{ind} = j\omega L_{12} I_1$$

For a balanced twisted receptor, there is no common mode coupling and only differential coupling need be considered. In this case the voltage induced in the twisted pair receptor loop can be found as

$$V_{ind} = j\omega L'_{12} I_1$$

where L'_{12} is the mutual inductance between the emitter circuit and the loop formed by the twisted receptor pair. The voltage at the receptor port is then calculated as

$$V_L = \frac{Z_{b2}}{Z_{b1} + Z_{b2}} V_{ind}$$

When the receptor circuit is shielded, the common mode current coupling is modified by the same factor as for single shielded wires while the coupling due to differential mode current is not changed by the presence of shields.

In the foregoing, account has been taken of inductive shielding effectiveness provided by shields. As discussed under capacitance, the reduction of this shielding effectiveness is considered due to the coupling into the pigtailed portion of the shields. It has been assumed in the wire to wire portion of this program that the area capable for both emission and reception is three inches in length and two inches above the ground plane.

Common Impedance - The fact that many circuits share a common return has caused many instances of EMI. The reason for this problem beyond the inductive and capacitive couplings already discussed is the return current of one circuit flowing through the non-zero impedance of the return path acts as a current generator of finite impedance into other commonly grounded circuits. This type of coupling has been modeled by assuming a wire as a common return element. This obviously is "worst case" since large metal portions of the ground return will generally provide less impedance than a typically large wire. By assuming that the receptor circuit does not load down the emitter circuit, this effect can be added into the calculation after considerations of inductance and capacitance have been calculated.

Port Impedance - The port impedances which form the terminations of the wire segments are modeled as the R-L-C configuration shown in Figure 67. This model allows any finite value of R, L, and C to be used in specifying the port impedance (Note: both R and L cannot be zero).

The total impedance connected to each end of a wire segment is computed by use of these port impedances and the wire map data. These segment termination impedances then allow computation of the wire to wire coupling according to the equations previously given.

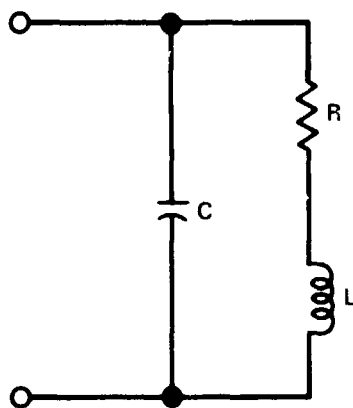


FIGURE 67
PORT TERMINATION IMPEDANCE CONFIGURATION

GP73 1075 29

6.3.7 Case to Case

The case to case model uses the emission and susceptibility levels as specified in Section 3.3.1.3, Non-Required Emission and Susceptibility. These levels are related to the system configuration by modelling each case as though it were a dipole. The source model assumes a fall off of $\left(\frac{1}{r}\right)^3$ for both the electric and magnetic fields.

6.4 PROGRAMMED FORMULAS

6.4.1 Spectrum Models

The programmed spectrum model formulas are expressed, as follows, in tabular form in terms of the program input parameters. All input parameters are defined and, where applicable, illustrated in pictorial representations.

For emitters both broadband and narrowband spectra are given, while only narrowband spectra are given for receptors. The spectra in the required frequency range of emitters and receptors are given in MKS units for the sake of simplicity: watts/Hz and watts for broadband and narrowband respectively.

In the unrequired range of emitters and receptors, spectra are given in units of dB microamps/MHz and dB microamps. For a load of Z ohms, the conversion from watts/Hz to dBμA/MHz is

$$\text{dB}\mu\text{A}/\text{MHz} = 10 \log[\text{watts}/\text{Hz}] + 180 - 10 \log[\text{impedance}]$$

and the conversion from watts to dBμA is

$$\text{dB}\mu\text{A} = 10 \log[\text{watts}] + 120 - 10 \log[\text{impedance}]$$

6.4.1.1 RF Modulations

CW

$$P_{\text{NB}}(f) = P\delta(\Delta f)$$

where P = carrier power

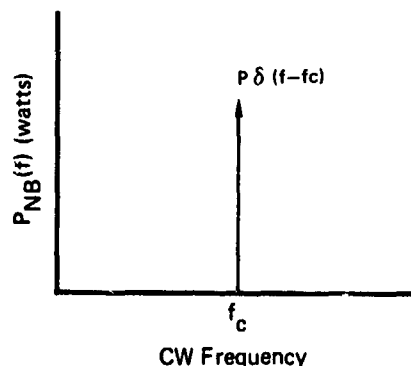


FIGURE 68 CW

$$\text{PDM/AM} \quad P_{BB}(f) = \frac{1}{6} \frac{P}{f_B} \quad ; 0 < |\Delta f| \leq \Delta f_M$$

$$P_{BB}(f) = \frac{1}{6} \frac{P}{f_B} \left(\frac{\Delta f_M}{\Delta f} \right)^2 \quad ; |\Delta f| \geq \Delta f_M$$

$$P_{NB}(f) = 0.25 P \delta(\Delta f)$$

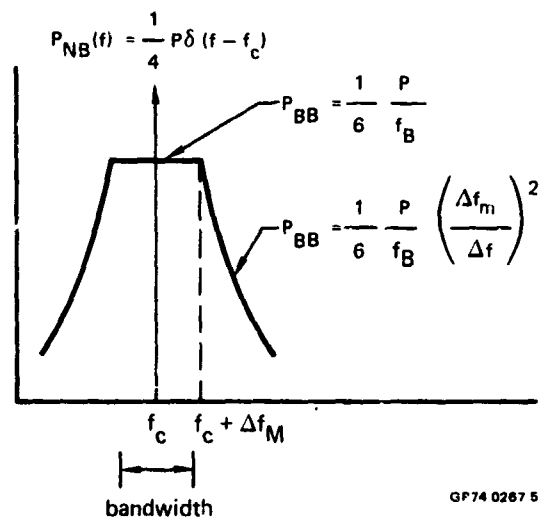
where

$$\text{bandwidth} = 2 f_B$$

$$\Delta f = f - f_c$$

P = peak RF power

$$\Delta f_M = \frac{\sqrt{3}}{\pi} f_M$$



GP74 0267 5

FIGURE 69 PDM-AM

PCM/AM-NRZ $P_{BB}(f) = 0.25 \frac{P}{f_B} ; 0 < |\Delta f| \leq \Delta f_M$

$$P_{BB}(f) = 0.25 \frac{P}{f_B} \left(\frac{\Delta f_M}{\Delta f} \right)^2 ; |\Delta f| > \Delta f_M$$

$$P_{NB}(f) = 0.25 P \delta(\Delta f)$$

where

$$\text{bandwidth} = f_B$$

$$\Delta f_M = \frac{f_B}{\pi}$$

P = peak transmitter power

$$\Delta f = f - f_c$$

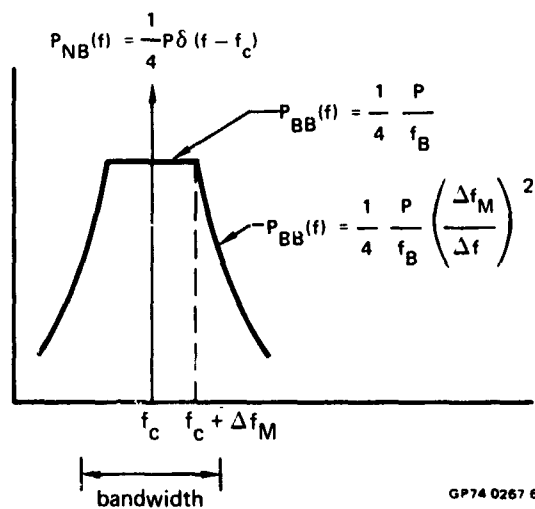


FIGURE 70 PCM-NRZ

$$\text{PCM/AM-Biphase} \quad P_{BB}(f) = \frac{4m^2P}{\pi^2 f_B} \quad ; 0 < |\Delta f| \leq \Delta f_M$$

$$P_{BB}(f) = \frac{4m^2P}{\pi^2 f_B} \left(\frac{\Delta f_M}{\Delta f} \right)^2 \quad ; |\Delta f| > \Delta f_M$$

$$P_{NB}(f) = P \delta(\Delta f)$$

$$\text{where } \Delta f_M = f_B$$

$$\text{bandwidth} = \frac{\tau^2}{16} f_B$$

$$\Delta f = f - f_c$$

$$P = \text{carrier power}$$

$$f_B = \text{bit rate}$$

$$m = \text{modulation index}$$

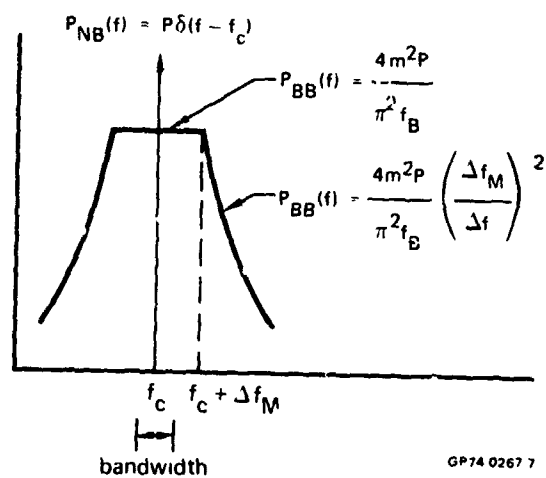


FIGURE 71 PCM/AM-BIPHASE

PPM/AM

$$P_{BB}(f) = P_T^2 f_B \quad ; 0 < |\Delta f| \leq \Delta f_M$$

$$P_{BB}(f) = P_T^2 f_B \left(\frac{\Delta f_M}{\Delta f} \right)^2 \quad ; |\Delta f| > \Delta f_M$$

$$\text{bandwidth} = \frac{1}{\tau}$$

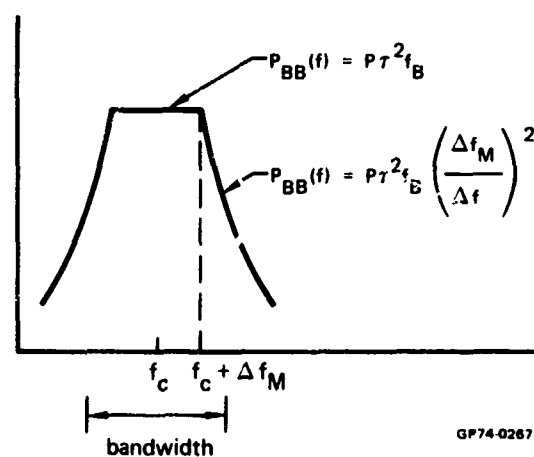
τ = pulse width

P = peak transmitter power

f_B = bit rate

$\Delta f = f - f_c$

$$\Delta f_M = \frac{1}{\pi \tau}$$



GP74-0267-B

FIGURE 72 PPM/AM

MORSE

$$P_{BB}(f) = G_0 \quad ; 0 < [|\Delta f| - f_{\text{tone}}] \leq \Delta f_1$$

$$P_{BB}(f) = G_0 (\Delta f_1)^2 / [|\Delta f| - f_{\text{tone}}]^2 \quad ; \Delta f_1 < [|\Delta f| - f_{\text{tone}}] \leq \Delta f_2$$

$$P_{BB}(f) = G_0 \times 10^{-6} (\Delta f_2)^4 / [|\Delta f| - f_{\text{tone}}]^4 \quad ; [|\Delta f| - f_{\text{tone}}] > \Delta f_2$$

for $f_{\text{tone}} = 0$

$$G_0 = \frac{P\delta}{4}$$

$$BW = \delta$$

$$P_{NB}(f) = \frac{P}{4} \delta (\Delta f)$$

$$\text{where } \delta = \frac{0.8}{\text{WPM}}$$

$$\Delta f = f - f_c$$

$$\Delta f_1 = \frac{1}{\pi\delta}$$

$$\Delta f_2 = 1000 \frac{1}{\pi\delta}$$

P = carrier power

for $f_{\text{tone}} \neq 0$

$$G_0 = \frac{P\delta}{16}$$

$$BW = 2\delta$$

$$P_{NB}(f) = \frac{P}{16} \delta (f - f_c - f_{\text{tone}}) + \frac{P}{16} \delta (f - f_c + f_{\text{tone}})$$

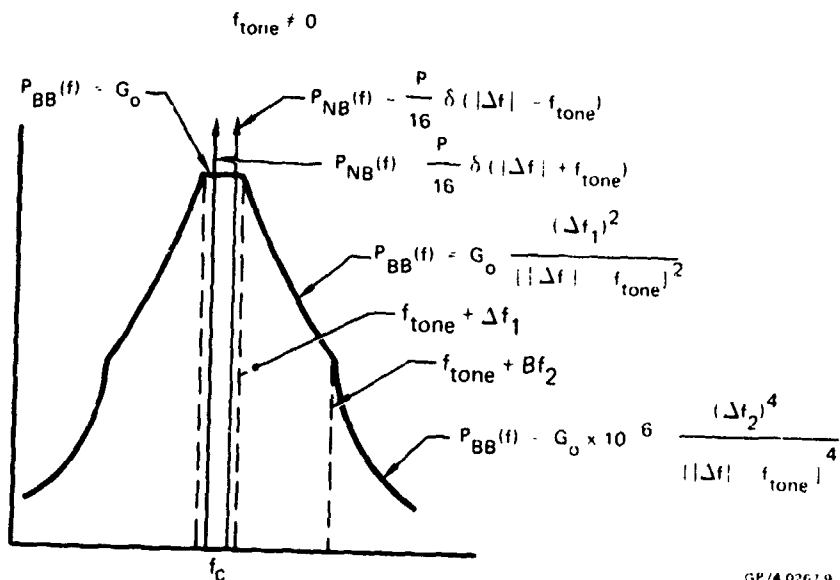
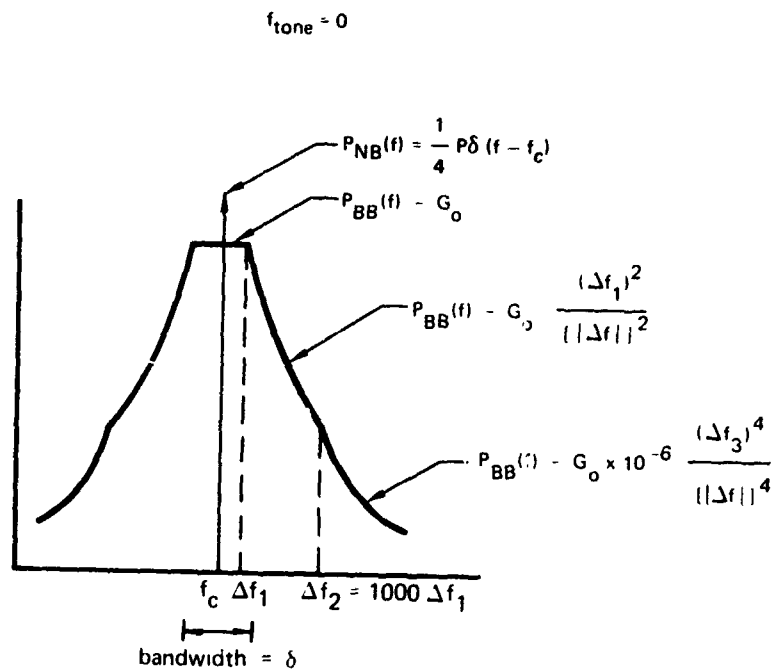


FIGURE 73 MORSE

GP/4 02619

FSK

$$P_{BB}(f) = P_o \quad ; |X| \leq X_M$$

$$P_{BB}(f) = \frac{4P}{\pi^2 f_B} \left(\frac{D}{D^2 - X^2} \right)^2 \quad ; |X| > X_M$$

$$\text{bandwidths} = f_{DEV} + f_B$$

$$\text{where } D = f_{DEV}/f_B$$

$$X = 2 \frac{\Delta f}{f_B}$$

$$\text{For } D < \frac{4}{\pi^2}$$

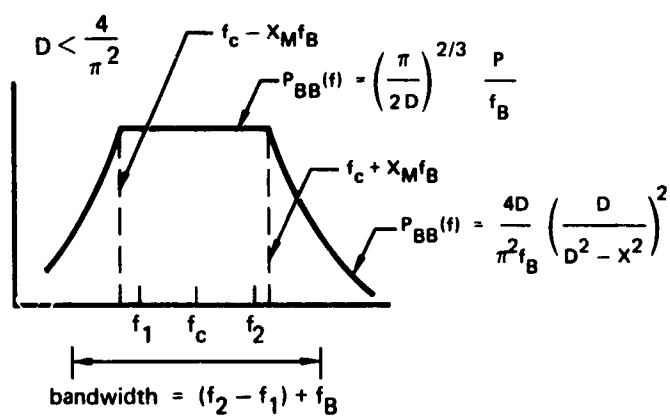
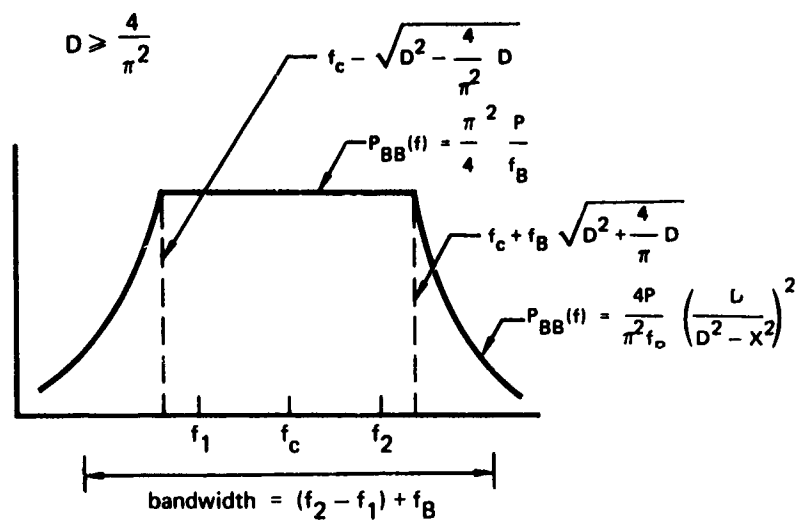
$$P_o = \left(\frac{\pi}{2D} \right)^{2/3} \frac{P}{f_B}$$

$$X_M = \sqrt{D^2 + \left(\frac{2D}{\pi} \right)^{2/3}}$$

$$\text{For } D \geq \frac{4}{\pi^2}$$

$$P_o = \frac{\pi^2}{4} \frac{P}{f_B}$$

$$X_M = \sqrt{D^2 + \frac{4}{\pi^2} D}$$



GP74-0267 10

FIGURE 74 FSK

PAM/FM

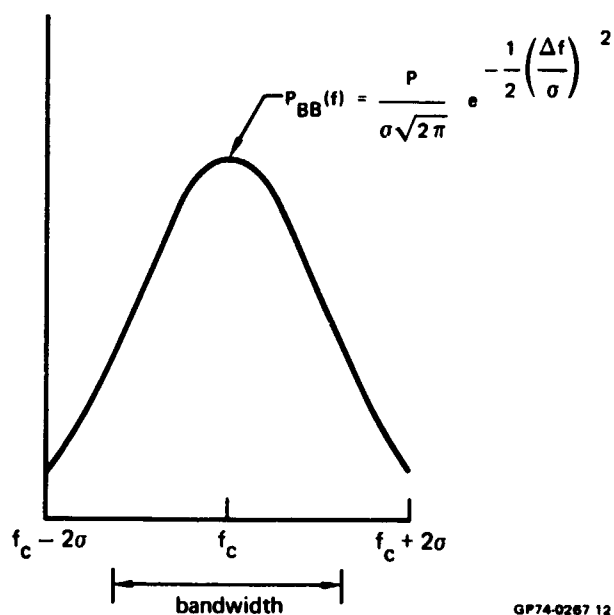
$$P_{BB}(f) = \frac{P}{\sigma\sqrt{2\pi}} \exp -\frac{1}{2} \left(\frac{\Delta f}{\sigma} \right)^2$$

$$\text{where } \sigma = \frac{f_{DEV}}{3}$$

$$\Delta f = f - f_c$$

P = transmitter power

$$\text{bandwidth} = \sigma\sqrt{2\pi}$$



GP74-0267 12

FIGURE 75 PAM/FM

RADAR

1) Rectangular Pulse

$$P_{BB}(f) = P_T^2 f_B \quad ; |\Delta f| \leq \Delta f_M$$

$$P_{BB}(f) = P_T^2 f_B \left(\frac{\Delta f_M}{\Delta f} \right)^2 \quad ; \Delta f_M < |\Delta f| \leq \Delta f$$

where

τ = pulse duration

f_B = bit rate

$$\text{bandwidth} = \frac{1}{\tau}$$

$$\Delta f_M = \frac{1}{\pi \tau}$$

$$\Delta f = f - f_c$$

P = peak power

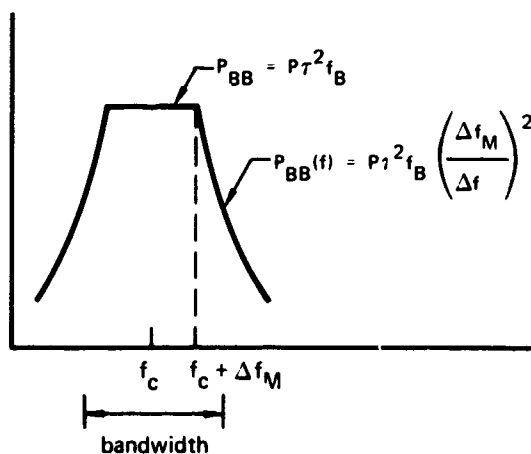


FIGURE 76 RADAR RECT

2) Trapezoidal Pulse

$$P_{BB}(f) = P\tau^2 f_B \quad ; |\Delta f| \leq \Delta f_1$$

$$P_{BB}(f) = P\tau^2 f_B \left(\frac{\Delta f_1}{\Delta f} \right)^2 \quad ; \Delta f_1 < |\Delta f| \leq \Delta f_2$$

$$P_{BB}(f) = P\tau^2 f_B \left(\frac{\Delta f_1}{\Delta f} \right)^2 \left(\frac{\Delta f_2}{\Delta f} \right)^2 \quad ; |\Delta f| > \Delta f_2$$

where

P = peak power

τ = pulse duration (between dB levels)

f_B = bit rate

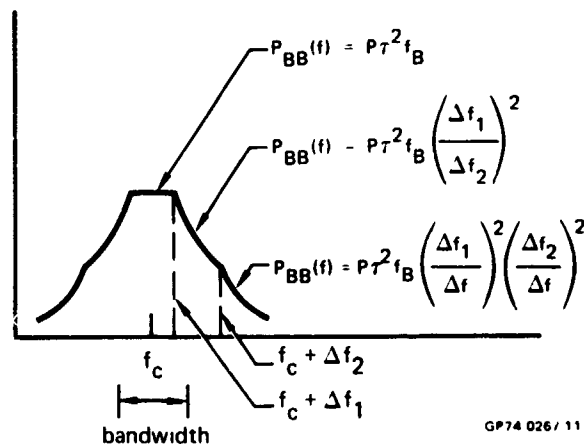
$$\text{bandwidth} = \frac{1}{\tau}$$

$$\Delta f_1 = \frac{1}{\pi \tau}$$

$$\Delta f_2 = \frac{1}{2\pi} \left(\frac{1}{\tau_r} + \frac{1}{\tau_f} \right)$$

τ_r = rise time

τ_f = fall time



GP74 026 / 11

FIGURE 77 RADAR TRAP

3) Cosine - squared

$$P_{BB}(f) = P\tau^2 f_B \quad ; |\Delta f| \leq \Delta f_M$$

$$P_{BB}(f) = P\tau^2 f_B \left(\frac{\Delta f_M}{\Delta f} \right)^6 \quad ; |\Delta f| > \Delta f_M$$

where

f_B = bit rate

$$\text{bandwidth} = \frac{1}{\tau}$$

τ = pulse width (between 6 dB levels)

P = peak power

$$\Delta f_M = \frac{1}{(8\pi)^{1/3} \tau}$$

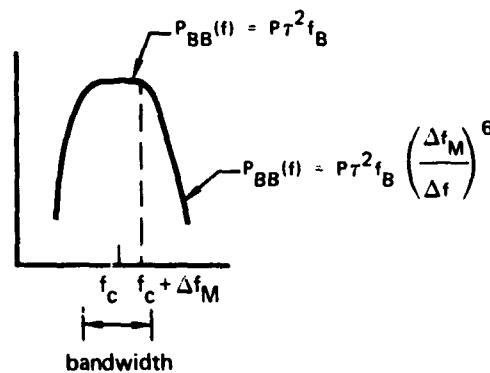


FIGURE 78 RADAR COSINE - SQUARED

4) Gaussian

$$P_{BB}(f) = 2\pi P T^2 f_B e^{-(2\pi T \Delta f)^2}$$

where

P = peak power

τ = pulse width (between half amplitude points)

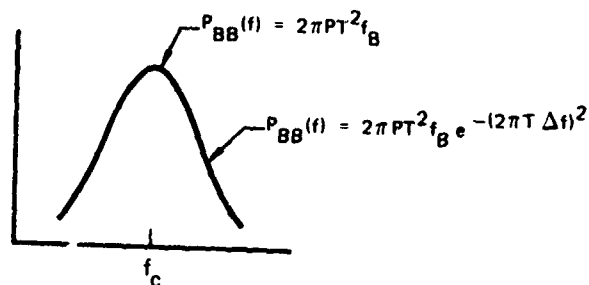
f_B = pulse repetition rate

f_c = carrier frequency

$\Delta f = f - f_c$

$$T = \frac{\tau}{2.3548}$$

$$\text{bandwidth} = \frac{1}{2\sqrt{\pi} T}$$



GP74 0267 13

FIGURE 79 RADAR GAUSSIAN

5) Linear Pulse Compression

$$P_{dB}(f) = P_0 \quad 0 \leq |\Delta f| \leq \Delta f_{aa}$$

$$P_{dB}(f) = P_0 - M \log \left| \frac{\Delta f}{\Delta f_{aa}} \right| \quad \Delta f_{aa} < |\Delta f| \leq \Delta f_b$$

$$\text{if } \Delta f_2 \geq \Delta f_b$$

$$P_{dB}(f) = P_0 - 20 \log \left| \frac{\Delta f}{\Delta f_1} \right| \quad \Delta f_b < |\Delta f| \leq \Delta f_2$$

$$P_{dB}(f) = P_0 - 20 \log \left| \frac{\Delta f_2}{\Delta f_1} \right| - 40 \log \left| \frac{\Delta f}{\Delta f_2} \right| \quad |\Delta f| > \Delta f_2$$

$$\text{if } \Delta f_2 < \Delta f_b$$

$$P_{dB}(f) = P_0 - 20 \log \left| \frac{\Delta f_2}{\Delta f_1} \right| - 40 \log \left| \frac{\Delta f}{\Delta f_2} \right| \quad |\Delta f| > \Delta f_b$$

where

$$P_0 = 10 \log \left[P \left(\tau + \frac{\tau_r}{2} + \frac{\tau_f}{2} \right)^2 f_B / D \right]$$

$$f_c = \text{carrier frequency}$$

$$f_0 = \text{function of } f_c, \tau, \tau_r, \tau_f, D$$

$$\Delta f = f - f_0$$

$$\Delta f_{aa}, \Delta f_b = \text{functions of } \tau, \tau_r, \tau_f, D, \text{sgn}(f - f_0)$$

$$P = \text{RF power}$$

$$\tau = \text{pulse width}$$

$$\tau_r = \text{rise time}$$

$$\tau_f = \text{fall time}$$

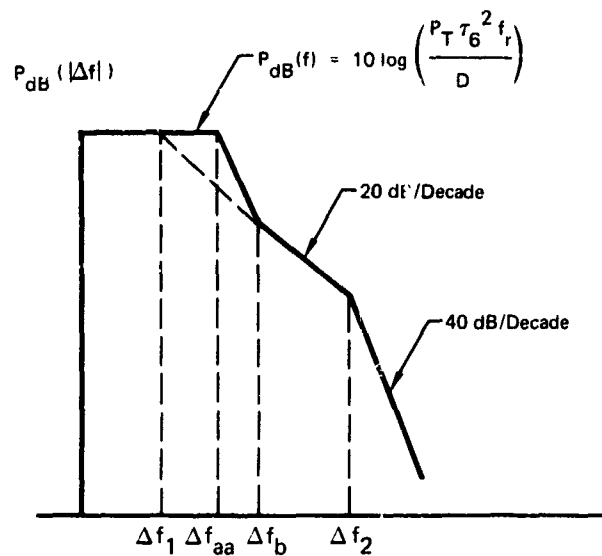
$$D = \text{pulse compression ratio (negative if frequency decreases during pulse)}$$

$$f_B = \text{bit rate}$$

$$\Delta f_1 = \frac{\sqrt{|D|}}{\pi \left(\tau + \frac{\tau_r}{2} + \frac{\tau_f}{2} \right)}$$

$$\Delta f_2 = \frac{1}{2\pi} \left(\frac{1}{\tau_r} + \frac{1}{\tau_f} \right)$$

$$P_{dB}(f) = 10 \log (P_{BB}(f))$$



GP74 0267 14

FIGURE 80 CHIRP

AM - DSB

$$P_{BB}(f) = \frac{m^2}{2} P g_i(|\Delta f|); i = 1, 2, 3$$

$$P_{NB}(f) = P \delta(\Delta f)$$

where P = carrier power

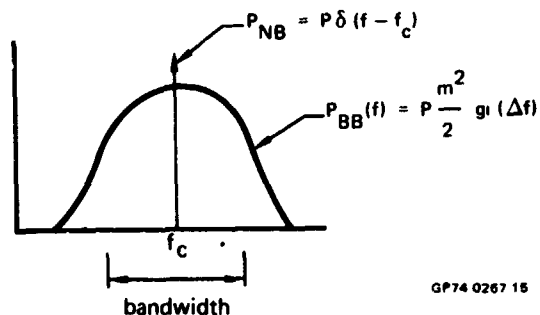
bandwidth = $2B$

m = modulation index

$$\Delta f = f - f_c$$

B = modulating signal bandwidth

$i = 1$ (voice), 2 (clipped voice), 3 (non-voice)



GP74 0267 15

FIGURE 81 AM-DSB

AM-DSB/SC

$$P_{BB}(f) = \frac{P}{2} g_i(|\Delta f|); i = 1, 2, 3$$

bandwidth = $2B$

where P = peak envelope power

$$\Delta f = f - f_c$$

B = modulating signal bandwidth

$i = 1$ (voice), 2 (clipped voice), 3 (non-voice)

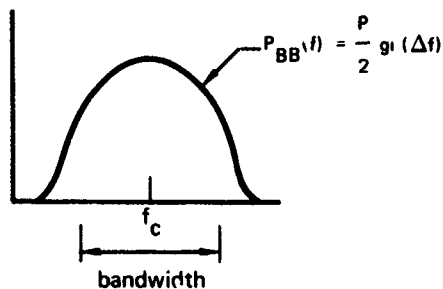


FIGURE 82 AM-DSB/SC

SSB-Lower

$$P_{BB}(f) = P g_i(-\Delta f); i = 1, 2, 3$$

bandwidth = B

P = peak envelope power

$$\Delta f = f - f_c$$

B = modulating signal bandwidth

i = 1 (voice), 2 (clipped voice), 3 (non-voice)

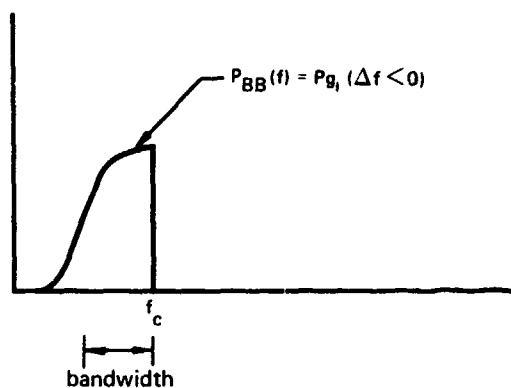


FIGURE 83 SSB - LOWER

SSB-Upper

$$P_{BB}(f) = P g_i(\Delta f), i = 1, 2, 3$$

where

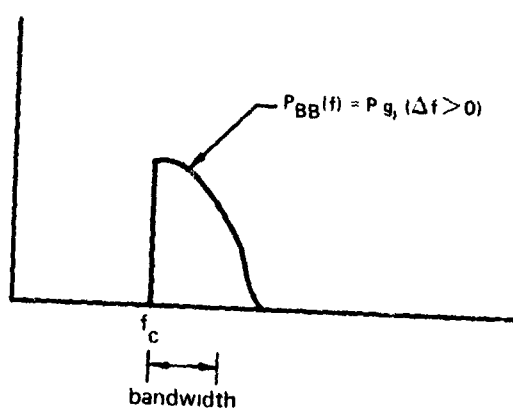
bandwidth = B

P = peak envelope power

$$\Delta f = f - f_c$$

B = modulation signal bandwidth

$i = 1$ (voice), 2 (clipped voice), 3 (non-voice)



GP74 0267 16

FIGURE 84 SSB - UPPER

FM

$$P_{BB}(f) = \frac{P}{2.062 B_{FM}} \quad ; |\Delta f| \leq B_{FM}$$

$$P_{BB}(f) = \frac{P}{2.062 B_{FM}} \left(\frac{B_{FM}}{f} \right)^{33.219} \quad ; B_{FM} < |\Delta f| \leq 2 B_{FM}$$

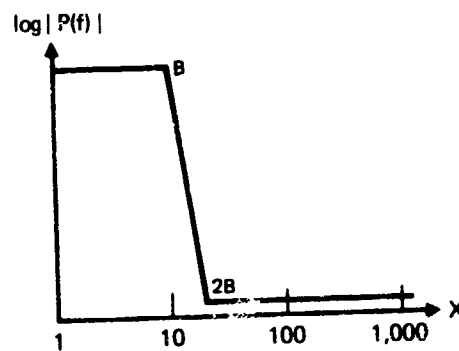
$$P_{BB}(f) = \frac{P}{2.062 B_{FM}} \times 10^{-10} \quad ; |\Delta f| > 2 B_{FM}$$

where $B_{FM} = f_{DEV} + B$

f_{DEV} = peak frequency deviation

B = bandwidth of modulation process

P = transmitter power



GP74-0287 17

FIGURE 85 FM

$g_1(x)$

1) Voice

$$g_1(x) = 0 \quad ; x < 0$$

$$g_1(x) = \frac{1}{712} (0.0008485) \quad ; 0 < x \leq 8$$

$$g_1(x) = \frac{1}{712} \left(\frac{x}{100} \right)^{2.8} \quad ; 8 < x \leq 100$$

$$g_1(x) = \frac{1}{712} \left(\frac{100}{x} \right)^{0.7} \quad ; 100 < x \leq 4000$$

$$g_1(x) = \frac{1}{712} \left(\frac{4000}{x} \right)^6 \quad ; x > 4000$$

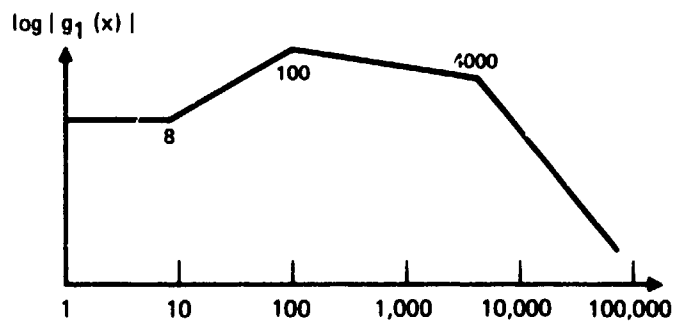


FIGURE 86 VOICE

$g_2(x)$

2) Clipped Voice

$$g_2(x) = 0 \quad ; x < 0$$

$$g_2(x) = \frac{1}{622} (0.0023) \quad ; 0 \leq x \leq 8$$

$$g_2(x) = \frac{1}{622} \left(\frac{x}{70} \right)^{2.8} \quad , 8 < x \leq 70$$

$$g_2(x) = \frac{1}{622} \quad ; 70 < x \leq 350$$

$$g_2(x) = \frac{1}{622} \left(\frac{350}{x} \right)^2 \quad , 350 < x \leq 3500$$

$$g_2(x) = \frac{1}{62200} \left(\frac{3500}{x} \right)^6 \quad ; x > 3500$$

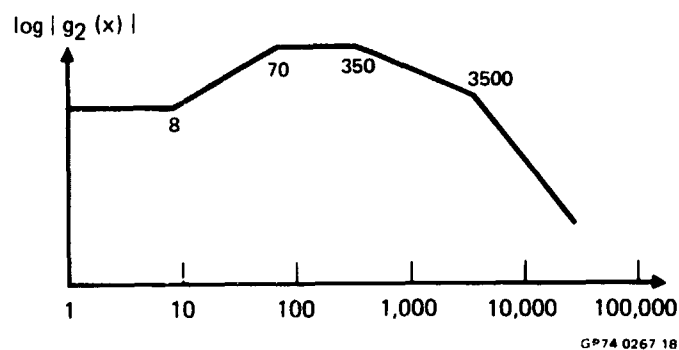


FIGURE 87

CLIPPED
VOICE

$g_3(x)$

3) Nonvoice

$$g_3(x) = 0 \quad ; x < 0$$

$$g_3(x) = \frac{1}{B} \quad ; 0 \leq x \leq B$$

$$g_3(x) = \frac{1}{B} \left(\frac{B}{x} \right)^{13.28} \quad , B < x \leq 2B$$

$$g_3(x) = 0.0001 \frac{1}{B} \left(\frac{2B}{x} \right)^{5.8} \quad , 2B < x \leq 40B$$

$$g_3(x) = 0 \quad ; x > 40B$$

where B = modulating signal bandwidth
 x = frequency relative to carrier

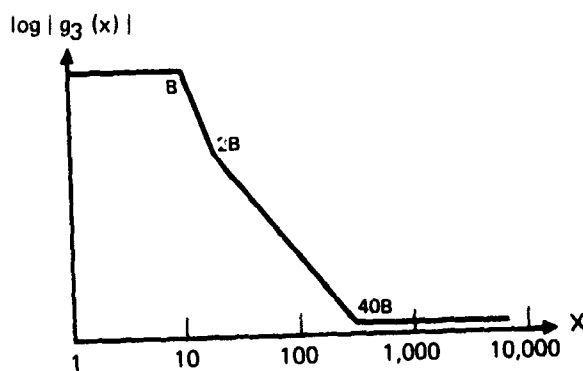


FIGURE 88 NON-VOICE

6.4.1.2 Signal/Control Modulations -

PDM $P_{BB}(f) = \frac{1}{3} \frac{A^2}{f_B} ; 0 < f \leq f_M$

$$P_{BB}(f) = \frac{1}{3} \frac{A^2}{f_B} \left(\frac{f_M}{f} \right)^2 ; f > f_M$$

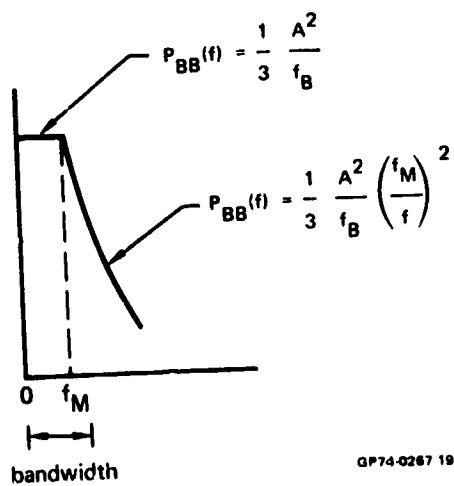
where

A = peak voltage/current into 1 ohm

f_B = bit rate

$$f_M = \frac{\sqrt{3}}{\pi} f_B$$

bandwidth = f_B



GP74-0287 19

FIGURE 89 PDM

PCM-NRZ

$$P_{BB}(f) = \frac{1}{2} \frac{A^2}{f_B} \quad ; 0 < f \leq f_M$$

$$P_{BB}(f) = \frac{1}{2} \frac{A^2}{f_B} \left(\frac{f_M}{f} \right)^2 \quad ; f > f_M$$

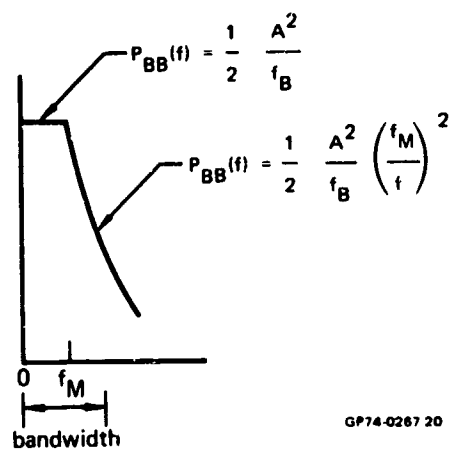
where

$$\text{bandwidth} = \frac{1}{2} f_B$$

$$f_M = \frac{f_B}{\pi}$$

A = peak voltage/current into 1 ohm

f_B = bit rate



GP74-0267 20

FIGURE 90 PCM-NRZ

PCM-Biphase

$$P_{BB}(f) = \frac{8m^2 A^2}{\pi^2 f_B} \quad ; 0 < f \leq f_M$$

$$P_{BB}(f) = \frac{8m^2 A^2}{\pi^2 f_B} \left(\frac{f_M}{f} \right)^2 \quad ; f > f_M$$

where

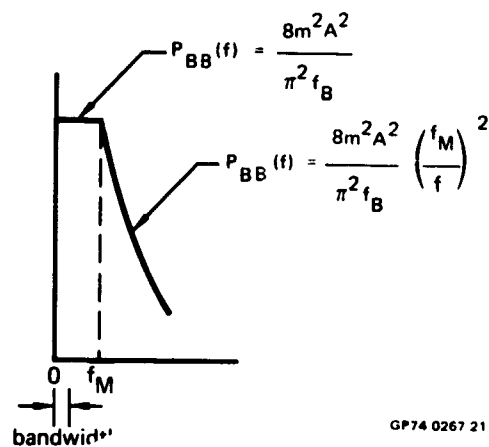
$$\text{bandwidth} = \frac{\pi^2}{32} f_B$$

$$f_M = f_B$$

m = modulation index

A = peak voltage/current into 1 ohm

f_B = bit rate



GP74 0267 21

FIGURE 91 PCM/AM - BIPHASE

PPM

$$P_{BB}(f) = 2A^2\tau^2f_B \quad ; 0 < f \leq f_M$$

$$P_{BB}(f) = 2A^2\tau^2f_B \left(\frac{f_M}{f} \right)^2 \quad ; f > f_M$$

where

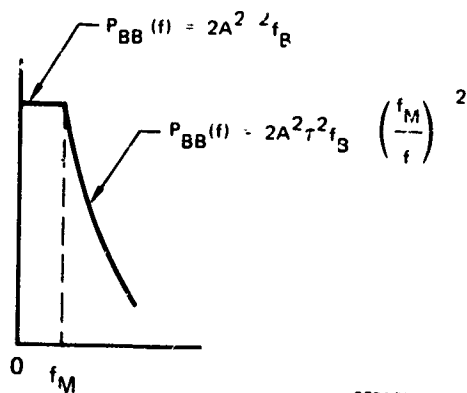
A = peak voltage/current into 1 ohm

τ = pulse duration

f_B = bit rate

$$f_M = \frac{1}{\pi \tau}$$

$$\text{bandwidth} = \frac{1}{2\tau}$$



GP74 0267 22

FIGURE 92 PPM

Morse

$$P_{BB}(f) = G_o \quad ; |\Delta f| \leq \Delta f_{M1}$$

$$P_{BB}(f) = G_o \left(\frac{\Delta f_{M1}}{\Delta f} \right)^2 \quad ; \Delta f_{M1} < |\Delta f| \leq \Delta f_{M2}$$

$$P_{BB}(f) = 10^{-6} \times G_o \left(\frac{\Delta f_{M2}}{\Delta f} \right)^4 \quad ; |\Delta f| > \Delta f_{M2}$$

where $\delta = 0.8/\text{WPM}$

A = peak voltage/current into 1 ohm

$$\Delta f = f - f_{\text{tone}}$$

$$\Delta f_{M1} = \frac{1}{\pi \delta}$$

$$\Delta f_{M2} = 1000 \times \Delta f_{M1}$$

$$f_{\text{tone}} = 0$$

$$G_o = \frac{A^2 \delta}{2}$$

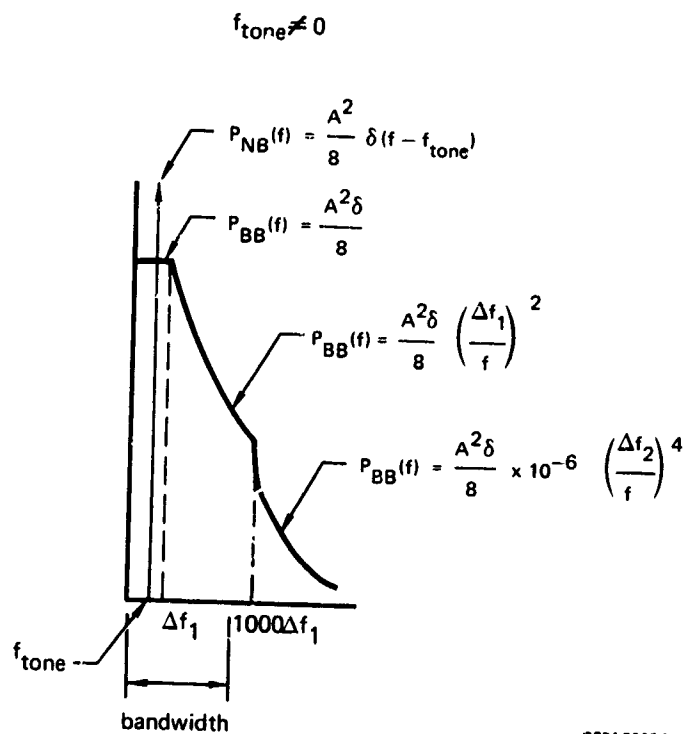
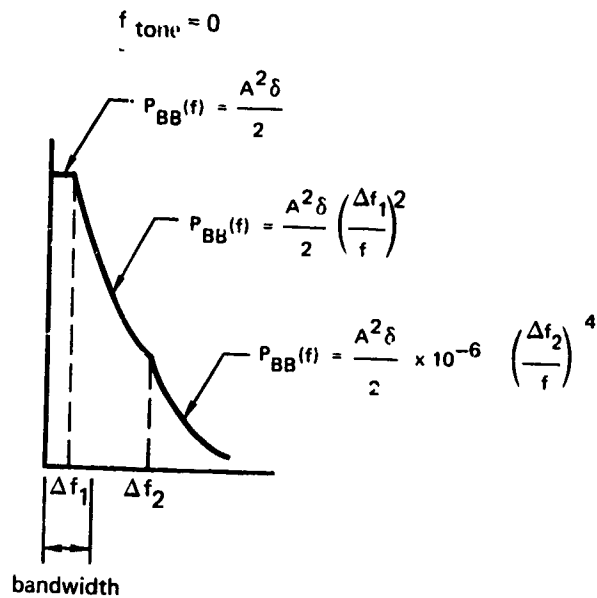
$$\text{bandwidth} = \frac{1}{2\delta}$$

$$f_{\text{tone}} \neq 0$$

$$G_o = \frac{A^2 \delta}{8}$$

$$\text{bandwidth} = \frac{1}{\delta}$$

$$G_{NB} = \frac{A^2}{8} \delta (f - f_{\text{tone}})$$



GP74 0267 23

FIGURE 93 MORSE

PAM

$$P_{BB}(f) = 2A^2\tau^2f_B \quad ; 0 < f \leq f_M$$

$$P_{BB}(f) = 2A^2\tau^2f_B \left(\frac{f_M}{f} \right)^2 \quad ; f > f_M$$

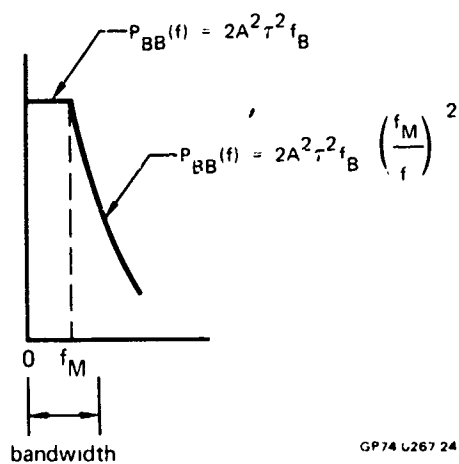
$$\text{where } f_M = \frac{1}{\pi \tau}$$

$$\text{bandwidth} = \frac{1}{2\tau}$$

τ = pulse width

f_B = bit rate

A = peak voltage/current into 1 ohm



GP74 L267 24

FIGURE 94 PAM

ESPIKE

$$P_{BB}(f) = \frac{2A^2 f_B}{[(2\pi f)^2 + (1/\tau)^2]}$$

where

A = peak voltage/current into 1 ohm

f_B = bit rate

$$\text{bandwidth} = \frac{1}{4\tau}$$

τ = decay time constant

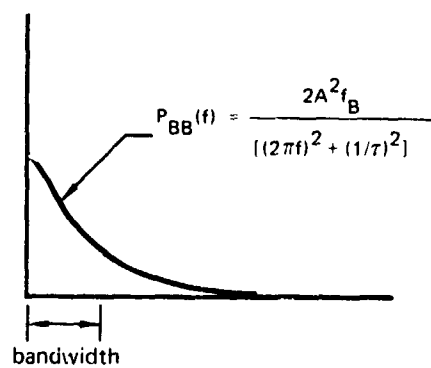


FIGURE 95 ESPIKE

Rectangular Pulse $P_{BB}(f) = 2A^2\tau^2f_B$; $0 < f \leq f_M$

$P_{BB}(f) = 2A^2\tau^2f_B \left(\frac{f_M}{f}\right)^2$; $f > f_M$

where

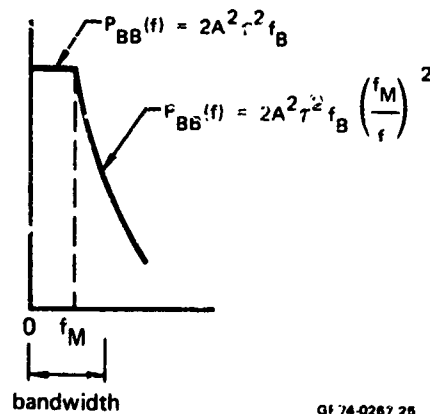
bandwidth $= \frac{1}{2\tau}$

f_B = bit rate

A = peak current/voltage into 1 ohm

$f_M = \frac{1}{\pi\tau}$

τ = pulse width



Q174-0267 25

FIGURE 96 RECTANGULAR

Trapezoidal Pulse $P_{BB}(f) = 2A^2\tau^2f_B$; $0 < f \leq f_{M1}$

$$P_{BB}(f) = 2A^2\tau^2f_B \left(\frac{f_{M1}}{f} \right)^2 ; f_{M1} < f \leq f_{M2}$$

$$P_{BB}(f) = 2A^2\tau^2f_B \left(\frac{f_{M1}}{f_{M2}} \right)^2 \left(\frac{f_{M2}}{f} \right)^4 ; f > f_{M2}$$

where

$$f_{M1} = \frac{1}{\pi\tau}$$

$$f_{M2} = \frac{1}{\pi\tau_r}$$

τ = pulse duration

τ_r = rise time

$$\text{bandwidth} = \frac{1}{2\tau}$$

A = peak current/voltage

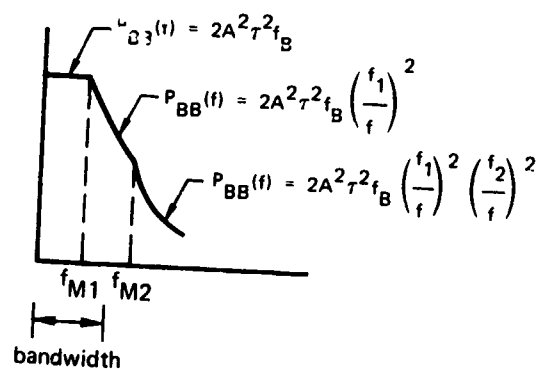


FIGURE 97 TRAPEZOIDAL

Triangular Pulses $P_{BB}(f) = 2A^2\tau^2f_B$; $0 < f \leq f_M$

$$P_{BB}(f) = 2A^2\tau^2f_B \left(\frac{f_M}{f}\right)^4 ; f > f_M$$

where

$$\text{bandwidth} = \frac{1}{2\tau}$$

$$f_M = \frac{1}{\pi\tau}$$

A = peak current/voltage into 1 ohm

$$f_M = \frac{1}{\pi\tau}$$

f_B = bit rate

τ = pulse duration

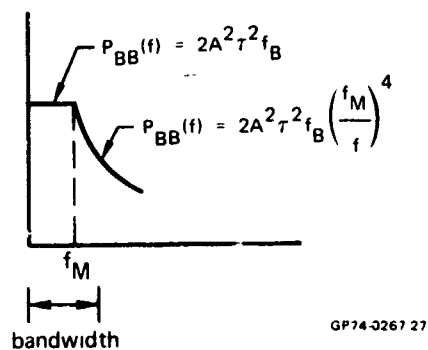


FIGURE 98 TRIANGULAR

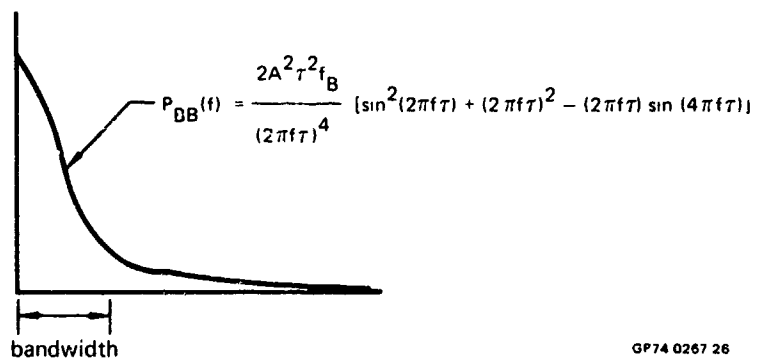
Sawtooth

$$P_{BB}(f) = \frac{2A^2\tau^2f_B}{x^4} [\sin^2 x + x^2 - x \sin 2x]$$

$$BW = \frac{1}{2\tau}$$

where $x = 2\pi f\tau$

τ = pulse width at half amplitude



GP74 0267 26

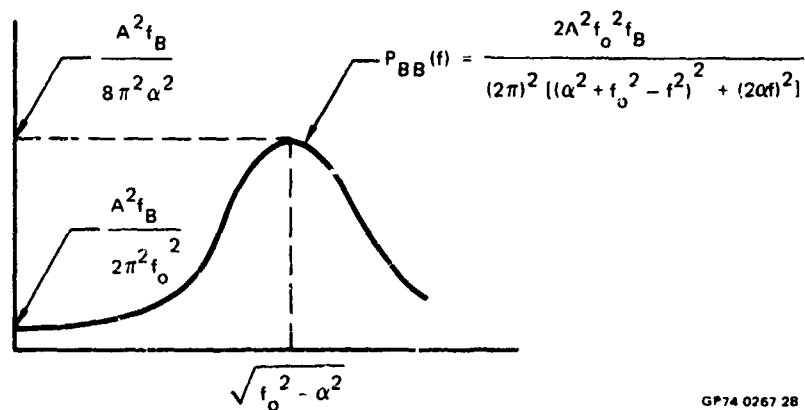
FIGURE 99 SAWTOOTH

Damped Sinusoid
$$P_{BB}(f) = \frac{2A^2 f_o^2 f_B}{(2\pi)^2 [\alpha^2 + f_o^2 - f^2]^2 + (2\alpha f)^2}$$

$$BW = 2\pi^2 \alpha$$

f_o = carrier frequency

α = inverse of decay time required to reach A/e



GP74 0267 28

FIGURE 100 DAMPED SINUSOID

6.4.1.3 Non-Required Emission and Susceptibility

This section gives the initial unrequired spectra based on MIL-STD-461A, MIL-STD-6181D and MIL-STD-704. Unless otherwise noted, the units for the spectrum levels are in dB microamps or dB microamps/MHz.

o MIL-STD-461A for RF Ports

Susceptibility:

$$G_{NB}(f) = 120. - ZDB \text{ (dB}\mu\text{A)}$$

where $ZDB = 10 \log [\text{impedance}]$

This is equivalent to one watt at the receptor terminals.

Emission:

o Local Oscillator

$$G_{NB}(f) = RLON \text{ (user supplied narrowband emission)}$$

$$G_{BB}(f) = RLOB \text{ (user supplied broadband emission)}$$

o Final Stage

$$PDBW = 10 \text{ LOG}_{10}(P) \quad P = \text{power}$$

$$\text{if } PDBW < 20 \quad G_{NB}(f) = 68.666 - 0.4333 \times PDBW - ZDB$$

$$\text{if } PDBW > 40 \quad G_{NB}(f) = 42.666 + 0.4333 \times PDBW - ZDB$$

$$\text{if } 20 \leq PDBW \leq 40 \quad G_{NB}(f) = 60. - ZDB$$

o MIL-STD-461A for Equipment Case

For an equipment case only, specification limits are in units of $G_{BB}(f)$ = dB (microvolts/meter/MHz) and $G_{NB}(f)$ = dB (microvolts/meter).

Susceptibility:

(log linear interpolate from the following table)

<u>f (Hz)</u>	<u>$G_{NB}(f)$ (dBμV/m)</u>
14×10^3	140
35×10^6	140
35.001×10^6	134
9.999×10^9	134
1×10^{10}	146
2×10^{10}	146

Emission:

(log linear interpolate from the following tables)

<u>f (Hz)</u>	<u>$G_{NB}(f)$ (dBμV/m)</u>
14×10^3	35
25×10^6	20
1×10^{10}	60

<u>f (Hz)</u>	<u>$G_{BB}(f)$ (dBμV/m/MHz)</u>
14×10^6	100
2×10^8	55
1×10^9	70

MIL-STD-461A For Power, Signal or Control Ports

Susceptibility:

- o Signal/Control

$$G_{NB}(f) = 120. - ZDB$$

- o Power

$$VSP = \text{RMS Voltage} \times 1.414$$

$$G_{NB}(f) = 8.686 \times \log_e [\text{MIN} (.1 \times VSP, 3)] + 120 - 2 \times ZDB$$

$$30 \leq f \leq 1250 \text{ Hz}$$

$$G_{NB}(f) = 8.686 \times \log_e [\text{MAX} (.01 \times VSP, 1)] + 120 - 2 \times ZDB$$

$$50,000 \leq f \leq 4 \times 10^6 \text{ Hz}$$

Levels between 1250 Hz and 50,000 Hz are linearly interpolated

Emission:

(log linear interpolate from the following tables)

<u>f (Hz)</u>	<u>G_{NB}(f) (dBμA)</u>
30	130
2000	130
2×10^4	80
2×10^6	20
5×10^7	20

<u>f (Hz)</u>	<u>G(f) (dBμA/MHz)</u>
10	132
2×10^4	132
2×10^6	50
5×10^7	50

MIL-STD-6181D For RF Ports

Emission:

(a) Final Stage

$$G_{NB}(f) = 40 - ZDB \text{ (dBμA)}$$

$$G_{BB}(f) = 60 - ZDB \text{ (dBμA/MHz)} - \text{only below the required frequency range}$$

(b) Local Oscillator

$$G_{NB}(f) = RLON \text{ (user supplied narrowband emission)}$$

$$G_{BB}(f) = RLOB \text{ (user supplied broadband emission)}$$

Susceptibility:

$$G_{NB}(f) = \text{Sensitivity (in dB watts)} + 200 - ZDB \text{ (dBμA)}$$

MIL-STD-6181D For Power, Signal or Control Ports

Emission:

(a) Power Line

(log linear interpolate from the following tables)

<u>f (Hz)</u>	<u>G_{NB}(f) (dBμA)</u>
1.5 x 10 ⁵	62.5
5 x 10 ⁶	34.0
25 x 10 ⁶	34.0

<u>f (Hz)</u>	<u>G_{BB}(f) (dBμA/MHz)</u>
1.5 x 10 ⁵	115
2 x 10 ⁶	81
25 x 10 ⁶	81

(b) Signal/Control Ports

(log linear interpolate from the following tables)

<u>f (Hz)</u>	<u>G_{NB}(f) (dBμA)</u>
1.5 x 10 ⁵	50
2 x 10 ⁶	5
25 x 10 ⁶	0

<u>f (Hz)</u>	<u>G_{BB}(f) (dBμA/MHz)</u>
1.5 x 10 ⁵	105
2 x 10 ⁶	50
25 x 10 ⁶	46

Susceptibility:

$$G_{NB}(f) = 132.55 - 2 \times \text{ZDB (dB}\mu\text{A)}; f < 15,000 \text{ Hz}$$

$$G_{NB}(f) = 100 - 2 \times \text{ZDB (dB}\mu\text{A)}; f > 150,000 \text{ Hz}$$

MIL-STD-6181D For Equipment Cases

Emission:

(log linear interpolate from the following tables)

<u>f (Hz)</u>	<u>G_{NB}(f) (dBμV/meter)</u>
150,000	29.
3 x 10 ⁶	29.
25 x 10 ⁶	22.
25.001 x 10 ⁶	4.
35 x 10 ⁶	10.
1 x 10 ⁹	60.

<u>f (Hz)</u>	<u>G_{BB}(f) (dBμV/meter/MHz)</u>
150,000	83.
500,000	76.
25 x 10 ⁶	73.
25.001 x 10 ⁶	36.
35 x 10 ⁶	41.
1 x 10 ⁹	80.

Susceptibility:

(log linear interpolate from the following table)

<u>f (Hz)</u>	<u>G_{NB}(f) (dBμV/meter)</u>
150,000	88.
25 x 10 ⁶	88.
25.001 x 10 ⁶	104.
35 x 10 ⁶	110.
1 x 10 ⁹	110.5
10 x 10 ⁹	111.5

MIL-STD-704 For Power Line Emission

$$G_{NB}(f) = 20 \log V + 120 \text{ (Fundamental)}$$

$$G_{NB}(f) = 20 \log V + 96 \text{ (Second, Third and Fourth Harmonic)}$$

where V = RMS Voltage

6.4.2 TRANSFER MODEL EQUATIONS

6.4.2.1 FILTER MODELS

Single Tuned Filter

$$T(f) = \left(\frac{1}{1 + x^2} \right)$$

$$\text{where } x = \frac{f_0}{\beta} \left(\frac{f}{f_0} - \frac{f_0}{f} \right)$$

f_0 = tuned frequency in Hz

f = frequency in Hz

β = filter bandwidth in Hz

Transformer Coupled

$$T(f) = \left(\frac{K/4Q}{\sqrt{(\delta^2 - 1/4Q^2 - K^2/4)^2 + (\delta/Q)^2}} \right)^n ; |\delta| < 4$$

$$T(f) = \left(\frac{K/Q}{\delta^3} \right)^n ; |\delta| \geq 4$$

$$\text{where } \delta = \frac{f - f_o}{f_o}$$

f_o = tuned frequency in Hz

f = frequency in Hz

Q = circuit "Q"

K = coupling coefficient $0 < K \leq 1$

n = number of stages

Butterworth Tuned Filter

$$T(f) = \frac{1}{1 + x^{2n}}$$

$$\text{where } x = \frac{f_o}{\beta} \left(\frac{f}{f_o} - \frac{f_o}{f} \right)$$

f_o = tuned frequency in Hz

f = frequency in Hz

β = filter bandwidth in Hz

n = order of filter

Low-Pass

$$T(f) = 1; \quad f \leq f_o$$

$$= (f_o/f)^{2n}; \quad f > f_o$$

where f_o = high frequency limit in Hz

f = frequency in Hz

n = order of filter

High Pass

$$T(f) = (f/f_o)^{2n}; \quad f < f_o$$

$$= 1; \quad f \geq f_o$$

where f_o = low frequency limit

f = frequency in Hz

n = order of filter

Band Pass

$$T(f) = (f/f_{low})^{2n}; \quad f < f_{low}$$

$$= 1 \quad ; \quad f_{low} \leq f \leq f_{high}$$

$$= (f_{high}/f)^{2n}; \quad f > f_{high}$$

where f_{low} , f_{high} = pass band limits in Hz

f = tuned frequency in Hz

n = order of filter

Band Reject

$$\begin{aligned} T(f) &= 1 && ; f < f_{low} \\ &= \text{Max} \left[\left(\frac{f_{low}}{f} \right)^{2n}, \left(\frac{f}{f_{high}} \right)^{2n}, T_{min} \right] && ; f_{low} < f < f_{high} \\ &= 1 && ; f > f_{high} \end{aligned}$$

where T_{min} = user supplied isolation limit

where f_{low} , f_{high} = rejection band limits in Hz

f = tuned frequency in Hz

n = order

6.4.2.2 Field Propagation Models

6.4.2.2.1 Aircraft/Spacecraft

$$P_R = P_T + TFS + SF$$

P_T = transmitter power in dBm

TFS = free space transmission factor in dB

SF = shading factor in dB

$$TFS = G_T + G_R + 20 \log_{10} \left(\frac{\lambda}{4\pi D} \right)$$

G_T = gain of transmitting antenna in dB

G_R = gain of receiving antenna in dB

λ = wavelength in meters

D = distance between two antennas in meters

o Antenna Separation

D is determined by using the combination of straight lines, conical spirals, and/or cylindrical spirals that gives the shortest distance between the two antennas over the vehicle surface.

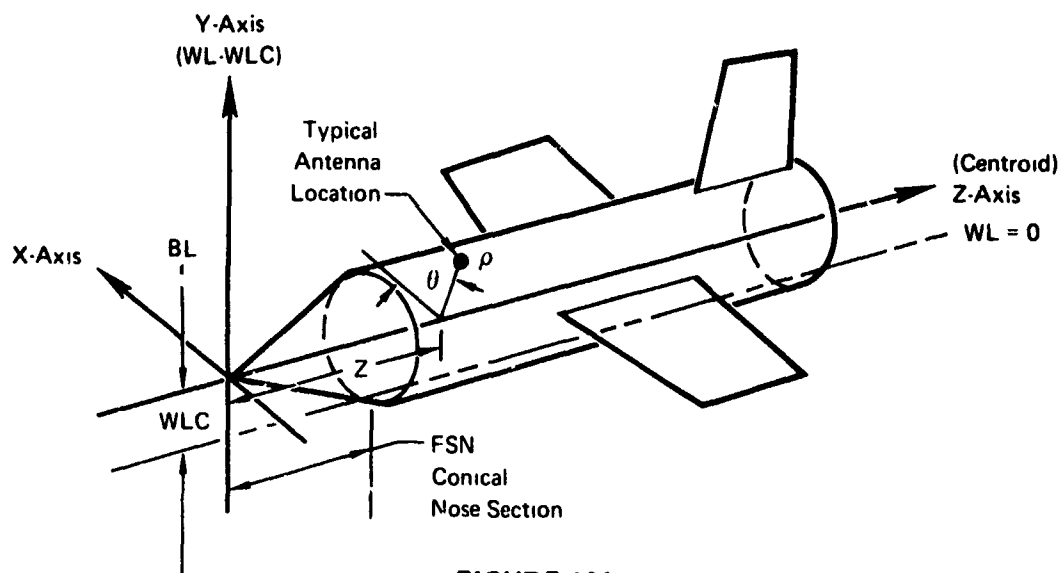


FIGURE 101
MODEL USED TO APPROXIMATE AIRCRAFT

GP73 0495 22

For the conical spiral, the distance between two points,

$P_1 (\rho_1, \theta_1, Z_1)$ and $P_2 (\rho_2, \theta_2, Z_2)$ is

$$D_{\text{con}} = \left| \frac{\rho_1 c - \rho_2 d}{2a} + \frac{a^2 + b^2}{2a} \ln \left| \frac{\rho_1 + c}{\rho_2 + d} \right| \right|$$

$$\text{where } a = \frac{\rho_2 - \rho_1}{\theta_2 - \theta_1}$$

$$b = \frac{Z_2 - Z_1}{\theta_2 - \theta_1}$$

$$c = \sqrt{a^2 + b^2 + \rho_1^2}$$

$$d = \sqrt{a^2 + b^2 + \rho_2^2}$$

For the cylindrical spiral ($\rho_1 = \rho_2 = \rho_f$),

$$D_{cyl} = \sqrt{\rho_f^2 (\theta_2 - \theta_1)^2 + (Z_2 - Z_1)^2}.$$

Straight line distances are found using

$$D_{sl} = \sqrt{\rho_1^2 + \rho_2^2 - 2\rho_1\rho_2 \cos(\theta_2 - \theta_1) + (Z_2 - Z_1)^2}.$$

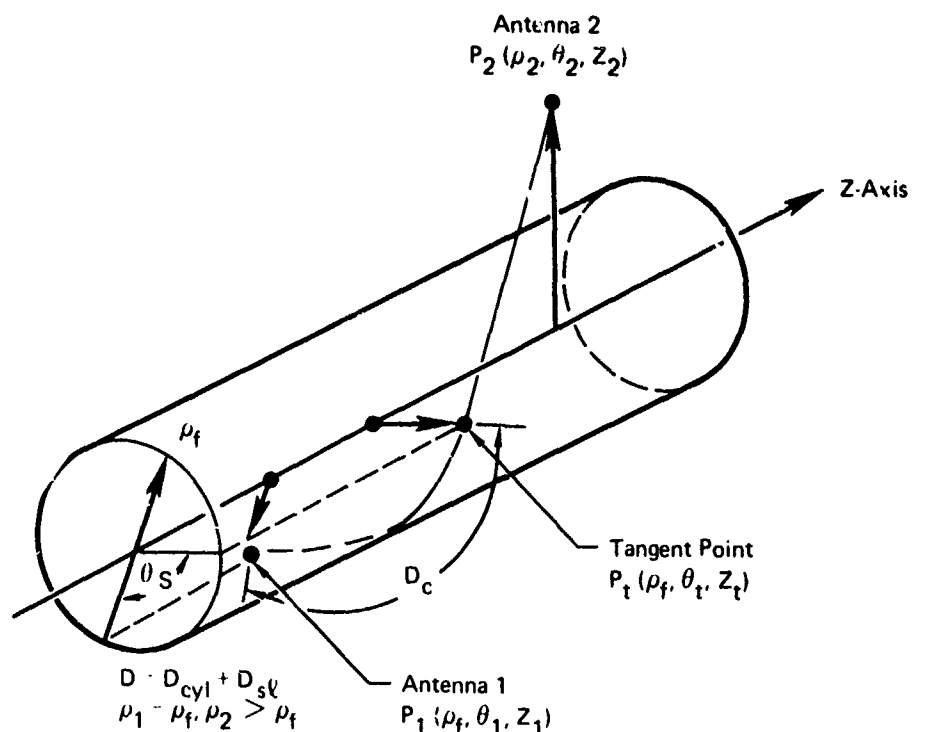
For one antenna off the cylinder (assume ρ_2, θ_2, Z_2 is off the cylinder) a tangent point is found using

$$\theta_t = \theta_2 \pm \tan^{-1} \left[\frac{\sqrt{\rho_2^2 - \rho_1^2}}{\rho_1} \right]$$

The appropriate sign is used that produces minimum D.

$$Z_t = \frac{\rho_1 |\theta_1 - \theta_t| Z_2 + Z_1 \sqrt{\rho_2^2 - \rho_1^2}}{\rho_1 |\theta_1 - \theta_t| + \sqrt{\rho_2^2 - \rho_1^2}}$$

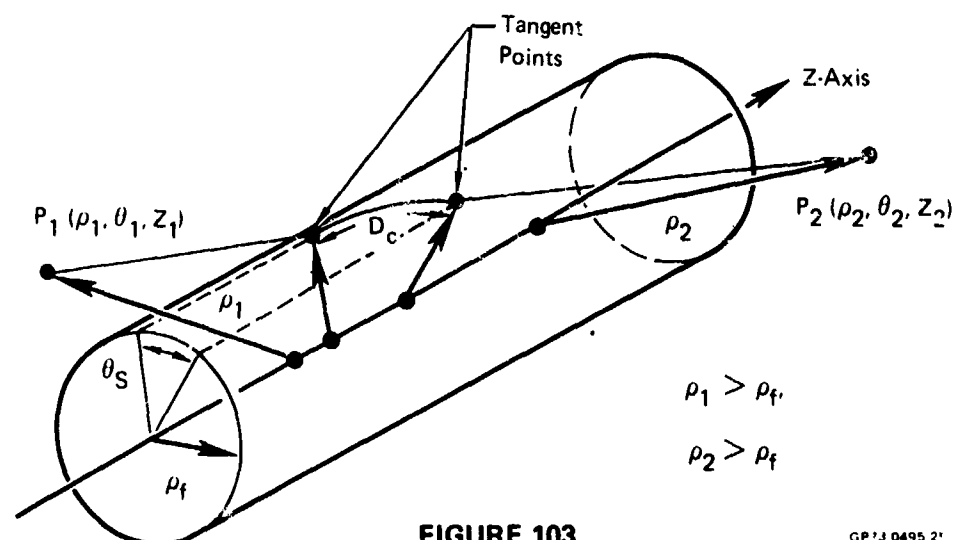
These formulas are used twice if both antennas are off the cylinder.



GP73-0495-20

FIGURE 102

DISTANCE BETWEEN TWO ANTENNAS WHEN ONE IS LOCATED OFF FUSELAGE AND A PORTION OF THE PATH IS AROUND THE FUSELAGE



GP73-0495-21

FIGURE 103

DISTANCE BETWEEN TWO ANTENNAS WHEN BOTH ARE OFF THE FUSELAGE AND THE PATH IS AROUND THE FUSELAGE

o Cylindrical Shading

The following is used for curved surface shading

$$SF_C = \frac{-A}{(\eta A + \xi)}$$

$$\text{where } A = \rho_f \theta_s^2 \sqrt{\frac{2\pi}{\lambda D_c}}$$

$$\eta = \begin{cases} 5.478 \times 10^{-3}, & \text{for } A < 26 \\ 3.340 \times 10^{-3}, & \text{for } A \geq 26 \end{cases}$$

$$\xi = \begin{cases} 0.5083, & \text{for } A < 26 \\ 0.5621, & \text{for } A \geq 26 \end{cases}$$

and SF_C = fuselage (cylindrical) shading factor (dB)

ρ_f = radius of cylinder (meters)

θ_s = angle around cylinder of propagation path (radians)

λ = wavelength (meters)

D_c = distance of cylindrical segment of propagation path (meters)

o Wing Diffraction

The following formula from optics is used to relate the diffracted electric field to the incident field

$$SF_w = 20 \log_{10} (SF'_w) + 78.73$$

$$SF'_w = \frac{\max |\sec \frac{1}{2} (\alpha_x - \alpha_r) \pm \csc \frac{1}{2} (\alpha_x + \alpha_r)| \cos \beta}{\sqrt{f D_{wr}}}$$

$$\cos \beta = \sqrt{\frac{y_{x2}^2 + z_{x2}^2}{x_{x2}^2 + y_{x2}^2 + z_{x2}^2}}$$

and SF_w = Wing shading factor (dB)

E_x = Incident electric field from transmitter at wing point

E_r = Received electric field at receiver antenna

α_x = Angle between Z_2 axis and incident wave propagation vector projected onto $Y_2 - Z_2$ plane

α_r = Angle between Z_2 axis and receptor wave propagation vector projected onto $Y_2 - Z_2$ plane

β = Azimuthal angle of incident wave propagation vector to $Y_2 - Z_2$ plane

D_{wr} = Distance from wing point to recaptor point (inches)

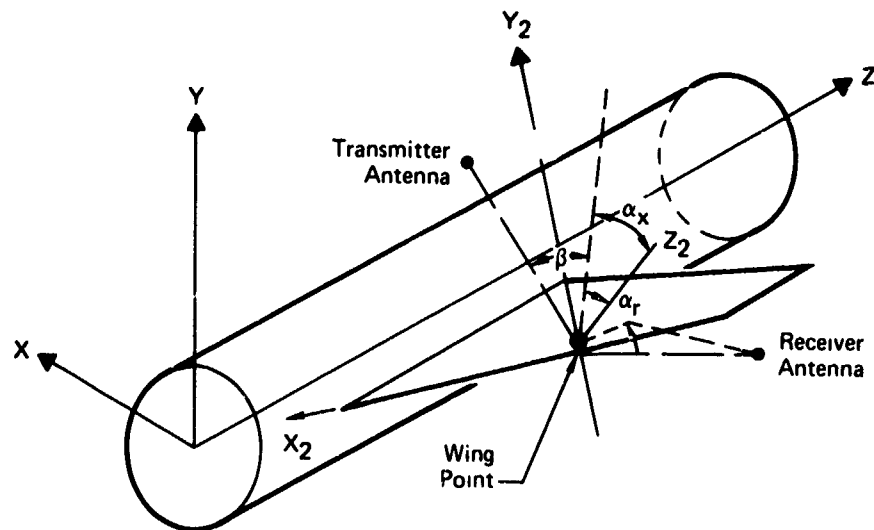


FIGURE 104
DIFFRACTION COORDINATE SYSTEM WHEN THE PROPAGATION PATH IS
AROUND THE WING EDGE. ATTENUATION FUNCTION IS CALCULATED
USING ANGLES IN THIS COORDINATE SYSTEM

GP73 0495 21

6.4.2.2.2 Ground Propagation Model

The following equations apply to ground propagation loss

$$L_t = L_o - 6 \quad ; d \leq \frac{d_{FSM}}{2}$$

$$L_T = L_o - 20 \log_{10} \left| \frac{d}{d_{FSM}} \right| \quad ; d > \frac{d_{FSM}}{2}$$

where

L_T — total propagation loss

L_o — free space loss

$$= 20 \log_{10} f + 20 \log_{10} d + 32.45$$

$$d_{FSM} = \frac{4 h_1' h_2'}{\lambda}$$

$$h_1' = \text{Maximum } [h_1, h_u]$$

= Effective Antenna Height of A

$$h_2' = \text{Maximum } [h_2, h_o]$$

= Effective Antenna Height of B

$$h_o = \frac{\lambda [\epsilon_r^2 + (0.06 \lambda \sigma)^2]^{1/2}}{2 \pi [(\epsilon_r - 1)^2 + (0.06 \lambda \sigma)^2]^{1/4}}$$

= Minimum Effective Antenna Height for Vertical Polarization

$$h_o = \frac{\lambda}{2 \pi [(\epsilon_r - 1)^2 + (0.06 \lambda \sigma)^2]^{1/4}}$$

= Minimum Effective Antenna Height for Horizontal Polarization

The antenna heights must not be so large that the quantity $\frac{h_1 h_2}{79.6 \lambda}$ is greater than d_c and antenna separation should not be greater than d_c where

$h_{1,2}$ = antenna heights in meters

λ = wavelength in meters

d_c = maximum plane earth distance

$$= \frac{150}{0.5305f}$$

$$1 \leq f \leq 100 \text{ MHz}$$

$$= \frac{60.4}{0.3337f}$$

$$100 < f \leq 1000 \text{ MHz}$$

The total propagation loss is the sum of the free space loss and the loss relative to free space (ground wave).

For near field coupling the propagation loss is linearly interpolated between values of zero and the far field value calculated at a distance of $2D^2/\lambda$ where D is the maximum antenna dimension. Propagation loss is taken as zero whenever the distance between antennas is less than or equal to the maximum antenna dimension.

6.4.2.3 Field to Wire (Via Aperture)

Upon determining a field to wire coupling path the program uses the appropriate propagation model or environmental field exposed on the wires, in volts/meter, to determine the current in amperes flowing through the loads. This is done on a segment basis and the total is summed irrespective of phase. The following definitions will be used throughout

$$\lambda = \frac{3 \times 10^8}{f}$$

$$X = 2\pi \frac{\ell}{\lambda}$$

$$Z_c = 120 \ln \left(\frac{b}{r} \right) = \text{characteristic impedance}$$

$Z_{o,L}$ = respective equivalent load impedances on either end of segment in question

b = separation between wires in two wire circuit

= twice height if ground reference

ℓ = length of transmission line segment

r = radius of wire

f = frequency

Assuming Z_L is the load in question

$$\text{if } Z_o > Z_c \text{ and } X \leq \left| \frac{2 Z_o}{Z_c + Z_o} \right|$$

$$|I'_L| = b X \left| \frac{Z_o + Z_c}{Z_c (Z_o + Z_L)} \right|$$

$$\text{if } Z_o > Z_c \text{ and } X > \left| \frac{2 Z_o}{Z_c + Z_o} \right|$$

$$|I'_L| = 2b \left| \frac{Z_o}{Z_c (Z_o + Z_L)} \right|$$

$$\text{if } Z_0 < Z_c \text{ and } X \leq \left| \frac{2 Z_c}{Z_c + Z_0} \right|$$

$$|I'_L| = b X \left| \frac{Z_0 + Z_c}{Z_c (Z_0 + Z_L)} \right|$$

$$\text{if } Z_0 < Z_c \text{ and } X > \left| \frac{2 Z_c}{Z_c + Z_0} \right|$$

$$|I'_L| = 2b \left| \frac{1}{Z_0 + Z_L} \right|$$

The induced current is

$$|I_L| = \text{Min}[|I'_L|, I_{\text{Bound}}]$$

where

$$I_{\text{Bound}} = \frac{\frac{\lambda}{\text{Max}[\sqrt{4\pi}, 1]}}{\sqrt{377 \times R_e(Z_L)}}$$

If a shield is present and the frequency is greater than 7228 Hz but less than 9×10^5 Hz

$$I_L = I_L \times 10^{[4.8 \log_{10} f - 70.8] \log_{10} f + 201.5}$$

If the frequency is greater than 9×10^5 Hz

$$I_L = I_L \times 10^{[(-67 \log_{10} f + 42.5) \log_{10} f - 345.8] \log_{10} f + 855}$$

If a double shield is present, the above powers of ten are multiplied by $\frac{3}{2}$.

6.4.2.4 Wire-to-Wire Coupling

The following formulas have been incorporated into IEMCAP to account for wire to wire coupling via mutual inductance and mutual capacitance.

The following factors and transfer models are included

- o Mutual inductance coupling
- o Mutual capacitance coupling
- o Common impedance coupling
- o Unshielded wires
- o Shielded wires (single and double)
- o Shield terminations (single and multiple)
- o Twisted wires (Balanced and Unbalanced)
- o Shield Pigtail Length and Area
- o Shield coverage factors

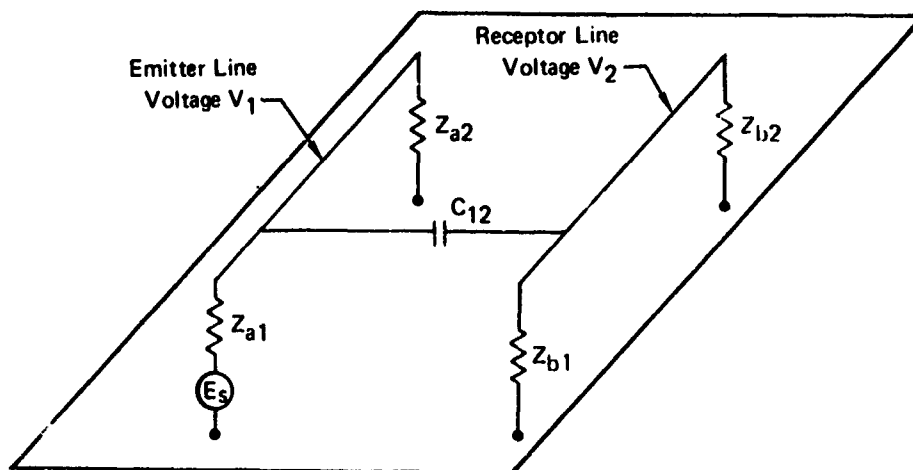
Wire-to-Wire Capacitance

The wire-to-wire capacitance is used to calculate the capacitive coupling of the emitter segment to the receptor segment according to the relation

$$\frac{V_{\text{rec}}}{V_{\text{em}}} = \frac{1}{1 + \frac{1}{j\omega C_{12} \ell_s Z}}$$

$$Z = \frac{Z_{b1} Z_{b2}}{Z_{b1} + Z_{b2}}$$

ℓ_s = segmen. length



CP 73-4959

FIGURE 105
CIRCUIT REPRESENTATIVE OF CAPACITIVE COUPLING BETWEEN
PARALLEL WIRES OVER A GROUND PLANE

With reference to Figure 101, the capacitance per unit length between the two wires is given by

where

$$C_{12} = - \frac{2\pi\epsilon_{\text{eff}}P_{12}}{\det}$$

$$P_{12} = \frac{1}{2} \left[\cosh^{-1} \left(\frac{s^2 + (r_1^2 - r_2^2)}{2sr_1} \right) + \cosh^{-1} \left(\frac{s^2 - (r_1^2 - r_2^2)}{2sr_2} \right) \right. \\ \left. - \cosh^{-1} \left(\frac{s'^2 + (r_1^2 - r_2^2)}{2s'r_1} \right) + \cosh^{-1} \left(\frac{s'^2 - (r_1^2 - r_2^2)}{2s'r_2} \right) \right]$$

$$s' = \sqrt{4h_1h_2 + s^2},$$

$$\det = \cosh^{-1} \left(\frac{h_1}{r_1} \right) \cosh^{-1} \left(\frac{h_2}{r_2} \right) - P_{12}^2.$$

V_{em} = voltage on source wire

V_{rec} = voltage on receptor wire

o Shielded emitter wire

$$\frac{V_{rec}}{V_{em}} = \left(\frac{1}{1 + \frac{1}{j\omega C_{ws} \ell_s}} \right) \left(\exp \left(-\frac{t_e}{\delta_e} \right) + F_e \right) \left(\frac{1}{1 + \frac{1}{j\omega ZC_{12} \ell_s}} \right)$$

$$C_{ws} = \frac{2\pi \epsilon}{\ln \left(\frac{R_{s1}}{r_1} \right)}$$

where ϵ = permittivity of material between the wire and shield.

R_{s1} and r_1 = shield inner radius and emitter wire radius, respectively

$F_e = .02$

C_{12} = as before with r , equal to shield outer radius

$$R_s = R_o \left(\frac{t_e}{\delta_e} \right) \frac{\sin h \frac{2t_e}{\delta_e} + \sin \frac{2t_e}{\delta_e}}{\cos h \frac{2t_e}{\delta_e} - \cos \frac{2t_e}{\delta_e}}$$

$$R_o = \frac{\ell_s}{2\pi \sigma r_1 t}$$

o Double shielded emitter wires

$$\frac{V_{rec}}{V_{em}} = \left(\frac{e^{-t_{e1}}}{\left(e \frac{\delta_{e1}}{\delta_{e1}} + F_{e1} \right)} \right) \left(\frac{e^{-t_{e2}}}{\left(e \frac{\delta_{e2}}{\delta_{e2}} + F_{e2} \right)} \right) \left(\frac{1}{1 + \frac{1}{j\omega C_{s1s2} \ell_s R_{s1}}} \right) \left(\frac{1}{1 + \frac{1}{j\omega C_{s1s2} \ell_s R_{s2}}} \right) \left(\frac{1}{1 + \frac{1}{j\omega C_{s2 rec} \ell_s Z}} \right)$$

where

C_{s1s2} = capacitance between shields

$C_{s2 rec}$ = capacitance between the outer shield and the receptor

subscripts 1 and 2 refer to inner and outer shields

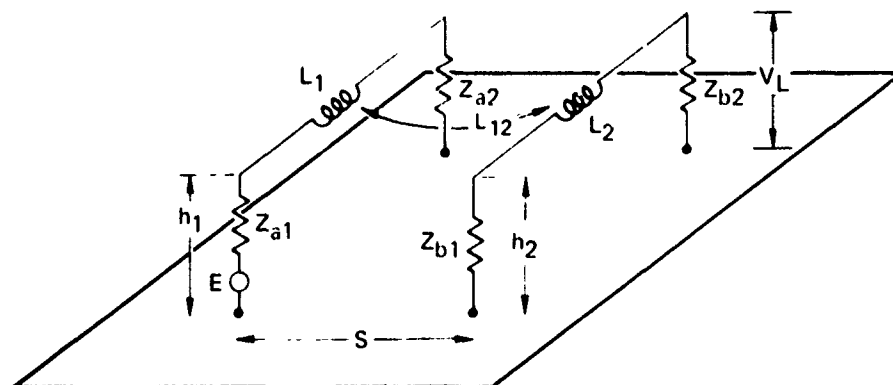
V_{em} = voltage on emitter wire

V_{rec} = voltage on receptor wire

- Notes:
- 1) The same factors are used to compute the shielding through the receptor shield(s).
 - 2) Pigtail shield terminations are assumed to have three inches of exposed wire.
 - 3) The capacitive coupling of a twisted pair circuit with another circuit is treated as the coupling of single wire circuits.

Inductive Coupling

The calculation of inductive coupling between emitter and receptor circuits is computed using the mutual inductance between the circuits as shown in the following figure.



GP 7.3-0495 10

FIGURE 106
CIRCUIT REPRESENTATIVE OF INDUCTIVE COUPLING BETWEEN
PARALLEL WIRES OVER A GROUND PLANE

- With reference to Figure 106, the voltage induced in the receptor load is

$$V_L = j\omega L_{12} I_1 \ell_s \frac{Z_{b2}}{Z_{b1} + Z_{b2} + j\omega L_2 \ell_s}$$

where

I_1 = current in emitter wire

$$L_{12} = \frac{\mu_0}{4\pi} \ell_n \left[\frac{(h_1 + h_2)^2 + s^2}{(h_1 - h_2)^2 + s^2} \right]$$

μ_0 = permeability of free space

$$L_2 = \frac{\mu_0}{2\pi} \ell_n \left[\frac{2h_2}{r_2} - 1 \right]$$

For multiple ground shielded emitter, the shield current is

$$I_{sh} = \frac{V_s}{R_s + j\omega L_{sw} \ell_s}$$

where

R_s = total shield resistance

$$L_{sw} = \frac{\mu_0}{2\pi} \ln \left(\frac{2h_1}{r_s} \right)$$

h_1 = height (above ground)

r_s = shield radius

$V_s = j\omega L_{sw} I_1 \ell_s$

ℓ_s = length of wire segment

The net emitter current I_{eff} is

$$I_{eff} = I_1 - I_{sh} = \frac{R_s}{R_s + j\omega L_{sw} \ell_s} I_1$$

The voltage induced in shielded receptor wires

$$V_2 = j\omega L_{ew2} \ell_s I_1 - j\omega L_{s2w2} \ell_s \frac{j\omega L_{es2} I_1}{R_{rs} + j\omega L_{rs} \ell_s}$$

where

L_{ew2} = mutual inductance per unit length between the receptor

L_{s2w2} = mutual inductance per unit length between the receptor wire and its shield

L_{es_2} = mutual inductance between the emitter circuit and receptor shield

L_{rs} and R_{rs} are the self inductance and shield resistance of the receptor circuit.

I_1 = emitter current or effective emitter current

For circuits composed of twisted pairs, both common mode currents and differential mode currents are considered in the coupling.

For an unbalanced twisted pair emitter circuit as shown below, the common mode current can be expressed as

$$I_c = j\omega C_s V_1$$

where

$$C_s = \frac{2\pi \epsilon_0 \ell_s}{\ln \left(\frac{2h}{r_w} \right)}$$

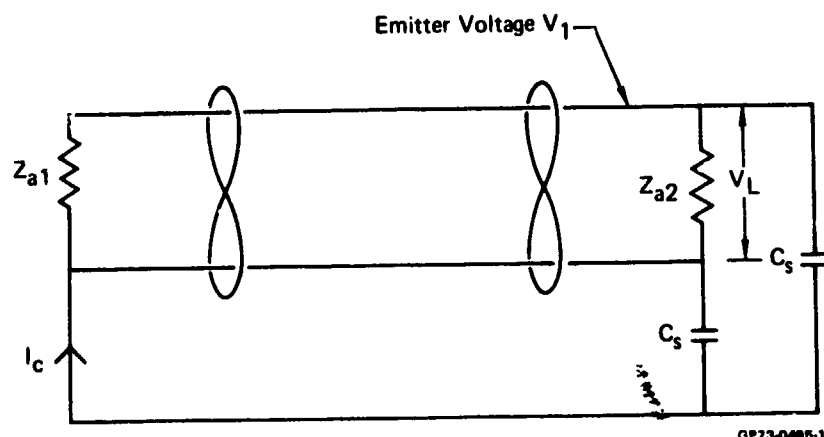


FIGURE 107
INDUCTIVE MODEL FOR UNBALANCED, TWISTED EMITTER WIRE PAIR

This common mode current is used as the single wire equivalent emitter current.

For a perfectly balanced twisted pair emitter circuit the voltage induced in the receptor circuit by the differential mode current is

$$V_L = j\omega L'_{12} \ell_s I_d$$

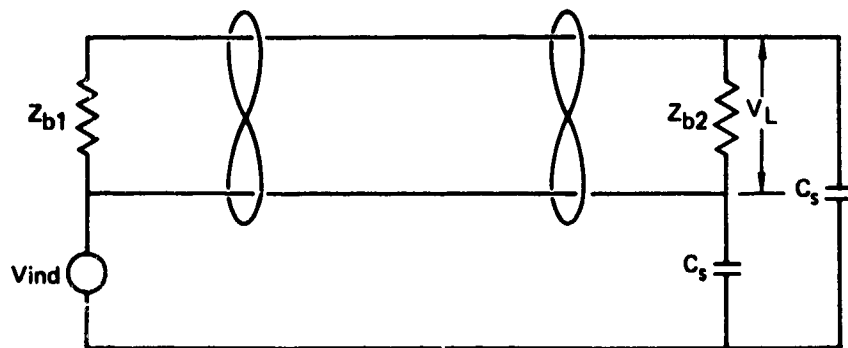
where

$$L'_{12} = \frac{\mu_0}{4\pi} \ln \left[\left(\frac{d}{s} \right)^2 + 1 \right]$$

- = mutual inductance of twisted pair loop and receptor circuit
- d = separation between twisted pair wires
- s = average separation between emitter circuit and receptor
- I_d = differential current

For a shielded twisted pair emitter, the common mode current is computed as for single wire circuits while the coupling due to the differential mode currents is unaffected by the presence of the shield.

For an unbalanced twisted pair receptor circuit, the load voltage produced by the common mode currents can be written as



GP73-0486-12

FIGURE 108
INDUCTIVE MODEL FOR UNBALANCED, TWISTED RECEPTOR WIRE PAIR,

$$V_L = \frac{j\omega Z_{eq} C_s}{1 + j\omega Z_{eq} C_s} V_{ind}$$

where

$$Z_{eq} = \frac{Z_{b1}Z_{b2}}{Z_{b1} + Z_{b2}}$$

$$V_{ind} = j\omega L_{12} I_1$$

For a balanced twisted receptor the voltage caused by the differential mode coupling is

$$V_L = j\omega L'_{12} I_1 \frac{Z_{b2}}{Z_{b1} + Z_{b2}}$$

where

L'_{12} = emitter circuit to receptor loop mutual inductance

For a shielded receptor circuit, the common mode current coupling is modified in the same manner as the single wire receptor and the induced differential mode currents are unaffected by the presence of the shield.

Common Impedance - The fact that many circuits share a common return has caused many instances of EMI. The reason for this form of EMI is the return current of one circuit flowing through a non-zero impedance return acts as a current generator of finite impedance into other commonly grounded circuits. This coupling mode has been modeled by assuming a wire as a circuit return. By assuming that the receptor circuit does not load down the emitter circuit, this effect is added into the calculation after considerations of inductance and capacitance have been completed.

6.4.2.5 Case to Case

The case to case model uses the emission and susceptibility levels as specified in Section 6.4.1.3, Non-Required Emission and Susceptibility. These levels are related to the system configuration by modelling each case as though it were a dipole. The source model assumes a fall off of $\left(\frac{1}{r}\right)^3$ for both the electric and magnetic fields.

REFERENCES

1. M. G. Pelchat, "The Autocorrelation Function and Power Spectrum of PCM/FM with Random Binary Modulating Waveforms," IEEE Transactions on Space Electronics and Telemetry, March 1964, pp. 39-44.
2. J. Morini, "Simplified Equations for the Power Spectrum of Binary Frequency Shift Keying," ECAC-TN-003-241, February 1966.
3. S. Cohen, "Spectrum Model for Amplitude Modulations with Stochastic Process," ECAC-TN-003-252, April 1966.
4. T. Lawson, "A Transmitter Spectrum Synthesis Techniques for EMI Prediction," ECAC-MD-111.
5. W. Shelton, "Spectrum Model for Angle Modulation with Stochastic Process," ECAC-TN-003-264, December 1966.
6. S. Cohen, "Spectral Characteristics of Single Sideband Amplitude, Phase and Frequency Modulation with a Stochastic Process," ECAC-TN-003-265, February 1967.
7. P. Newhouse, "A Simplified Method for Calculating the Bounds on the Emission Spectra of Chirp Radars," ECAC-TN-002-27, June 1970.
8. N. M. Shehodeh and R. Chiu, "Spectral Density Functions of a Carrier Amplitude Modulated by a Biphasic PCM Code," IEEE Transactions on Communications Technology, pp. 263-265, June 1970.
9. N. Solat, "On the Spectra of Wave-Shaped Binary Sequences," Proc. IEEE, April 1964.
10. S. A. Cohen and W. T. Shelton, "Spectral Analysis of a PAM-FM Signal," IEEE Transactions on Communication Technology, p. 487-494, June 1968.
11. Ibid.
12. Y. W. Lee, Statistical Theory of Communications, New York, London, Sidney: John Wiley & Sons, Inc., January 1967.
13. M. Maiuzzo, "Two Simplified Theoretical Ground Wave Models," ECAC-TN-003-315, June 1968.
14. J. L. Bogdanor, M. D. Siegel, G. L. Weinstock, "Intra-Vehicle Electromagnetic Compatibility Analysis," AFAL-TR-71-155, July 1971.
15. G. Hasserjian, A. Ishimaru, "Excitation of a Conducting Cylindrical Surface of Large Radius of Curvature," IRE Trans. on Antennas and Propagation, pp. 264-273, May 1962.

REFERENCES (Continued)

16. C. Taylor, S. Satterwhite, C. Harrison, Jr., "The Response of a Terminated Two-Wire Transmission Line Excited by a Nonuniform Electromagnetic Field," IEEE Trans. on Antennas and Propagation, pp. 987-989, November 1965.
17. J. L. Bogdanor, M. D. Siegel, G. L. Weinstock, op. cit.
18. Greenstein and Tobin, "Analysis of Cable Coupled Interference," IEEE Transactions on RFI, p. 43-44, March 1963.
19. Mohr, "Coupling Between Lines at High Frequencies," IEEE Transactions on EMC, p. 127-129, December 1967.
20. Mohr, "Coupling Between Open and Shielded Wires Lines Over a Ground Plane," IEEE Transactions on EMC, p. 34-35, September 1967
AFSC DH 1-4 DN 5B4 p. 1-3.
21. "Development of a Space Vehicle Electromagnetic Interference/Compatibility Specification," NASA Contract Number 9-7305.

Appendix A

SIGNALS, NOISE AND INTERFERENCE IN A LINEAR DEVICE

A.1 INTRODUCTION

The purpose of this discussion is to provide insight into the concept of "standard response" of a power sensitive linear device and to relate this quantity to more widely known parameters of receptor devices employed in electronic systems. In the conventional sense, the standard response of a device is that power level at its output terminals which is just sufficient to convey intelligence that a signal is present. For some kinds of receptors this power level is just that amount necessary to change the state of the device. In other cases the power level must be sufficiently above noise (or noise plus interference) to ensure a high probability of recovery of the intelligence present in the signal. The present discussion develops the concept of standard response of a device along these conventional lines and suggests how the concept can be related to electromagnetic interference (EMI) susceptibility criteria for devices. Use of the device susceptibility in the calculation of EMI margins and of integrated EMI margin is treated in Section 2.2 of this manual.

A.2 TECHNICAL DISCUSSION

Assume a linear filter with power transfer function, $|H(f)|^2$, and suppose there is signal power spectral density, $\eta(f)$, at its input terminals. Then, the output power spectral density (o.p.s.d.) due to this input is

$$\text{o.p.s.d.} = \eta(f)|H(f)|^2 \quad \text{watts/Hz} \quad (1)$$

This is the component of o.p.s.d. due to input signal only and does not consider the components due to thermal noise power spectral density or to interference power spectral density. The output noise power spectral density component is given by:

$$\text{o.n.p.s.d.} = FkT|H(f)|^2 \quad \text{watts/Hz} \quad (2)$$

where

k = Boltzman's constant in watts per degree Kelvin per Hz,

T = device temperature in degrees Kelvin

and

F = device noise figure, a numeric that is greater than or equal to unity. For lossy networks, F is identical with the network loss factor, $L = 1/G_o$.

Thus, the total input power spectral density, for an idealized (interference-free) environment, is given by:

$$\text{i.p.s.d.} = \eta(f) + FkT \quad (3)$$

The total output power spectral density corresponding to (3) is, therefore

$$\text{o.p.s.d.} = [\eta(f) + FkT] |H(f)|^2 \quad (4)$$

Integration of (4) over all frequencies gives the total output power as follows:

$$\hat{P}_{\text{out}} = \int_0^{\infty} \eta(f) |H(f)|^2 df + G_o FkTB_n \quad (5)$$

where

$$B_n \triangleq \frac{1}{|H(f_o)|^2} \int_0^{\infty} |H(f)|^2 df \quad (6)$$

and

$$G_o \triangleq |H(f_o)|^2 \quad (7)$$

Thus, the total output power contains a noise power component $\hat{N}_o = G_o FkTB_n$ where kTB_n can be said to be the input noise power. B_n in these expressions is the effective noise bandwidth of the device and is defined by equation (6).

Now, denote by \hat{S}_o the component of output power due to input signal power spectral density. Then total output power may be expressed:

$$\hat{P}_{\text{out}} = \hat{S}_o + \hat{N}_o \quad (8)$$

Examine for the moment the result of a cw signal centered in the tuned pass band of the filter (i.e., a delta function at frequency f_o). Then, $\eta(f) = \hat{P}_{\text{in}} \delta(f - f_o)$, and the quantity \hat{S}_{oN} is given by

$$\hat{S}_{oN} = \int_0^{\infty} \hat{P}_{\text{in}} \delta(f - f_o) |H(f)|^2 df = \hat{P}_{\text{in}} |H(f_o)|^2 \text{ or, } \hat{S}_{oN} = G_o \hat{P}_{\text{in}} \quad (9)$$

$$\text{and } \hat{P}_{\text{out}} = G_o \hat{P}_{\text{in}} + \hat{N}_o = \hat{S}_{oN} + \hat{N}_o \quad (10)$$

Now, for a desired probability of detection of intelligence in a signal, it is usual to specify for a device that its output signal power must have some minimum value compared with the output noise power. Thus, it may be said that the "standard response" of the device is such that the signal-to-noise power ratio has a required minimum numeric value of $\overline{\text{SNR}}$. Then, the "standard response" is defined as an output signal power, \hat{K} , given by

$$\hat{K} = \hat{N}_O \overline{\text{SNR}} \quad (11)$$

where $\overline{\text{SNR}}$ = output signal-to-noise power ratio.

For the case of the narrowband (cw) signal centered in the filter pass band, the following would obtain:

$$\hat{K}_N = \hat{N}_O \overline{\text{SNR}} = \hat{S}_{ON}(\text{min}) = G_O \hat{P}_{in}(\text{min}) \quad (12)$$

and it can be said that the device "cw sensitivity" (at its input terminals) is

$$\hat{K}_N / G_O = FkTB_n \overline{\text{SNR}} = \hat{P}_{in}(\text{min}) \text{ watts} \quad (13)$$

Consider now the EMC problem of utilizing the previously discussed "ideal" filter in a system where it is subject to one or more sources of interfering signals. These interference signals can be expected to introduce a third term in the output power expression for the filter which, for ease of identification, will be denoted \hat{I}_O . This interference signal power is of the general nature of noise power when considering the problem of detecting desired signal intelligence in the presence of thermal noise plus these interfering signals. Thus, it is clear that these additional interfering signals will, of necessity, degrade the so-called ideal response characteristic of the filter. In order for the EMC engineer to establish realistic interference criteria for this device, he must obtain from the systems engineer the "tolerable degradation" for the device when it is situated in the interference environment of the system.

When interference signals are present, in addition to a desired signal and thermal noise, it is appropriate to define a quantity, $\overline{\text{SNIR}}$, which is the signal-to-noise plus interference power ratio at the output of the device.

Some guidelines will now be developed to aid in judging the allowable interference power at the input of the receptor device in order for it to perform within its "tolerable degradation" specification. The development proceeds with the previously stated assumption that the power spectral density at the device input terminals is comprised of three components:

one due to the desired signal, a second due to interfering signals and a third due to thermal noise. Then the output power spectral density in this case is just:

$$\text{o.p.s.d.} = [\eta(f) + I(f) + FkT]|H(f)|^2 \quad (14)$$

Integrating over all frequencies, as in the case of the filter in the "ideal" environment, it is found that the total output power consists of:

$$\hat{P}_{\text{out}} = \hat{S}_o + \hat{I}_o + \hat{N}_o = (\hat{N}_o + \hat{I}_o)(1 + \overline{\text{SNIR}}) \quad (15)$$

It is logical to assert that, for a required probability of signal detection, the $\overline{\text{SNIR}}$ for the device operating in the interference environment must be at least equal in value to the $\overline{\text{SNR}}$ that was specified for the device in the ideal environment. There is no doubt that this necessitates a higher level of signal power if the thermal noise power is the same for both ideal and interference environments and if the interference power is non-zero.

If the filter under discussion happened to represent the receiver portion of a communications transceiver, the impact of a requirement for higher received signal power to overcome interference is clearly either reduced communication range or else a need for higher transmitter power for maintenance of communication range. If the filter represents a logic circuit device, the interpretation would be somewhat different: the added interference power would be specified to remain within a known noise immunity threshold when considered in conjunction with thermal noise.

Regardless of the specific circuit application of the filter, the general problem to be solved by the EMC engineer, in establishing interference criteria for the device, involves a modification of the previous concept of "standard response" of the device when considering the interference environment. When interference is present, the standard response is re-defined as an output signal power, \hat{K}' , given by

$$\hat{K}' = (\hat{N}_o + \hat{I}_o) \overline{\text{SNIR}} = (\hat{N}_o + \hat{I}_o) \overline{\text{SNR}} \quad (16)$$

Equation (16) reflects the idea that $\overline{\text{SNIR}}$ must remain identical to $\overline{\text{SNR}}$, so that signal power must increase to compensate the added interference power.

Minimum input signal power for the "ideal" case was previously given by equation (13). The relationship for a revised minimum input signal power, corresponding to the interference situation of equation (16), is just:

$$\hat{P}_{\text{in}}(\text{min. rev.}) = (\hat{N}_i + \hat{I}_i) \overline{\text{SNR}} \quad (17)$$

Equations (17) and (13) enable determination of the tolerable input interference power for a given permissible performance degradation.

The discussion about "tolerable degradation" of a receptor's performance deserves some further clarification. The prime objective of any system design is to achieve required performance at a minimum cost. Therefore, the systems engineer does not, in general, have much, if any, performance to "give away." However, for those "new" elements of a system, some performance trades will be possible to accommodate some reasonable interference levels in the system. For "old" elements (say GFE equipments whose parameters are established) the problem will often be to keep the interference signal levels low enough that the performance degradation is a small fraction of a modest performance margin that would normally exist for that equipment.

A.3 EXAMPLES

Some specific numerical values for the parameters of certain types of receptors common in systems will now be assumed for the purpose of illustrating a possible approach to establishing interference criteria for devices of these types. The reader will appreciate that the numerical results obtained are presented only as general guidelines and should not be considered hard and fast rules; each particular situation will require its own careful assessment of tolerable interference and of suitable safety margins.

Example 1 - Communications Receiver

The first example is a communications receiver characterized by the following parameters:

$$\text{On-Tune Sensitivity} = 10 \log_{10} [P_{in}(\text{min})] = -100 \text{ dBm}$$

$$\text{Noise Figure} = 10 \log_{10} [F] = 8 \text{ dB}$$

$$\text{Signal-to-Noise Ratio} = 10 \log_{10} [\overline{\text{SNR}}] = 10 \text{ dB}$$

$$\text{Now, } \hat{P}_{in}(\text{min}) = FkTB_n \overline{\text{SNR}} = 10^{-10} \text{ mw } (-100 \text{ dBm})$$

$$\text{Therefore, } \hat{N}_i = kTB_n = 1.6 \times 10^{-12} \text{ mw } (-118 \text{ dBm})$$

This receiver is part of a communication system that is assumed to have little margin to spare since both transmitter and receiver equipment exist. It is assumed, however, that it is decided the system can tolerate a receiver sensitivity degradation of +1 dB (perhaps brought about because of favorable antenna locations which minimize transmission line losses). Therefore, the following relation obtains:

$$\hat{P}_{in}(\text{min. rev.}) = [FkTB_n + \hat{I}_i] \overline{\text{SNR}} = 1.26 \times 10^{-10} \text{ mw } (-99 \text{ dBm})$$

Then, $FkTB_n + \hat{I}_i = 1.26 \times 10^{-11} \text{ mw } (-109 \text{ dBm})$

Consequently, the interference signal level at the input terminals can be allowed to be no greater than

$$\hat{I}_{in}(\text{max}) = 1.26 \times 10^{-11} - 1 \times 10^{-11} = 2.6 \times 10^{-12} \text{ mw}$$

or $I_{in}(\text{max}) = -116 \text{ dBm}$

Example 2 - Logic Circuit

In this example it is assumed that the receptor is a 5V logic circuit which has a "noise immunity" specification of 1.0V r.m.s. corresponding to some very low error rate. That is, the circuit will not change states a very large proportion of the time until a signal in the circuit changes in level by at least 1.0V r.m.s. The circuit is assumed to have no power gain, so that power relations at its output terminals reflect directly to its input. Now, suppose the load impedance (resistive) across which input signal voltage is impressed is 1000 ohms. Then the signal power required to just trigger the device is simply $V^2/R = 1 \text{ mw}$, or 0 dBm. Thus, the "standard response" of this circuit is exactly 1 mw and the combination of interference power plus thermal noise power in the circuit must not exceed this value. It is probably safe to say that the thermal noise power is many orders of magnitude less than 0 dBm so that, for practical purposes, the tolerable interference power could conceivably be allowed to assume this quite high level. Since this is such a high tolerance on interference and since little penalty would ordinarily result from playing it a bit safe in this instance, an interference power of perhaps -10 dBm could probably be specified with little impact on economy or weight in the system.

A.4 CONCLUSIONS

The "standard response" of a receiving device has been defined as that output signal power which just gives required output signal-to-noise power ratio, SNR. This conventional interpretation pertains to desired signals. When considering interference signals the permissible interference signal power at the device output generally differs in level from, but is related to, the device standard response. If output interference power were permitted to be identical with the standard response, the interference would compete directly with a desired signal and this would generally result in excessive degradation of device performance. Consequently, permissible output interference power will usually be specified such that, when combined with thermal noise power, only moderate degradation of device sensitivity results.

In IEMCAP interference signal power is computed at the input terminals of a receptor and is compared with the device "interference susceptibility" power level for determination of an EMI margin. The discussion in this appendix has shown the relationship of device standard response (for desired signals) to the interference susceptibility power at the device input terminals for a given tolerable degradation of device sensitivity in the system environment. In the communication receiver example it was seen that a sensitivity degradation of 1 dB corresponded to an interference susceptibility power level (in the tuned pass band) of -116 dB for the assumed device. This level was seen to be -17 dB relative to device desired signal sensitivity. Thus, in the pass band of this receiver, an interference signal exceeding -116 dBm at the device input terminals would result in EMI while interference less than this amount would be relatively compatible. Since such a receiver is a power sensitive device, it can also be concluded that the result of integrating input interference power spectral density over all frequencies must also be less than -116 dBm for avoidance of EMI in the example device.

MISSION of Rome Air Development Center

RADC is the principal AFSC organization charged with planning and executing the USAF exploratory and advanced development programs for electromagnetic intelligence techniques, reliability and compatibility techniques for electronic systems, electromagnetic transmission and reception, ground based surveillance, ground communications, information displays and information processing. This Center provides technical or management assistance in support of studies, analyses, development planning activities, acquisition, test, evaluation, modification, and operation of aerospace systems and related equipment.

Source AFSCR 23-50, 11 May 70